

Some pages of this thesis may have been removed for copyright restrictions.

If you have discovered material in AURA which is unlawful e.g. breaches copyright, (either yours or that of a third party) or any other law, including but not limited to those relating to patent, trademark, confidentiality, data protection, obscenity, defamation, libel, then please read our [Takedown Policy](#) and [contact the service](#) immediately

Steric Stabilization and Dissolution Characteristics
of Aqueous Suspensions of Pharmaceutical Interest

by

David Alexander Rawlins

A thesis presented for the degree of

DOCTOR OF PHILOSOPHY

of the

University of Aston in Birmingham

November 1979

Steric Stabilization and Dissolution Characteristics of
Aqueous Suspensions of Pharmaceutical Interest

by

David Alexander Rawlins

Submitted for the degree of Doctor of Philosophy, 1979.

The adsorption of two groups of nonionic surface active agents and a series of high molecular weight hydrophilic polymer fractions onto a polystyrene latex and a drug substance diloxanide furcate H.P. has been investigated. The presence of pores within the drug surface has been demonstrated and this is shown to increase the adsorption of low molecular weight polymer species. Differences in the maximum amount of polymer adsorbed at both solid-solution interfaces have been ascribed to the different hydrophobicities of the surfaces as determined by contact angle measurements.

Adsorbed layer thicknesses of polymer on polystyrene latex have been determined by three techniques: microelectrophoresis, intensity fluctuation spectroscopy and by viscometric means. These results, in combination with adsorption data, were used to interpret the configuration of the adsorbed polymer molecules at the interface.

The type of drug suspension produced on adsorbing the different polymers in the absence of electrostatic stabilization was correlated with theoretical predictions of suspension characteristics deduced from potential energy diagrams. The agreement was good for the adsorption of short chain length surfactants, but for the polyvinylalcohols, discrepancies were found between experiment and theory. This was attributed to the inappropriate use of a mean segment density approximation within the adsorbed layer to calculate attractive potentials between particles. A maximum in the redispersibility values for suspensions coated with adsorbed nonylphenylethoxylates was attributed to 'partial steric stabilization' of the particles in conjunction with the attractive forces operating in the sediment between bare surface patches on neighbouring particles.

No significant change in the dissolution of the drug was observed when nonylphenylethoxylates were adsorbed due to desorption upon contact with the dissolution medium. Pluronic F68 and all the polyvinylalcohol fractions caused a reduction in the dissolution rate which is explained by the decreased diffusion of drug through the adsorbed polymer layer.

KEYWORDS

Steric stabilization + dissolution +
pharmaceutical suspensions.

Contents

	<u>Page</u>
Summary	1
Memorandum	1
Acknowledgements	1
Section 1 Introduction	1
1:1 Suspensions	1
1:2 Historical Review of Suspension Formulation	3
1:3 Aims of the Present Work	15
Section 2 Theory	18
2:1 Adsorption	18
2:2 Solvent Conditions	26
2:3 Steric Stabilization	27
2:3:1 Entropy Theories	31
2:3:2 Enthalpy Theories	31
2:3:3 Entropy plus Enthalpy Theories	36
2:3:4 Elastic Theories	42
2:4 Electrical Stabilization	43
2:4:1 The Diffuse Double Layer	46
2:4:2 The Inner Part of the Double Layer	48
2:4:3 Double Layer Repulsion	49
2:5 Hydration Forces	50
2:6 Attraction Between Particles	51
2:6:1 The Microscopic Approach	53
2:6:2 The Retardation Effect	55
2:6:3 The Macroscopic Approach	57
2:6:4 The Effect of Adsorbed Layers	60
Section 3 Materials	64
3:1 Water	64
3:2 Surface Active Agents and Polymers	64
3:3 Adsorbents	69
3:3:1 Drug - Diloxanide Furoate B.P.	69
3:3:2 Polystyrene Latex	69
3:4 Characterization of Materials	70
3:4:1 Surface Active Agents	70
3:4:2 Polymers	74
3:4:3 Polystyrene Latex	79
3:4:4 Drug Powder	88
Section 4 Adsorption	97
4:1 Methods	97
4:1:1 Adsorption Isotherms	97
4:1:2 Mercury Porosimetry	98

	<u>Page</u>
4:1:3 Nitrogen Adsorption Measurements	102
4:1:4 Contact Angle Measurements	104
4:2 Results and Discussion	105
4:2:1 <u>Adsorption of Nonylphenylethoxylates</u>	105
4:2:1:1 Polystyrene Latex	105
4:2:1:2 Diloxanide Furoate B.P.	110
4:2:2 <u>Adsorption of Pluronics</u>	112
4:2:2:1 Polystyrene Latex	112
4:2:2:2 Diloxanide Furoate B.P.	119
4:2:3 The Rate of Surfactant Adsorption	120
4:2:4 <u>Adsorption of Polyvinylalcohol</u>	124
4:2:4:1 Polystyrene Latex	124
4:2:4:2 Diloxanide Furoate B.P.	128
4:2:5 The Rate of PVA Adsorption	134
4:2:6 The Hydrophobic Nature of Surfaces	136
 Section 5 Adsorbed Layer Thickness	 158
5:1 Methods	158
5:1:1 Microelectrophoresis	158
5:1:1:1 Electrodes	160
5:1:1:2 Stationary Levels	161
5:1:1:3 Optical Correction for Cylindrical Cells	161
5:1:1:4 Operation	162
5:1:1:5 Conversion of Mobility to Zeta-potentials	162
5:1:2 The Viscometric Thickness of the Adsorbed Layer	165
5:1:3 Intensity Fluctuation Spectroscopy	167
5:2 Results and Discussion	169
5:2:1 Microelectrophoresis	169
a) Polystyrene Latex	170
b) Diloxanide Furoate B.P.	176
5:2:1:1 Estimation of Adsorbed Layer Thickness from Microelectrophoretic Measurements	177
5:2:2 Adsorbed Layer Thickness from Intensity Fluctuation Spectroscopy Measurements	183
5:2:3 Adsorbed Layer Thickness by Viscometric Means	184
 Section 6 Stability	 198
6:1 Methods	198
6:1:1 Coarse Suspension Stability	198
6:1:2 Polystyrene Latex Stability	200
6:1:3 Determination of Hamaker Constants	202
6:1:4 Potential Energy Diagrams	204
6:2 Results and Discussion	205
6:2:1a Suspension Characteristics	205
6:2:1b Long Term Storage of Suspensions	219
6:2:2 Polystyrene Latex Stability	223
6:2:3 Hamaker Constants	226
6:2:4 Potential Energy Diagrams	228
 Section 7 Dissolution Studies	 265
7:1 Methods	267
7:1:1 Saturated Solubility of Drug in Water	267
7:1:2 Polymer Desorption	267
7:1:3 Solubility in Polymer Solutions	268
7:1:4 Dissolution Studies	268
7:1:5 Preparation of Drug Crystals	268
7:2 Theory	269

	<u>Page</u>
7:3 Results and Discussion	270
7:3:1 Solubility of Drug in Water and Polymer Solutions	270
7:3:2 Desorption of Polymers from the Drug Surface	273
7:3:3 The Effect of Stirring Rate on Suspension Dissolution Rates	275
7:3:4 The Effect of Drug Quantity on Dissolution Rate	277
7:3:5 The Effect of Adsorbed Layers on Dissolution Rate	278
Section 8 Conclusions	293
References	298

Characteristics of
Polystyrene

102

Characteristics of
Polystyrene

111

Characteristics of
Polystyrene

116

Characteristics of
Polystyrene

120

Characteristics of
Polystyrene

122

Characteristics of
Polystyrene

124

Characteristics of
Polystyrene

127

Characteristics of
Polystyrene

130

Characteristics of
Polystyrene

133

Characteristics of
Polystyrene

137

Characteristics of
Polystyrene

140

Characteristics of
Polystyrene

141

Characteristics of
Polystyrene

145

Characteristics of
Polystyrene

146

List of Tables

Table	Title	Page
1	Critical Micelle Concentrations of Surface Active Agents in Water (25°C)	71
2	N.M.R. Analysis of Ethylene Oxide Content of Surfactants	73
3	Physical Characteristics of Polyvinyl-alcohol Fractions	78
4	Adsorption Characteristics of Nonylphenylethoxylates on Polystyrene Latex	108
5	Adsorption Characteristics of Nonylphenylethoxylates on Diloxanide Furoate B.P.	111
6	Molecular Areas of Pluronics at the Polystyrene Latex Solution Interface	118
7	Adsorption Characteristics of Pluronics on Diloxanide Furoate B.P.	120
8	Adsorption Characteristics of Polyvinylalcohols on Polystyrene Latex	125
9	Adsorption Characteristics of Polyvinylalcohols on Diloxanide Furoate B.P.	129
10	Molecular Dimensions of Polyvinyl-alcohols in Dilute Aqueous Solution	133
11	Contact Angle Measurements of Drug and Latex with Equilibrium Solutions	138
12	Adsorbed Layer Thickness of Surfactants by Microelectrophoretic Measurement on Latex	179
13	Adsorbed Layer Thickness of Surfactants by Microelectrophoretic Measurement on Diloxanide Furoate B.P.	182
14	Adsorbed Layer Thickness of Surfactants by Intensity Fluctuation Spectroscopy	183
15	Adsorbed Layer Thickness of PVA by Viscometry	185
16	Adsorbed Layer Thickness of PVA on drug from Equivalent Hydrodynamic Volumes	186

Table	Title	Page
17	Characteristics of Suspensions with Adsorbed Nonylphenylethoxylates after 3 Days Storage	200
18	Characteristics of Suspensions with Adsorbed Pluronic Layers after 3 Days Storage	210
19	Characteristics of Suspensions with Adsorbed PVA Layers After 3 Days Storage	212
20	Surface-Volume Mean Diameters of Suspensions After One Years Storage	221
21	Optical Dispersion Data of Materials	227
22	Restricted Primary Minimum Depth and Suspension Types	233
23	Concentrations of Polymer in the Adsorbed Phase	234
24	The Desorption of Polymers from the Drug Surface	274

	PVA Fractions	23
	Distributions of Latices	25
	...	21
	...	22
	...	23
	...	24
	...	25
	...	26
	...	27
	...	28
	...	29
	...	30
	...	31
	...	32
	...	33
	...	34
	...	35
	...	36
	...	37
	...	38
	...	39
	...	40
	...	41
	...	42
	...	43
	...	44
	...	45
	...	46
	...	47
	...	48
	...	49
	...	50
	...	51
	...	52
	...	53
	...	54
	...	55
	...	56
	...	57
	...	58
	...	59
	...	60
	...	61
	...	62
	...	63
	...	64
	...	65
	...	66
	...	67
	...	68
	...	69
	...	70
	...	71
	...	72
	...	73
	...	74
	...	75
	...	76
	...	77
	...	78
	...	79
	...	80
	...	81
	...	82
	...	83
	...	84
	...	85
	...	86
	...	87
	...	88
	...	89
	...	90
	...	91
	...	92
	...	93
	...	94
	...	95
	...	96
	...	97
	...	98
	...	99
	...	100

List of Figures

Figure	Title	Page
1	Potential Energy Diagram for Electrostatically Stabilized Particles	5
2	Effect of Electrolyte Concentration on Potential Energy Curves	6
3	Potential Energy Diagram for Sterically Stabilized Particles	8
4	The Configuration of Polymer Molecules Adsorbed at the Solid-Liquid Interface	10
5	Schematic Representation of Enthalpic Stabilization According to Hydration Theories	20
6	Schematic Representation of Entropic Stabilization	31
7	Definitions used in the Fischer Osmotic Model	33
8	The Free Energy of Interaction Between Flat Plates Covered with Polymer Loops or Tails	44
9	The Pluronic Grid	66
10	Huggins Plots for PVA Fractions	89
11	Particle Size Distributions of Latices	90
12	Conductometric Titration of Latex B	91
13	Conductometric Titration of Latex A	92
14	pH-Mobility Plot of Latex A	93
15	Effect of pH on Surface Group Dissociation	94
16	Diagram of the Helium-Air Pycnometer	95
17	Diagram of the Coulter Counter	95
18	Particle Size Distribution of Diloxanide Furoate B.P.	96
19	Penetration Volume-Pressure Curves for Diloxanide Furoate B.P. by Mercury Porosimetry	140
20	Pore Size Distribution by Mercury Porosimetry of Diloxanide Furoate B.P.	141
21	Pore Size Distribution of Diloxanide Furoate B.P. Batch 2616 by Nitrogen Adsorption	142

Figure	Title	Page
22	Adsorption Isotherms (25°C) of Nonylphenylethoxylates on Polystyrene Latex	143
23	Adsorption Isotherms (25°C) of NPE 13 on Latex in distilled water and at pH 2.3	144
24	Adsorption Isotherms (25°C) of Nonylphenylethoxylates on Diloxanide Furoate B.P.	145
25	The Dependence of Molecular Area of Nonylphenylethoxylates on the Number of Ethylene Oxide Units Per Molecule	146
26	Adsorption Isotherms (25°C) of Pluronics on Polystyrene Latex	147
27	Adsorption Isotherms (25°C) of Pluronics on Polystyrene Latex	148
28	The Dependence of Molecular Area of Pluronics on the Ethylene Oxide Content per Molecule	149
29	Adsorption Isotherms (25°C) of Pluronics on Diloxanide Furoate B.P.	150
30	Effect of Time on Surfactant Adsorption	151
31	Adsorption Isotherms (25°C) of PVA on Polystyrene Latex	152
32	Adsorption Isotherms (25°C) of PVA on Diloxanide Furoate B.P.	153
33	The Dependence of Saturation PVA Adsorption on Diloxanide Furoate B.P. on the Square Root of Molecular Weight	154
34	Stockmayer-Fixman Plot for the Polyvinylalcohol Fractions	155
35	Adsorption of Fractionated and Unfractionated PVA on Polystyrene Latex and Diloxanide Furoate B.P.	156
36	Adsorption Rate of Polyvinylalcohol onto Diloxanide Furoate B.P.	157
37	Schematic Representation of Adsorbed Polymer at a Charged Interface	170
38	Mobility-concentration Plot of Latex A in the Presence of Nonylphenylethoxylates	170
39	Mobility-concentration Plot of Latex A in the Presence of Pluronics	170

Figure	Title	Page
40	The Effect of Hydrophilic Chain Length on the Mobility of Latex A	190
41	Mobility-concentration Plot for Latex A in the Presence of PVA	191
42	pH - Mobility Plot of Diloxanide Furoate B.P. (Batch 224231)	192
43	Mobility - concentration Plot of Diloxanide Furoate B.P. in the presence of Nonylphenylethoxylates	193
44	Mobility - concentration Plot of Diloxanide Furoate B.P. in the presence of Pluronic	194
45	Mobility - concentration Plot for Diloxanide Furoate B.P. in the presence of Polyvinylalcohol	195
46	Graph of Relative Viscosity Against Particle Volume Fraction	196
47	Graph of Reciprocal Logarithm (relative viscosity) Against the Reciprocal of Particle Volume Fraction	197
48	Redispersibility Data for Drug Suspensions in the Presence of Nonylphenylethoxylates After 3 Days Storage	239
49	Redispersibility Data for Drug Suspensions in the Presence of Polyvinylalcohols After 3 Days Storage	240
50	Suspension Characteristics in the Presence of NPE 20 After 3 Days Storage	241
51	Suspension Characteristics in the Presence of PVA 34,500 After 3 Days	242
52	Schematic Representation of Partial Stabilization	243
53	Redispersibility Data for Drug Suspensions in the Presence of Nonylphenylethoxylates After 1 Year Storage	244
54	Redispersibility Data for Drug Suspensions in the Presence of Polyvinylalcohols After 1 Year Storage	245
55	Log τ' vs Log λ Plots for 0.716 Micron Diameter Latex for Two Particle Concentrations	246
56	n' vs Time Plots for Latex in the Presence of Adsorbed Pluronic	247

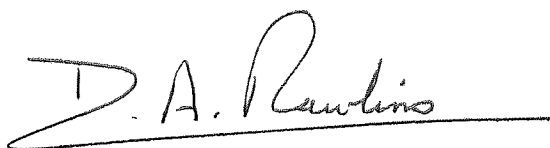
Figure	Title	Page
57	The Effect of Surfactant Concentration on Latex Stability	248
58	The Effect of Latex Concentration on Stability	249
59	Optical Dispersion Plots for Pluronics; at 25°C	250
60	Optical Dispersion Plots for Pluronics at 60°C	251
61	Optical Dispersion Data for Nonylphenyl-ethoxylates at 60°C	252
62	Optical Dispersion Plots for Diloxanide Furoate B.P. and Polyvinylalcohol	253
63	The Effect of Particle Core Hamaker Constant on the Primary Minimum	254
64	The Effect of Adsorbed Layer Hamaker Constant on the Primary Minimum	255
65	Potential Energy Disgrams for Semi-Infinite Flat Plates of Drug Coated With Adsorbed Nonylphenylethoxylates	256
66	Potential Energy Diagrams for Semi-Infinite Flat Plates of Drug Coated with Adsorbed Pluronics	257
67	Potential Energy Diagrams for Semi-Infinite Drug Plates of Drug Coated With Adsorbed Polyvinylalcohols	258
68	Variation of Restricted Primary Minimum Depth as a Function of Polyvinylalcohol Molecular Weight	259
69	Cloud Point Diagrams for some Surfactants	260
70	Potential Energy Diagrams for 0.716 μ Coated with Adsorbed Nonylphenylethoxylates	261
71	Potential Energy Diagrams for 0.716 μ Diameter Latex Coated with Adsorbed Pluronics	262
72	POTential Energy Curves for V_A , V_{RS} $V_{OSMOTIC}$ Calculated for an Exponential Segment Density Distribution for PVA 37,800	263
73	Potential Energy Diagrams for Semi-Infinite Flat Plates of Drug Coated with Adsorbed Polyvinylalcohols Using HVO Theory	264
74	Solubility of Diloxanide Furoate B.P. in Polyethylene Glycol Solutions	265
75	Solubility of Diloxanide Furoate B.P. in Polyvinylalcohol Solutions	266

Figure	Title	Page
76	Dissolution Curves of Diloxanide Furoate B.P.	285
77	Effect of Agitation on Drug Dissolution	286
78	Effect of Quantity of Drug on Dissolution Rate	287
79	Effect of Adsorbed Nonylphenylethoxylates on Dissolution Rates	288
80	Effect of Adsorbed Pluronics on Dissolution Rate	289
81	Effect of Adsorbed Polyvinylalcohols on Dissolution Rate	290
82	Effect of PVA Molecular Weight on Dissolution Rate at 200 r.p.m.	291
83	Relative Diffusion Rates of Molecules Through Polymer Solutions	292

Memorandum

This dissertation, which is being submitted for the degree of Doctor of Philosophy in the University of Aston in Birmingham, is an account of the work carried out under the supervision of Dr J.B. Kayes in the Department of Pharmacy the University of Aston in Birmingham from October 1976 to November 1979.

Except where acknowledged by references in the text, the work described herein is claimed to be original and has not been submitted for any other award.



David A. Rawlins

November 1979.

ACKNOWLEDGEMENTS

It is a particular pleasure to thank Dr J.B.Kayes for the guidance and encouragement given to me throughout the duration of this work.

I am indebted to Professors M.R.W. Brown and C.B. Ferry for the opportunity to conduct this research and for making available to me the facilities of the Department of Pharmacy.

Thanks are also due to Dr T.King of the Physics Department, Manchester University for making available the I.F.S. equipment and to the Boots Co. Ltd., Nottingham for the provision of measurement facilities and generous gifts of drug samples. I should also like to thank Dr B.Vincent (University of Bristol), Dr Th. Tadros (I.C.I. Plant Protection Division) and Professor I.W. Kellaway (UWIST) for their useful discussions.

Financial assistance is gratefully acknowledged from the West Midlands Regional Health Authority and from the Pharmaceutical Society of Great Britain for the provision of the Burroughs' Scholarship.

Finally, I wish to express my thanks to my wife for her help and encouragement during the preparation of this thesis.

SECTION 1

Introduction

In Memory of my Father

SECTION I

introduction

... dispersed phase is suspended.

... particles those

... then.

... particles

... rate

... of

... eq. bentonite, ...

... mechanically preventing

... is reduced by these methods

... is practical

... suspension

... time being

... this is ...

...

...

...

INTRODUCTION1:1 Suspensions

A suspension may be defined as a heterogeneous two phase system consisting of an external liquid or semi-solid phase in which the finely divided particulate matter or dispersed phase is suspended. In general, pharmaceutical suspensions contain particles whose dimensions are in excess of one micron and this distinguishes them, albeit arbitrarily, from true colloidal systems where the particles are relatively smaller with at least one dimension in the one nanometer to one micron range and where, in a stable system, Brownian motion usually maintains suspension of the particles. Sedimentation of larger particles may present a problem to the formulator. The rate of sedimentation may be retarded by increasing the bulk viscosity of the system through the addition of gums and high molecular weight polymers or by introducing structure builders eg. bentonite, which trap the particles in their mesh-like structure, mechanically preventing sedimentation. Although sedimentation rate is reduced by these methods complete suspension of the particles cannot be achieved in practical terms and the formulator is faced with the task of producing a suspension in which the sediment is easily redispersable and at the same time being aesthetically acceptable to the patient. As discussed later this is not always a simple objective to achieve. In addition to these two requirements a suspension must remain uniformly dispersed for a sufficient length of time to allow removal and administration of the correct dose of drug after shaking.

Two types of suspension may be prepared namely aqueous or non-aqueous depending on the nature of the external phase. In the pharmaceutical field the vast majority of suspensions are aqueous in nature as they are intended for oral administration. Non-aqueous suspensions are used

principally for the intra-muscular injection route.

A review of the number of mixtures prepared as suspensions listed in past and present official compendia indicates an increasing use of this formulation as a dosage form. For example the B.P.C. 1954 (1) lists eighteen different suspensions compared with thirty two preparations in the present edition (2). The number of suspensions produced by the pharmaceutical industry exceeds one hundred and twenty (3) and this figure does not include injections, the insulins and antibiotic syrup formulations which may, when reconstituted, form suspensions. This increase in use may be attributed to the advantages which these formulations possess. The high surface area of powder exposed to the gastric fluids on ingestion provides high availability of the poorly soluble drug for absorption. For those suspensions used in cases of gastro-intestinal upset, adsorption of toxins onto the powder is increased by the high surface area exposed. The comparative ease of masking the unpleasant taste of many insoluble drugs by the addition of suitable flavours to the external phase demonstrates a further application of suspension formulation. This is seen for example with the antibiotic 'syrups', many of which are formulated for children. Products formulated in this manner may not possess the unwanted local side effects that are observed with other formulations. For example it has been observed (4) that a suspension of aspirin does not cause mucosal ulceration in contrast with the same drug formulated as a tablet. Other preparations prepared as suspensions include dermatological applications, shampoos, parenteral injections and eye drops.

In the veterinary field many suspensions are produced by the addition of water to dry granules of drug. For pest control, pesticides are formulated as concentrated dispersions which must be diluted on site to produce a homogeneous suspension capable of being sprayed through

orifices without blockage. In this case a readily dispersible concentrate is required which will produce individual particles on dilution.

Other areas where suspensions are utilized include mining engineering, printing and paint technology although in the last two cases non-aqueous dispersions are often prepared.

Stability of dispersions in the pharmaceutical sense differs from the true colloidal meaning of the word. Where particles are very small and Brownian motion maintains uniform dispersion, it is only necessary to prevent aggregation by means of a suitable repulsive force between particles. In coarse suspensions, particles in this deflocculated state will be able to roll over each other on sedimentation and produce a very compact non-redispersible sediment. It is therefore necessary for particles to undergo limited aggregation before complete sedimentation occurs in order to produce a high sedimentation volume product.

In this work it is the aggregation phenomenon between particles which will be discussed. Rheological properties of suspensions are not investigated.

Martin et al (5) have listed the desirable properties of pharmaceutical suspensions and it was with these in mind that the present work was undertaken:

- a) ease of redispersability of the suspension on storage
- b) appearance of the suspension
- c) suitable flow properties of the final product

1:2 Historical review of suspension formulation

It was only during the 1960's that the scientific principles of

colloid chemistry were applied to pharmaceutical systems. Up to this time, formulation appears to have been rather empirical in nature. The vast majority of work on pharmaceutical suspensions is concerned with the electrical stabilization of such systems and this is a consequence of work carried out in the Netherlands and Russia on colloidal systems by Deryaguin and Landau (6) and Verweey and Overbeek (7). Their combined theory - the so called DLVO theory - has been used with refinements to predict colloidal behaviour and to explain aggregation of particles in electrically stabilized dispersions. On the other hand stabilization produced by the adsorption of polymers onto the particle surfaces has not been extensively investigated in the area of pharmaceutical suspensions. It is only recently that theories describing this 'steric stabilization' have been introduced and these may be used only with certain restrictions (see Section 2).

In order to control the forces acting between particles it is necessary to understand them. The following section describes in general terms the understanding of such forces and the use to which this has been put by workers in the pharmaceutical field.

The basic premise of the DLVO theory is that the attractive and repulsive forces operating between particles can be considered to be additive. Thus for the long range attractive van der Waals potential V_A , and the potential energy of repulsion due to electrostatic means V_R , the total energy of interaction V , may be given by:

$$V = V_A + V_R$$

Graphically this can be represented by Figure 1 where these values are plotted as a function of the distance between two similar particles, H .

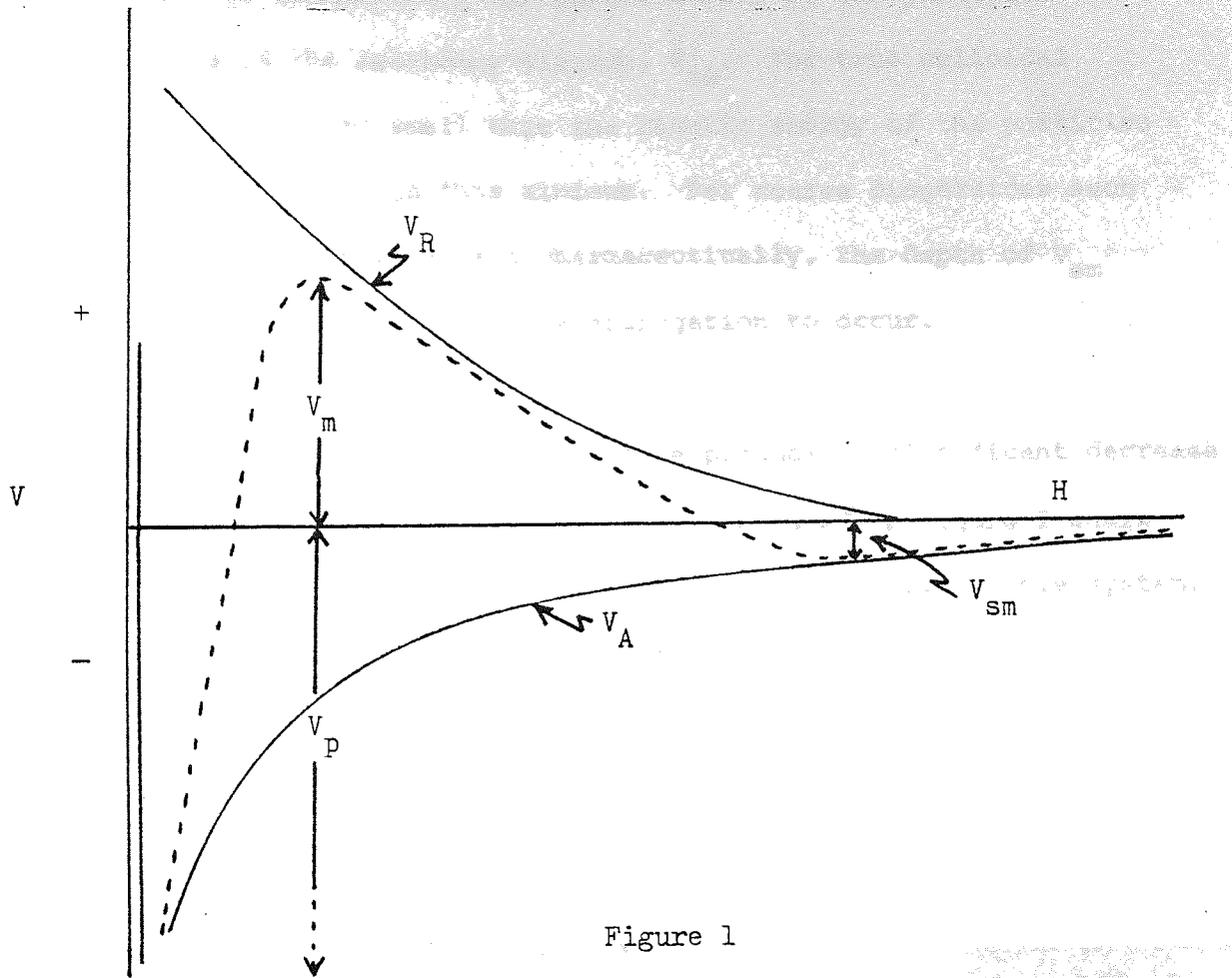


Figure 1

At very short distances of separation the attraction between particles becomes enormous and will overcome all repulsive potentials producing a deep minimum in the curve termed the primary minimum, V_p . The depth of V_p is limited by the strong close range Born repulsion due to overlap of electron clouds on the molecules of the attracting surfaces. At larger separations V_R may become dominant resulting in the primary maximum V_m . The position and height of this maximum are determined by the ionic strength of the bulk solution and by the surface potential of the particles themselves. V_A is unaffected by these parameters and therefore they can be used to restrict the height of V_m . At further separations V_R decays more rapidly than V_A and a small minimum may be

observed which is dependent on the particle size of the particles involved. This is the secondary minimum, V_{sm} . For true colloidal particles V_{sm} will be so small that the kinetic energy of the particles will prevent association in this minimum. For coarse dispersions such as emulsions and suspensions used pharmaceutically, the depth of V_{sm} may become large enough for particle aggregation to occur.

Addition of non-adsorbing electrolyte produces a significant decrease in colloid stability and this is clearly demonstrated in Figure 2 where increasing amounts of electrolyte are added to a previously stable system.

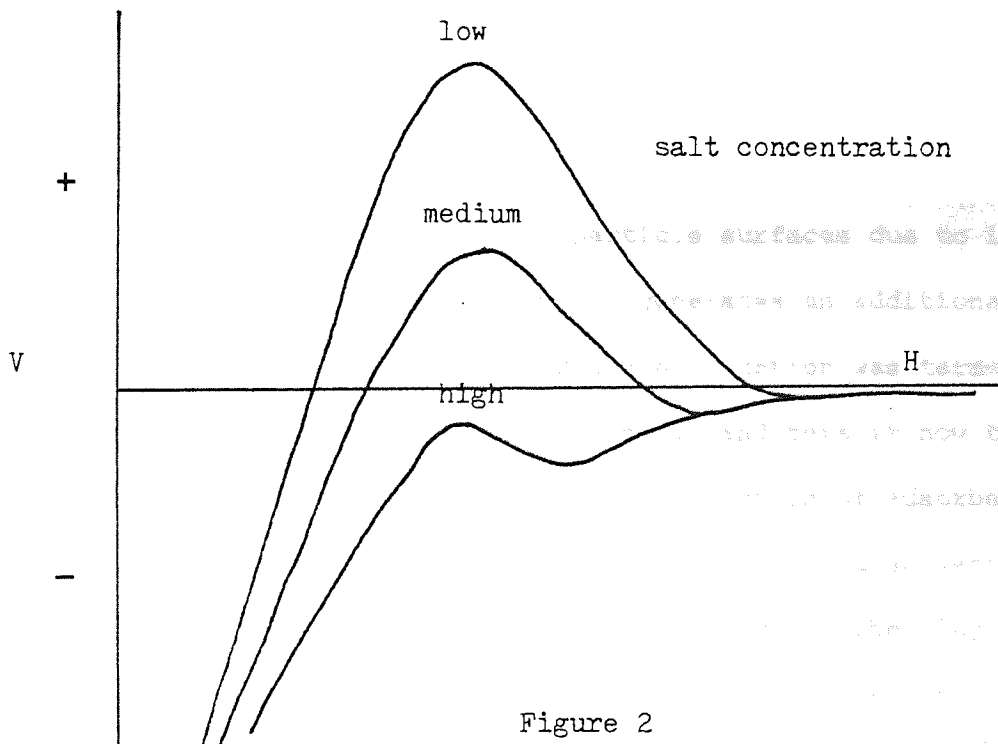


Figure 2

With low ionic strengths and high surface potentials the primary maximum is maximal and aggregation of particles in the primary minimum is prevented by this repulsive barrier. The secondary minimum will not be deep enough to cause aggregation as the kinetic energy of the particles will overcome the attractive forces. Under these conditions a stable colloidal system will result. On the addition of further

quantities of electrolyte the repulsive barrier V_R is reduced. This causes a reduction in V_m and a deepening in the secondary minimum V_{sm} . When sufficient salt is added V_{sm} will become deep enough for attraction to occur and a loosely aggregated system will form. Further electrolyte addition suppresses the repulsive barrier to such an extent that these barriers become ineffective stabilizers and association in the primary minimum will occur. The adhesive forces existing deep in the primary minimum are complex and are not obtained simply by extrapolating the attractive and repulsive forces to separational distances of interatomic dimensions. For example Israelachvilli (8) has discussed that changes in pH may affect the Born repulsion to such an extent that no deep primary minimum is observed. No experimental evidence is available to confirm this point.

The addition of a polymer to a dispersion will result in the adsorption of some material onto the particle surfaces due to interfacial or specific mechanisms. This adsorption generates an additional repulsive force on overlap of these layers. Such stabilization was termed 'steric stabilization' by Heller and Pugh (9) and this is now the accepted generic name used to describe the stabilizing action of adsorbed layers of nonionic polymers and surface active agents. In a good solvent environment for the polymer the repulsion between overlapping adsorbed layers increases rapidly with interpenetration providing a very strong repulsive force. This is shown graphically in Figure 3.

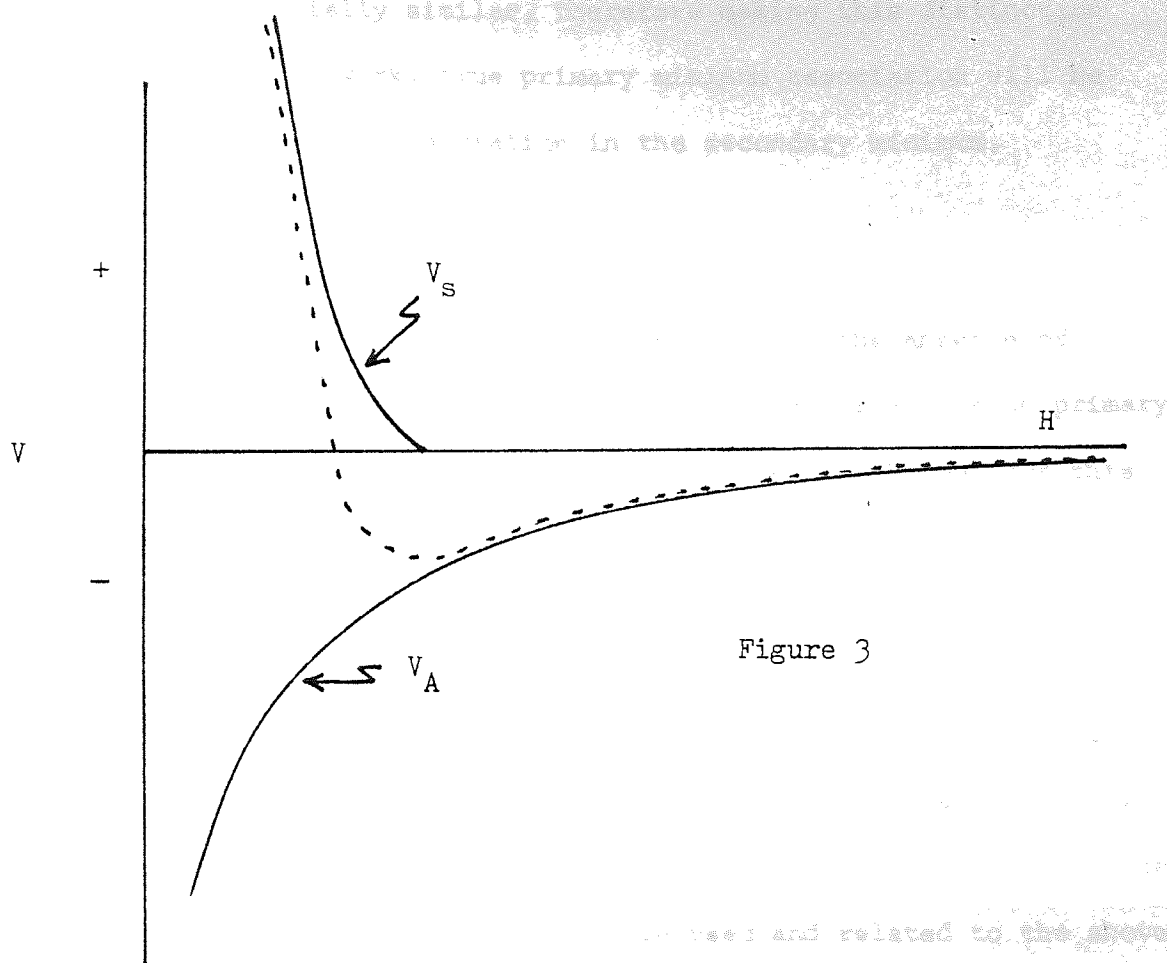


Figure 3

The depth of the attractive potential in this case is controlled by the thickness of the adsorbed layer δ , the strength of the barrier described by the slope of the ascending repulsive V_S curve and V_A . Summation of these terms yields the total interactive potential energy,

$$V = V_S + V_A$$

The terms used to describe the aggregation of particles on the reduction of repulsive forces are somewhat misleading. The terms 'coagulation' and 'flocculation' have been used in recent literature to describe the aggregation phenomenon. However in many cases no distinction is made between primary and secondary minimum aggregation. Perhaps one

explanation of this is that the aggregates produced in both cases will appear essentially similar, therefore making this distinction uncertain. In this work, true primary minimum association will be termed coagulation and association in the secondary minimum, flocculation (10).

Where steric stabilization is considered in the absence of electrostatic potentials these terms become less certain as no primary maximum will exist as a reference point (Figure 3). Throughout this work aggregation produced in this manner will be called restricted coagulation.

In the pharmaceutical literature up to the early part of this decade, the words coagulation and flocculation are used synonymously, and this makes comparison between results difficult. In this work the following suspension characteristics are used and related to the above terminology as follows:-

- a) Deflocculation - repulsive potentials between particles are high and attractive forces are insufficient to cause aggregation. The particles will settle as discrete entities and on sedimentation, repulsion will cause the particles to roll over each other establishing a dense, hard, low volume sediment. Smaller particles will be able to enter the voids created by larger, irregularly shaped crystals thereby enhancing the compact nature of such a system.
- b) Flocculation - this term covers two aspects of aggregation, namely secondary minimum association and aggregation induced by the bridging of polymers or metal ion - polyelectrolyte. Healy and La Mer (11) have described a simple mechanism to account for polymer bridging. In their explanation, the polymer adsorbs onto the surface to partially cover the particles. This sterically stabilizes this region of the surface from aggregation with similar regions on

neighbouring particles. Polymer molecules then produce flocculation by adsorbing simultaneously onto two particles. The bridging mechanism does not occur between all particles due to the partially covered areas on the surfaces. This reduces the particle-particle contacts producing the high sedimentation volume observed experimentally. Although some workers do not agree with this mechanism (12) polymer bridging is now widely accepted as the explanation for flocculation at low polymer concentrations. Both mechanisms result in the formation of loose aggregates or 'flocs' which sediment rapidly producing an open textured sediment with a high sedimentation volume.

- c) Coagulation - the repulsive forces between particles are so low that the long range van der Waals forces predominate and aggregation occurs in the primary minimum. The rate of aggregation will be fast if a deep minimum exists and this combined with strong interparticulate forces on contact produces a high sedimentation volume. Several authors have stated that coagulation of particles produces a caked suspension (13,14). This general conclusion may be disputed and as an example the area of clay colloid science may be cited. Being mineral materials clays are virtually insoluble in water and aggregation is not complicated by Ostwald ripening which is discussed below. Results with sodium montmorillonite (15) show that at high sodium chloride concentrations the sediment is voluminous. Coagulation must therefore occur in the absence of any steric stabilization, but this dispersion is easily redispersible. On these grounds it may be expected that Kaolin and Morphine Mixture B.P.C. should be coagulated as the ionic strength of sodium bicarbonate present is high (0.6M) and no added stabilizing polymers are present. Certain clays however are associated with appreciable quantities of organic material in the form of ill-defined lignites or humus (16). Such species are known to impart a deflocculating effect (17) presumably by steric stabilization. This suspension sediments slowly, indicative of a deflocculated state

although redispersion is easily obtained. This may be explained by restricted coagulation.

Hiestand has remarked that flocs produced by the addition of electrolyte would be expected to produce coarse compact masses with a curdled appearance. The appearance of the sediment is determined by the floc size which in turn is determined by the kinetics of aggregation (18). Bagchi (19) has developed a theoretical approach to show that the rate of aggregation is a function of the depth of the minimum in the potential energy curve. The curdled appearance observed with such systems may be due to too high a collision rate between particles. Contrary to Hiestand's results, Matthews and Rhodes (20) have shown that both the flocculation and coagulation mechanisms may be used to produce suspensions which do not cake and that for particles in the range 0.5 - 20 microns, coagulation may produce suspensions that are pharmaceutically more elegant than those produced by flocculation.

Where a drug powder is soluble to a limited extent in the external phase a thin layer of supersaturated solution will exist between crystal faces such as those found in coagulated systems. Solubility increases with decreasing particle size (21) and the large crystals will grow at the expense of the smaller ones. This phenomenon, Ostwald ripening (22), causes an overall coarsening of the sediment and crystal bridges between particles may occur. Kolthoff (23) drew attention to this effect and considered that over a long period of time crystal bridging may result in the complete unification of the particles. When this occurs the sediment is no longer easily redispersible and this may explain the caking observed by the above authors when coagulation is evident.

The use of 'controlled flocculation' in pharmaceutical suspension formulation has been widely accepted as the fundamental approach to producing

elegant, redispersible suspensions. This approach, first proposed by Haines and Martin (24 a,b,c) considers that the interparticulate forces may be controlled by addition of electrolyte or polymer to the dispersion with the effect that the suspension characteristics may be altered. However - Kayes (25) has pointed out that this term describes several aspects of aggregation which may lead to confusion.

These are:-

- a) secondary minimum flocculation
- b) flocculation produced by bridging of polymers or metal ion - polyelectrolyte complexes
- c) primary minimum coagulation

In the second of their papers (24b) Haines and Martin demonstrated the relationship between the zeta potential (an index of surface charge) and sedimentation volume of sulphamerazine and bismuth subnitrate dispersions produced by the addition of electrolyte. At very low or very high electrolyte concentrations a high zeta potential was observed with a corresponding low sedimentation volume. At intermediate concentrations the zeta potential was low producing a non-caked 'flocculated' sediment. They interpreted these results as showing that a large electrostatic repulsion signified by the high zeta potential gave rise to a deflocculated system with a compact sediment. The reverse situation also applies.

This work is often quoted without reference to the criticisms levelled at it by Ecanow and co-workers (26,27). Repetition of the work of Haines and Martin by these authors revealed a precipitation reaction occurring between the electrolyte used to promote flocculation and the surface active agent used as a wetting agent and they attributed the aggregation observed to this reaction. They also doubted whether the measured zeta potentials in the original work were valid as flocculation

was said to have occurred spontaneously. This, they claim, prevented measurement of true zeta potentials although no basis for this reasoning exists. The third criticism referred to the attractive forces between macroscopic particles. They stated that the presence of long range van der Waals forces, sufficient for aggregation to occur with coarse particles, had not been clearly demonstrated experimentally and they thought attraction would only occur where particles were finely subdivided ($<2\mu$). However the existence of secondary minimum flocculation has been demonstrated experimentally with 10μ latex particles (28) and direct measurements of the forces of attraction between molecularly smooth sheets of mica at relatively large surface separations (29 a,b,c) confirm the presence of such forces. It can be shown from theory (Section 2) that in its simplest form the potential energy of attraction between two spheres is proportional to the radius of the interacting particles. Therefore larger particles will be more liable to aggregate than small particles in the presence of the same repulsive barrier.

Using wetting agents and electrolyte solutions which do not interact, Matthews and Rhodes (30) have shown that a reduction in zeta potential does lead to a high sedimentation volume and that the 'flocculation' is dependent on the particle size of the powders under study. Using sulphaguanidine powder wetted with polysorbate 80, a nonionic surface active agent, Jones et al (31) have shown an increased sedimentation volume on the addition of non interacting electrolyte. These results differ completely from those of Ecanow and Takruri (32) who found that addition of the same electrolyte to a suspension of the same drug prepared in an identical manner to that of Jones et al produced no increase in sedimentation volume. However comparisons are difficult as in the case of reference 32 no details of particle size are mentioned. This is important for two main reasons. a) the particle size has a great effect on the attractive forces between particles (see above) b) the surface area of drug powder controls

the extent of adsorption of wetting agent from the solution onto the powder surface. With smaller particles there will be a larger surface area per unit weight of powder to cover and adsorption will occur to a lesser extent than on the larger particles. Depending on the interactions involved, the steric stabilizing effect of the adsorbed polymer on the smaller particles will therefore be less and aggregation will be more likely to occur.

Extending their work to cover 'flocculation' with hydrocortisone, coarse and fine griseofulvin and sulphamerazine, Matthews and Rhodes (33) have shown that the DLVO theory of colloidal particles may be extended to use in systems of coarse dispersions. They correlated the observed physical stability of the suspensions to the type of dispersion predicted on theoretical grounds. Generally the agreement was good, but a number of assumptions had to be made with regard to the attractive and repulsive potentials involved. These authors have given guidelines for the formulation of suspensions using the controlled 'flocculation' technique. Their work is further supported by that of Short and Rhodes (34) who investigated the stability of steroidal suspensions. Bondi et al (14) have investigated to a limited extent the effect of an adsorbed anionic surface active agent on suspension stability. They have shown that the amount of surfactant adsorbed at the interface can dramatically affect the stability in the presence of added electrolyte. Further support for the controlled aggregation approach is forwarded by Kayes (25) who studied the effect of anionic, cationic and nonionic surfactants on the stability of four drug suspensions - betamethasone, thiabendazole, griseofulvin and naladixic acid. Agreement was found between the type of sediment formed and that predicted by DLVO theory and confirms the conclusion of Matthews and Rhodes (33) that a theoretical treatment of interparticulate forces can be applied to coarse systems. Otsuka (35) studied the effects of nonionic surfactants on suspension

stability and related the adsorption isotherms of the surfactant to the sedimentation volume.

Examples of recent work performed with polymer adsorption in the area of pharmaceutical suspensions include Caramella (36) who examined the effects of wetting agents on suspension characteristics; Felmeister et al (37) who studied polymer bridging; Najib et al (38) who investigated the adsorption of polyvinylpyrrolidone (PVP) and sodium carboxymethylcellulose onto a polystyrene latex, and Otsuka and Kakuichi (39) who studied flocculation-deflocculation behaviour of chloramphenicol with PVP-sodium dodecyl sulphate complexes.

Farley and Lund (40) have defined criteria necessary in the preparation of extemporaneously prepared suspensions and have evaluated the use of several polymeric materials as alternatives to tragacanth for use as suspending agents. The polymer concentrations used were relatively high (0.4 - 5%) and no mechanism of suspension stability was proposed. It must be recognised however that in addition to producing a high viscosity external phase, polymer adsorption will occur at the particle interface. As a result of this a steric stabilizing effect will operate.

1:3 Aims of the present work

It has been shown in the above references that suspension stability may be controlled through the addition of electrolyte solution. This approach suffers from one major disadvantage. The addition of ionic excipients to the formulation such as flavours, colourings, preservatives and changes of pH may well affect the final product. Possible leaching of ionic species from glass containers may give a similar effect. Stabilization of particles through the adsorption of polymers avoids this problem as the steric effect is independent of added electrolyte

and very high ionic strengths are usually required to affect the solution properties of nonionic polymers.

Use of sterically stabilized latex

In this work, the adsorption of two groups of nonionic surface active agents and one series of a long chain polymer are studied. The type of sediment observed is related to potential energy diagrams obtained from modern theories of particle interactions. In all the above references where polymer adsorption was utilized, no attempt has been made to suppress the electrostatic repulsion between the particles. This prevents a true assessment of the stabilizing capabilities of the polymer alone. The conditions used in this report are such that electrostatic repulsion can be considered negligible. The observed effects on stability are therefore due to the adsorption of polymers.

Comparisons are made between adsorption on a polystyrene latex dispersion and that of a drug material. With regard to stability, latex systems have been shown to be good models for coarse suspensions (30). In addition to particle size measurement, the surface characteristics of latices may easily be determined experimentally and the factors permit a more accurate interpretation adsorption data.

Dissolution data of sterically stabilized pharmaceutical suspensions is scant and there is a greater need to understand the role that adsorbed polymers may play. Seager (41) has shown that the inclusion of methylcellulose as a suspending agent to a nitrofurantoin dispersion retarded the adsorption of the drug from the gastro-intestinal tract. Although this may be due to several effects such as a) a viscosity increase of bulk solution in the presence of polymer, b) modification of gastric emptying rates, c) possible complex formation between drug and polymer, the in vitro dissolution was not determined and reduced

absorption may have been due to the presence of an adsorbed layer surrounding the particles. Part of this work describes in vitro determinations of dissolution rates of sterically stabilized drug dispersions.

SECTION 2

SECTION 2

theory, a knowledge of

theory

the definition of surface

the definition of

SECTION 2

Theory2:1 Adsorption

Before consideration can be given to the interaction between particles which are covered with an adsorbed layer, a knowledge of the mechanism of the adsorption of polymers is required. Several theories have been proposed to account for the observed adsorption and these will be discussed. In general these theories relate to long chain flexible macromolecules composed of polymer segments. Each segment has the potential to adsorb at the interface. It may be seen that this definition excludes surface active agents as this type of molecule has relatively short chains and includes at least two different types of segment, one of which will normally be preferentially adsorbed to the others. The discussion is therefore limited to macromolecular adsorption although the adsorption of surface active agents may follow these equations in special cases.

The driving force of adsorption is the change in the free energy of the system which is made up of the changes in enthalpy and entropy of surface, solvent and polymer. During deposition of the polymer the total free energy must be a negative value, otherwise adsorption will not occur. Generally, in the adsorption of a polymer from solution onto a non-porous solid the relationship between the maximum amount adsorbed A_s , and the molecular weight M of the polymer may be written as :

$$A_s = k M^a \quad (2.1) \text{ where } k \text{ and } a \text{ are constants}$$

for the given system.

This was first appreciated by Perkel and Ullman (42) who interpreted the configuration of the polymer in terms of the constant a . In ideal

conditions where $a = 0$, the molecule is tightly adsorbed onto the surface through all segments. Where $a = 1$ the plateau adsorption is proportional to molecular weight. The polymer is attached to the surface by very few segments with the remainder extending into solution. For $0 < a < 1$ polymer adsorption occurs through several segments along the polymer chain and other segments extend away from the surface in the form of 'loops' and 'trains'. This is shown diagrammatically in Figure 4.

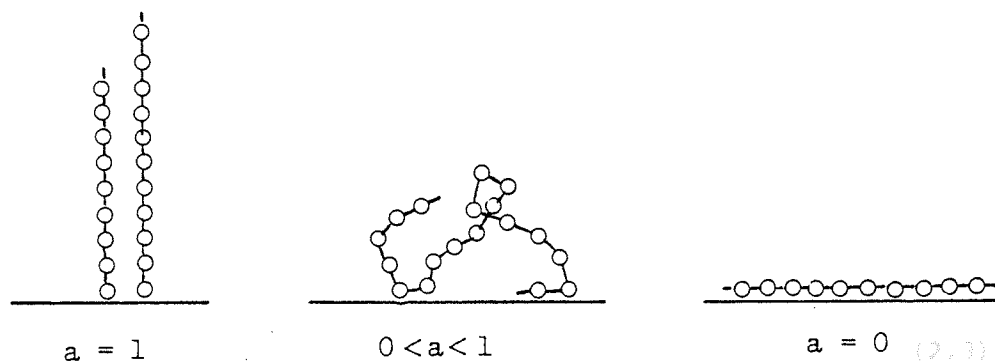


Figure 4

It was first recognised by Jenckel and Rumbach (43) that adsorption of polymers could not be accounted for by the usual processes of monolayer formation as this would lead to an adsorbed layer of more than ten molecules thick if adsorption occurred via all the polymer segments. They proposed that only a few segments were adsorbed with the remainder projecting out into the solvent in the form of loops.

The first quantitative approach to polymer adsorption was that by Frisch, Simha and Eirich (F.S.E.) who used the model of Jenckel and Rumbach as the basis of their analysis (44). The polymers were assumed to have Gaussian distribution of end to end distances and the change in this distribution upon adsorption was determined. The model also

assumed that there would be random placing of segments upon the surface and that adsorption occurred from dilute solution with no interaction between polymer chains at the interface. The probability, p , averaged over t segments that an arbitrary segment is adsorbed is

$$p = 2\alpha/(\pi ft)^{1/2} - O(1/t) \quad (2.2)$$

where α is the probability that a segment is adsorbed upon contact and where f accounts for the bond angle between successive chain segments as well as for the flexibility of the chain. For large values of t , the coefficient of the second term on the right hand side of the equation becomes zero but for small values of t , where flexibility is restricted, it takes on a finite value. In the limiting case of p becoming zero, the following adsorption isotherm is obtained:

$$\frac{\theta}{1-\theta} \exp(2K_1\theta) = (Kc)^{1/\langle v \rangle} \quad (2.3)$$

where θ is the fraction of the surface covered, c is the polymer concentration in bulk solution and K_1 , K are constants. $\langle v \rangle$ is the average number of segments adsorbed per chain. This equation requires a steep rise in the isotherm at low concentrations after which the dependence of θ on c becomes less. Competitive solvent adsorption is not allowed for in this equation, but inclusion of such an effect does not alter the equation significantly. For single point attachment, $\langle v \rangle = 1$ and K_1 tends to zero. Under these conditions the equation reverts to the Langmuir isotherm for monolayer formation. The equation shows a dependence of $\langle v \rangle$ on $t^{1/2}$ and also predicts that the average loop size increases with molecular weight of polymer. In poor solvents, the flexibility of the chain, which is related to f , will be low and therefore $\langle v \rangle$ will be small. The effect of solvent on the polymeric chain during adsorption is also accounted for by an interaction constant K_2 . In a

poor solvent K_2 is higher than in a good solvent and this causes the constant K in equation 2.3 to increase. The quality of the solvent therefore affects the adsorption through $\langle v \rangle$ and K , and as a result of this, greater adsorption is predicted in poor solvents.

Higuchi (45) has developed equations relating the fraction of segments adsorbed to the surface interaction parameter K_2 , where

$$K_2 = \alpha \exp(\epsilon/kT) (1-\theta) \quad (2.4)$$

where ϵ represents the surface segment interaction energy. This predicts that small changes in ϵ will produce large changes in the number of segment contacts. Small values of ϵ give few attachment points per chain, whereas a value of $4kT$ for ϵ would give a polymer with practically all segments in surface contact. Lal and Stepto (46) have characterized the configuration behaviour of macromolecules adsorbed at an interface in terms of the adsorption energy $\Delta\epsilon$. This they define as the energy change on breaking a segment-solvent bond and forming a segment-surface bond. In agreement with the earlier predictions of Higuchi they demonstrate that for $\Delta\epsilon = -0.9kT$ the chains strongly adsorb and are extended on the surface. For $\Delta\epsilon = -0.5kT$ adsorption only just occurs with the thickness being determined by the length of the tails.

Forsman and Hughes used a statistical mechanical approach (47) to relate the adsorption process to the change in free energy that occurs as a polymer molecule approaches the surface. For extremely dilute solutions with low surface coverages and slight polymer-surface interactions, θ increases with the square root of molecular weight. They conclude that the driving force for adsorption is the polymer-surface interaction energy which is counteracted by the loss of polymer configurational entropy opposing adsorption. In the plateau region of the

isotherm molecular weight dependence is predicted to be small. Increasing temperatures cause increasing adsorption as the polymer will be more extended at the surface with fewer surface contacts thereby requiring more polymer to occupy the available surface sites.

The F.S.E. approach has been criticised by Silberberg (48a,b) on the grounds that i) the conformation of the polymer on adsorption was not considered to be a variable in the treatment of the thermodynamic equilibrium between the surface and the solution and ii) the shape of the molecule was determined incorrectly. He developed a theory based on the partitioning of segments between the surface and the bulk solution. Segments in contact with the surface were described by an internal partition function determined by the surface attraction forces. Those segments arranged in loops were considered identical with those in solution. Several conclusions may be drawn from this treatment i) For polymer molecules of sufficiently large size, the composition and structure of the surface phase is independent of the molecular weight. Thus the size of loops and trains does not depend on the degree of polymerization but only on the nature of the polymer involved. This contrasts with the F.S.E. theory where large loops are predicted proportional to the square root of molecular weight. ii) Segment concentration at the interface is high and the molecule is held in a compact series of loops even if the segment-surface interaction is low. iii) The exact state of the adsorbed polymer is a function of interactions between segments, solvent and the surface.

Although these predictions are substantiated by much of the experimental evidence (see(48b)), there are many reports which are not consistent with the above results.

Hoeve et al (49) thought the uniform size loops and uniform size

trains used by Silberberg far too restrictive and developed a theory based on Gaussian statistics for loops. In the case of an isolated flexible molecule they predict very large loops for small adsorption energies. Smaller loops are found with a large fraction of segments adsorbed as the energy increases. This contrasts with the work of Silberberg. Using a different approach, the work of Roe (50) gave similar results.

Extending his work, Silberberg (51a,b) considered adsorption accounting for polymer concentration, solvent interactions and self-exclusion effects. He concluded that with high degrees of adsorption, there were fewer surface-segment contacts and larger loops than previously predicted. Under the special conditions of theta-solvency the adsorbed layer thickness was predicted to be proportional to the square root of molecular weight.

In dealing with a long polymer chain permanently attached at one end Rubin (52) has found that a molecule can adsorb in three ways depending on the energy change per segment on adsorption $\Delta\epsilon$. If $\Delta\epsilon$ is more negative than a critical value, $\Delta\epsilon_c$, the number of segments in contact with the surface is proportional to the molecular weight. In this case such a molecule would stay in contact with the surface even if it was not terminally anchored. If $\Delta\epsilon$ is more positive than $\Delta\epsilon_c$, the number of additional contacts with the surface is of the order of one, and desorption is likely to occur. When $\Delta\epsilon = \Delta\epsilon_c$ the number of contact points becomes proportional to the square root of molecular weight.

Clark et al (53) also considered interaction energies between segments, solvents and surfaces and interpreted the conformation of the molecule in terms of these interactions. In the presence of a good solvent there is a strong tendency for the formation of a long 'train'

in that part of the chain close to a terminally anchored point. A high proportion of the unadsorbed segments exist in tail configurations. Bad solvent environments decrease the likelihood of the initial train, and in most situations a loop-train configuration occurs with a small or non-existent tail. It is unfortunate that in this study and most of the other studies mentioned above concerned with adsorbed polymer configuration, consideration is given only to the case of a single, isolated, adsorbed molecule. This corresponds to a situation of very low adsorption approaching zero coverage. Experimental measurements of adsorption and adsorbed layer thickness are more difficult to obtain in this region and application to higher surface coverages where lateral interactions occur must be considered doubtful.

Hoeve (54) introduced a model in which the flexibility of the chain is accounted for. Agreement was found between this model and his previous model, and in addition he found that the volume fraction of segments in the diffuse layer containing loops did not exceed 0.1 even when the surface was completely saturated with polymer segments.

Hoffman and Forsman (55) extended their earlier theory to allow for segment density distributions in the adsorbed phase. They applied the Flory-Huggins theory to give the free energy of mixing solvent and segments and allowed for configurational entropy changes on adsorption. They point out that for a sparsely covered surface where intermolecular interaction is negligible the equilibrium solution concentrations are below those that can be measured experimentally. This shows the limited applicability of theories that assume no lateral interactions between adsorbed molecules.

In order to allow calculation of the steric repulsion between

particles covered with a high molecular weight polymer, the segment density distribution of the polymer $\rho_{(H)}$, must be derived. Such a distribution for a single loop has been given by Hesselink (56) in terms of the number of segments per loop i , and the length of a segment l , at a distance H from the surface

$$\rho_{(i,H)} = 12H(i l^2)^{-1} \exp(-6H^2/i l^2) \quad (2.5)$$

Combination of this equation with the loop size distribution of an adsorbed polymer derived by Hoeve et al (49,57) yields the segment density distribution $\rho_{(H)}$ for an adsorbed homopolymer (88,89).

$$\rho_{(H)} = 2a\sqrt{6} (\bar{i}l)^{-1} \exp(-2aH\sqrt{6}/\bar{i}l) \quad (2.6)$$

where $\bar{i}l$ is the average loop size and a is a numerical constant ~ 0.7 . Segment density distribution have been derived in the case where an impenetrable surface is brought into close proximity with the adsorbed polymer. The exponential decrease of $\rho_{(H)}$ with distance from the surface is a characteristic of high polymer adsorption and emerges from most treatments of the problem (49,50,52).

The general picture that emerges from the theories outlined above can be summarized as follows:

- 1) At low equilibrium concentrations the amount adsorbed, Γ , rises steeply until lateral interactions between neighbouring molecules occur when adsorption tends to plateau values.
- 2) Plateau values increase with increase in molecular weight, M , with the possible exception of very large values of M where Γ_{\max} is independent of M .
- 3) Adsorbance is greater from poor solvents than from good in any given system. The effect of temperature is in general not very great and

increases or decreases in adsorption may be observed on raising the temperature.

- 4) The loop size distribution is high and the average loop size is affected by conditions of solvency, flexibility and adsorption energies.
- 5) The segment density distribution in the outer layers decays exponentially away from the surface.
- 6) Although the fraction of segments adsorbed is usually small, desorption is unlikely to occur as all segment-surface interactions must be simultaneously broken.

With surface active agents the above treatments cannot be used; however, it is often found that adsorption follows the Langmuir isotherm (e.g. 82), which is indicative of monolayer formation. Adsorption may occur via the hydrophobic or hydrophilic regions of the molecules depending on the polymer-substrate-solution interactions. This is discussed in Section 4.

2:2 Solvent Conditions

Before discussing theories of steric stabilization, it is pertinent to discuss conditions of solvency which affect a polymer in solution, and hence its stabilizing effectiveness. For a high molecular weight polymer chain in a good solvent environment, the segments of which the chain is composed, are subject to two opposing factors which govern the spatial configuration of the molecule in solution. These may be termed short range interactions due to local interactions between atoms and groups which are near neighbours in the sequence along the polymer chain, and long range interactions due to pairs of segments remote in the chain sequence, but near to each other during interactions (58). A configurational parameter $\langle h^2 \rangle$ or mean square end-end distance of the molecule may be defined as that distance which would be obtained in the absence of perturbations caused by the long range effects. In

non-ideal solutions the experimentally determined root mean square end-end distance $\langle h^2 \rangle^{1/2}$ is related to $\langle h^2 \rangle_0$ by

$$\langle h^2 \rangle = \alpha^2 \langle h^2 \rangle_0 \quad (2.7)$$

where α is the linear expansion coefficient attributable to the long range or excluded volume effect. α depends markedly on the solvent and also on temperature. In circumstances where the macromolecule is unperturbed due to excluded volume effects being absent the solvency conditions are termed 'ideal' and the polymer is said to be under Theta (θ) conditions (59).

There is an exact analogy for this with the Boyle point of a real gas. At the Boyle Temperature gas molecules behave ideally as the repulsion between a pair of molecules is exactly compensated by their mutual attraction. The Theta point can be defined as that temperature at which deviations from the Van't Hoff osmotic pressure law do not occur, and at which the second virial coefficient (B) becomes zero. Under these conditions, α becomes equal to unity. Comparisons of polymer coil dimensions are normally made in θ -solvents, so that solvent effects may be neglected. Under these conditions the excess free energy of mixing ΔF_m , of polymer and solvent is zero.

$$\Delta F_m = a \left(\frac{\theta}{T} \right) - 1 \quad (2.8)$$

Napper (60) has demonstrated that for polyethylene oxide, the θ temperature is independent of the molecular weight of the polymer.

2:3 Steric Stabilization

As colloidal particles covered with an adsorbed polymer layer often exhibit stability in the absence of an electrostatic repulsion,

the polymer layers must provide an additional stabilizing force. In discussing the total changes in free energy, ΔG_s , as two such particles approach each other, Ottewill (61) considered the most likely contributions to ΔG_s to be the change in surface free energy on close approach, the excess chemical potential caused by the overlapping of layers and an elastic contribution arising from compression of the layers.

$$\Delta G_s = \Delta G_{\text{surface}} + \Delta G_{\text{osmotic}} + \Delta G_{\text{elastic}}$$

According to the second law of thermodynamics if ΔG_s is suitably positive, a net repulsion will occur. Napper and Hunter (62) have demonstrated three different mechanisms by which a positive value of ΔG_s may be obtained from its constituent enthalpy (ΔH) and entropy (ΔS) changes on close approach of the particles.

1) enthalpic stabilization : both ΔH and ΔS are positive but $\Delta H > T\Delta S$. The net enthalpy change opposing flocculation outweighs the net effect of the increase in entropy which promotes flocculation. Such stabilization is normally characterized by 'flocculation' on heating as $T\Delta S$ usually increases more rapidly than ΔH .

A possible origin of the enthalpic mechanism may be due to the hydration of polymers in aqueous solution. If two particles coated with adsorbed layers approach each other there is an increased probability of polymer - polymer contacts in the interaction zone. As a result of this, some of the previously associated molecules are excluded from the overlap region and these molecules have greater degrees of freedom than those in the polymer associated state (Figure 5).

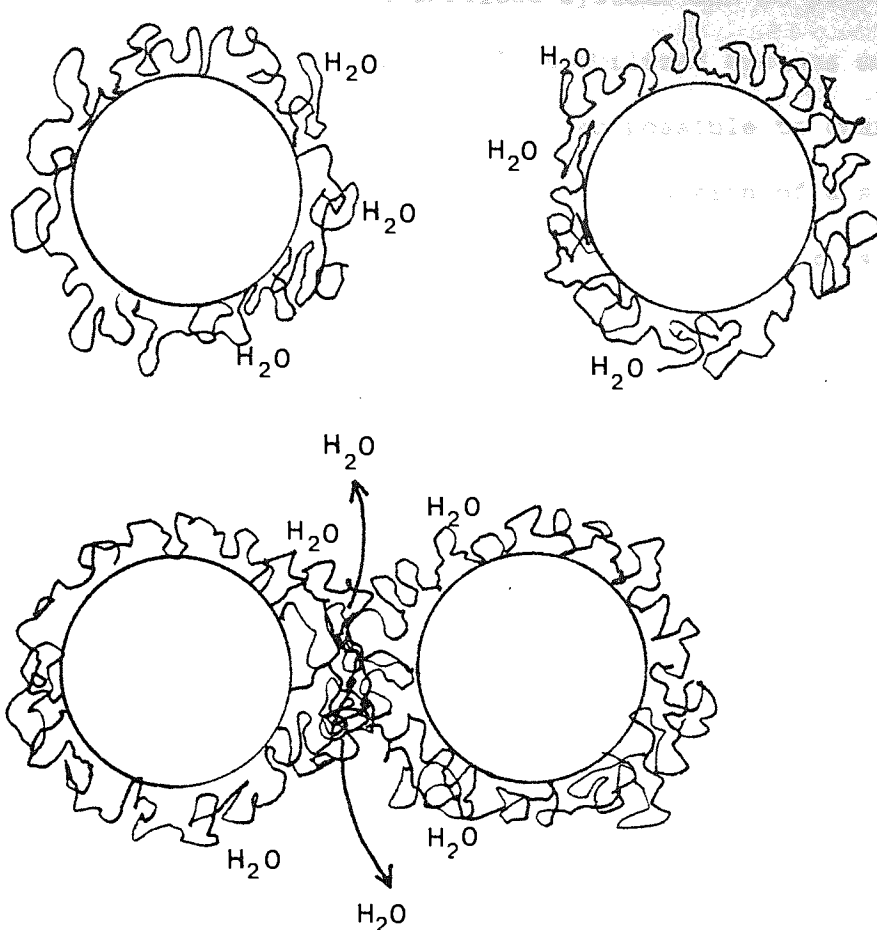


Figure 5 Schematic Representation of Enthalpic Stabilization
According to Hydration Theories.

The energy requirement necessary to provide this greater freedom provides the positive enthalpy of interpenetration capable of imparting stability. There is much evidence to show that nonionic surfactants of the ethylene oxide type are highly hydrated in aqueous solution (63-66) although this may be partly due to water being trapped in the interstices of the ethylene oxide chains (63). Corkill et al (67) have experimentally shown large heats of solution for ethylene oxide chains in aqueous solution and these results led Ottewill (68) to conclude that the enthalpic mechanism is more important in aqueous systems and the entropic contribution more important in the

stabilization of non-aqueous systems. However Napper et al (69) have shown that entropically stabilized systems can be prepared in aqueous dispersion and that enthalpically stabilized systems may be prepared in non-aqueous media (70). It is also possible to change from enthalpic to entropic stabilization on addition of a suitable solvent (71). The understanding of the enthalpic mechanism is therefore far from certain. Napper has suggested (72) that a more rigorous analytical approach to steric stabilization should include the free volume effects of mixing polymer and solvent. This involves assessing the changes in volume of polymer and solvent on mixing to which enthalpic and entropic parameters may be ascribed. Flory and co-workers (73) have used this approach in the dissolution of polymer in solvent and although this has not yet been attempted with regard to the stabilization of particles by an adsorbed layer it is clear that the same principles may be applied when these layers overlap and 'mixing' of polymer segments occurs.

- 2) entropic stabilization: ΔH and ΔS are both negative, but $T|\Delta S| > |\Delta H|$. The effect of the entropy change opposes flocculation and outweighs the enthalpy term. In principle, entropically stabilized dispersions are characterized by 'flocculation' on cooling.
- 3) combined enthalpic - entropic stabilization: ΔH is positive and ΔS is negative. Napper (71) considered that this type of stabilization occurred on changing from an enthalpic to an entropic mechanism. Dispersions stabilized in this way cannot in principle be 'flocculated' at any temperature.

The simple temperature change method of distinguishing between the three types of mechanism is not unambiguous as both ΔS and ΔH may themselves be temperature dependent. In addition, some dispersions 'flocculate' both on cooling and heating and those that are combined enthalpic - entropically stabilized may not flocculate at all. Modern

theories of polymer solutions imply that any polymeric stabilizer should be capable of both enthalpic and entropic stabilization in any dispersion medium if a wide enough temperature-pressure range can be scanned (74). The term steric stabilization covers these three types of stability produced by adsorbed polymers and the use of 'entropic stabilization' to refer to polymer stabilization as a whole is incorrect (75).

2:3:1 Entropy Theories

The first quantitative assessment of the forces generated on overlap of two adsorbed layers was that due to Mackor (76). He attempted to explain the results of van der Waerden (77) on the stabilization of carbon black in non-aqueous solvents produced by adsorbed alkyl benzenes. The model invoked was that of a rigid rod-like molecule freely jointed at one end to an impenetrable flat surface (Figure 6).

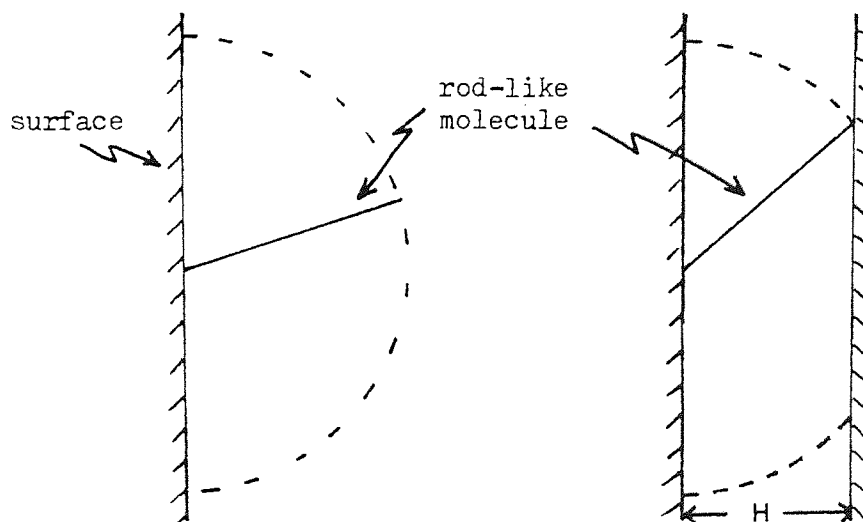


Figure 6 Schematic Representation of Entropic Stabilization

The molecule was free to move within a hemisphere described by the rod about its point of attachment to the surface, and the number of possible configurations available to the molecule was assumed proportional to the surface area of the hemisphere swept out by the end of the rod. On approach of a second flat surface to a distance of less than the length of the rod, the number of configurations possible was reduced resulting in a decrease in entropy of the rod. The second law of thermodynamics predicts an increase in the free energy of the system as a consequence of decreased entropy (enthalpic contributions being assumed constant), and repulsion between the particles will occur.

Using the same approach, Clayfield and Lumb (78,a,b,c) have performed elaborate computer-aided calculations to determine the reduction in configurational entropy, ΔS . They extended Mackors original work to the case of terminally anchored flexible chains of up to 100 segments. This involved determining the number of statistically possible configurations of a polymer-in-a-box as two sides of the box approached each other. Bond angles were restricted to 90° , and the excluded volume effect of the segments was considered by excluding occupied sites. These authors derived equations for spheres and a sphere and plate. Increasing the flexibility of the chain was shown to increase the repulsion. In the situation where more than one segment may be adsorbed the repulsion is greater than for a terminally anchored chain of the same root mean square thickness.

This approach to quantifying steric repulsion assumes that the quality of the solvent does not have any effect on the effectiveness of the steric barrier. It is only the macromolecules themselves that contribute towards ΔS and hence ΔG . There is however a wealth of evidence to show that the solvency of the dispersion medium can influence the repulsion between particles (79,80). Effects of

enthalpy changes are also ignored in these calculations, although as discussed above, enthalpically stabilized dispersions do exist.

Fischer (81) was the first to point out that the solvent could have a critical effect on the steric stabilization of dispersed particles. He proposed that on overlap of adsorbed layers, the chemical potential of solvent in the interaction zone would decrease and a chemical potential gradient would be set up between those solvent molecules in the overlap region and those in the bulk medium. To counteract this effect, solvent molecules would flow into the interaction zone from the bulk and in so doing, force the particles apart. This is equivalent to the generation of an excess osmotic pressure. The case of two spherical particles was considered, having identical adsorbed layers of polymer molecules colliding under the action of Brownian movement in a common solvent (Figure 7). When the particles are far apart, the solution is ideal, but on overlap the solution deviates from ideality and a change in the solvent chemical potential occurs.

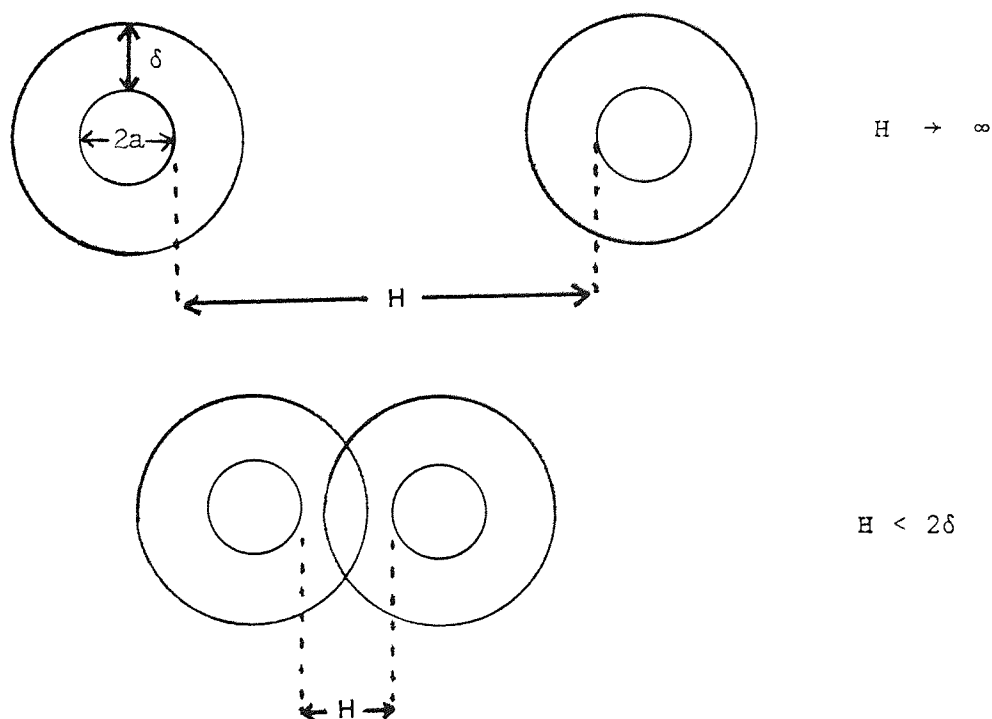


Figure 7

$$\Delta\mu = \Delta\mu_H - \Delta\mu_\infty$$

$$\text{and } \Delta\mu = -\pi_E \bar{V}_1 \quad (2.9)$$

where π_E is the excess osmotic pressure generated in the overlap volume δV , and \bar{V}_1 is the partial molar volume of the solvent. π is related to the second virial coefficient, B , and the mean segment concentration, c , in the adsorbed layer by

$$\pi = RTBc^2 \quad (2.10)$$

$$\text{giving } \Delta G_{\text{osmotic}} = 2 \int_0^{\delta V} RTBc^2 dV = 2RTBc^2 \delta V$$

The volume of a segment of a sphere was then substituted for δV giving

$$\Delta G_{\text{osmotic}} = \frac{4BN_A c^2 \pi kT}{3} \left(\frac{\delta - H}{2} \right)^2 \left(3a + 2\frac{\delta + H}{2} \right) \quad (2.11)$$

Since B is related to the polymer solvent interaction, the role of the solvent is implicitly included in this theory. In good solvent B is positive and hence ΔG_s is positive which gives rise to a repulsion between adsorbed layers. In the special case of theta solvents $B = 0$ and flocculation is predicted.

Ottewill and Walker (82) extended this theory so that readily obtainable parameters could be used to define the repulsive potential. The second virial coefficient is related to the polymer solvent interaction parameter χ by

$$B = \frac{RT (\psi_1 - \chi)}{V_1 \rho_2^2} \quad (2.12)$$

where V_1 is the solvent molecular volume and ρ_2 the density of the

polymer. ψ_1 is an entropy parameter which is given the ideal value of 0.5. For spherical particles such as those described above, the following expression was obtained:

$$\Delta G_s = \frac{4kT\pi c^2}{3V_1\rho_2^2} (0.5-\chi) \left(\frac{\delta-H}{2}\right)^2 \left(\frac{3a+2\delta+H}{2}\right) \quad (2.13)$$

Doroszkowski and Lambourne (83) have pointed out that the above model does not take into account the situation where $H < \delta$. In these circumstances the overlap volume is decreased, as part of the interaction zone is occupied by the solid particle core. These workers allowed for this effect and showed that ΔG_s increases more rapidly on overlap than is predicted by equation 2.13.

The equation of Fischer and its subsequent refinements suffers from several shortcomings. The use of a mean segment concentration in the adsorbed layer is an obvious approximation and it has been shown in the previous section (2:1) that the segment density is a function of the distance normal to the particle surface. These theories do not take into account compression of the polymer chains on overlap, as only interpenetration of the chains is considered. Thirdly, these theories disregard all virial coefficients higher than the second. This is an acceptable approximation in good solvents, but as χ approaches a value of 0.5 this approximation may become less reliable.

Bagchi has derived analytical expressions in terms of his denting model (84). This model assumes that when the stabilizing chains come into contact they are compressed as if they had come into contact with an impenetrable surface. Such a model may be satisfactory for short chain surfactants at high surface coverage, but this is unlikely to apply to high molecular weight adsorbed polymers where the outer regions

are relatively diffuse. However, Bagchi does claim good agreement between his model and experimental stability data of Fleer et al (85) who used a silver iodide-polyvinyl alcohol system.

2:3:3 Entropy Plus Enthalpy Theories

Meier evaluated the segment density distribution at planar interfaces for linear chains terminally adsorbed at one end and combined the entropy approach of Mackor with Fischers solvency theory to produce a generalized theory of steric stabilization. The specific case of an adsorbed 'tail' was considered using random flight statistics with appropriate boundary conditions. The volume restriction term, ΔG_{VR} , was calculated by determining the probability, $P_N(H)$, that all chain segments lie within a distance H of the surface where H is the particle surface separation. The equation derived was (86),

$$\Delta G_{VR} = -2\eta kT \ln P_N(H)$$

where $P_N(H)$ is given by

$$P_N(H) = \sum_{m=-\infty}^{\infty} \left[\exp(-6m^2 H^2 / Nl^2) - \exp(-3(2m-1)^2 H^2 / 2Nl^2) \right] \quad (2.14)$$

η is the number of molecules adsorbed per unit area, $(Nl^2)^{1/2}$ is the root mean square end to end distance of the polymer chain in free solution.

The osmotic (mixing) term, $\Delta G_{osmotic}$, was obtained by application of the Flory-Krigbaum theory (87) to calculate the free energy change of mixing on overlap of adsorbed layers. In this model low surface coverage is implied in order that lateral overlap of polymer molecules may be neglected.

$$\Delta G_{\text{osmotic}}^{(H)} = 6(2\pi)^{1/2}(\alpha^2 - 1)kT\eta \left[B_{jj}^{(H)} + \eta \zeta^2 B_{jk}^{(H)} - B_{ii}(\infty) \right] \quad (2.15)$$

where α is the chain expansion factor, ζ accounts for the probability of polymer chains not opposing each other on approaching particles and B_{jj} , B_{jk} and B_{ii} are complex statistical functions of chain dimensions.

Meier showed that the osmotic effect contributes substantially to the stabilization particularly at high surface coverages. This is because V_{RS} increases linearly with the amount of polymer adsorbed whereas V_{osmot} increases quadratically, this being due to overlap of two polymeric clouds.

Meier's results are however in error because he allowed polymer segments to penetrate the impenetrable particle surfaces, thereby underestimating the value of ΔG_{osmot} . Hesselink and co-workers (88,89) have corrected this mistake and also extended Meier's work to the cases of adsorbed loops, homopolymers and copolymers. When macromolecules adsorb at an interface, the overlaps will form loops of a certain size distribution. For an adsorbed homopolymer this is given by

$$n_i = n a \pi^{-1/2} (\bar{l})^{-1} i^{-3/2} \exp(-i a^2 / (\bar{l})^2) \quad (2.16)$$

where n_i is the number of loops of i segments per unit area, \bar{l} the average number of segments per loop, n the total number of segments in loops per unit area and a is a numerical constant ≈ 0.7 . This equation only applies if the majority of segments are in loops and end effects due to tails can be considered negligible. For a copolymer where attachment to the surface is through anchor segments randomly distributed along the polymer chain, the equivalent expression is

$$n_i = n (\bar{l})^{-2} \exp(-i/\bar{l}) \quad (2.17)$$

The relative loss of configurations, $(R_{(i,H)})$ for a single loop on approach of a second surface is given by:

$$R_{(i,H)} = \sum_{m=-\infty}^{\infty} (1 - 12m^2 H^2 / i l^2) \exp(-6m^2 H^2 / i l^2) \quad (2.18)$$

The resulting rise in free energy ΔG_{VR} per unit area due to volume restriction is:

$$\Delta G_{VR} = -2kT \sum_i n_i \ln R_{(i,H)} \quad (2.19)$$

Substitution of equation 2.18 into equation 2.19 and integrating yields

$$\Delta G_{VR} = 2vkTV_{(i,H)} \quad (2.20)$$

where v is the number of loops or tails per unit area.

For the case of equal loops and $H/\sqrt{i l^2} \gg 1$ a good approximation for $V_{(i,H)}$ is given by

$$V_{(i,H)} = -2(1 - 12H^2 / i l^2) \exp(-6H^2 / i l^2) \quad (2.21)$$

The osmotic contribution towards ΔG_s was originally given by Meier

$$\Delta G_{\text{osmotic}} = 2(2\pi/9)^{3/2} (\alpha^2 - 1) kTv^2 \langle h^2 \rangle M_{(i,H)} \quad (2.22)$$

where $\langle h^2 \rangle^{1/2}$ is the r.m.s. end to end distance of the chain, and

$M_{(i,H)}$ as formulated by Hesselink et al for a homopolymer is

$$M_{(i,H)} = 2a(6/i)^{1/2} p [1 - 2bHp - p^2]^{-2} [3bH - 7 + p(1 + 10bH - 2b^2 H^2) + p^2(7 - bH) - p^3] \quad (2.23)$$

where $p = \exp(-bH)$ and $b = 2a\sqrt{6}/il$

With equal loops and $H/\sqrt{i l^2} \gg 1$ equation 2.23 reduces to

$$M(i,H) = (3\pi)^{\frac{1}{2}} (6H^2/(il^2) - 1) \exp(-3H^2/il^2) \quad (2.24)$$

These results show that under identical conditions a cover of equal tails is more effective in preventing 'flocculation' than a cover of loops distributed as in a copolymer, and also more effective than a cover of equal loops. An important point to note is that because of the exponential segment density distribution given by Meier and Hesselink, repulsion is predicted to occur at all separations from the surface to infinity. This obviously cannot be so as adsorbed layers will be of finite thickness. Vincent (90) has attempted to correct for this by providing a quadratic equation which describes the exponential form to within a few percent but which gives a segment density distribution of zero when the distance from the surface is equal to the contour length of the adsorbed polymer. This equation applies only to homopolymers.

Criticism of the analytical theories of Hesselink, Vrij and Overbeek (HVO) have been given by Evans and Napper (80,91). In their experimental observations, these authors have shown that under the special conditions of theta solvents, where $\chi = 0.5$ or $\alpha = 1$, physical instability of sterically stabilized dispersions results. They argue that according to the HVO theory, this incipient flocculation will not be predicted as a volume restriction potential ΔG_{VR} is present which does not vanish under these conditions. They postulate that all theories advanced to predict steric stabilization with the exception of Fischers solvency theory, are in conflict with experimental evidence. It is suggested that the volume restriction term V_{RS} is implicitly allowed for in the derivation of the osmotic term $V_{osmotic}$ and that V_{RS} is therefore superfluous. These authors also give equations using a segment density distribution model applicable to spherical particles.

The explanation why flocculation occurs at the theta point as determined by Napper was considered by Osmond et al (92). To determine the theta temperature experimentally Napper used a technique which involves extrapolating a plot of reciprocal phase separation temperature against polymer concentration to a point corresponding to pure polymer. This point gives the theta temperature. In the pure polymer, translational configurational entropy will approach zero and only the internal configurational entropy remains. This situation is also the case for an irreversibly adsorbed polymer and correlation between theta temperatures measured in this way and incipient flocculation caused by phase separation of the adsorbed layers is not unexpected. Osmond et al reconcile the differences in interpretation of flocculation between Evans and Napper and Hesselink et al on the grounds that they are comparing different modes of flocculation. The latter authors are considering flocculation due to the attractive forces outweighing the steric effect, whereas the former are concerned with a phase separation type flocculation.

In reply to the criticism of Napper outlined above, Hesselink (93) has shown that Napper's contention is based on a comparison of experimental evidence and theoretical predictions that are calculated for different experimental conditions. These authors compared Hesselink's theory of low surface coverage with their own results, where maximum surface coverage was used. At low coverage V_{RS} is dominant and some repulsion may be observed in solvents of poor quality (i.e. $\chi \approx 0.5$). At high surface coverage $V_{osmotic}$ dominates over the volume restriction term and results of flocculation observed under such conditions are explicable solely on the basis of the osmotic term as was found by Evans and Napper.

Doroszkowski and Lambourne (94) have found that on compressing

small particles covered with an adsorbed polymer using a surface balance technique, a small repulsion was observed when worse-than-theta-conditions were studied. They attribute this repulsion to the loss of configurational entropy of the polymer chains on close approach of the particles as the osmotic repulsion is theoretically very small or zero in such solvents. This would therefore support the claims of Hesselink that a configurational volume restriction term must be included in the equations describing steric stabilization. However, it is perhaps confusing that in the same paper (94) these authors conclude that expressions of V_g , the potential energy of repulsion due to the adsorbed layer, best fitted their experimental data in better-than-theta-conditions when the volume restriction term was omitted. This is probably due to the fact that in such solvents the osmotic term is dominant and that volume restriction is relatively unimportant as suggested by Hesselink (93).

Extending their earlier theories, Smitham, Evans and Napper have proposed a model in which lateral interactions between adjacent polymer chains on the same particle are taken into account (95). They adopt two segment density models and show that a combined constant segment density plus symmetrical gaussian model gives the best agreement with the results of Doroszkowski and Lambourne (94). It is also concluded that interpenetration of chains is far more likely to occur than the 'denting' mechanism proposed by Bagchi.

The statistical calculations of Dolan and Edwards (96) make allowance not only for the restriction of configurational freedom caused by the second particle but also for excluded volume effects due to the polymer segments. The entropic and enthalpic interactions between solvated segments are taken into account which makes analysis of an

osmotic term superfluous. The results of Dolan and Edwards agree closely with the HVO theory for large overlaps although for large surface separations, Dolan and Edwards find higher repulsions.

Under certain conditions dispersions may be prepared which are stable in solvent conditions markedly worse than θ solvents i.e. $\chi > 0.5$. Dobbie et al (97) have prepared a polystyrene latex stabilized with various molecular weight polyethylene oxides in aqueous dispersion and subjected it to increasing temperatures, thereby increasing the polymer-solvent interaction parameter χ . The majority of dispersions were stable under worse than θ conditions. This stability was attributed to the multipoint anchoring of the polymer along the latex surface which causes perturbations in the conformation of the macromolecules. This renders the free solution properties of the molecules (under which θ conditions are determined) no longer relevant.

2:3:4 Elastic Theories

The least developed aspect of steric stabilization is the contribution first proposed by Jäckel (98) and subsequently modified by Evans et al (99) for the elasticity on compression of the adsorbed layers. The latter authors have quantified this contribution in terms of a compression ratio. Comparison between this theory and the results of Doroszkowski and Lambourne (94) show good agreement at large distances of separation, but on close approach the theory predicts much stronger interactions than were observed experimentally.

The disagreements between the above authors on formulating a suitable analytical solution to steric stabilization outline the difficulties which the problem presents. Despite this, the main factors

governing the extent of steric stabilization can be summarized:

- a) molecular weight of stabilizer
- b) flexibility of the molecule
- c) solvent quality
- d) amount of polymer adsorbed
- e) adsorption energy
- f) dimensions of the polymer at the interface governed by factors (a-c)
- g) attractive potentials between particles V_A

The relative effect of tails and loops on the depth of the interaction minimum can be seen from the example given by Hesselink (88) in Figure 8. He calculates for a polymer of molecular weight 6000, $\alpha = 1.2$, and amount of polymer adsorbed $2 \times 10^{-8} \text{ g cm}^{-2}$, the repulsion obtained between two flat plates. The attractive potential is given by the simple Hamaker equation:

$$V_A = \frac{-A}{12\pi H^2} \quad \text{where } A = 10^{-13} \text{ ergs} \quad (2.25)$$

Curve (a) shows the interaction for equal loops; curves (b) and (c) indicate the volume restriction and osmotic repulsions respectively for a cover of equal tails, which comprise the total interaction curve (f) for this case. This illustrates that the depth of the minimum is dependent on the mode of adsorption and on the relative magnitudes of V_A and ΔG_s , although in this case the magnitude of A would appear to be an order of magnitude too high.

2:4 Electrical Stabilization

Most solids, when brought into contact with a polar medium such as water, acquire a surface charge through one of the mechanisms listed below.

$10^{-3} \text{ erg cm}^{-2}$

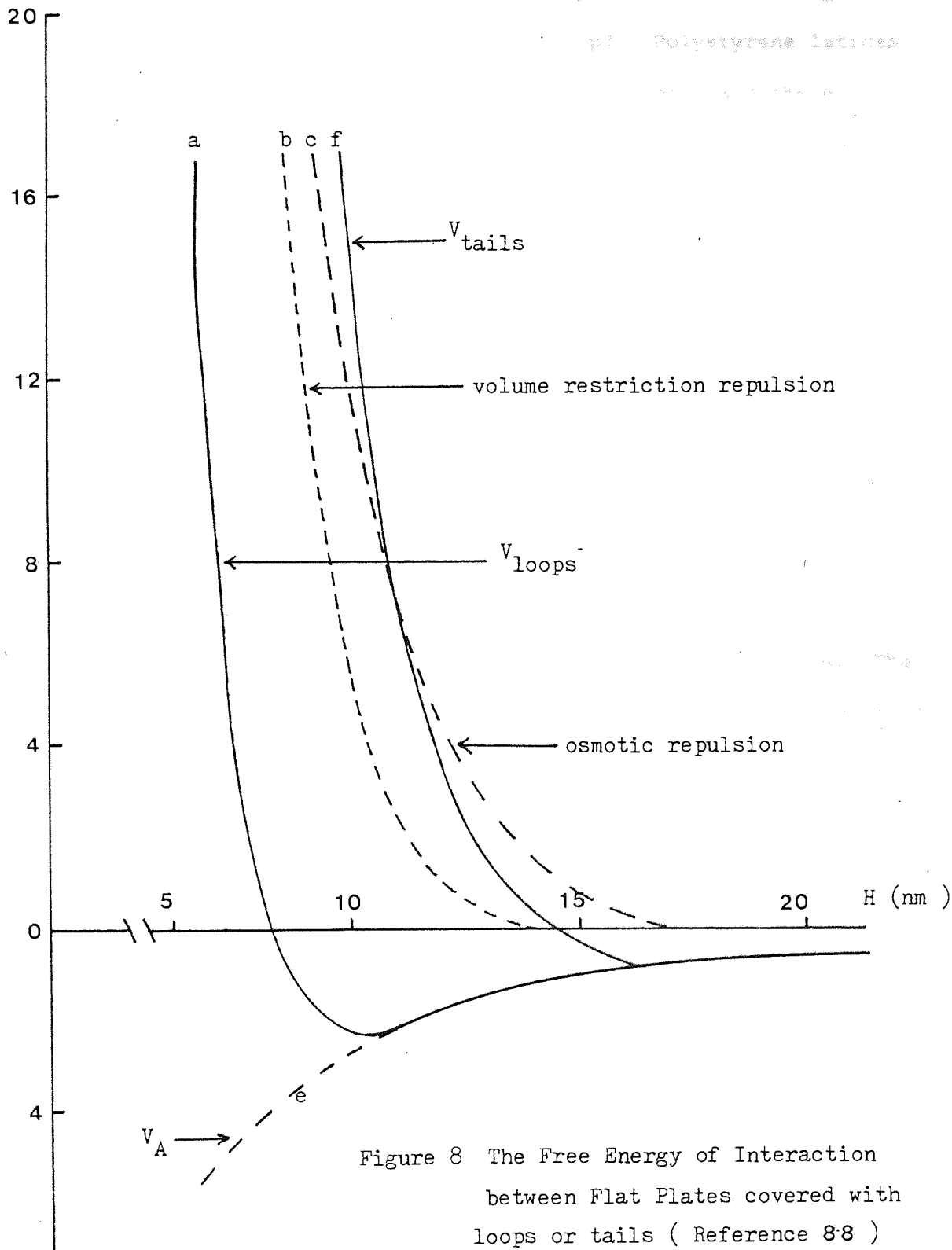


Figure 8 The Free Energy of Interaction between Flat Plates covered with loops or tails (Reference 8:8)

ionization: This is produced by surface groupings which are an integral part of the surface and which may ionize completely under suitable conditions of pH. Examples are proteins which carry both positive or negative charges depending on pH. Polystyrene latices have been widely used as model systems for colloids and these usually carry negative carboxylic acid and/or sulphate surface groupings.

ion adsorption: Surfaces may acquire charge by adsorption of ions of one sign in preference to those of the opposite sign. Haydon has argued (100) that the principal reason why negative zeta-potentials are found on many substances is due to the fact that the hydrated cations cannot approach the surface as closely as the anions and that true adsorption of negative ions need not be assumed in order to explain the negative zeta-potentials observed. Where ionization of the surface occurs via mechanism (1) it is possible that counter ions of high charge number may adsorb causing a reversal of charge. The adsorption of ionic surface active agents will normally determine the surface charge.

ion-dissolution: Ionic substances, such as $AgCl$, may acquire surface charge through unequal dissolution of oppositely charged ions from the crystal lattice.

Isomorphic Substitution: This results from the replacement of one type of ion by another of the same sign in the crystal lattice. Examples of this are found in clays where for example a tetravalent silicon atom is replaced by a trivalent aluminium atom in the structure of the montmorillonite group. This replacement leaves a net negative surface charge.

The surface charge influences the distribution of ions in the surrounding medium. Ions of opposite charge (counter ions) are attracted towards the surface. This produces a localized high concentration of

these ions near the surface causing partial diffusion of counter ions away from the interface. In addition to repulsion of ions of like charge (co-ions) thermal mixing of all these ions leads to the formation of an electric double layer. This consists of the electrically charged surface around which is distributed in a diffuse manner a neutralizing excess of counter ions.

2:4:1 The Diffuse Double Layer

A theory for the diffuse region of the double layer for plane surface was developed by Gouy (101) and Chapman (102). The conditions for the Gouy-Chapman model are that the concentration of ions in the dispersion medium must be low in order that interactions between ions may be neglected and that these ions are treated as point charges. The surface charge is distributed evenly over the solid surface and the medium is treated as a continuum, influencing the double layer only through its permittivity ϵ . The interaction of ions with the surface is subject to their random thermal motions and the distribution of ions will be determined by the Boltzmann law :

$$n_i' = n_o \exp(-z_i' e \psi / kT) \quad (2.26)$$

where n_o is the bulk concentration of the ions and n_i' is the concentration of ions of one particular type, i , at a point where the potential is ψ . z represents the ion valency and e the charge on the electron.

The net volume charge density p at a point where the potential is ψ is:

$$p = e \sum z_i n_i \quad (2.27)$$

and this may be combined with equation 2.26 to give for a 1:1 electrolyte:

$$p = -2ze n_0 \sinh (ze\psi/kT) \quad (2.28)$$

p is related to ψ through the Poisson equation which for a flat double layer is of the form

$$\frac{d^2\psi}{dH^2} = \frac{-p}{\epsilon} \quad (2.29)$$

Combining equations 2.28 and 2.29 and integrating twice yields

$$\psi = \frac{2kT}{ze} \ln \left(\frac{1+\gamma \exp(-\kappa H)}{1-\gamma \exp(-\kappa H)} \right) \quad (2.30)$$

where

$$\gamma = \frac{\exp(ze\psi_0/2kT)-1}{\exp(ze\psi_0/2kT)+1} \quad (2.31)$$

and

$$\kappa = \left(\frac{2e^2 N_A c^2}{\epsilon kT} \right)^{1/2} \quad (2.32)$$

and H is the distance from the surface.

At low surface potentials ψ_0 , equations 2.30 and 2.31 can be reduced by making use of the Debye-Hückel approximation:

$$\exp \left(\frac{ze\psi_0}{2kT} \right) \approx 1 + \frac{ze\psi_0}{2kT}$$

These equations then become

$$\psi = \psi_0 \exp(-\kappa H) \quad (2.33)$$

showing that at low potentials, the potential decreases exponentially from the surface over a distance $1/\kappa$. The value of $1/\kappa$ is customarily referred to as the 'thickness of the diffuse double layer'.

2:4:2 The Inner Part of the Double Layer

The relatively simple model adopted above is based on the assumption of point charges in the dispersion medium. Stern (103) overcame this difficulty by postulating that the finite size of ions placed limitations on the number of ions that could be adsorbed at the interface. He recognised that an ion may not approach closer to the surface than a distance equal to the hydrated ion radius and that in some cases specific adsorption of ions may occur. Where specific adsorption occurs, the ion may lose part of its hydration shell and consequently may come into intimate contact with the surface.

In this region the ions are not subject to the normal thermal motions which affect ions in the diffuse region. The Stern plane is located at about a hydrated ion radius from the surface and the corresponding potential ψ_s is termed the Stern potential. ψ_s may be used in place of the surface charge ψ_0 in the Gouy-Chapman treatment of the diffuse double layer.

Grahame (104) proposed a modification of Stern's idea and subdivided the Stern region into an inner and outer Helmholtz plane (I.H.P., O.H.P.). The I.H.P. is the region closest to the surface consisting of specifically adsorbed ions plus some solvent molecules not associated with the adsorbed ions. The outer Helmholtz region contains the hydrated counter ions and the outermost region corresponds to the outer limit of the Stern region. Equations are available to treat the inner region of the double layer in terms of both Stern and Grahame models (105). Both these models assume that the surface charge is uniform. However, charges exist at discrete sites on the surface and where an ion is adsorbed it will rearrange neighbouring charges thereby altering the potential that the ion itself experiences. This effect has been incorporated into the Stern equation by Levine et al (106) and by use of this equation, is it possible to

explain the observations on AgI sols that ψ_s goes through a maximum as ψ_0 is increased.

2:4:3 Double Layer Repulsion

The important consequence of an electric double layer surrounding a particle is that the repulsion occurring on overlap of two such layers may be sufficient to prevent particle aggregation. Deryaguin and Landau (6) and Verwey and Overbeek (7) considered such an interaction in terms of the Gouy-Chapman theory for the diffuse region. For flat plates Verwey and Overbeek derived an approximate expression for the potential energy of repulsion, V_R :

$$V_R = \frac{64nkT\gamma^2 \exp(-\kappa H)}{\kappa} \quad (2.34)$$

where

$$\gamma = \frac{\exp(ze\psi_0/2kT) - 1}{\exp(ze\psi_0/2kT) + 1}$$

and where n is the number of ions per unit volume of solution.

The repulsive energy is therefore a function of the surface potential ψ_0 as defined by γ . ψ_0 may be replaced by the Stern potential ψ_s for which a valid approximation is the experimentally determined zeta potential, ζ . This approximation is valid only under certain conditions and Lyklema and Overbeek (107) have discussed that differences between ψ_s and ζ will be most pronounced at high potentials and high electrolyte concentrations. For spheres the derivation of an exact equation for the repulsive barrier is more difficult. Hogg, Healy and Furstenau (108) derived a general equation for two spheres of radii, a_1 and a_2 and surface potentials ψ_{01} and ψ_{02} which applies only when ψ_0 is less than 25mV.

$$V_R = \frac{\epsilon a_1 a_2 (\psi_{01}^2 + \psi_{02}^2)}{4(a_1 + a_2)} \left[\frac{2\psi_{01} \psi_{02}}{(\psi_{01}^2 + \psi_{02}^2)} \ln \left(\frac{1 + \exp(-\kappa H)}{1 - \exp(-\kappa H)} \right) + \ln(1 - \exp(-2\kappa H)) \right]$$

(2.35)

In the case usually considered of equal spheres and identical charges equation 2.35 reduces to

$$V_R = \frac{\epsilon a \psi_0^2}{2} \ln[1 + \exp(-\kappa H)] \quad (2.36)$$

2.5 Hydration Forces

An additional repulsive force may exist at interfaces where the solvent molecules are in some way structured.

Van Olphen (109) has argued against the solvation theory stating that the orientation effect of solvent molecules through dipole interactions with the surface may be expected to be significant only up to a few water-molecule diameter away from the surface. Therefore these forces will not be large enough to affect the balance between attractive forces and double layer repulsive forces. He does however agree that a few solvent molecules may be bound to the surface and that the work required to desorb these molecules may manifest itself as a very short range repulsion.

Le Neveau et al (110) have demonstrated the existence of such forces between lipid bilayers and Hunter and Leyendekkers (111) found similar results on mineral clay surfaces. Using crossed mica surfaces Israelachvilli measured the repulsion exerted by structured water at the interfaces and concluded that these forces may cause repulsions at distance up to 7.5nm from the surface (8). This force appears to be independent of electrolyte concentration and pH but it does depend on the nature of the surfaces involved and to some extent on the cations

which may be present in solution.

Theoretical consideration to the problem has been attempted by Marcejla et al (112) who have shown that the decay of the repulsion should be exponential - a fact which is verified by the work of Israelachvilli.

In compression studies of sodium montmorillonite particles in aqueous solution, no evidence of primary minimum coagulation could be detected even at surface separations of 1.5nm and repulsive potentials were always greater than those predicted by potential energy curves (113). The authors suggest that these observations are due to solvation forces although it is possible that the model of the electrostatic repulsion was an oversimplification.

2:6 Attraction Between Particles

Interactions between molecules were first quantitatively assessed by van der Waals (114) in the modified equation of state for gases in which departures from the ideal gas law occurred. The deviations from this law were due to the finite size of the molecules effectively causing repulsion and also due to attractions of the molecules for each other. These attractions comprise the van der Waals forces and they can be sub-divided into three groups according to the type of interaction that occurs.

1) Keesom effect (115)

Keesom investigated the attractive force between two molecules with permanent dipole moments. As the maximum attraction occurs when the dipoles are aligned end to end, this effect is sometimes called the orientation effect. For two different interacting dipoles (μ_1 and μ_2), the potential energy of attraction, V_K is given by

$$V_K = \frac{-2}{3kT} \cdot \frac{\mu_1^2 \mu_2^2}{r^6} \quad (2.37)$$

where r is the distance between the centres of the dipoles.

2) Debye Effect

Debye observed (116) that if the attractive forces were due solely to the Keesom effect, then a reduction in the attraction potential should occur at high temperatures in accordance with equation 2.37. This however was not confirmed by experimental evidence and Debye proposed that an additional attractive effect existed which depended on the induction of a dipole in one molecule by the dipole of a neighbouring molecule. These are sometimes termed dipole-induced dipole effects. For two molecules of different polarisabilities (α_1 and α_2).

$$V_D = - \frac{\alpha_1 \mu_2^2 + \alpha_2 \mu_1^2}{r^6} \quad (2.38)$$

Both the first two effects depend on the existence of permanent dipole moments in the molecules and therefore play no part in cases where the molecules are non-polar.

3) London Effect (117)

The third effect, known as the London or dispersion effect is completely general and operates whenever two molecules, ions or atoms are in close contact. It is the result of an interaction between the random motions of the electrons in the two species. Although non polar materials have zero permanent dipole moments because, averaged over a period of time the rapid motions of the electrons result in a symmetrical distribution of charge, there will exist instantaneous dipole moments. These are influenced by corresponding moments in neighbouring species and distributions which lead to an attractive potential are favoured over those corresponding to repulsion.

The energy of attraction for hydrogen like atoms is given by:

$$V_L = - \frac{3hv_0\alpha^2}{4r^6} \quad (2.39)$$

where h is Planck's constant and v_0 represents the characteristic oscillatory frequency of the electrons.

One important conclusion reached by London was the fact that this type of force is additive. All three types of van der Waals attraction decay inversely as the sixth power of distance and for single molecules they are essentially short-range forces. Kallman and Willstatter (118) however suggested that because of the additive nature of van der Waals forces they may be able to explain the long range attractive forces that are observed with colloidal systems.

Two methods of calculating van der Waals forces exist. The first - the microscopic approach - starts from the interactions between individual molecules and postulates their addativity by integrating over all pairs of atoms and molecules. The second approach - macroscopic - originates directly from the optical properties of the interacting macroscopic bodies. We shall consider these approaches in turn.

2:6:1 The Microscopic Approach

Summation of the London forces for molecules in one flat plate, and evaluation of their interaction with similar arrays of molecules in another flat parallel plate in vacuum where the plates are separated by a distance H leads to the following expression for the potential energy of interaction (7)

$$V_A = - \frac{\pi^2 q^2 \lambda'}{12} \left[\frac{1}{H^2} + \frac{1}{(H+2T)^2} - \frac{2}{(H+T)^2} \right] \quad (2.40)$$

where T is the thickness of the plate and q is the number of molecules per unit volume of the plates. λ' is equal to $\frac{1}{2} h\nu_0 a^2$. The quantity $\pi^2 q^2 \lambda'$ is a constant for a given material and is usually given the symbol A , and referred to as the Hamaker constant. When the distance between the plates is small compared to their thickness, expression 2.40 becomes:

$$V_A = - \frac{A}{12\pi H^2} \quad (2.25)$$

The potential energy of interaction for plates is now seen to vary inversely as the square of separational distance, and under these conditions, the attractive van der Waals forces can exert their influence over a comparatively long range.

For spheres, Hamaker derived expressions for the attraction in a vacuum (119):

$$V_A = \frac{\pi^2 q^2 \lambda'}{12} \left[\frac{y}{x^2 + xy + x} + \frac{y}{x^2 + xy + x + y} + 2 \ln \left(\frac{x^2 + xy + x}{x^2 + xy + x + y} \right) \right] \quad (2.41)$$

where x is the ratio of surface separation to the largest particle diameter and y is the ratio of the smaller to the larger diameter.

For spheres of equal size and where the separational distance is less than the diameter of the spheres

$$V_A = - \frac{Aa}{12H} \quad (2.42)$$

where a is the particle radius.

The above equations refer to interactions between particles in vacuo. However, for real systems such as pharmaceutical suspensions, aerosols etc, account must be made for the presence of a dispersion medium

between particles. Hamaker derived expressions to allow for this in terms of the in vacuo Hamaker constants for the particles (A_{11}) and the dispersion medium (A_{22}). The effective Hamaker constant (A_{eff}) is then given by

$$A_{\text{eff}} = A_{11} + A_{22} - 2A_{12}$$

or assuming a geometric mean relationship:

$$A_{12} = (A_{11}A_{22})^{\frac{1}{2}} \quad (2.43)$$

then

$$A_{\text{eff}} = (A_{11}^{\frac{1}{2}} - A_{22}^{\frac{1}{2}})^2 \quad (2.44)$$

Depending on the relative values of A_{11} and A_{22} , the potential energy of interaction may be greater or less than that observed in a vacuum.

2:6:2 The Retardation Effect

The expressions for the attractive potential between particles in Equations 2.25, 2.42 are valid only when the distance of surface separation is less than $0.1\lambda_0$ where λ_0 represents the wavelength corresponding to the intrinsic oscillations of the atoms. This is because London - van der Waals forces are electromagnetic in nature and a finite time is necessary for the propagation of such waves. During this time period, the dipoles of the interacting species will have altered and as a consequence the attractive energy will be reduced. This was appreciated by Casimir and Polder (120) who found that for large distances between atoms V_A decreases inversely with the seventh power of distance instead of as the sixth.

The correction for this can be made simply by adding a correction

factor to equation 2.39 so that

$$V_A = - \frac{3h\nu_0 \alpha^2}{4 r^6} \cdot f(p) \quad (2.45)$$

where $p = 2\pi r/\lambda_0$ with the conditions that

$$f(p) = 1.01 - 0.14p \quad 0 < p < 3$$

$$f(p) = \frac{2.45}{p} - \frac{2.04}{p^2} \quad 3 < p < \infty$$

Schenkel and Kitchener (121) derived empirical equations to determine V_A allowing for the retardation effect for spheres.

At large separations ($>2\lambda$) where attraction is fully retarded:

$$V_A = - \frac{2.45 Aa \lambda}{120\pi H^2} \quad (2.46)$$

For distances between the fully retarded situation and that where the simple Hamaker expression may be used (i.e. Equation 2.25) a more complex equation was derived:

$$V_A = Aa \left[\frac{-2.45\lambda}{120\pi H^2} + \frac{2.17\lambda^2}{720\pi^2 H^3} + \frac{0.59\lambda^3}{3360\pi^3 H^4} \right] \quad (2.47)$$

Clayfield, Lumb and Miller (122) have also derived expressions for the retarded attraction between spheres of equal radii. Both sets of equations have been criticised by Vincent (90) as they do not represent V_A continuously as a function of separational distance. The equations of Schenkel and Kitchener appear to be more in error than the original unretarded Hamaker function for small particles and the expressions of Clayfield et al deviate grossly at small separations. In his paper Vincent has produced equations to allow for retardation and it is claimed that these represent V_A continuously as a function of H . These

equations were used in this work and they will be presented in section 2.7. Experimental verification of retardation at small distances of separation has come from the work of Tabor and Winterton (29a,b,c) who used crossed mica cylinders for which the geometry represents a sphere approaching a planar surface. For this situation the non-retarded force of attraction depends inversely on H^2 while for the fully retarded situation it is inversely proportional to H^3 . Their experimental results demonstrate a gradual transition between these two power laws with the retardation effect operating from a surface separation of 8nm.

2:6:3 The Macroscopic Approach

In this treatment of attractive forces between particles the interacting phases are thought of as being continuous and the interaction as occurring through a continuous medium. No assumption is made as to the additivity of dispersion forces - it is recognised that the atomic and molecular forces that contribute towards attraction may be non-additive, and temperature dependent. In the 'microscopic approach' the forces responsible for attraction are regarded as originating from electromagnetic fluctuations due to fluctuations occurring in a narrow frequency band in the ultra-violet region of the spectrum. In the Lifshitz approach (123) it is recognised that contributions come from polarizations at microwave and infrared frequencies in addition to ultraviolet. The original Hamaker concept of interaction between particles was based on a procedure that is valid for dilute gases. Parsegian and Ninham (124) suggest that this procedure is not suitable for the study of condensed medium interactions particularly those involving highly polar substances such as water.

For small distances of separation between the surfaces of two flat plates the non-retarded force of attraction is given by (123)

$$F = \frac{h \bar{\omega}}{16\pi^3 H^3} \quad (2.48)$$

where for identical plates of medium 1 interacting in medium 2

$$\bar{\omega} = \int_0^{\infty} \left(\frac{\epsilon_1(i\xi) - \epsilon_2(i\xi)}{\epsilon_1(i\xi) + \epsilon_2(i\xi)} \right)^2 d\xi \quad (2.49)$$

where $\epsilon(i\xi)$ is the relative permittivity expressed as a function of the frequency of the field in rad.s^{-1} . The frequency dependent relative permittivity $\epsilon(\omega)$ is expressed as a complex function $\epsilon^1(\omega) + i\epsilon^{11}(\omega)$ of a complex frequency $\omega = \omega_{\text{real}} + i\xi$ where $\epsilon^{11}(\omega)$ is the imaginary part of the relative permittivity and can be obtained from spectroscopic measurements.

It would therefore appear that the use of the macroscopic approach may be limited by the complex variables which must be determined experimentally. In recent years however advances in this theoretical field have been made and approximations have been derived which account for experimentally determined values of attraction between macroscopic objects. The first use of the Lifshitz theory was applied to experimental results (125) of the forces of attraction between two water media separated by a bi-molecular leaflet. The experimentally determined value of the Hamaker constant was 4.66×10^{-14} erg. This may be compared with a value of $4.5 - 5.4 \times 10^{-14}$ obtained from Lifshitz theory (126). Parsegian and Ninham have extended their earlier work to provide a general theory applicable in the case of two parallel lipid slabs separated by an aqueous medium (124). Several features are predicted as a result of this.

1) As water is highly polar much of the van der Waals forces originate from polarizations at infrared and microwave frequencies, rather than the ultraviolet.

2) The idea of a Hamaker 'constant' is quite misleading.

In this approach the potential energy of interaction between two flat slabs is given by $V_A = A/12\pi H^2$ and is similar to that derived from the microscopic approach. However the term A is not a constant, but is a function of the distance between the plates and temperature. A is therefore termed the "Hamaker function".

- 3) The van der Waals force contains a large temperature - dependent component.
- 4) Dielectric data may be obtained through a whole range of frequencies so that numerical estimates may be evaluated.

Suitable equations have now been derived for the interaction between spherical particles (127,128). Smith et al (127) predict that if the dielectric properties of the medium and the particles are similar the Hamaker approach may be used both qualitatively and quantitatively to express the interaction. Evans and Napper (128) have critically discussed the work of Parsegian and Ninham, and have suggested that the use of ionization potentials of vapours instead of liquids as used by the latter authors may not be a justifiable approximation to determine the permittivity of the materials. These authors also evaluate the Hamaker function of polystyrene latices at various distances of separation but note that comparison with experimentally determined values is difficult due to the wide spread of values listed in the literature.

Nir et al (129) have given the complete dielectric properties of water and calculated the attractive forces for the water-vacuum-water system. It was shown that the Hamaker function more than doubled on reducing the surface separation from 100 to 5nm, and that the percentage contribution from the ultraviolet region of the spectrum decreased with increasing surface separation.

The computation of an interaction constant for the Lifshitz approach can be seen to require considerably more data than the simpler microscopic approach of Hamaker. At present the literature describes determinations of Hamaker functions for relatively simple substances such as water, liquid hydrocarbons and gases, as the dielectric data of these substances may be obtained from information readily available in handbooks. The microscopic method will continue to be used in the future until the techniques adopted for simple molecules can be easily adapted for more complex practical systems. The advantage of the Hamaker approach is that values for A , the Hamaker constant, may be readily determined by extrapolation of results obtained in the visible region of the spectrum to the ultraviolet region (90). In the light of the criticisms of the Hamaker approach, it is surprising to see that good correlations are observed between experimentally determined results and this simple theory of attraction (see for example (113)). In addition, Vincent has stated (90) that where comparisons are made between the two theories the agreement is not unreasonable.

2:6:4 The Effect of Adsorbed Layers

In addition to providing a force capable of stabilizing a dispersion through the steric effect, adsorbed polymers may affect the electrostatic repulsion and the attractive forces by their presence at the interface. Ionic polymers may increase or decrease V_R depending on the nature of the surface charge and the nature of the polymer. Nonionic polymers in general tend to lower V_R due to the displacement of the plane of shear at constant surface potential. The effective Hamaker constant of the particles may be altered if that of the adsorbed polymer is sufficiently different. This effect was recognised by Vold (130) and she derived general equations for V_A to allow for the presence of such layers. The net interaction energy was always negative

(i.e. interaction) regardless of the magnitude of the Hamaker constants of the particles and the medium and stabilization was found to be most effective when the Hamaker constant of the adsorbed layer (A_s) was either greater or less than the Hamaker constants of both the particles, (A_p), and the medium, (A_m). It was shown that in the presence of an adsorbed layer the attractive potential was always decreased and that this effect was only significant with very small particles (<50nm) or thick sheaths (>2nm). However, in re-evaluating the 'Vold effect' Osmond, Vincent and Waite (131) have determined conditions under which an adsorbed layer may cause an increase in the attraction between particles.

In both the above theoretical considerations, the adsorbed layers have been treated as being homogeneous and uniform. This model is reasonable for short chain length polymers and surfactants, but it breaks down for high molecular weight polymers where a segment density distribution in the adsorbed layer must be considered. In extending Vold's work to cover interactions between particles of geometrics other than spheres, Vincent (90) has provided equations allowing the retardation effect to be taken into account.

For identical flat plates, thickness T , covered with an adsorbed layer, thickness δ , V_A is given by:

$$\begin{aligned}
 V_A = & \frac{-1}{12} \left[(H_o + H_i - 2H_{oi}) (A_s^{\frac{1}{2}} - A_m^{\frac{1}{2}})^2 \right. \\
 & + H_p (A_p^{\frac{1}{2}} - A_m^{\frac{1}{2}})^2 + 2(H_{op} + H_{ip}) \\
 & \left. \times (A_s^{\frac{1}{2}} - A_m^{\frac{1}{2}}) (A_p^{\frac{1}{2}} - A_m^{\frac{1}{2}}) \right] \quad (2.50)
 \end{aligned}$$

Two H functions were derived corresponding to short range (H_s) and long range (H_L) interactions.

$$\begin{aligned}
 H_s &= \frac{a}{\pi} \left[\frac{1}{\Delta^2} + \frac{1}{(\Delta+t_1+t_2)^2} - \frac{1}{(\Delta+t_1)^2} - \frac{1}{(\Delta+t_2)^2} \right] \\
 &\quad - \frac{4b}{\pi} \left[\frac{1}{\Delta} + \frac{1}{\Delta+t_1+t_2} - \frac{1}{\Delta+t_1} - \frac{1}{\Delta+t_2} \right] \\
 H_L &= \frac{a'}{2.5\pi} \left[\frac{1}{\Delta^3} + \frac{1}{(\Delta+t_1+t_2)^3} - \frac{1}{(\Delta+t_1)^3} - \frac{1}{(\Delta+t_2)^3} \right] \\
 &\quad - \frac{b'}{5\pi} \left[\frac{1}{\Delta^4} + \frac{1}{(\Delta+t_1+t_2)^4} - \frac{1}{(\Delta+t_1)^4} - \frac{1}{(\Delta+t_2)^4} \right]
 \end{aligned}
 \tag{2.51}$$

$$a = 1.01, \quad b = 0.14 (2\pi/\lambda), \quad a' = 2.45 (\lambda/2\pi), \quad b' = 2.04 (\lambda/2\pi)^2$$

where for:

H_o	: $\Delta = H+2T+2\delta$	$t_1 = \delta$	$t_2 = \delta$
H_i	: $\Delta = H$	$t_1 = \delta$	$t_2 = \delta$
H_{oi}	: $\Delta = H+T+\delta$	$t_1 = \delta$	$t_2 = \delta$
H_f	: $\Delta = H+2\delta$	$t_1 = T$	$t_2 = T$
H_{of}	: $\Delta = H+2\delta+T$	$t_1 = \delta$	$t_2 = T$
H_{if}	: $\Delta = H+\delta$	$t_1 = \delta$	$t_2 = T$

The critical separation point Δ^* , at which the short range interaction changes to the long range interaction is given by $\Delta^* = 36.9 - 17.5 \log_{10} t + 4.1 (\log_{10} t)^2 - 0.25 (\log_{10} t)^3$ where for semi-infinite plates $\Delta^* = 10\text{nm}$. Vincent has given plots of $\log H_s$ and $\log H_L$ against distance and has shown these variables to be continuous at the cross-over point.

These expressions are employed in the present work to correlate

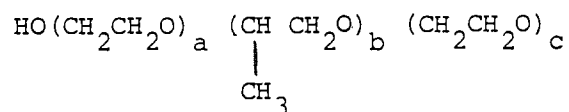
observed suspension stability with that predicted from the above equations. To use such equations the conformation of the adsorbed molecules at the interface must be understood and to achieve this, measurements on the thickness of the adsorbed layers and the total quantity of material adsorbed must be determined. These measurements form the basis of the work in sections 4 and 5.

SECTION 3

materials

<u>Trade Name</u>	<u>n</u>	<u>Source</u>	<u>Molecular Weight based on molecular formula</u>
Synperonic	8	I.C.I. Petrochemical Div.	572
Synperonic	13	"	792
Synperonic	20	"	1100
Synperonic	30	"	1540
Ethylan HA	35	Lankro Chemicals Ltd.	1760

b) the Pluronics which are block co-polymers of polyoxyethylene (POE) and polyoxypropylene (POP) having the general formula:



where a and c are statistically equal

They vary in form depending on the relative amounts of the hydrophobic and hydrophilic parts of the molecule. Those products which are liquid, paste or flakes at room temperature are designated L, P or F respectively. The 'Pluronic Grid' (132) shows the relationship between the polymers in terms of the hydrophilic and hydrophobic content (Figure 9).

Pluronic Grid

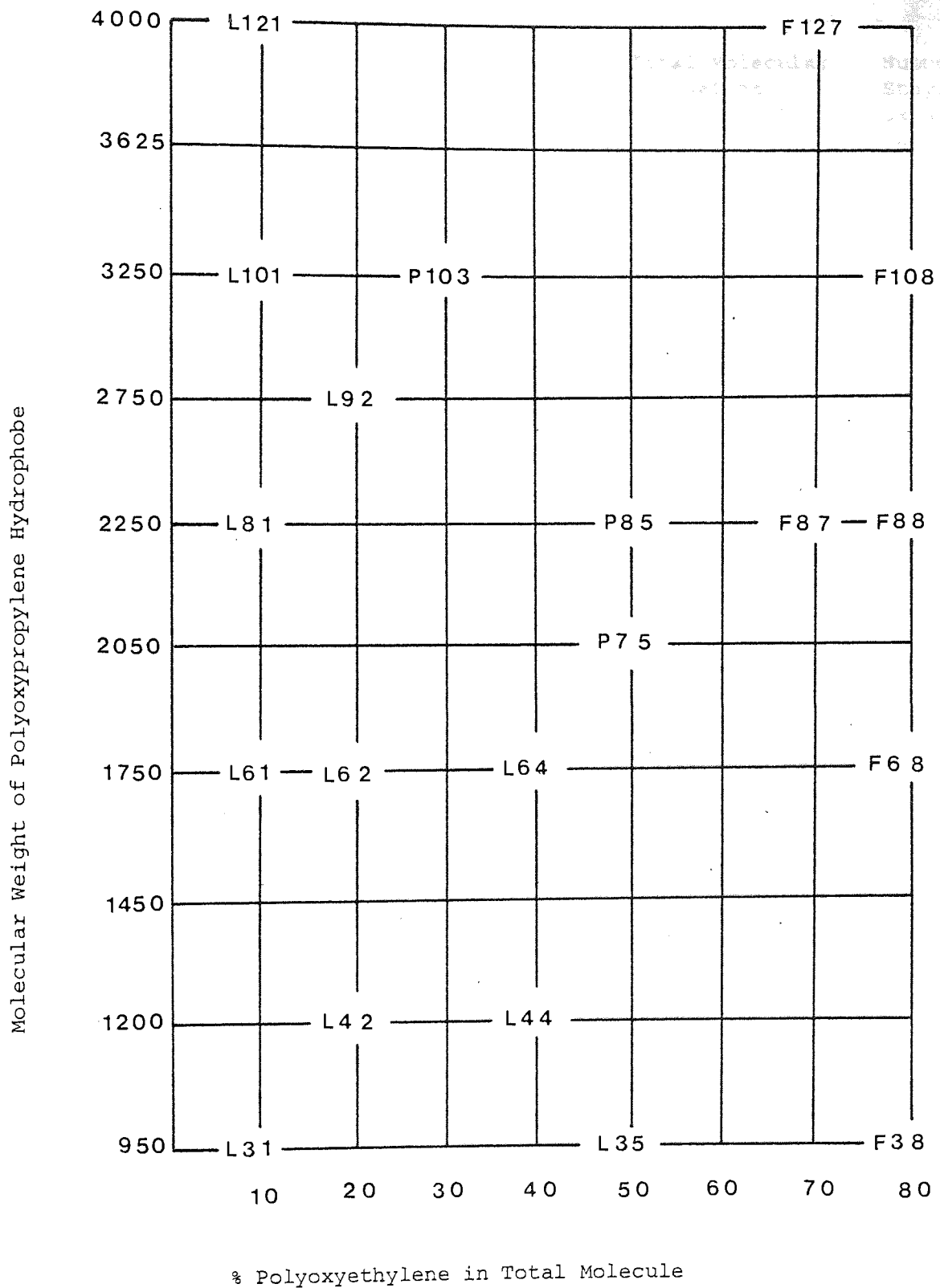


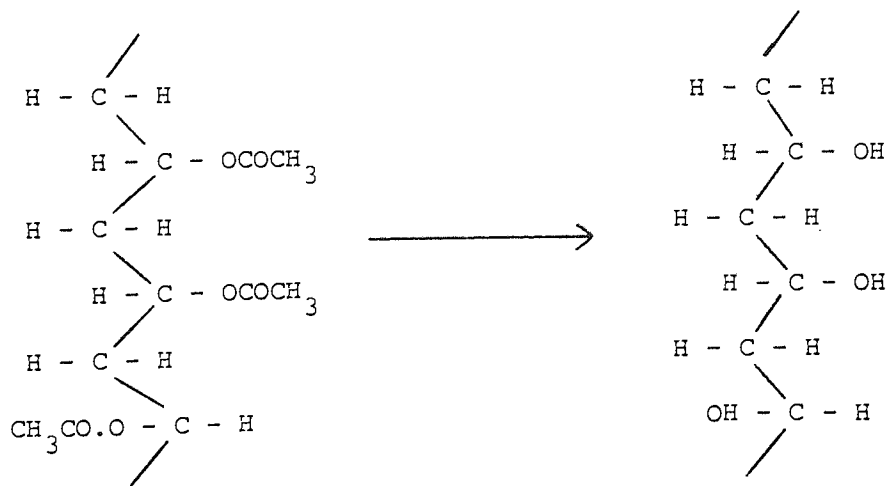
Figure 9: Pluronic Grid

Missing page(s) from the bound copy

The Pluronic used in this study are summarized below.

<u>Polymer Pluronic</u>	<u>Manufacturer</u>	<u>Total Molecular Weight</u>	<u>Number of Ethylene Oxide units per hydro- philic chain (i.e. a or c)</u>
L61	Ugine Kuhlmann Chemicals Ltd.	1944	2.2
L62	"	2188	5.0
L64	"	2916	13.3
F68	"	8750	79.7
F38	"	4750	43.2
F88	"	11,250	102.3
F108	"	16,250	147.7

Polyvinyl alcohol (PVA) was chosen as a suitable macromolecular substance for this study as its properties have been extensively studied in the past and its fractionation and characterisation are relatively simple (133). It is manufactured by hydrolysis of the parent compound polyvinyl acetate (PVAc) and the extent of this reaction may be controlled to give different grades of PVA with varying degrees of hydrolysis. For 100% hydrolysis



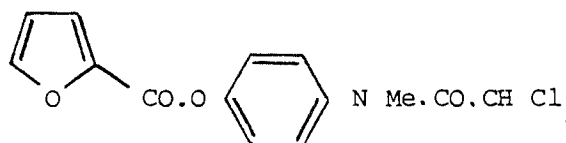
Two commercially available samples of PVA were used in this study, both being 88% hydrolysed :

Mowiol 8 - 88	MW ~ 30,000	Harco Chemical Company Ltd
Polyviol W 25/140	MW ~ 80,000	Wacker Chemicals UK Ltd

3:3 Adsorbents

3:3:1 Drug:- Diloxanide Furoate B.P. Boots Co. Ltd Nottingham

(4-(N-methyldichloroacetomido)phenyl 2-furoate)



Molecular Weight 328.2

The drug is described as insoluble in water and is formulated industrially as a suspension for use in cases of chronic amoebiasis. Two batches were obtained (Batch No. 2616, 224231) and used as received without purification.

3:3:2 Polystyrene Latex

Two monodisperse latices (A and B) were prepared by an aqueous phase initiation suspension polymerization process according to the technique of Goodwin and others (134). Potassium persulphate (Fisons A.R. grade) was used as the initiator and was recrystallized twice from water at temperatures no greater than 30°C to avoid decomposition. The crystals obtained were dried overnight in a vacuum oven and subsequently stored over silica gel. Styrene (B.D.H. Reagent Grade) was distilled at reduced pressure at 40 - 50°C in an atmosphere of oxygen free nitrogen (B.O.C. White Spot) and stored under nitrogen before use. Both latices were prepared under the

same conditions. The polymerization was carried out in a 1 litre round bottom flask with stirring effected by a PTFE T-paddle revolving at 360 r.p.m.. 700 ml of distilled water were allowed to equilibrate for 1 hour with the temperature of the water bath (95°C). The required amount of styrene was then added and after a further equilibration period of 30 minutes, 30ml of a $2.9 \times 10^{-4} \text{ mol dm}^{-3}$ solution of the initiator was added and washed in with a further 20ml of water. The reaction time was 24 hours during which the temperature for latex A dropped to a final value of 84°C . The reaction temperature for latex B was maintained throughout the reaction at $92 - 95^{\circ}\text{C}$. At the end of the reaction time the latices were steam stripped to remove any remaining unreacted monomer and filtered through a packed bed of glass wool to remove any coagulum formed. The latices were dialysed against distilled water in well boiled Visking dialysis tubing for several days with numerous changes of water until the conductivity of the dialysate approached that of pure water. The ratio of latex to dialysate was ca. 1:10. As the initial ionic strength was very low this process was found to take a relatively short time of approximately 10 days after which the latices were stored in Pyrex containers.

Yields from this process were very low (53% for latex A, 6.4% latex B) and percentage solids content for each dispersion were $4.02\% \frac{\text{w}}{\text{v}}$ for A and $0.51\% \frac{\text{w}}{\text{v}}$ FOR B determined by evaporation of a known volume of latex. On drying, latex A exhibited irridescent red and green colours of a higher order Tyndall spectrum indicative of a concentrated, highly monodispersed system.

3:4 Characterization of Materials

3:4:1 Surface Active Agents

The surface active agents used were characterized by measurement

of the critical micelle concentration cmc. The method used for the nonylphenylethoxylates and for the Pluronics was an iodine solubilization technique (135). However, for the Pluronics it was necessary to modify the method using half the concentration of iodine in order to detect changes in the absorbance - concentration plot.

Results are given in table 1 together with literature values. Further comment on these values will be made in Section 4:3.

Table 1

Critical micelle concentrations of surfactants in water at 25°C.

Surfactant	c.m.c. $\mu\text{mol dm}^{-3}$	Literature Values $\mu\text{moles dm}^{-3}$	References
NPE 8	51	44	136
NPE 13	71		
NPE 20	68	135-175, 79	136, 137
NPE 30	100	250-300, 185	136, 138
NPE 35	114	—	—
Pluronics	g dl^{-1}	g dl^{-1}	
L61	.0026	0.0014	139
L62	0.0020	0.0017, 2.4	139, 135, 141
L64	0.0014	0.0016, 0.026, 2.2	139, 140, 141
F68	0.0053	0.0085, 0.1	139, 141
F38	0.0030	—	—
F88	0.0048	0.0055	139
F108	0.0072	0.0073	139

These nonionic surfactants were also characterized in terms of the percentage of ethylene oxide units per molecule by means of nuclear magnetic resonance spectroscopy. Measurements were made on a Varian A-60 spectrometer at ambient temperature. In general operating conditions were : filter bandwidth 4, sweep time 250 sec, sweep width 500 cps, spectrum amp 16 and integral amp 80. A 5 % solution of surfactant in deuteriochloroform was made and the spectrum recorded using trimethylsilane as the internal reference. The value of the integrals was obtained from the average reading of three successive 250 second scans and from these values the relative amount of ethylene oxide per chain was calculated. The number of protons present in the polyoxyethylene chain of the nonionics was determined by using the ratio of the integral of the ethylene oxide peak to that of the hydrophobic group which was assumed to have the number of protons indicated by the manufacturers. For the nonylphenylethoxylates three signals were obtained corresponding to the protons of the alkyl chain ($\tau = 8.7 - 9.2$), benzene ring ($\tau = 2.9 - 3.2$) and ethylene oxide units ($\tau = 6.4$). The determination of ethylene oxide was made relative to the proton signal of the benzene ring. Two strong signals were obtained with the Pluronics, one corresponding to the protons of the methyl group in the polyoxypropylene unit ($\tau = 8.8 - 9.0$) and the other to all remaining protons of the backbone chain ($\tau = 6.4$). Table 2 gives a summary of these results. It may be seen that for the nonylphenylethoxylates and the low ethylene oxide content Pluronics, agreement between the observed results and those given by the manufacturers is good. However there is a marked discrepancy with the higher molecular weight Pluronics. These were subjected to a crude purification procedure to determine if the high ethylene oxide contents were present as an integral part of all molecule, or whether they were present as free polyethylene glycols. A concentrated solution of the surface active agent in water was made and heated to approximately

65°C at which point no phase separation was apparent. Sodium chloride was then added until a large proportion of the surfactant had separated. The supernatant was decanted and the surfactant dried before dissolving in acetone to remove any salt and redrying in a vacuum oven at 50°C. This process was repeated twice more. NMR data of the treated Pluronics show ethylene oxide contents tending towards the manufacturers stated values (Table 2). It would therefore appear that although in commercial samples of Pluronics the ethylene oxide content may be higher than expected, the excess found is not an integral part of the molecule

Table 2

N.M.R. Analysis of Ethylene Oxide Content of Surfactants.

<i>Surfactant</i>	<i>Manufacturers stated % POE</i>	<i>% POE from NMR</i>	<i>% POE of treated pluronics from NMR</i>
L61	10	-	-
L62	20	20	-
L64	40	44	-
F38	80	86	83
F68	80	90	81
F88	80	93	85
F108	80	92	84
	<i>E.O. units / molecule (manufacturer)</i>	<i>E.O. units / molecule from NMR</i>	
NPE8	8	8.4	
NPE13	13	12.8	
NPE20	20	20.1	
NPE30	30	31.7	
NPE35	35	35.8	

3:4:2 Polymers

The polyvinyl alcohol was fractionated by a sequential precipitation technique. This involved adding increasing quantities of acetone, which is a poor solvent for the polymer, to a concentrated solution of the polymer in water. The precipitated fraction was collected by centrifugation and decantation, redissolved in water and dried for 48 hours in a vacuum oven at 70°C. To obtain the low molecular weight fractions from Mowiol 8-88 it was found necessary to add quantities of propan-2-ol to the polymer solution. As these lower fractions could only be obtained in very small quantities several fractionations were performed and these fractions were combined to give manageable amounts. The transparent films so obtained were shredded and stored under nitrogen until required. Altogether 15 fractions were obtained and designated A to O according to their molecular weight. This provided the first means of characterizing the polymers.

Molecular weights of the fractions were determined by viscometric means using a Grade A U-tube viscometer (Technico Ltd) giving a flow time for doubly distilled water of 288.4 sec. Before each measurement the viscometer was cleaned with chromic acid and rinsed thoroughly with water. Drying was accomplished by rinsing with acetone and evaporation of solvent under reduced pressure. Each solution was allowed to equilibrate with the temperature of the surrounding water bath for no less than 30 min. The temperature was stabilized at $25 \pm 0.05^\circ\text{C}$ during all experiments (Townson and Mercer Ltd viscometer bath Series III). Flow times were measured using a hand held stop watch and the time for each solution was determined at least three times until agreement between successive timings was within ± 0.2 sec. Relative viscosities η_r of the solutions were calculated using the following equation

$$\eta_r = t_1 \rho_1 / t_2 \rho_2 \quad (3.1)$$

where t_1 and t_2 are the mean flow times of solutions having densities ρ_1 and ρ_2 respectively. In this case solution 1 refers to the

polymer solution and solution 2 refers to the reference liquid, distilled water.

The specific viscosity is given by

$$\eta_{sp} = \eta_r - 1 \quad (3.2)$$

and the intrinsic viscosity by $[\eta] = \left(\frac{\eta_{sp}}{c} \right)_{c \rightarrow 0}$ (3.3)

Huggins (142) has shown how to relate the intrinsic viscosity to polymer concentration when dilute solutions are considered by

$$\left(\frac{\eta_{sp}}{c} \right) = [\eta] + k^1 [\eta]^2 c \quad (3.4)$$

where k^1 is constant for a given polymer fraction and is termed the Huggins constant. For rigid uncharged spheres k^1 is approximately 2.0 (144a) while for flexible macromolecules, values of 0.35 are often found. However k^1 depends strongly on the quality of the solvent and in poor solvents values of 1.4 have been reported (145a). Plots of reduced viscosity (η_{sp}/c) against concentration will be linear from which values of the intrinsic viscosity and Huggins constant may be obtained. Such plots for the different fractions are shown in Figure 10 for polymer concentrations up to ca. 0.4%^{w/v} and values of $[\eta]$ and k^1 for each fraction are given in Table 3.

The intrinsic viscosity is one of the most useful parameters in characterizing polymers as it is a function of the molecular weight, M , and can be expressed as an exponential form of M (143) as

$$[\eta] = K M^a \quad (3.5)$$

where K and a are both constants and depend on the nature of the solvent, polymer and temperature. For flexible linear macromolecules

$0.5 < a < 0.8$.

Many determinations of the constants in equation 3.5 have been made using different methods to obtain independent values of the molecular weight (see 145, 146). The values of K and a used here are those from the work of Garvey, Tadros and Vincent (145) namely 2.7×10^{-4} and 0.71 respectively. Justification for using these values is demonstrated by the intrinsic viscosity results for the unfractionated samples which if substituted into equation 3.5 with K and a having the above values yields molecular weight of 35,600 and 81,700 which are in reasonable agreement with figures quoted by the suppliers. It should be noted that details of the experimental procedure used by the suppliers to determine M is not available and that different methods used to determine molecular weight of polymers often give different results. The values of the molecular weights employed in this work are weight-averaged as they are related to the sedimentation results of Garvey et al.

The second method of characterizing the fractions was by measuring the percentage of hydrolysis of the parent compound PVAc to PVA. Determination of the acetate content was performed by refluxing a known weight of polymer (ca. 30mg) with 5ml of $M/10$ sodium hydroxide for 30 minutes and back-titrating the excess with $M/10$ hydrochloric acid solution using phenol red as the indicator. CVS ampoules of acid and alkali were used diluted to the appropriate strength.

Using a preparative gel permeation chromatographic technique to separate the various fractions it was shown that there was no significant variation in the degree of hydrolysis with molecular weight (145). However, using a fractional precipitation method on

the same PVA sample, van den Boomgaard et al (133) have demonstrated that the higher molecular weight fractions have a greater degree of hydrolysis. This was accounted for by the fact that the g.p.c. method fractionates only according to the size of the molecule whereas the latter method depends on the solubility of the fractions in the water-acetone system.

Values of the polymer fractions are listed below in Table 3

Table 3

Physical Characteristics of Polyvinylalcohol Fractions.

Fraction	$[\eta]$ (dl g ⁻¹)	k ¹	M	% hydrolysis	Sample Source	
A	1.10	0.74	121,500	90	<p>Polyviol W24/140</p> <p>Mowiol 8-88</p>	
B	1.07	0.76	116,800	91		
C	1.03	0.73	110,700	88		
D	0.94	0.71	97,400	88		
E	0.83	0.82	81,700	87		
F	0.80	0.74	77,600	88		
G	0.65	0.93	57,900	86		
H	0.62	0.72	54,200	86		
I	0.56	0.84	46,900	89		
J	0.48	0.79	37,800	87		
K	0.45	0.86	34,500	88		
L	0.38	-	27,200	88		
M	0.34	-	23,200	89		
N	0.24	-	14,200	87		*
O	0.12	-	5,400	86		*
Unfractionated Mowiol 8-88	0.46	-	35,600			
Unfractionated Polyviol W25/ 140	0.83	-	81,700			

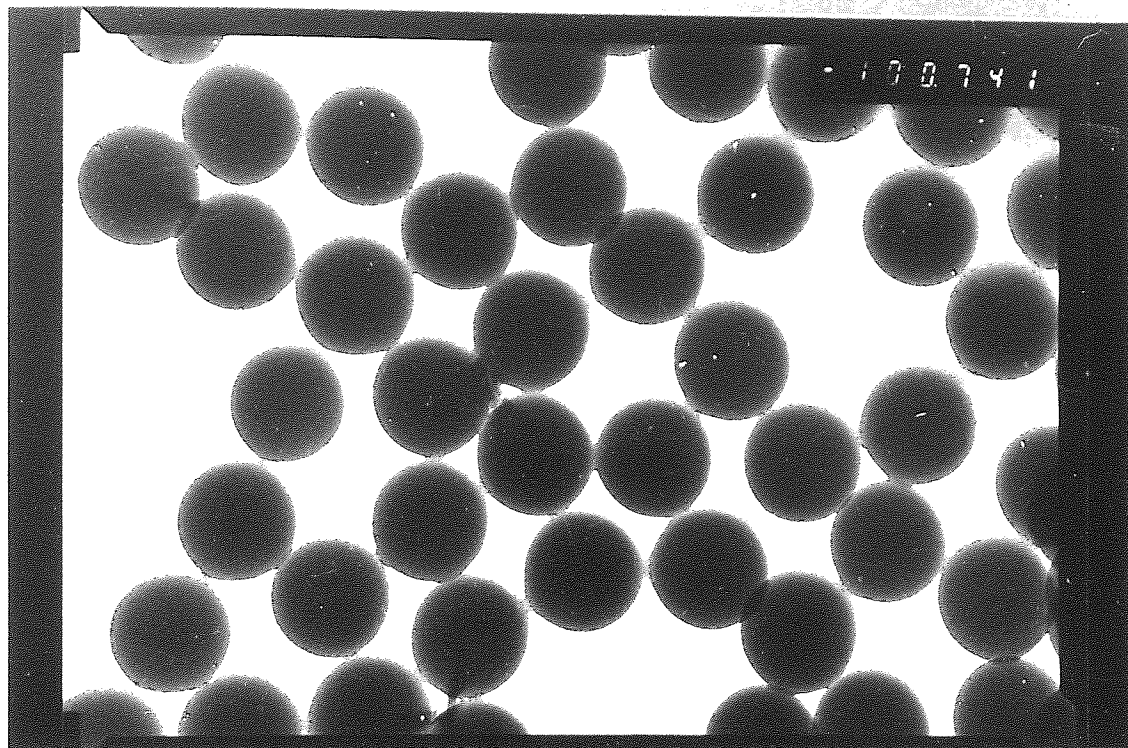
* denotes use of propan-2-ol in fractionation

As Garvey has shown (145) small errors in flow time may give rise to large errors in k^1 and this is particularly evident for the low molecular weight fractions. Values for the Huggins constant for fraction L to O have therefore been omitted as an error of ± 0.2 sec in the measured flow time ^{gives} an error of $\pm 40\%$ for fraction L. The values of k^1 reported here can be considered constant in agreement with previous results (146) and the theoretical approach of Huggins (142) who proposed that the constant is independent of molecular weight. These results differ from those of Fleer (147) who found that k^1 increases with molecular weight indicating that water becomes a worse solvent as M increases. In contrast however to Garvey et al, it is found that values of k^1 are considerably higher than those reported by these authors and it is concluded that this may be a result of different methods of manufacture between samples.

The degree of hydrolysis of the fractions of PVA show slight molecular weight dependence although this is not as marked as in the results of van den Boomgaard (133). The accuracy of the procedure was $\pm 1\%$ and it may be observed that the lower molecular weight fractions are hydrolysed to a slightly lesser extent than higher fractions in the series.

3:4:3 Polystyrene Latex

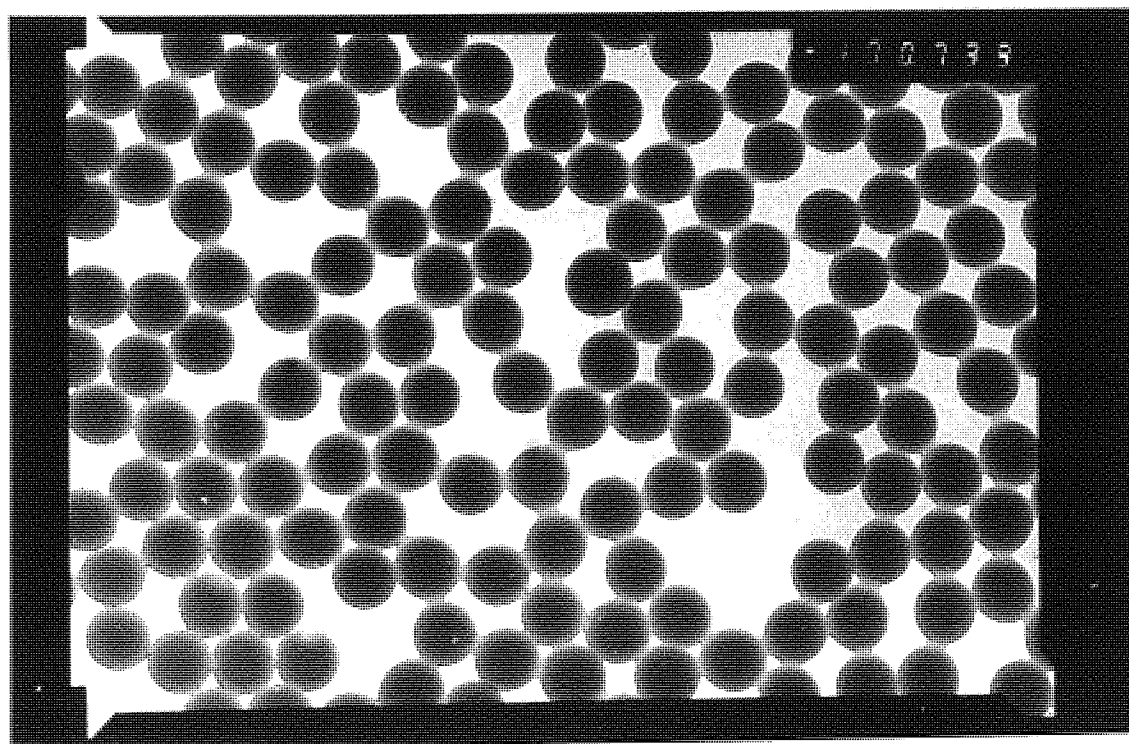
a) Particle size analysis of the latices was performed on a Jeol JEM100B transmission electron microscope operating with a magnification of $\times 32,600$. Prints of the negatives were magnified by a factor of 1.5 and the diameters of the particles determined manually. For latex A 657 particles were measured, while for latex B, a total of 534 were analysed. Sample photographs of both latices are given overleaf and demonstrate the monodispersity obtained in their preparation. Histograms of the particle size distributions are given in Figure 11.



LATEX A



1 micron



LATEX B

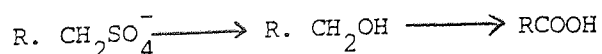
The results of the analysis may be summarized as follows:

Latex A - mean diameter 312nm, modal diameter 315nm
coefficient of variation of the mean 2.6%

Latex B - mean diameter 172.5nm, modal diameter 172.5nm
coefficient of variation of the mean 3.2%

The large difference in particle diameters between the batches of latex which were prepared under identical initial conditions may be attributed to the drop in the reaction temperature for latex A during preparation. Goodwin et al have demonstrated (148) that reaction temperature has a great effect on the size of the final product and that higher temperatures produce smaller diameter particles.

b) Conductometric Titration - It is well known that polystyrene latices are normally negatively charged (149) and that the type of ionizing species present on the surface depends on the method of preparation. In the method used here, namely persulphate initiation, three types of groups are often found, two of which are acidic - one being stronger than the other. These acidic groups are sulphate and carboxylic acid groups (151) while the third species is a hydroxyl group. The sulphate groupings are a consequence of the interaction between polystyrene molecules in the aqueous phase and sulphate free radicals. Hydroxyl groups are formed through the hydrolysis of surface sulphate groups and in addition they may form as a product of the reaction between monomer molecules and hydroxyl radicals created by the reaction of water with persulphate. Two mechanisms exist for the production of carboxyl groups. Goodwin et al (148) have shown the reaction to occur through oxidation of the sulphate and hydroxyl groups by means of a Kolthoff reaction as follows



The second method occurs during the purification stage when a dialysis technique is used. Yates (151) has shown that under prolonged exposure to Visking dialysis tubing in acid conditions, some of the sulphate

groups are converted to weak acid residues. This process also occurs at neutral pH although to a lesser extent and is therefore applicable to this work. The explanation as to why this occurs was thought to be due to hydrolysis and oxidation of the tubing leading to carboxylated polysaccharides which can then adsorb onto the particle surface.

The type and quantity of surface ionizable groupings may be determined by conductometric titration (152) of the latex with carbonate free sodium hydroxide solution. A known volume of latex (10ml for latex A, 50ml latex B) was thermostatted at $25 \pm 0.1^{\circ}\text{C}$ and allowed to attain equilibrium for 15 minutes. Small incremental volumes of 0.01M NaOH solution were added from a Alga syringe and the conductivity of the dispersion was monitored as a function of alkali added by means of a Wayne Kerr conductivity meter-type B642 - and platinum electrodes. The titration was performed under nitrogen to exclude carbon dioxide and stirring was achieved by means of a magnetic follower. In order to standardize the procedure 0.1ml of 10^{-2} HCl were added before titration was started and the first part of the graphs so obtained, represent the initial neutralization of this added acid. Figures 12 and 13 show the results obtained for latices A and B respectively and it is apparent that differences in the surface groups between the two batches are present. Neutralization of the hydrochloric acid occurs at 0.1ml added NaOH and for latex A a gradual rise in conductivity occurs after this point, indicative of surface carboxyl groups only. Two neutralization points for latex B indicate the presence of two surface groups and the continued decrease in conductivity after 0.1ml of NaOH have been added demonstrates the presence of strong, i.e. sulphate groups. In addition, carboxylic acid groups are present as shown by the rise in conductivity after the sulphate neutralization.

Knowing the particle size, particle concentration and equivalence

points the number of charge groups per unit area may be estimated.

Summarizing the results:

Latex A : Number of charge groups (COOH) per unit area = $6.12 \times 10^{16} / \text{m}^2$

Area per charge group = 16.3 nm^2

Surface charge at complete ionization = $0.98 \mu\text{C cm}^{-2}$

Latex B : Number of $-\text{SO}_4$ groups per unit area = $3.43 \times 10^{16} / \text{m}^2$

Number of $-\text{COOH}$ groups per unit area = $1.03 \times 10^{17} / \text{m}^2$

Area per $-\text{SO}_4$ group = 29.2 nm^2

Area per $-\text{COOH}$ group = 9.17 nm^2

Surface charge at complete ionization = $(1.1 + 1.65) \mu\text{C cm}^{-2}$

c) Microelectrophoresis - Confirmation of the type of surface groups found by conductometric titration can be made using this technique.

The procedure adopted and the underlying theory is detailed in section 5 where microelectrophoresis is extensively employed. Essentially the velocity of particles in a given electric field is measured and this can be used to indicate surface groupings if determined as a function of pH. In the case of the latex a cylindrical cell was used and the particles visualized by scattering of light. Measurements were made in 10^{-3} M NaCl and at $25 \pm 0.1^\circ \text{C}$. Adjustment of pH was made by the addition of sodium hydroxide or hydrochloric acid solutions. The amount of light scattered by latex B was too low to monitor particle migration and only latex A could be observed in this way. Figure 14 shows the results obtained with this latex. An initial steep rise in mobility over the range pH 2 - 6 is indicative of surface carboxyl groups only (149) and the plateau above pH6 demonstrates complete ionization of groupings at this value. Ottewill and Shaw (149) have found that where sulphate groups are present the mobility falls off more slowly below this pH and that the mobility does not tend to zero at pH2 in contrast to the results reported here. The increase in mobility above pH 10 cannot be ascribed to groups which are an integral part of the surface

as both carboxyl and sulphate groups (if present) will be fully ionized, and hydroxyl groups are very weak acid groups which will not be ionized until much higher pH values are reached. (153) It would appear that this increase is due to a surface excess of hydroxyl ions formed either by specific adsorption or by the ability of these ions to approach closer to the surface than anions, in the manner described by Haydon (100). This would not be unreasonable as relatively large concentrations of sodium hydroxide are required to obtain high pH values and as a consequence hydroxyl ion concentrations will be high.

The mobility may be assumed constant between pH 6 - 9.5 and in subsequent measurements where polymers and surfactants are adsorbed onto the latex surface, determinations were carried out between these pH limits.

These results confirm the conclusion previously found with conductometric titration that for latex A the only ionizing surface groups present are carboxyl groups.

Surface dissociation constants

Ottewill and Shaw (149) have examined the use of microelectrophoresis to determine dissociation constants of acidic surface groups and the use of these values to identify the nature of these groups.

Neglecting activity coefficients the dissociation constant at the surface of shear K_s , of an acidic molecule HA_s may be defined as

$$K_s = \frac{[H_s^+][A_s^-]}{[HA_s]} \quad (3.6)$$

The hydrogen ion concentration $[H_s^+]$ in the surface of shear is related to

the zeta potential ζ and the bulk hydrogen ion concentration $[H_b^+]$ through the Boltzmann equation:

$$[H_s^+] = [H_b^+] \exp(-e\zeta/kT) \quad (3.7)$$

Combining (3.6) with (3.7) gives

$$pK_s = pH_b - \log \frac{[A_s^-]}{[HA_s]} + e\zeta/2.303kT \quad (3.8)$$

For monovalent charged groupings the surface charge density per unit area is given by

$$\sigma = e n_{A_s^-} \quad (3.9)$$

where $n_{A_s^-}$ is the number of ionized groups per unit area.

If σ is the surface charge at complete ionization

$$[A_s^-] / [HA_s] = \sigma / (\sigma_0 - \sigma) \quad (3.10)$$

At low potentials σ and ζ are proportional, therefore

$$[A_s^-] / [HA_s] = \zeta / (\zeta_0 - \zeta) \quad (3.11)$$

At the bulk pH where $2\zeta = \zeta_0$, equation (3.11) becomes equal to unity and equation (3.8) reduces to

$$pK_s = pH_b + e\zeta/2.303kT \quad (3.12)$$

The pK_s values of the surface group may then be calculated using equation (3.12) where the above conditions apply.

From figure 14, the maximum mobility attained when ionization is complete is $-3.55 \times 10^{-8} \text{ m.s.}^{-1} \text{ v.}^{-1}$ corresponding to a zeta potential

of -70mV (149). Where the measured zeta potential is -35mV ($u = -2.05 \times 10^{-8} \text{ m}^2 \text{ s}^{-1} \text{ v}^{-1}$) the bulk pH is 3.38. Substitution of these values into equation (3.12) gives a value for pK_s of 3.97 which is in excellent agreement with the results of Ottewill and Shaw (149) on carboxylated latices prepared by an emulsion polymerization method. These authors determined the pK_s values of a number of latices as a function of $\zeta_0/2$ and by extrapolating to zero zeta potential found a pK_s ($\zeta = 0$) of 4.64 which agrees well with the value of 4.31 for phenylacetic acid and acids of similar structure which may be regarded as the parent compounds of the polystyrene acid groupings. Stone-Masui and Watillon (154) determined pK_s at zero surface charge by potentiometric titrations and found values ranging between 4.7 and 5.0 which were within the limits of experimentally determined values of pK_a for the parent acid of the emulsifier used to prepare the latices.

The number of carboxylic acid groups ionized at a particular pH value may be obtained from the use of the dissociation constant in the surface of shear. If α is the degree of dissociation then

$$\alpha = \frac{[A_S^-]}{[A_S^-] + [HA_S]} \quad (3.13)$$

and combining this with equation (3.6) gives

$$pK_s = \text{pH} - \log \frac{\alpha}{1-\alpha} \quad (3.14)$$

Figure 15 shows the results of using this approach and again demonstrates the rapid fall off in the number of ionized groups below pH consistent with the presence of carboxyl groups.

3:4:4 Drug Powder

a) The melting point of the crystals was determined and found to be

112-114°C compared with a literature value of 114-116°C. This was the only procedure adopted to ensure the authenticity of the samples. Both batches of drug gave very similar results and the above figures encompass results for the two batches.

b) True density measurements of the diloxanide furoate powders were obtained using a helium air pycnometer (Micromeritics Instrument Corporation, Model 1302). The instrument operates on the principle that the change in pressure of a non-adsorbing gas (helium) in an enclosed chamber due to changes of free space within the chamber, is proportional to the volume of any solid material therein. The true volume of the sample is therefore determined and from this the true density is obtained. A diagram of the apparatus is given in Figure 16. The position of the piston, indicated by the relative position marker, is adjusted until the pressure within the sample chamber becomes equal to that within the bellows. This position is measured first with the chamber empty (R_2) and then with a stainless steel ball of known volume V_{STD} (movement R_1). The ideal gas laws may be considered to apply under the imposed conditions and a calibration factor, β , may be defined:

$$\beta = \frac{V_{STD}}{R_2 - R_1} \quad (3.15)$$

The process is then repeated with a sample of unknown volume V giving a corresponding piston movement R_s . The unknown volume is calculated from equation (3.16)

$$V = \beta(R_2 - R_s) \quad (3.16)$$

True densities of the materials obtained were as follows:

Batch 224231	$1.520 \times 10^3 \text{ kg m}^{-3}$
Batch 2616	$1.516 \times 10^3 \text{ kg m}^{-3}$

c) Particle size distributions for diloxanide furoate powder were determined on a Coulter Counter Model TA at Boots Co. Ltd., Nottingham. The apparatus analyses the size and number of particles suspended in an electrically conductive liquid by forcing the suspension to flow through a small orifice having electrodes on either side (Figure 17). On passing through the orifice a particle changes the resistance between the electrodes generating a voltage pulse whose amplitude is proportional to the volume of the particle. These signals are amplified, scaled and counted and from the derived data the particle size distributions are obtained.

The conducting electrolyte used was 0.9% $\frac{w}{v}$ sodium chloride solution (Polyfusor Boots Co. Ltd.) normally used for intravenous administration. Background counts due to extraneous matter in the solution were therefore low and could be neglected as these counts contributed less than 0.1% of the total count. The size of the orifice used was 140 μ and calibration of the instrument was performed using an 18.26 μ diameter divinylbenzene latex. Measurements were performed over a period of 100sec which permits a low rate of particle counting. The low counting rate avoids the use of co-incidence corrections due to two or more particles arriving in the sensing zone giving rise to unresolvable, overlapping signals. This model of Coulter Counter has the facility of measuring the number of particles in a given size range over sixteen different channels simultaneously and outputting the results in the form of cumulative percentage frequencies or relative percentage frequencies on a graph plotter.

The results of the particle size distribution for both batches are given in Figure 18 expressed on log-probability paper. The mean value diameter, d_{50} , for the powders are:

Batch 224231

=

12.5 μ

Batch 2616 = 16.0 μ

Specific surface areas may be calculated from this data providing the graphs are linear using the appropriate Hatch-Choate equation (155) which in this case is

$$\log d_s = \log d_{50} - 1.151 \log^2 \sigma \quad (3.17)$$

where d_s = surface area diameter

and σ is the geometric standard deviation defined by

$$\sigma = \frac{d_{84}}{d_{50}} = \frac{d_{50}}{d_{16}} \quad (3.18)$$

To obtain approximate specific surface areas the graphs in Figure 18 were redrawn between d_{16} and d_{84} using straight lines and the above parameters determined from these graphs. The specific surface areas S may then be calculated using

$$S = \frac{6}{d_s \rho} \text{ m}^2 \text{ g}^{-1} \quad (3.20)$$

where ρ is the true density of the powder. Using the result previously obtained in section 3:4:4:b for ρ , the following specific surface areas are obtained.

Batch	224231	0.37 m ² g ⁻¹
Batch	2616	0.29 m ² g ⁻¹

Equation 3.20 is, strictly speaking, applicable only to spherical particles and this demonstrates the limitations of the technique to determining surface areas of coarse drug particles. In addition it is only the projected surface area that will be measured and the contribution of interparticulate pores to the total surface area will be unresolved.

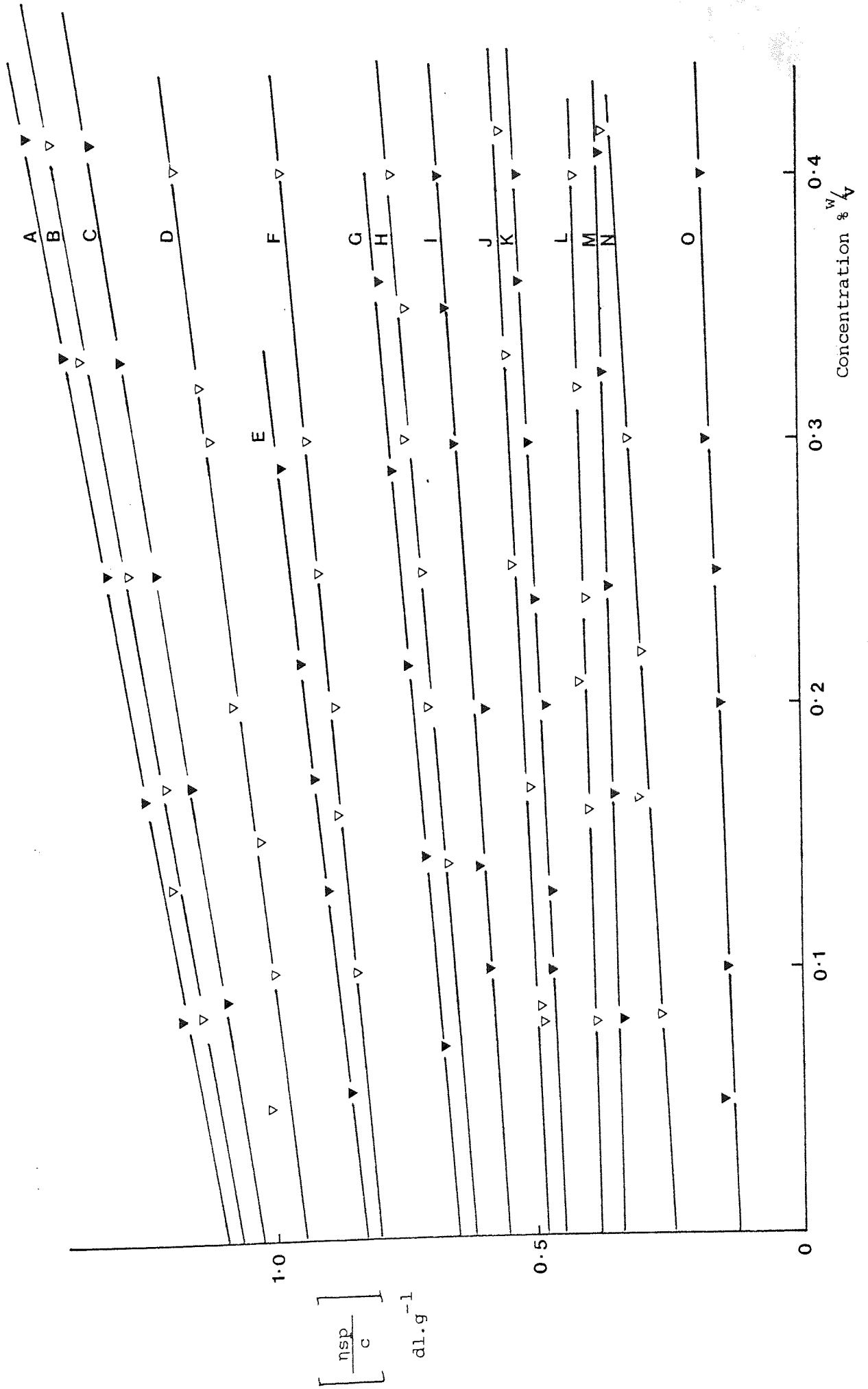


Figure 10 - Huggins Plots for PVA fractions

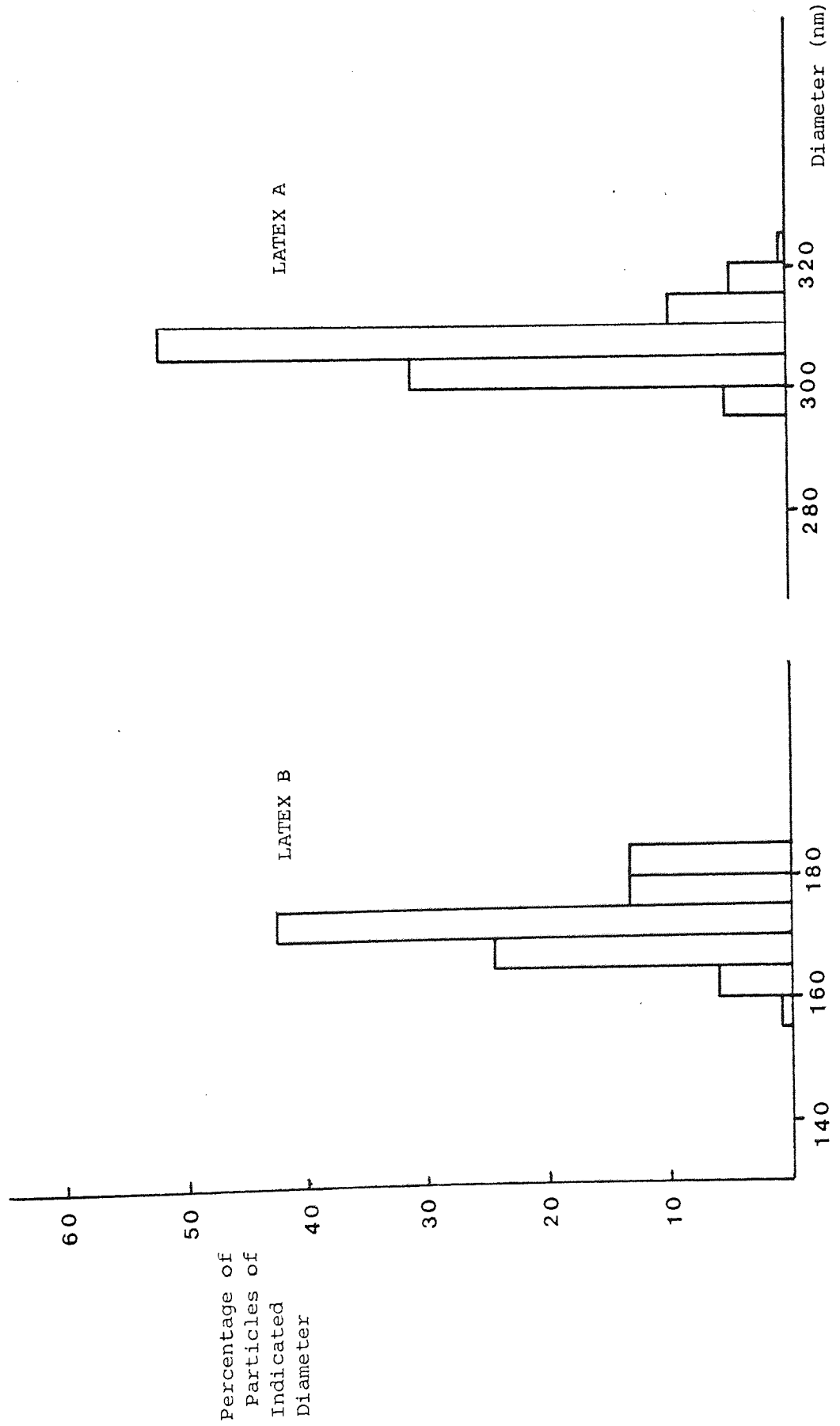


Figure 11 - Particle Size Distributions of Latices

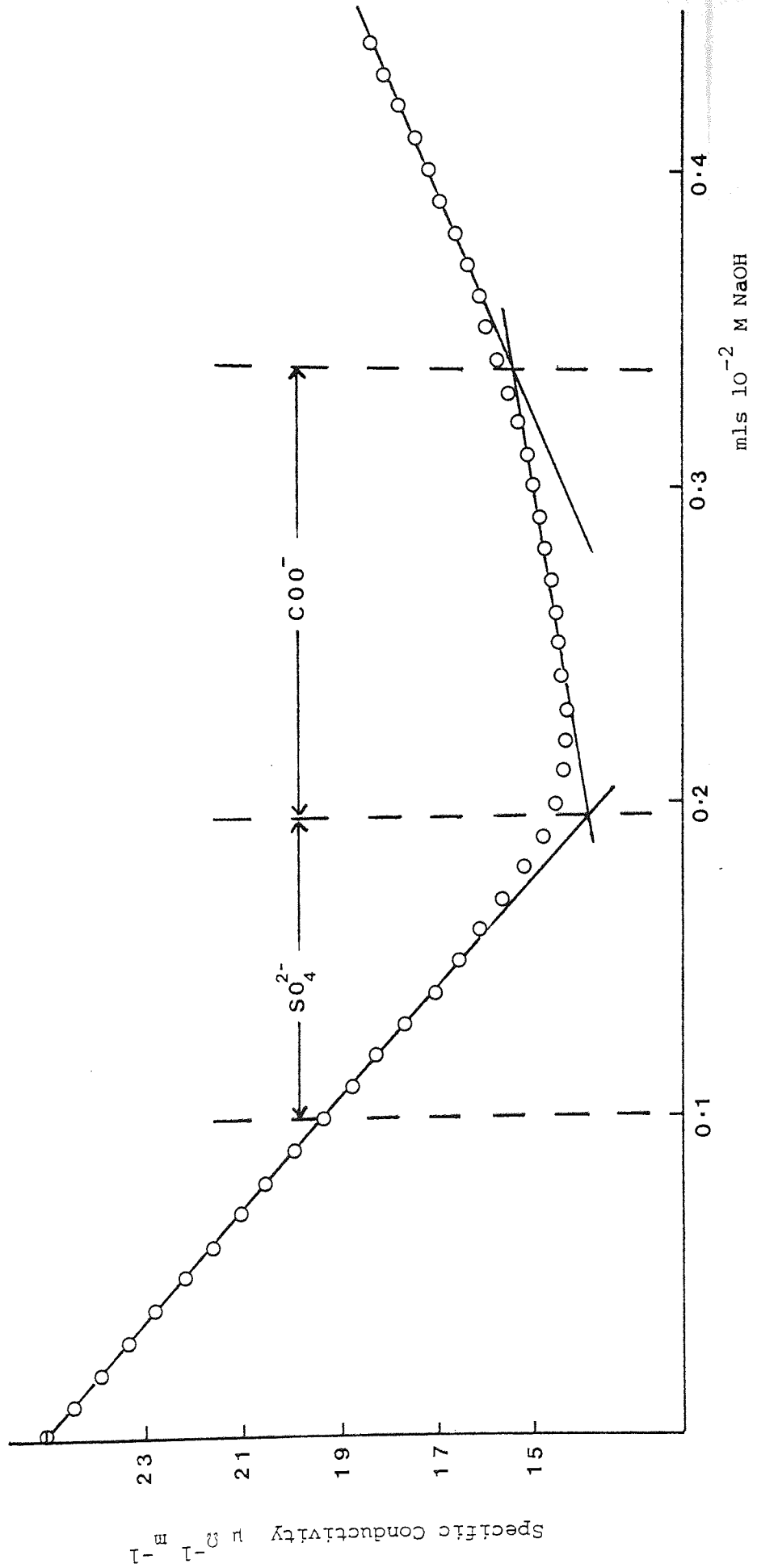


Figure 12 - Conductometric titration of Latex B

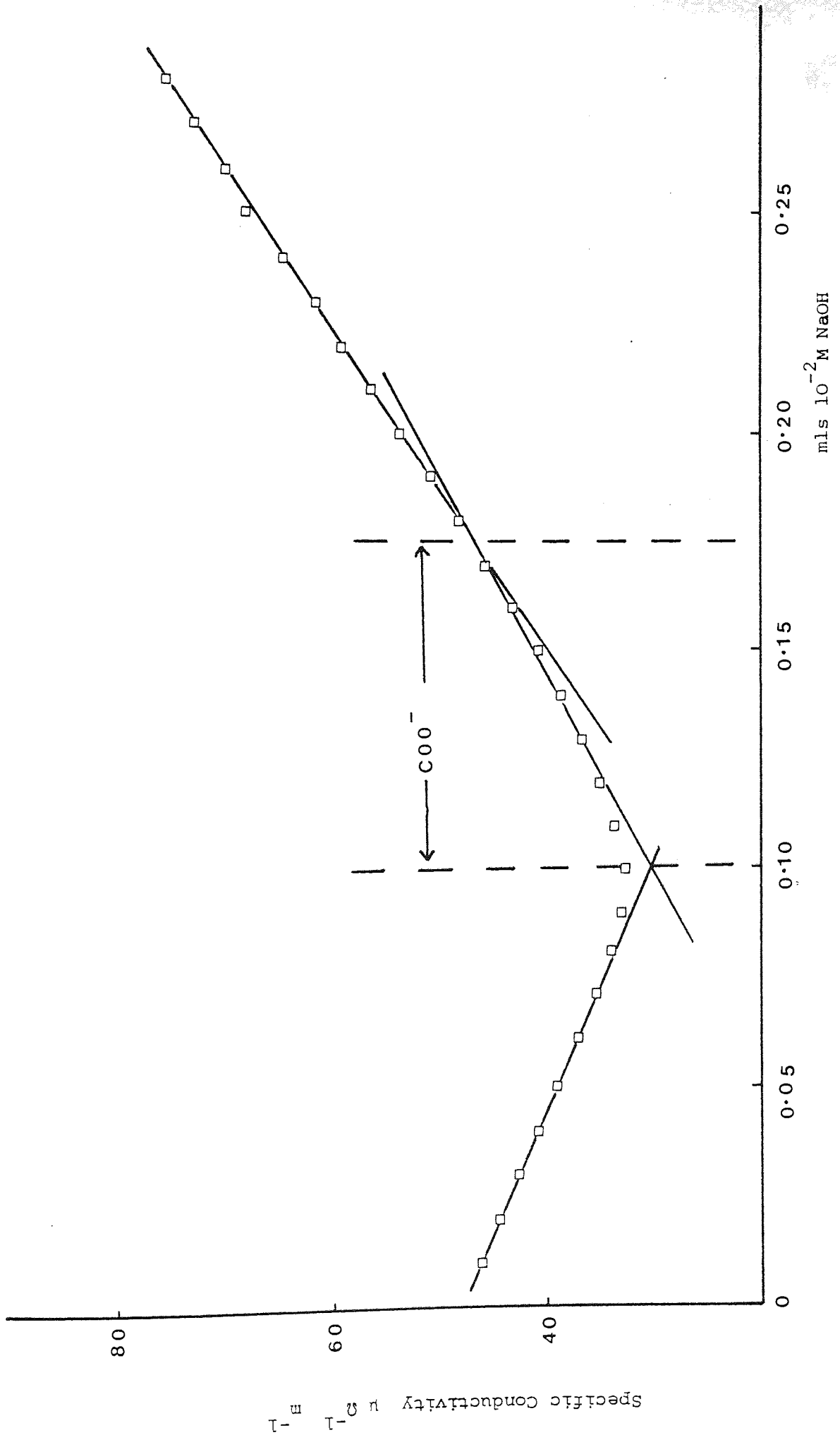


Figure 13 - Conductometric titration of Latex A

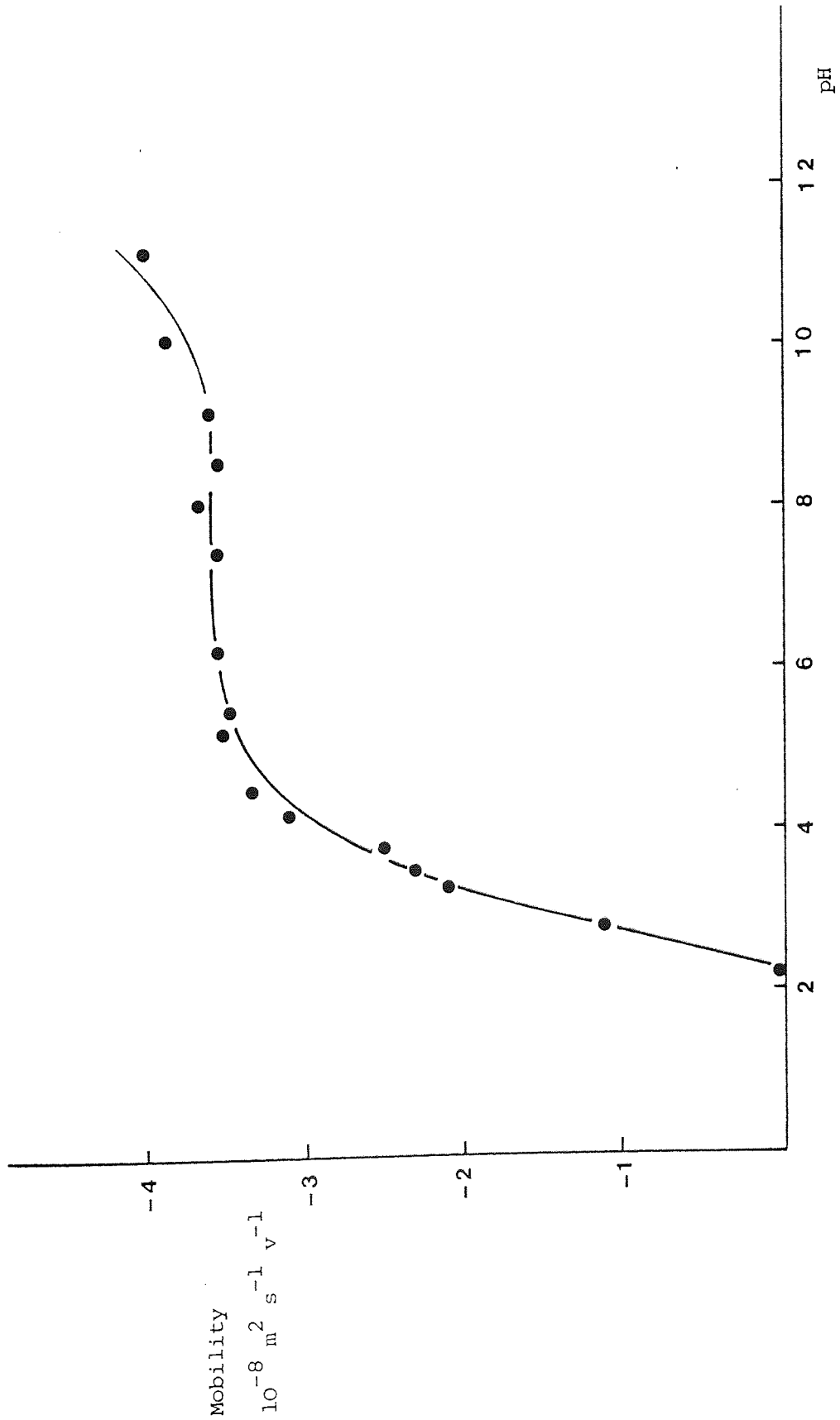


Figure 14 - pH-Mobility Plot of Latex A

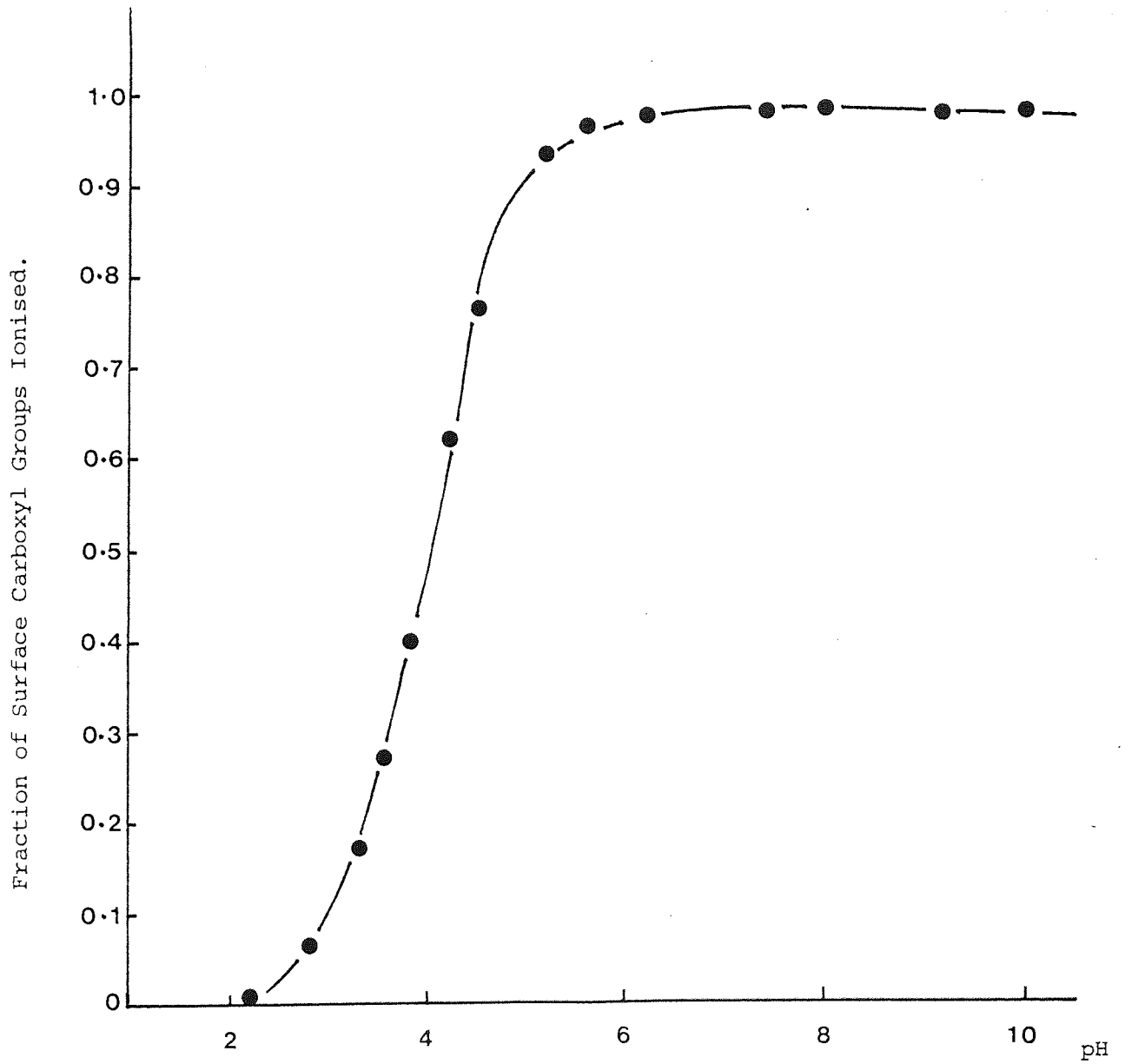


Figure 15 Effect of pH on Surface Group Dissociation

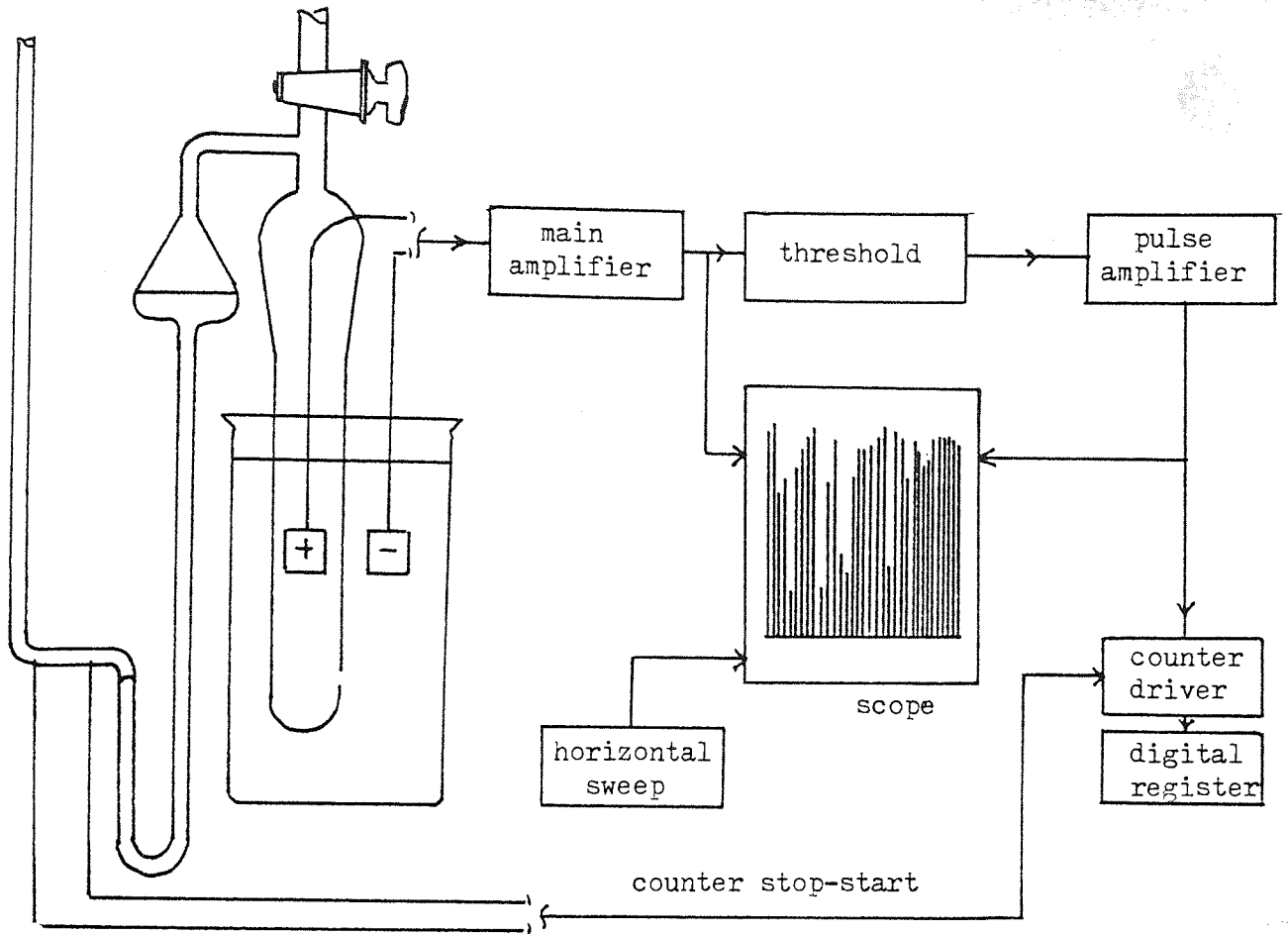


Fig. 17 Diagram of the Coulter Counter

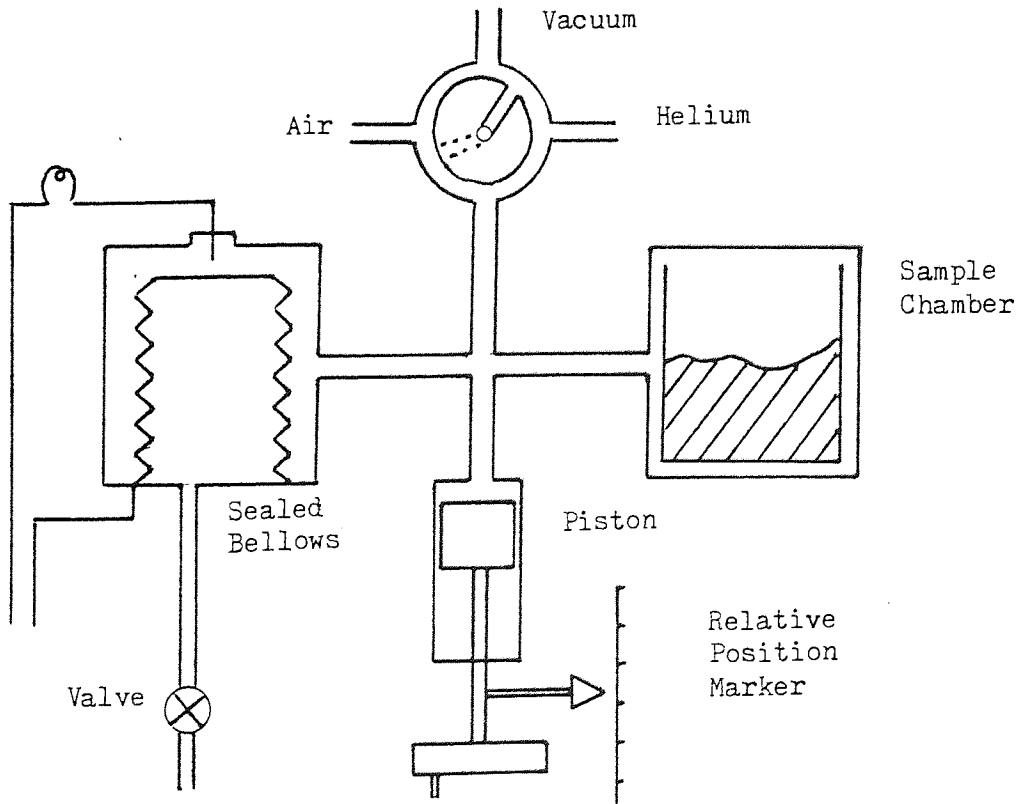


Fig. 16 Diagram of the Helium-Air Pyknometer

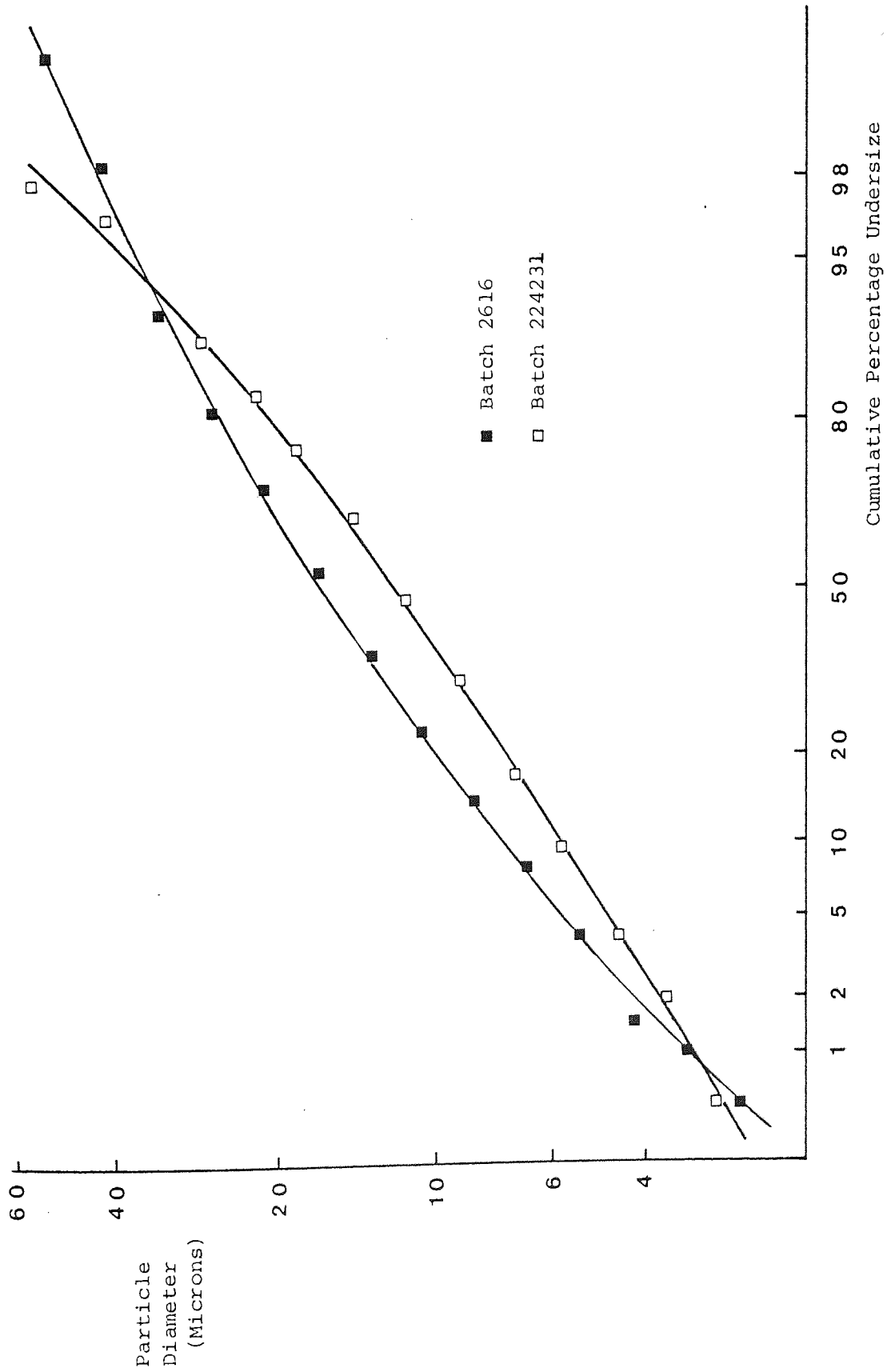


Figure 18 - Particle Size Distribution Diloxanide Furoate B.P.

SECTION 4

adsorption

SECTION 4 - Adsorption

4:1 Methods

4:1:1 Adsorption Isotherms

In this work all adsorption isotherms were determined at $25 \pm 0.1^{\circ}\text{C}$. A known weight of drug powder was weighed into 25ml glass vials which could be stoppered with polyethylene lids. Batch 224231 was used as adsorbent in the case of Pluronics and NPE's, and Batch 2616 was used for polyvinyl alcohol adsorption. The required amount of water was then added and by careful manipulation it was found that the powder would remain at the base of the tube. The correct volume of a stock solution of the surface active agent was added and the tube shaken vigorously by hand for ca. 10 seconds to permit dispersion of the powder. The tube was then subjected to ultrasonification for periods of up to one minute to further assist dispersion and to allow the release of entrapped air. Heating of the tube and its contents became apparent if ultrasonification was continued for times in excess of one minute and where further dispersion was required an interval of three minutes was allowed to elapse before further sonification was applied. Dispersion was achieved using a sonification bath (Kerry Ltd) and cooling of the suspension could be performed by replacing the bath water with cold tap water. A Coulter Counter analysis of a suspension produced in this way, which had been deflocculated with NPE20, revealed little change in the particle size distribution indicating that attrition of the particles was minimal. The surface area available for adsorption can therefore be considered to be that of the dry powder. In order to achieve equilibrium of the adsorbing species the tubes were wrapped in water repellent film (Parafilm) and clamped horizontally under water in a shaking water bath - the long axes of the tubes in line with the direction of movement. Suspensions produced in this way were well dispersed and lumps of

undispersed powder constituted less than 3% of the total powder weight.

Adsorption onto polystyrene latex (latex A) was achieved in 10ml polypropylene, stoppered centrifuge tubes. The required volumes of water and surfactant stock solution were mixed together in the tubes and latex (2ml) added. The method of mixing adopted for the latex and powder decreases the likelihood of concentrated polymer solutions coming into contact with the adsorbent surfaces. This is particularly important where adsorption is likely to be non-reversible.

Adsorption of polymers onto the container walls was determined by blank runs to be negligible. Washing of the tubes between experiments was by the use of copious amounts of tap and distilled water only. In this way the walls will be covered with irreversibly adsorbed polymer which will prevent further adsorption occurring. The internal surface area of the containers is ca. 0.5% of the area of the powders in the vial and therefore adsorption onto container walls can be neglected.

To assay the supernatant for residual polymer content after equilibrium, the suspensions were allowed to stand for 30 minutes and the top portion of the resulting dispersion was filtered through well soaked 0.45 μ membrane filters into glass containers. The first portion of the filtrate was discarded in the event of adsorption occurring on the filtration assembly.

For the latex, the solids content was removed by centrifuging (M.S.E. HS18) at 16,000 rpm for 20 minutes in a thermostatted chamber.

To assay the supernatants containing ethylene oxide nonionic surfactants the technique of Baleux was adopted (156). 1g of iodine and 2g potassium iodide were dissolved in 100ml water. 0.26ml of this

reagent were added to 10ml of a suitable dilution of the supernatant and after 5 minutes the absorbance of the solution was measured on a scanning spectrophotometer (Pye Unicam SP800) against a blank of reagent and water. The wavelength of maximum absorption, λ_{\max} , was found to be slightly concentration dependent and calibration graphs corrected for this deviation were linear over the range measured.

For polyvinyl alcohol the analytical procedure of Garvey, Tadros and Vincent was used (145) in which the reagent consists of 0.255g iodine, 0.45g potassium iodide and 3.6g boric acid per 100ml of solution. 1ml of this reagent was added to 2ml of polymer solution in 10mm absorbance cells and after gentle mixing the absorbance was read at 670nm (Pye Unicam SP600, Series 2). Care was taken to avoid excessive agitation of the resulting solution as the formation of blue 'specks' may occur.

The presence of dissolved drug did not interfere with either assay.

4:1:2 Mercury Intrusion Porosimetry

In order to obtain a value of the specific surface area of the drug suitable for determining molecular areas of polymers at the interface, mercury porosimetry was used as this is a liquid penetration method and will therefore give a surface area measurement of the powder which describes the accessibility of the liquid to the powder surface. Of the methods useful in determining surface areas (e.g. nitrogen adsorption, coulter counter, air permeability) this is the most representative of the experimental situation where penetration of the aqueous polymer solution into interparticulate pores occurs. In addition to providing an estimate of this value, the technique may also be used to determine the pore size distribution of the sample.

For circular pores and void spaces, the surface tension of the mercury, γ , acts along the circle of contact for a length equal to the circumference of the pore. If the pore is of radius r , the resulting force is equal to $2\pi r\gamma$ and the force tending to push the mercury out of the pore in a direction normal to the pore opening is $2\pi r\gamma \cos\theta$, where θ is the contact angle. The force applied to the mercury to achieve penetration acts over an area equal to the circle of contact between mercury and pore and is equal to $\pi r^2 P$ where P is the applied pressure. At equilibrium these two forces are equal and hence

$$\pi r^2 P = 2\pi r\gamma \cos \theta$$

This reduces to the Young-Laplace equation:

$$r = \frac{-2\gamma \cos\theta}{P} \quad (4.1)$$

Pore volume distributions are measured by determining the cumulative volumes of mercury entering the pores as the pressure is increased in steps. The radii of the pores are then determined using the above equation.

A knowledge of the contact angle is required and in accordance with the manufacturers recommendation this is taken to be 130° .

The instrument used was a Model 910 mercury intrusion porosimeter (Micromeritics Instrument Corporation) having the facility to measure in the pressure range 0-50,000 psi corresponding to pore diameters of down to 3 nm. The procedure recommended by the manufacturers was followed. Essentially the technique involves initially removing any air or vapour from around the powder sample and replacing it by mercury.

The pressure inside the sample chamber is again reduced and according to equation 4.1, at such low pressures, little penetration of voids and pores occurs with a non-wetting liquid. Pressure is then applied to the mercury and the volume of penetration is measured by a moveable contact following the mercury meniscus inside a precision bore tubing connected to the sample chamber. A blank run was made with no powder inside the chamber. This allows for pores present in the chamber walls and also for the compressibility of the mercury and such readings are subtracted from the runs where powder samples are present.

Rootare and Prenzlou (157) have shown how to derive specific surface areas from pressure penetration - volume curves provided there are no pores with entrance regions smaller than their dimensions elsewhere. Under these conditions

$$S = \frac{PdV}{\gamma \cos \theta_c} \quad (4.2)$$

and PdV may be evaluated graphically between appropriate limits.

Figure 19 shows the penetration volume-pressure curves for the two batches of diloxanide furoate. The surface area is then given by the area underneath the graphs. For batch 2616 maximum penetration is not achieved until very high pressures are applied and the surface area determined becomes less reliable if this region is included. This high pressure region corresponds to the limit of accuracy of the instrument and for this reason the specific surface area of this batch was taken between the limits of 0 - 13,000 psi corresponding to surface areas where the contribution from pores below 10 nm diameter is neglected.

Batch 224231	Specific Surface Area = 1.206m ² g ⁻¹
Batch 2616	Specific Surface Area = 1.055m ² g ⁻¹

These values are far greater than results obtained from Coulter

Counter measurements and demonstrates the limited applicability of the latter method to determining surface areas of non-spherical particles with non-homogeneous surfaces.

Suitable manipulation of the data in Figure 19 permits the evaluation of a pore size distribution for the samples and these are given in Figure 20. As the mean particle sizes of the batches are 12.5μ and 16.0μ , it is most likely that down to pressures of 350 psi, corresponding to pore diameters of 500nm, the voids between particles are filled. Below this values both batches contain pores in the region of 5 - 10nm and batch 224231 contains pores with diameters of 40nm.

4:1:3 Nitrogen Adsorption Measurements

Substantiation of the pore size distribution measurements obtained by mercury porosimetry is necessary as the pore diameters found using this method are very small and correspond to pressures at the upper range of the instrument where the accuracy is limited. Gas adsorption is frequently used as an alternative as the range in which accurate pore size distributions may be made corresponds to the low values reported above.

A Quantasorb surface area analyser (Quantochrome Corporation, New York) was used for this determination. The principle of operation is that mixtures of helium and nitrogen are passed through the sample bed contained in a U-shaped cell. At the temperature of operation (liquid nitrogen) helium will not adsorb onto any surface while nitrogen is physically adsorbed onto all surfaces. The pore structure is then calculated from the amount of nitrogen adsorbed at various partial pressures. Adsorption and desorption of nitrogen occur when the sample is immersed and withdrawn from a liquid nitrogen filled vacuum flask. Changes in the amount of nitrogen in the flowing stream are sensed by a thermal conductivity detector which outputs its response onto a chart

recorder. The area of the peaks caused by adsorption or desorption should be equal, and the area of such peaks is proportional to the quantity of gas adsorbed.

Condensation of the gas occurs within the pores resulting in a thin film, thickness t , of liquid nitrogen being deposited on the walls of the pores. Lowering of the vapour pressure over the concave meniscus of the condensed vapours is related to radius r_K , of a capillary causing such an effect through the Kelvin equation

$$RT \ln \frac{p}{p_0} = - \frac{2\gamma V_L \cos\theta}{r_K} \quad (4.3)$$

where γ and V_L are the surface tension and molar volume of the condensed vapour respectively and θ is the angle of contact between the liquid and the walls of the pores. For liquid nitrogen this reduces to

$$r_K = \frac{-4.1}{\log p/p_0} \quad (4.4)$$

Thus the amount of nitrogen adsorbed is measured at various partial pressures corresponding to pores of radius r_K . The radius determined by equation 4.4 is not the true value for the pore, but corresponds to the true radius minus the thickness of the adsorbed condensed vapour film t . Values of t depend upon the packing of the nitrogen molecules at the surface and are related to the thickness of one adsorbed molecule, y , by

$$(159) \quad t = y \left[\frac{5}{\ln p/p_0} \right]^{1/3} \quad (4.5)$$

Wheeler assumed an open packing of the nitrogen molecules giving a value to y of 4.3 \AA while de Boer assumed hexagonal close packing giving a value of 3.5 \AA (158). The choice of y is critical in determining the true radius, particularly for very small pores where the adsorbed film contributes a significant amount to the pore volume. In this work the

value of 4.3 \AA for γ was used and the t values were calculated accordingly. Results of Batch 2616 shown in Figure 21 demonstrate the existence of pores with very small radii occurring below 4 nanometers. This is in reasonable agreement with determinations by mercury intrusion porosimetry where values of ca 5nm for the pore diameters were shown. A large fraction of pores is shown to exist with radii of 1-2nm. Use of the value of 3.5 \AA for γ produces a shift in the graph of Figure 21 to the left indicating even smaller pores. However, for the purpose of this work it is sufficient only to demonstrate the existence of such pores with small radii, rather than to give absolute measurements of pore size distributions.

4:1:4 Contact Angle Measurements

The contact angle between a liquid and a surface may be taken as an index of the hydrophobicity of that surface. For hydrophilic materials the contact angle ϕ will be less than 90° and some penetration of the material by the liquid will occur if a porous material is being studied. Hydrophobic materials have contact angles in excess of 90° and penetration into pores is difficult.

Kossen and Heertjes (159) have developed a method to determine contact angles on powder compacts and Lerk et al (160) have demonstrated its applicability to pharmaceutical materials. Essentially the method involves measuring the height of a liquid drop that can be supported on a powder compact by interfacial forces, as a function of the porosity of the compact.

$$\text{For } \phi > 90^\circ, \quad \cos \phi = -1 + \frac{(2-Bh^2) \cdot 2}{3(1-\epsilon_v)} \quad (4.6)$$

$$\text{for } \phi < 90^\circ, \quad \cos \phi = 1 - \frac{2}{3(1-\epsilon_v)} \cdot Bh^2 \quad (4.7)$$

where h is the height of the drop, ϵ_v is the volume porosity of the

$$\text{compact and } B = \frac{\rho_l g}{2\gamma} \quad (4.8)$$

where ρ_L is the liquid density and γ is its surface tension.

Compacts of diloxanide furoate were prepared in $\frac{1}{4}$ inch diameter dies on a Wilkinson STD1 reciprocating tablet machine. Only a small range of porosities could be measured due to lamination of the discs at high compaction forces. Porosities were determined from a knowledge of the compact volume and the true powder volume which was found from the weight and true density of the powder. The compacts were placed on a horizontal surface and enclosed within a small perspex box where two sides were lined with filter paper soaked in the liquid under test. A single drop of liquid was placed on the compact surface through a small aperture in the enclosure lid and the height of this drop was measured by a cathetometer. Additional drops were then added to the initial drop until no detectable change in the height was observed. This value was then substituted into equation 4.6 together with the values of γ and ρ_L of a saturated aqueous solution of diloxanide furoate determined by du Nuoy tensiometer and Lipkin pyknometer respectively.

When dried, polystyrene latex is too static to be compressed and in order to determine the contact angle, a film of polystyrene was prepared by dissolving dried latex in dioxan and evaporating the solvent after spreading on a microscope slide. Distilled water was used as the contact liquid.

4:2:1 Adsorption of Nonylphenylethoxylates

4:2:1:1 Polystyrene Latex

Results for the nonylphenylethoxylates on polystyrene latex are shown in the five isotherms of Figure 22. All are of the same general form. Adsorption increases with concentration until, at a point greater than the measured critical micelle concentration, the amount adsorbed tends to a saturation value. These graphs are Langmurian in form and may

be fitted to the linear derivation of the equation. This indicates that only a monolayer of the adsorbing species has formed at the interface and therefore the molecular areas at the interface may be derived. At high surface coverages the adsorbed surfactant may attach to the surface via the hydrophobic chains or through both. Anchoring of the non-polar alkyl-benzene group to the surface may occur as a result of hydrophobic bonding which is a unique property of non-polar groups. On dissolving a liquid hydrocarbon in water a large negative entropy change occurs which is directly related to the structuring of solvent molecules around the non-polar chain. Counteracting this effect, the apolar groups withdraw from the aqueous phase and tend to cluster together. For surface active agents the clustering takes the form of micellization with the result that structured water around the hydrocarbon chains is released and this gain in entropy of solvent molecules far outweighs the enthalpic requirements of breaking solvent-solute bonds (161).

A similar entropy increase will occur on adsorption of a hydrocarbon chain at a solid hydrophobic interface. As hydrophobic bonding is related to the structuring of solvent molecules around the apolar chain, a greater entropy gain will occur on the adsorption of a longer hydrocarbon chain and hence adsorption will become more favourable.

The hydrophilic ethylene oxide chains may adsorb as a result of one or more of several mechanisms. Corkill, Goodman and Tate (67) have demonstrated that hexaoxyethylene glycol will adsorb at a Graphon interface from aqueous solution. No charged groups are present on this material and these authors showed by water adsorption measurements that the surface was extremely hydrophobic. Adsorption may occur through hydrophobic bonding between the surface and the constituent- CH_2 - groups of the ethylene oxide chain. Such an explanation may be used to interpret the data obtained with

The non-ionic surface active agents above. Alternatively hydrogen bonding may occur between the ether oxygen atoms of the hydrophilic chain and the polar surface groups of the polystyrene latex. Dobbie et al (97) have shown that such bonding does occur at low pH values where surface carboxyl groups are present in the unionized state. It may be expected therefore that under conditions where these surface groups are ionized, less adsorption will occur. However results with NPE13 in distilled water (pH 5.6) and in acid conditions of pH 2.3 show no significant difference (Figure 23) demonstrating that adsorption is independent of the state of ionization, in accord with the results of Ottewill and Walker (162) who studied the adsorption of a homogenous alkyl polyoxyethylene glycol monoether onto a latex. This mechanism is therefore unable to account for the adsorption observed. A further bonding mechanism may be due to hydrogen bonding between ether oxygen atoms and surface hydroxyl groups but this is difficult to substantiate as the number of such surface groups is unknown and their presence cannot be demonstrated using conductometric titration. Recently Barnett et al (see 163) have shown that for long chain polyoxyethylene glycols attachment occurs via the carboxyl surface grouping, though whether this is independent of pH is not stated. It therefore remains a possibility that bonding occurs between the solvation sheaths surrounding the carboxyl head group and the ether oxygens and that such bonding will be independent of pH.

Details of the adsorption data are given in Table 4.

Table 4

Adsorption Characteristics of Nonylphenylethoxylates on Polystyrene

Latex

	<i>Adsorption</i> $\mu\text{moles m}^{-2}$	<i>Area/molecule</i> nm^2	<i>Area/molecule at</i> <i>air/solution</i> <i>interface</i> nm^2
NP8	3.07	0.55	0.53*
NP13	1.84	0.90	-
NP20	1.20	1.38	0.82 ⁺
NP30	0.89	1.85	1.01 ⁺
NP35	0.68	2.43	-

* Ref (35)

+ Ref (137)

Molecular areas were determined from the plateau region of the isotherms. The increase in surface area covered with increasing chain length would suggest that the molecule adopts a somewhat flattened configuration at the interface. If adsorption occurred via the hydrophobic moiety only, vertical stacking would be expected to occur and the area occupied would be independent of chain length. It has been shown that for short chain surfactants a close-packed vertically orientated monolayer occurs (82). With higher ethylene oxide contents the molecules tend to loop themselves around the surface (154) and the monomolecular area will hence be greater in these cases.

Kuno and Abe (136) have previously reported details of NPE adsorption onto calcium carbonate and have shown that the areas occupied at the interface are smaller than those at the air-water interface. They

considered that the surfactant is not adsorbed as individual molecules but as micelles. Mathai and Ottewill (164) considered it misleading to assume that the aggregates on the solid-solution interface have the same structure as micelles in the bulk solution. The NPE's studied were of low ethylene oxide content and the adsorption may be explained by considering the low cloud points of the materials used. Ottewill has suggested that when adsorption occurs with such materials the surface may assist in nucleation and condensation of the surfactant causing a reduction in the lower consolute boundary and hence adsorption in a condensed state (61). Repetition of the above work by Akers and Riley (165) gave substantially different results with high molecular areas at the interface. They extended the original work to include chain lengths of up to 50 ethylene oxide units. The surfactants used were similar to those of Kuno and Abe, and it must be concluded that the differences observed between the two sets of results are a consequence of different powder samples employed. Continuing their work on NPE adsorption Kuno and Abe (166) gave details of results found on adsorbing the surfactants onto a more hydrophobic powder, carbon black. Langmurian curves were obtained in all cases and the cross sectional areas per adsorbed molecule were far greater than those observed on calcium carbonate. They considered that adsorption occurred through the lipophilic part of the molecule and a general relationship was found between the molecular area and the number of moles of ethylene oxide, n , per molecule.

$$46.7n^{0.74} = A \text{ nm}^2$$

Expressions of form in the above equation have been found for many systems when a homologous series of surfactants is studied.

From Table 4 it is apparent that the areas occupied on polystyrene latex are greater than those at the air-water interface, with the possible

exception of NPES. This is consistent with the idea that these molecules lie in an extended configuration on the surface. For NPES the results may indicate that the molecules are vertically orientated with the alkyl chain adsorbed on the surface and the hydrophilic ethylene oxide chain projecting into the aqueous phase. Confirmation of this is provided by a discussion of the thickness of the adsorbed layer in Section 5.

A general relationship between molecular area and ethylene oxide content has been provided by McCracken and Datyner (167) for the NPE - latex system:

$$A = 0.21n^{0.5} \text{ nm}^2 \quad (4.9)$$

However such an equation does not fit the data in Table 4. and neglecting NPES, the equation

$$A = 0.068n \text{ nm}^2 \quad (4.10)$$

can be used to determine molecular areas determined in this work. The discrepancy between equations 4.9 and 4.10 may be related to the type of surfaces found on the latex, although this cannot be definitely concluded as no details of the method of preparation of the latex used in reference 169 are provided. Relationships of the form in equation 4.10 (i.e. proportionality between A and n) have been found by several authors e.g. Stryker, Helin and Mantell (168) who measured adsorption on polystyrene latices and Rupprecht and Liebl (169) who measured adsorption on silica.

4:2:1:2 Diloxanide Furoate

Figure 24 illustrates the adsorption isotherms obtained on the drug powder and again these show Langmuirian isotherms with the formation of a monolayer of material where the graphs level out. Measured c.m.c. values do not coincide exactly with the attainment of the plateau region, but

are in general some way below. Values of the area occupied per molecule at the drug interface based on specific surface area measurements determined by mercury porosimetry are shown in Table 5.

Table 5

Adsorption Characteristics of Nonylphenyethoxylates on Diloxanide Furoate B.P.

<i>Surfactant</i>	<i>Amount adsorbed</i> $\mu\text{moles g}^{-1}$	<i>Area/molecule</i> nm^2
NP8	1.95	1.02
NP13	1.30	1.54
NP20	0.60	3.22
NP30	0.43	4.65
NP35	0.39	5.00

The values here reported are far greater than those obtained previously on polystyrene latex and this may be a result of using surface area measurements obtained by different means. While surface area measurements from electron micrographs will be fairly accurate, those from mercury porosimetry are subject to errors inherent in the technique such as insufficient evacuation of the sample although reasonable steps were taken to ensure that this did not occur.

It is well known however that the amount of adsorption strongly depends on the nature of the surface onto which the polymer adsorbs. This is clearly demonstrated by the work of Kuno and Abe (136,166) who used two powders as adsorbents and whose surface areas were determined by the same means - nitrogen adsorption. Vast differences in the amount adsorbed at each interface indicate the effect that the surface has on adsorption.

In agreement with the results on polystyrene latex a linear relationship was observed between the molecular area and ethylene oxide

content. Graphs relating these two parameters are shown in Figure 25 for both materials to demonstrate this effect.

The adsorption of nonylphenylethoxylates onto other materials of pharmaceutical interest has been investigated by Otsuka et al (35) who used sulphathiazole and naphthalene as substrates. In the case of sulphathiazole S-shaped isotherms were obtained and molecular areas indicated multilayer formation. This was in contrast to the results with naphthalene where Langmuirian curves were found. Values of molecular areas with this material gave results more in accord with values obtained in this work on diloxanide furoate.

Elworthy and Guthrie have investigated the adsorption of nonionic surfactants of the alkyl polyoxyethylene glycol type onto griseofulvin (170) as a function of temperature. Langmuir isotherms were obtained and molecular areas of surfactant at the interface indicated that the hydrocarbon chain was adsorbed end on to the surface with the polyoxyethylene groups bent towards the surface and also attached to it. Their results showed greater areas at the solid-solution interface than at the air-solution interface showing that the hydrophilic groups contribute more towards the occupied area on the solid than at the air interface. It is interesting to note that these authors found little difference between the amounts adsorbed for commercial surfactants and synthetic materials of the same chain length where the chain width distribution may be considered narrow.

4:2:2 Adsorption of Pluronics

4:2:2:1 Adsorption on Polystyrene Latex

Little published data is available concerning the adsorption characteristics of the Pluronics at the solid-liquid interface and as far as is known, none has appeared in the pharmaceutical literature

despite the fact that such surfactants are used in the manufacture of pharmaceutical preparations.

Adsorption isotherms for Pluronics L61, L62, L64 and F68 are shown in Figure 26 and those of F38, F68, F88 and F108 in Figure 27. The former group of surfactants form a homologous series, the ethylene oxide content increasing with the last digit in the code while the hydrophobic polyoxypropylene (POP) region remains constant. It should be noted that the latter group does not constitute a homologous series as the POP region increases in molecular weight from F38 to F108 and the ethylene oxide content is expressed as a percentage of the total molecular weight. In order to prepare solutions of L61 it was found necessary to prepare a stock solution of surfactant in ice cold water before diluting to the required strength and warming to 25°C, the equilibration temperature.

In all cases the curves may be fitted to the Langmuir isotherm with maximum plateau values occurring near the measured critical micelle concentration. Measurements on quartz show similar isotherms for Pluronic L64 with attainment of a plateau in the region of 300 p.p.m. (171) and adsorption was found to be reversible. For Pluronic L44, a more hydrophobic surfactant, adsorption onto sand was shown to be of the multilayer type (172) with adsorption continually increasing with equilibrium concentration. The explanation for this behaviour was interpreted by means of the equilibrium equation:

Micelles in solution \rightleftharpoons Single molecules in solution \rightleftharpoons Molecules adsorbed at the surface.

In cases where micelles are present, the micelles compete with surface adsorption for the individual surfactant monomers preventing a build-up of single molecules in solution so that adsorption will not change significantly above the c.m.c. For Pluronics the author stated that

little micellization occurs and consequently the equilibrium is shifted to the right in the above equation. Ottewill has given an alternative explanation in terms of the configuration that an adsorbed molecule adopts at the interface (61). He considered that at high surface coverages the molecules were orientated in such a way that the hydrophilic chains prevented exposure of the hydrophobic chains to the aqueous phase, preventing further adsorption of surfactant molecules by hydrophobic bonding. In this case the ethylene oxide content per molecule of Pluronic is low and shielding of the polyoxypropylene units from further adsorption may be impossible causing the multilayer adsorption observed experimentally.

Howard and McConnell (173) have investigated the adsorption of several Pluronics onto carbon and nylon fibres and although a homologous series was not studied it was shown that for polymers of approximately the same molecular weight, adsorption decreases on a weight basis with an increase in ethylene oxide content. Molecular areas were not assessed due to difficulties in the measurement of the surface areas of the adsorbents.

The determination of the critical micelle concentrations of the Pluronics is a subject which has achieved considerable interest over the years. Wide variations in reported values are evident and in some cases no evidence of micellization has been found. It is therefore of interest to relate the adsorption isotherms to the critical micelle concentrations as there is often a correlation between them - usually maximum adsorption occurring at or near the cmc. For example the results of Corkill et al (67) show that the critical micelle concentration does not coincide exactly with maximum adsorption but may occur before or after the adsorption plateau. This is in agreement with Elworthy and Guthrie (170) for their work at the griseofulvin-solution interface.

The results of Mathai and Ottewill show that the critical micelle concentration occurs at the initial steep rise of the isotherm (164) although in this work multilayer adsorption was found to occur. In general it may be said that for nonionic surface active agents where micellization is known to occur the critical micelle concentration corresponds to a point between the equilibrium concentrations where adsorption increases rapidly and where maximum adsorption occurs. The values of cmc's in the literature for the Pluronic series vary considerably and appear to depend on the method used for its determination. From Table 1, it can be seen that using dye solubilizing techniques, Sasaki and Shah (142) obtained values for Pluronic L64 of 2.2g dl^{-1} (7.5×10^{-3} moles l^{-1}) and 2.4g dl^{-1} (1.1×10^{-2} moles l^{-1}) for Pluronic L62. These results are far greater than those usually observed for nonionic surfactants (ca. $0-300 \times 10^{-6}$ moles l^{-1}) and are in conflict with the results of Schmolka and Raymond (139) who again used dye solubilization but found typical c.m.c. values in the range $0.0014 - 0.0073\text{g dl}^{-1}$. These authors also found good agreement between these values and measurements from surface tension data. A value for L64 intermediate to these extremes has been reported by Becher (141) who determined the c.m.c. by iodine solubilization giving the value as 0.026g dl^{-1} . Commenting on the dye solubilization methods used, Anderson (174) states that the benzopurpurine solubilization method adopted by Schmolka and Raymond gives unsatisfactory results due to the low precision of the technique and that non-linear relationships between optical density and log concentration do not provide satisfactory evidence of micelle formation. From surface tension measurements the author concludes that micelle formation occurs around $3 \times 10^{-5}\text{g dl}^{-1}$ for L62 which is significantly lower than the results of Schmolka and Raymond.

Using light scattering Mankowich (175) and Cowie and Siriani (176) have shown that little or no aggregation takes place in an aqueous system

and this is corroborated by the measurements of Dwiggins et al (177) who performed ultracentrifugal measurements.

Results from this work tabulated in Table 1 show values in close agreement with Schmolka and Raymond despite the fact that different techniques were used. It should however be recognized that breaks in the iodine absorption concentration plots may be due to partial exhaustion of the dye as suggested by Anderson and not specifically due to micelle formation. Recent light-scattering studies by McDonald and Wong (178) show that Pluronic L64 does not form aggregates up to concentrations of 20% w/v at 25°C. On increasing the temperature, aggregation was shown to occur with concentrations in excess of 20% w/v. Results with L62 and F68 also demonstrate that no aggregation occurs at 25°C (179). These authors suggest that the Pluronics may behave in a different manner to other nonionic surfactants and conclude i) there are temperature ranges where no micellization occurs ii) growth of aggregates to a stable size takes place over far wider concentration ranges than for other nonionic surfactants iii) methods normally used to determine cmc's may be inaccurate in the case of the Pluronics.

Studying the interfacial properties of Pluronic solutions by surface tension, Prasad et al (180) have demonstrated the existence of one inflection at very low concentrations. The use of dye solubilization techniques revealed a break in the absorbance-concentration plots at much higher concentrations which were close to values found by Saski and Shah (142). These two breaks in the results were ascribed to the formation of two types of aggregate. At low concentrations the individual monomers undergo a conformational change in which the hydrophobic polyoxypropylene region is coiled in the centre and the polyoxyethylene chains form a shield around this core. The existence of such 'monomolecular-micelles' has previously been postulated by Sadron (181). At high

concentrations aggregation of the monomer units occurs resulting in a more conventional micelle.

The rapid rise in adsorption onto latex observed with all the Pluronics does occur in the region of the measured critical micelle concentration, as is also the case with the nonylphenylethoxylates. It is therefore possible that adsorption of monomolecular micelles occurs from solution onto the surface although the measured values of cmc used in this work are greater by approximately one order of magnitude than those reported by Prasad et al. Further association of monomers to multimolecular aggregates was shown to occur at 0.1 g dm^{-3} for F68 by these authors. The adsorption isotherm for this copolymer was extended to cover equilibrium concentrations in excess of this value however, within experimental error, no further adsorption could be detected above the plateau region previously attained at low concentrations. If adsorption of such aggregates occurs, re-arrangement of the molecules must take place after adsorption with the subsequent destruction of the micelle structure and release of some copolymer molecules into the bulk solution. Alternatively, an adsorbed layer of previously bound surfactant protects the surface from further adsorption in the manner suggested by Ottewill (61).

Consideration of the interfacial areas occupied on the latex surface is given in Figure 28 for the Pluronics forming a homologous series i.e. L61, L62, L64 and F68. Increasing the ethylene oxide content increases the area occupied as found previously for the nonylphenylethoxylates, and extrapolation of the curve to zero hydrophilic content indicates that the hydrophobic POP region adsorbs on the surface with an area of 2.4 nm^2 or 0.08 nm^2 per POP unit. This value is smaller than the value obtained for the polyoxyethylene unit of 0.13 nm^2 when it adsorbs on the surface as linear coils (182). The propylene oxide unit is more bulky than that of the ethylene oxide unit due to the presence of the methyl side chain and

it would appear that this region of the molecule forms small loops or is tightly coiled on the surface. The value of 0.08nm^2 per POP unit may be compared with values of $0.017 - 0.073\text{nm}^2$ per POP unit obtained at the solution - air interface for several of the Pluronics (180).

Values of the total molecular areas at the interface are reported in Table 6 for the plateau regions of the isotherms.

Table 6

Molecular areas of Pluronics at the Polystyrene latex - solution interface.

Surfactant	Area per molecule (nm^2)	
	Determined Experimentally	From Molecular Models (182)
L61	2.85	2.97
L62	3.20	3.69
L64	5.90	10.16
F38	6.51	(12.54)
F68	15.10	23.08
F88	17.52	(29.70)
F108	24.26	(42.90)

The results obtained are far greater than those observed at the air-solution interface (180), but considerably less than those at the solution-quartz interface (171) and again shows the great influence the nature of the interface has on adsorption. Molecular areas increase with increasing ethylene oxide content and may be explained by the adsorption occurring through the hydrophilic chains in addition to the POP chain for reasons stated previously where the adsorption of the nonylphenylethoxylates was studied.

The value of the molecular area obtained by adding the area of the polyoxypropylene region obtained above to the molecular model for the POE units of $0.13\text{nm}^2/\text{unit}$ gives close agreement with experimentally determined values for L61 and L62 indicating that for these copolymers the polyoxyethylene chains adsorb flat onto the surface and do not penetrate into the bulk solution. For Pluronics L64 and F68 the experimentally determined values of monomolecular areas are much less than those predicted by the models and if it is assumed that adsorption of the POP region proceeds as for surfactants of the same POP molecular weight i.e. L61 and L62, the polyoxyethylene chains must adsorb as loops on the surface. Using these models it may be shown that for the other Pluronics used (F38, F88 and F108) adsorption of the POE chains must also occur via loops. However for these surface active agents the picture is complicated by the fact that both the POE and POP regions vary. Glazman and Blashchuk (183) have shown that for a series of polyoxyethylene compounds the area per POE unit strongly depends on the hydrophobic chain attached to it. When the hydrophobic chains were straight chain alkyl groups, it was found that increasing the alkyl chain length decreased the area per POE unit. Values of the area per POE unit obtained varied between 0.13 and 0.07nm^2 on extending the alkyl chain length from C_4 to C_{16} and maintaining the hydrophilic chain constant. Therefore, as the hydrophobic and hydrophilic units are not constant for F38, F68, F88 and F108, molecular models for these surfactants based on 0.08nm^2 per POP unit and 0.13nm^2 per POE unit derived from those Pluronics which do form a homologous series should be treated with caution.

4:2:2:2 Adsorption on Diloxanide Furoate

Similar adsorption isotherms to those on polystyrene latex are found with diloxanide furoate (Figure 29). The molecular areas given in Table 7 show that far higher molecular areas are found with this substance than on the latex. Thus figures for Pluronic L64 are 18.20nm^2

and 5.90nm^2 for drug and latex respectively. This is in accordance with the adsorption characteristics of the nonylphenylethoxylates.

Table 7

Adsorption Characteristics of Pluronics on Diloxanide

Furoate B.P.

Surfactant	Plateau Adsorption $\mu\text{moles g}^{-1}$	Area per molecule nm^2
L61	0.192	10.42
L62	0.180	11.12
L64	0.110	18.20
F68	0.045	44.50

Discrepancies between the molecular areas determined on the two adsorbents may be explained by the different technique used to measure the specific surface areas as discussed in Section 4:2:2. Alternatively, polymer-adsorbent interactions will differ on the two surfaces and consequently the mode of adsorption may not be the same. It would appear reasonable to assume that in both cases the hydrophobic region of the molecule is adsorbed and that the ethylene oxide chains penetrate into the aqueous solution in the form of loops or tails. An indication of the conformation at the interface may be derived from measurements of the adsorbed layer thickness and such determinations are performed in Section 5.

4:2:3 Rate of Surface Active Agent Adsorption

In order to determine adsorption isotherms, true equilibrium must be established between surfactant molecules at the interface and those in the bulk aqueous phase. For short chain polymers it is often considered that saturation coverage occurs within 24 hours, although

times much less than this may actually be required (82). Elworthy and Guthrie (170) found that the adsorption onto griseofulvin of alkyl polyoxyethylene glycols was complete within 16 hours, while Kayes (154) using micro-electrophoresis, found adsorption of these compounds onto polystyrene latex to be almost instantaneous.

Initial results with polystyrene latex indicated that saturation coverage was complete with 1 hour. Due to the fairly lengthy procedure of preparation, centrifugation and assay of the supernatant, this was the minimum time in which adsorption onto latex could be monitored.

To prepare diloxanide furoate dispersions for kinetic adsorption studies the required volume of surfactant solution was added directly to the drug powder. This one stage process eliminates the possibility of concentrated surfactant solution coming into contact with the powder surface. Dispersion of the powder was achieved by hand shaking only, up to times of 10 minutes and incomplete exposure of the powder surface to the surfactant solution is possible. Rapid manipulation permitted adsorption during periods down to 2 minutes to be measured. Initial concentrations were chosen so that for each surfactant studied, two points were determined corresponding to maximum and sub-maximum adsorption at equilibrium.

Results are shown in Figure 30 where the amount adsorbed is plotted against the logarithm of time. For all surfactants used, the time needed to establish equilibrium for sub-maximum adsorption is very short. In these cases the change in the amount of polymer adsorbed after 2 minutes is negligible and the total amount adsorbed corresponds to a point on the Langmuir isotherms (Figures 24 and 29) indicating that adsorption is complete.

Where adsorption proceeds to maximum surface coverage (lines a,b and c) completely different results are obtained and time dependence is demonstrated. Initially high amounts of surfactant are adsorbed after which a gradual decrease occurs leading to equilibrium surface coverages after periods of greater than 5 hours. Equilibrium measurements determined after 24 hours are therefore fully justified.

Changes in surface area caused by dissolution or solubilization of the drug are not responsible for the apparent decrease in adsorption with time. For curve (a) this would require a decrease of nearly a third of the total accessible surface area, but measurements of the amount of drug remaining undissolved after 24 hours show that less than 2% of the drug had dissolved. Adsorption of micelles or surfactant aggregates may provide one explanation. Multilayer adsorption of surfactants has previously been demonstrated (136,164) although the exact nature of the adsorbed phase is not clear. For nonionic surfactant micelles and the monomolecular micelles proposed for the configuration of the Pluronic at low concentrations, the ethylene oxide chains surround the hydrocarbon core and initial contact of the micelle at the solid-solution interface will occur through those hydrophilic chains if micellar adsorption takes place. Rearrangement of the molecules within the adsorbed micelle may then occur leading to the release of some of the monomers into solution, and the extension of the remaining adsorbed molecules on the surface. For the Pluronic, the monomolecular micelle will be in a contracted form and will occupy a smaller interfacial area than the extended monomer when adsorbed. It is therefore possible that more surfactant can be accommodated at the surface initially. Extension of some molecules causes desorption of others resulting in a gradual loss of surfactant at the interface. For this to occur, the entropic and enthalpic considerations associated with desorption and extension of molecules leading to adsorption occurring via both hydrophobic and hydrophilic chains, must outweigh the

same considerations of the monomolecular micelles adsorbing via the ethylene oxide chains. Without further information on the number of segments adsorbed and the energetics associated with adsorbing the hydrophobic and hydrophilic segments, this conclusion remains speculative. Experiments performed on the breakdown of micellar aggregates in free solution show that the kinetics of this dissociation is very fast, being in the order of milliseconds (184).

This may mitigate against the above explanation as equilibrium takes approximately 5 hours to establish. A further explanation involves the heterogeneous nature of the surface active agents used. Commercial samples of nonylphenylethoxylates are known to possess ethylene oxide chain lengths distributed according to a Poisson distribution (185). In free solution there will be a range of monomer molecular weights and it is known that low molecular weight fractions adsorb at a faster rate than high molecular weight fractions due to greater diffusion rates (186). Displacement of the smaller molecules by larger ones may occur resulting in a decrease in the amount of surfactant adsorbed with time. Such displacement has previously been found by Kolthoff and Gutmacher (187) who examined the time dependent adsorption of butadiene-styrene copolymers on carbon black. Molecular weights of the polymers used were high and the displacement occurred over several hours. In the present work, molecular weights are comparatively low and the decrease in the amount of adsorbed surfactant occurs within a few minutes. This may be explained by the few points of contact between surfactant monomer and surface which facilitate desorption from the surface. It will be shown in Section 7 that desorption of the nonylphenylethoxylates from the diloxanide furoate surface is rapid - a point which substantiates the above reasoning.

4:2:4 Adsorption of Polyvinyl Alcohol

4:2:4:1 Polystyrene Latex

Six of the fractionated polyvinyl alcohol samples were used for adsorption studies in order that a molecular weight range of 5,000 to 100,000 would be studied. Adsorption of PVA is known to be affected by the degree of hydrolysis of the sample (85) and therefore samples were chosen which had less than 2% deviation in the experimentally determined hydrolysis values. The fractions used were: D, F, J, M, N, O.

Results of the adsorption obtained at 25°C are shown in Figure 31 where it may be seen that maximum adsorption increases with molecular weight. Adsorption is initially rapid with a levelling effect occurring around 400p.p.m. However a true plateau is not attained and adsorption continues to increase gradually over the concentration range studied. The maximum amount of polymer adsorbed may give an indication of the type of adsorption that has occurred. For example, the results of Garvey, Tadros and Vincent (145) for the adsorption of PVA onto a polystyrene latex show maximum adsorption values in the range 0.9 - 2.9mg m⁻² for molecular weight fractions of 8000 to 67,000. Monolayer formation was considered to have taken place as the values of the adsorbed layer thickness were in close agreement with twice the value of the radius of gyration of the polymer molecule in solution.

Values of the amount adsorbed and apparent molecular areas are given in Table 8.

Table 8

Adsorption Characteristics of Polyvinylalcohols on Polystyrene Latex

Fraction	Molecular Weight	Amount Adsorbed at 400 ppm (mg m ⁻²)	Apparent Molecular Area nm ²
D	97,400	5.9	27.4
F	77,600	4.2	30.7
J	37,800	3.6	17.4
M	23,200	3.0	12.8
N	14,200	2.2	10.7
O	5,400	1.4	6.4

It can be seen that for fractions of comparable molecular weight the 'plateau' adsorption values reported here are greater than those given by Garvey et al for true monolayer coverage. Fler, Koopal and Lyklema (85) have studied adsorption of the same polymer at the silver iodide - water interface and have demonstrated that for a molecular weight of 53,000, approximately 1.5mg PVA adsorbs per square metre at maximum monolayer coverage. Studies by Johnson and Lewis (188) on PVA adsorption onto carbon black have shown that monolayer coverage occurred around 0.25mg m⁻² but at higher concentrations further adsorption occurred with the lower molecular weight fractions. The results presented here would therefore indicate that either the molecule is adsorbed with a small area of surface contact and with the majority of the segments projecting outwards into the surrounding solution, or that some type of multilayer formation has taken place resulting in high saturation adsorption values. The former premise is doubtful as Garvey et al have shown that where a monolayer occurs, adsorption of polyvinylalcohol molecules onto polystyrene latex takes place in the form of distorted random coils. In order to observe molecular areas as small as those given in Table 8 considerable

deformation of the coils would have to occur through compression by neighbouring anchored molecules. However such a mechanism is unlikely to occur (145).

Multilayer adsorption of polyvinyl alcohol at the paraffin-solution interface was observed by Lankveld and Lyklema (189) although kinks in the isotherms, normally indicative of multilayer formation were difficult to detect for the high molecular weight fractions. The maximum amount of polymer adsorbed was more in accord with results reported here. The general features of multilayer adsorption have been discussed on theoretical grounds by Silberberg (190) who has shown that such adsorption is possible within 20°C of the θ temperature and that the number of additional macromolecules must be less than the number of those bound by segments in the initial monolayer. He considered that multilayer formation can be regarded as incipient surface phase separation which can occur in better-than- θ conditions, whereas phase separation in the bulk solution cannot occur except under worse than θ conditions.

Studies by van den Boomgaard et al (133) on the adsorption of polyvinylalcohol fractions prepared in a manner similar to that reported here, show plateau adsorption values in excess of those reported by Garvey et al (145) for PVA fractions obtained by gel permeation chromatography onto polystyrene latex. These authors considered that the observed differences were due to the type of latex surface used in both sets of experiments. In the former case, a surfactant-free technique was used to prepare the latex, while Garvey et al employed a latex prepared by emulsion polymerization, using sodium laurate as the emulsifier.

The latex, prepared by dispersion polymerization, was thought to have a more hydrophobic surface, accounting for the high adsorption values

observed. The nature of the surface has been shown to have a pronounced effect on PVA adsorption as the work by Tadros (191) on adsorption onto silica demonstrates. Increasing the negative surface charge, through increasing the pH, causes a reduction in the amount adsorbed and many explanations for this decrease are given. For example, it is suggested that this may be due to a screening effect of hydrated counter ions, or that hydrogen bonded water molecules are preferentially adsorbed compared to PVA segments at these negative sites. Figure 31 demonstrates the effect that a change in pH has on PVA adsorption onto polystyrene latex. For fraction F little change in the plateau value is observed on reducing the pH from that of distilled water (pH 5.6) where the vast majority of surface carboxyl groups are ionized, to a pH of 2.5 where 2% remain ionized. Complications caused by acid hydrolysis of the acetate groups may be discounted as this would lead to a reduction in the total amount adsorbed (85). Adsorption onto polystyrene latex and silica would therefore appear to occur via different mechanisms. From ellipsometric studies of PVA adsorption onto silicas of differing surface hydrophobicity, Fler and Smith (192) suggest that on hydrophilic surfaces, hydrogen bonding occurs between the silanol groups and the carboxyl group of the acetate residues, while for hydrophobic surfaces attachment occurs mainly through the acetate and methylene groups presumably by hydrogen bonding. For the polystyrene latex used in these experiments there are large areas of hydrophobic styrene residues between the surface carboxyl groups and the interface may be considered essentially hydrophobic, thus the mechanism suggested above for hydrophobic surfaces may apply and consequently adsorption will be independent of pH and surface ionization. For silica surfaces, Davydoŭ (193) has shown that the concentration of silanol groups per unit area is $2.6 \text{ groups nm}^{-2}$. Adsorption of PVA has been shown to occur via these groups (191) and with such a high concentration of closely packed groups it is perhaps not surprising that the ionization of these groups determines the extent of polymer adsorption.

Van den Boomgaard et al have concluded that even though no kinks were observed in the adsorption isotherms (except for low molecular weight fractions) multilayer adsorption of PVA onto the latex occurred. This was deduced from the quantity of material adsorbed and from the thickness of the adsorbed layer. Results reported here show plateau values greater than those reported for monolayer formation (145) but approaching the values for multilayer formation given in reference 133. Adsorbed layer thickness measurements are therefore necessary to confirm the existence of such adsorption.

4:2:4:2 Diloxanide Furoate

Figure 32 shows the adsorption obtained for polyvinyl alcohol onto the drug powder at 25°C. With these isotherms, adsorption continued up to a plateau region where saturation occurred and no further adsorption could be detected within experimental error, except for the two lowest molecular weight fractions.

Basing the specific surface area of the powder on $1.06\text{m}^2\text{g}^{-1}$ determined from mercury porosimetry, low saturation quantities are observed in comparison with adsorption onto polystyrene latex. The actual values compare favourably with the values for monolayer formation on latex reported by Garvey (145) and it is a reasonable conclusion that such adsorption occurs with this substance. It is found that the isotherms conform to the Langmuir isotherm, substantiating the claim that monolayer formation occurs. However for a true Langmuirian adsorption process, reversibility of this process is indicated. In general this is not a feature of macromolecular adsorption as contact occurs through many polymer segments and all such segments must be desorbed together for total desorption to occur. Apparent Langmuir adsorption has been observed by several authors (see 194) for long chain polymers. Attempts to apply the

simplified Frisch-Simha-Eirich equation (44) to the results were unsuccessful - deviations being observed at high concentrations. This is not unexpected as the equation only applies to low surface coverages where interactions from neighbouring molecules become insignificant. Data points at low surface coverage are too few to permit an accurate analysis of adsorption using this equation.

From molecular models it can be shown that the maximum amount of polymer which can be adsorbed onto flat surface in the form of a monolayer is approximately 0.5 mg m^{-2} , assuming a value of 0.165 nm^2 for the surface area occupied by a PVA segment (195). For complete surface coverage, the fraction of segments in contact with the surface is given by $p = 0.5/A_s$ where A_s represents the equilibrium saturation value. As the molecular weight of adsorbate increases, A_s increases and consequently the fraction of adsorbed segments decreases. Such results demonstrate that only a small fraction of the adsorbed polymer is in close contact with the surface; the remainder projecting into the bulk solution in the form of loops and tails. Values of A_s and the area occupied per molecule are given in Table 9.

Table 9

Adsorption Characteristics of Polyvinylalcohols on Diloxanide Furoate B.P.

Fraction	A_s mg m^{-2}	Area per molecule nm^{-2}	p
D	2.30	70.3	0.22
F	2.0	64.4	0.25
J	1.33	46.9	0.37
M	1.13	32.9	0.44
N	0.95 (0.78)	25.3 (30.8)	0.52(0.64)
O	0.71 (0.50)	10.1 (18.0)	0.70 (1.0)

(brackets denote correction for adsorption into pores)

These values of p are most likely to be an overestimate as complete saturation of the surface by segments is doubtful, and no provision is made to allow for the presence of the more bulky acetate groups which form 12% of the total chain and through which hydrophobic bonding is likely to occur with the surface. Microcalorimetric measurements of the fraction of segments bound to a polystyrene surface give a value of 0.16 for p with a PVA polymer of 67,000 molecular weight (196).

Application of the exponential expression derived by Perkel and Ullman (42), relating the maximum amount adsorbed to the molecular weight

$$A_s = KM^a \quad (2.1)$$

does not give a good linear fit when the data is plotted semi-logarithmically. Deviations are observed with the two low molecular weight fractions from a line giving a value of 0.5 to the exponent a . A graph of the maximum adsorbed against the square root of molecular weight is shown in Figure 33. The dependence of A_s on $M^{1/2}$ is predicted from the F.S.E. theory and is also found experimentally for the adsorption of PVA onto polystyrene latex (145). The observed deviation at low molecular weights is likely to be a result of the existence of pores within the surface which permit the entry of small molecules but prevent entry of polymer molecules whose dimensions exceed the pore dimensions. The surface area measurements neglect contributions from pores below 10nm diameter and consequently allowance must be made for this when molecular areas are discussed.

The dimensions of flexible polymer coils in solution may be obtained by the use of suitable equations applicable to dilute solutions. The Stockmayer - Fixman equation was used to relate the intrinsic viscosity ($[\eta]$) to the molecular weight (M) of the polymer (197)

$$[\eta] = K_{\theta} M^{\frac{1}{2}} + 0.51 \phi B M \quad (4.11)$$

A plot of $[\eta]/M^{\frac{1}{2}}$ vs. $M^{\frac{1}{2}}$ yields a straight line relationship from which the intercept K_{θ} may be obtained and in addition the parameter B is found from the slope. ϕ is a universal 'constant' to which a value of 2.8×10^{21} is ascribed in θ solvents when $[\eta]$ is in units of dl g^{-1} . (59). However, Ptitsyn and Eizner (198) have concluded that ϕ is not a constant but varies according to the solvent power of the medium for the polymer chains and decreases as the solvent power increases. Flerer showed water to be a moderately good solvent for PVA and chose a value for ϕ of 2.2×10^{21} (147) while Garvey has used a value of 2.1×10^{21} (145). K_{θ} is equal to $[\eta_{\theta}]/M^{\frac{1}{2}}$ where $[\eta_{\theta}]$ is the intrinsic viscosity in a theta-solvent (144). The polymer solvent interaction parameter χ may be obtained from the second virial coefficient B , through the relationship

$$B = \frac{2v_2^2 (k_2 - \chi)}{V_1 N_A} \quad (4.12)$$

where v_2 is the partial specific volume of the polymer and V_1 is the molar volume of the solvent.

The root mean square end to end distance of the polymer molecules in solution is given by the Flory - Fox relationship (199)

$$K_{\theta} = \frac{\phi \langle h_0^2 \rangle^{3/2}}{M^{3/2}} \quad (4.13)$$

where $\langle h_0^2 \rangle^{1/2}$ is the distance in a theta solvent i.e. it is the unperturbed dimension. The radius of gyration of the molecule, $\langle s^2 \rangle^{1/2}$, is given by

$$\langle s^2 \rangle = \langle h^2 \rangle / 6 \quad (4.14)$$

and consequently the unperturbed radius of gyration can be determined on substitution of $\langle h_0^2 \rangle$ in equation 4.14. The value of $\langle s^2 \rangle^{1/2}$ in any solvent is related to the unperturbed dimensions through the expansion

coefficient α by

$$\langle s^2 \rangle = \alpha^2 \langle s_0^2 \rangle \quad (4.15)$$

and as an approximation, α is given by (145)

$$\alpha^3 = [\eta] / K_0 M^{1/2} \quad (4.16)$$

The hydrodynamic radius R_h is then related to the radius of gyration by

$$R_G = \zeta' \langle s^2 \rangle^{1/2} \quad (4.17)$$

where ζ' is a constant, independent of molecular weight and whose value is theoretically equal to 0.665.

The Stockmayer - Fixman plot for the PVA fractions is shown in Figure 34. A good linear fit is obtained at higher molecular weight but deviation is found for the low molecular weight fractions as they are outside the range of the validity of equation 4.11. This equation applies to flexible polymer coils where draining effects through the coil are negligible. Berry (200) has applied a similar equation to polystyrene fractions in two solvents and observed a similar effect of downward curvature at low M values. This disparity was concluded to be due to chain stiffness effects which become significant at low molecular weights. With very stiff chains, these conditions are attained only at very high molecular weights. The results of Banks et al confirm this experimentally (201) for cellulose derivatives in a pyridine-water theta solvent.

The extrapolated value of K_0 is $1.58 \times 10^{-3} \text{ dl g}^{3/2} \text{ mole}^{1/2}$ which is in good agreement with previous results (145) and a value of 0.473 for the polymer solvent interaction parameter χ is obtained from the value of B . Combined values of the macromolecular dimensions of PVA in water at 25°C are given in Table 10.

Table 10

Molecular Dimensions of Polyvinylalcohols in Dilute Aqueous Solution.

Fraction	Molecular Weight, M	α	$\langle h^2 \rangle^{1/2}$ (nm)	$\langle s^2 \rangle^{1/2}$ (nm)	R_h (nm)
D	97,400	1.243	35.0	14.28	9.50
F	77,600	1.224	30.7	12.55	8.35
J	37,800	1.166	19.8	8.08	5.37
M	23,200	1.129	15.4	6.27	4.16
N	14,200	1.088	11.9	4.86	3.23
O	5,400	1.011	6.8	2.77	1.83

It may be observed that the hydrodynamic radius of the polymer coils where the deviation in the A_g versus $M^{1/2}$ plot occurs, corresponds approximately to the pore radius of the powder sample where significant numbers of pores are present. This substantiates the claim that the powder acts as a molecular sieve in preventing entry of larger polymer coils into the pores. The adsorption of polymers onto well characterized powder surfaces has been used by Eltekov and Kiseler (202) to obtain a molecular weight distribution for polydisperse polymers. Using silica samples containing pores in the range 5 - 160 nm diameter, adsorption of various rubber fractions was determined from organic solvents and it was demonstrated that bi-modal mass distributions occurred with these polymers. To confirm ^{that} the increase in A_g at low molecular weights is due to a greater surface area available for adsorption on the pore walls, the adsorption of the unfractionated sample of low molecular weight PVA was compared with the adsorption of a fractionated sample of similar molecular weight. Figure 35 shows the results obtained using polystyrene latex and diloxonide furoate as the adsorbent. Little difference is observed between the two samples with the latex; however, adsorption on the powder shows that the fractionated sample adsorbs to a lesser extent than the commercial sample. Polystyrene latices have been

shown not to possess any pores (203) and therefore adsorption of the unfractionated PVA sample will be largely determined by the higher molecular weight species present. Where pores are present, adsorption onto the external surface of the powder will proceed as for a non-porous material, but in this case the smaller molecular species will enter and adsorb in the pores giving an apparent increase in the total quantity adsorbed.

The values of A_s , and molecular area at the interface must therefore all be corrected to allow for pore adsorption. The specific surface area used to determine the above parameters corresponds to a value which neglects the pore surface area i.e. it represents the external surface area. Measurements of surface area by mercury porosimetry become less reliable at the high pressures corresponding to the pore diameters found in the powder sample. In order to correct for this effect the linear region of Figure 33 was extrapolated to the lower molecular weight fractions. Corrected values of these parameters are given in Table 9, shown in parenthesis.

4:2:5 Rate of PVA adsorption

The study of the kinetics of the establishment of adsorption equilibrium is necessary for an understanding of the mechanisms involved and for an evaluation of the reliability of the data. These rates depend on the polymer, solvent and substrate and the agitation applied during adsorption. The diffusion of molecules to the surface or into pores is almost always the limiting factor in adsorption kinetics (186). Results on the adsorption of polystyrene onto non-porous chrome surfaces (203_a) show that the rate of adsorption decreases with increase in molecular weight. Howard and McConnel studied the adsorption of polyethylene oxides onto activated carbon and showed a similar dependence on the size of the molecule. The difference in

rates is due to the slower diffusion of the larger species to the surface. In their analysis of the results, Howard and McConnell have attempted to apply kinetic equations to their data. Two expressions were used (204)

$$\Gamma_t = A_s (1 - \exp(-kt)) \quad (4.18)$$

$$\Gamma_t = A_s t / (t + k) \quad (4.19)$$

where k is the time taken to reach 50% saturation. Γ_t is the amount adsorbed at time t and A_s is the saturation coverage. Equation (4.19) was found to fit the data adequately and results of k for adsorption onto nylon and charcoal were estimated to be 3.5 and 0.12 hours respectively. The longer k values observed with nylon as the adsorbent reflect the adsorption of polymer into narrow pores. Peterson and Kwei (205) measured the adsorption of polyvinylacetate from benzene onto chrome and applied the kinetic equation of the Langmuir isotherm to the results i.e.

$$\frac{d\theta}{dt} = k_1(1-\theta)c - k_{-1}\theta \quad (4.20)$$

where k_1 and k_{-1} are the rates of adsorption and desorption respectively. The experimental results of the kinetics of adsorption of PVA onto diloxanide furoate are shown in Figure 36 for two fractions D and N. Comparison between the two graphs is difficult as the rate of adsorption has been shown to be concentration dependent (205). For the data presented here, equal initial concentrations on a weight basis were used sufficient to give saturation of the surface at equilibrium. The adsorption is initially rapid but tends to a limiting value after a period of a few hours. The measurement of equilibrium adsorption values after 24 hours is therefore justifiable. Neither of the plots in Figure 36 fit any of the three kinetic equations given above, however these expressions are applicable at low surface coverages where there are too few data points to permit an accurate assessment of the line

fitting procedure. The graph obtained for the high molecular weight polymer shows that after 2 hours contact time 90% of the equilibrium saturation value has been reached whereas for the low molecular weight fraction only 75% of saturation has been attained. Both dispersions were shaken at the same rate which reduces the effect that agitation has on adsorption rates. The slower rate found for fraction N may be due to the slow diffusion of small molecules into the pores.

4:2:6 The Hydrophobic Nature of Surfaces

It has been demonstrated previously that the quantity of polyvinyl alcohol and non ionic surface active agents adsorbed on polystyrene latex and dilaxonide furoate at equilibrium differ substantially. It has long been recognized that the nature of the interface has a great effect on adsorption (186) and some authors (133) have indicated that the degree of hydrophobicity of the surface determines the extent of adsorption. The relatively large amounts of PVA adsorbed onto polystyrene latex may be the result of one or more of the following processes:

- a) incipient phase separation of polymer at the surface
- b) the adsorption of PVA aggregates from solution
- c) preferential adsorption onto hydrophobic surfaces.

Silberberg has discussed the first possibility (190) and has shown that multilayer formation may be a result of phase separation at the surface. Assuming that adsorption of the first layer of PVA occurs as random coils (see Section 4:5:2) the concentration of polymer at the interface will be in the region of 5 - 20% w/v . To ascertain whether this mechanism is possible a 14% w/v solution of the unfractionated Mowiol 8-88 ($M \approx 30,000$) was heated to determine when phase separation occurred. None was detected, even on heating to the boiling point of the solution. It therefore appears unlikely that this process is

responsible for the apparent multilayer formation on the latex.

Latex with Equilibrium

Polyvinylalcohol is a long chain polymer known to aggregate in solution. Recent work by Eagland et al (206) confirms this point but in addition, they propose the existence of two aggregating species. The first occurs at $\sim 1\% \text{ w/v}$ and is due to the association of single random-coil macromolecules while the second occurs at $3\% \text{ w/v}$ and is attributed to aggregation of these micellar spheres. The second mechanism is therefore unable to account for the higher adsorption values found as the initial concentrations used to prepare the dispersions were far less than those where reported aggregation occurs. This process can also be discounted as the adsorption of aggregates would apply to both surfaces and if this were the only mechanism involved similar saturation values would be obtained at both interfaces.

To investigate the third possibility that the differences in adsorption are due to interactions between polymer and surface based on the hydrophobic extent of the surface, contact angle measurements were made between the surface and the solution that is in equilibrium with it. Hence the polystyrene-water and dilaxonide furoate - saturated solution contact angles were determined. The experimental technique and theory is discussed in Section 4:1:4. In addition to forming the powder compacts by compressing between the steel punches of the tablet machine, a few were also prepared by compressing between paper and polyethylene film to observe the effects of the punch face on contact angle. Results are given below in Table 11.

Table 11
*Contact Angle Measurements of Drug and Latex with Equilibrium
 Solutions*

<i>Material</i>	<i>Preparation</i>	<i>Contact Angle (θ_c)</i>
<i>Polystyrene Latex</i>	-	$102 \pm 3^\circ$
<i>Diloxanide Furoate Batch 2616</i>	<i>steel punches</i>	$92 \pm 3^\circ$
<i>Diloxanide Furoate Batch 2616</i>	<i>paper</i>	$91 \pm 2^\circ$
<i>Diloxanide Furoate Batch 2616</i>	<i>polyethylene film</i>	$93 \pm 2^\circ$
<i>Diloxanide Furoate Batch 224231</i>	<i>steel punches</i>	$92 \pm 2^\circ$

Little difference is observed between the contact angles of powder compacts prepared by the methods given above and it can be concluded that compression between the steel punches is not a source of surface contamination. Reproducibility between batches is good. The latex exhibits a significantly higher contact angle, showing this to have a more hydrophobic surface than drug. The results reported here are higher than those given by Ottewill and Vincent (207) who determined contact angles by the captive bubble method. The difference between values given in Table 11 and those in reference 207 (ca 90°) may be due to the difference techniques used to prepare the latices. Ottewill and Vincent used an emulsion polymerization technique and found values for the area occupied by the surface carboxyl groups to be 2.5nm^2 per group. This is a smaller value than the charge group area reported in Section 3 and therefore the surface used by these authors will be more hydrophilic, and consequently show a lower contact angle. The paper by Tadros (191) shows that the effect of decreasing the surface hydrophobicity is to reduce the amount of PVA adsorbed. This is in accord with the results reported here where the more hydrophilic drug surface adsorbs polymer to a lesser extent than the more

hydrophobic latex.

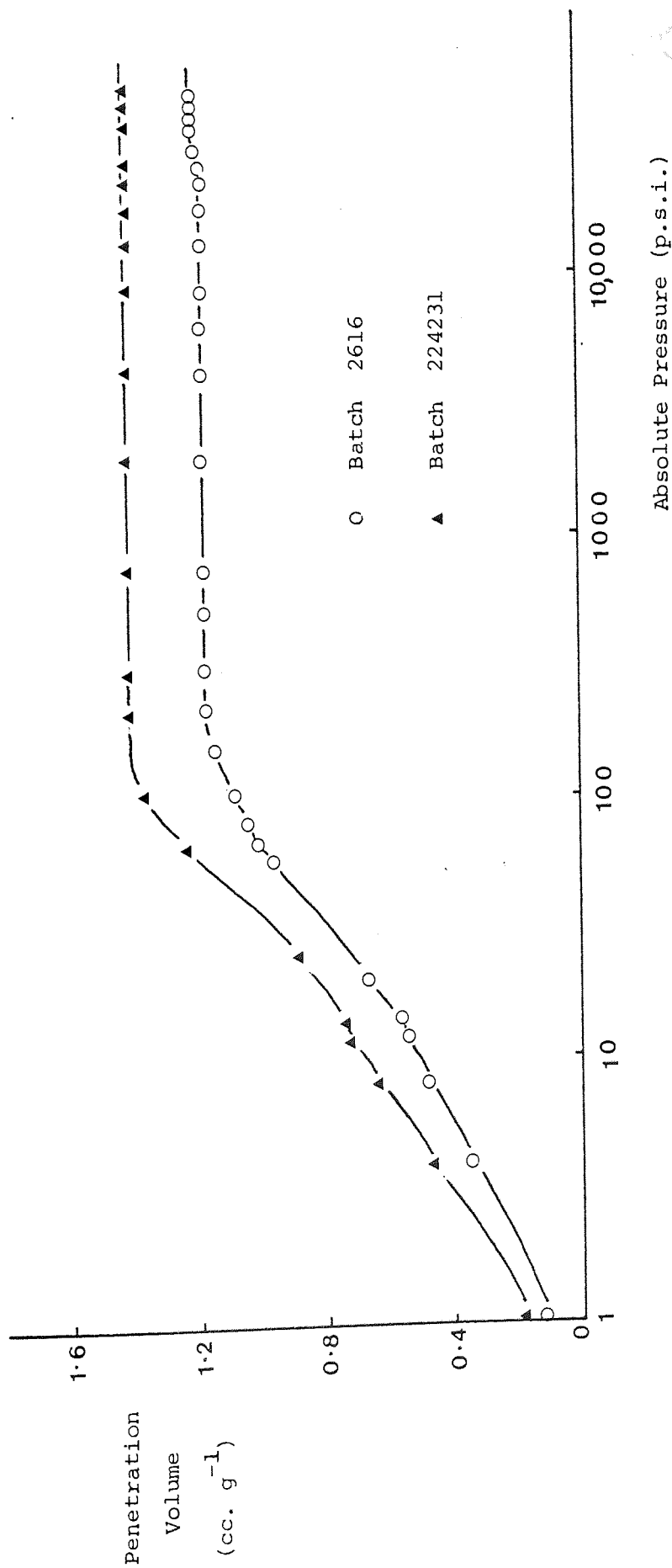


Figure 19 Penetration Volume - Pressure Curve for Diloxanide Furoate B.P.
by Mercury Porosimetry.

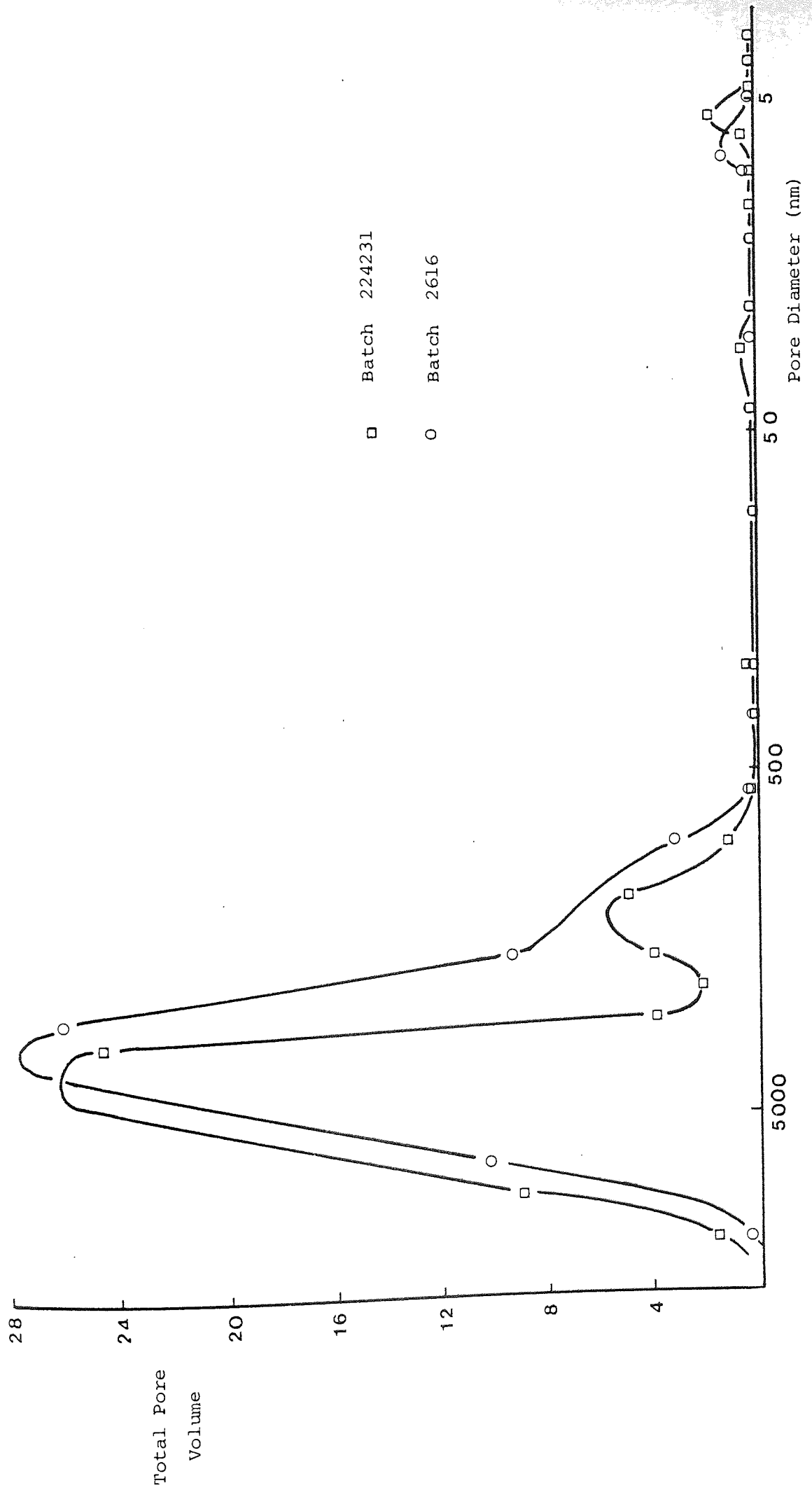


Figure 20 Pore Size Distribution for Diloxanide Furoate B.P.

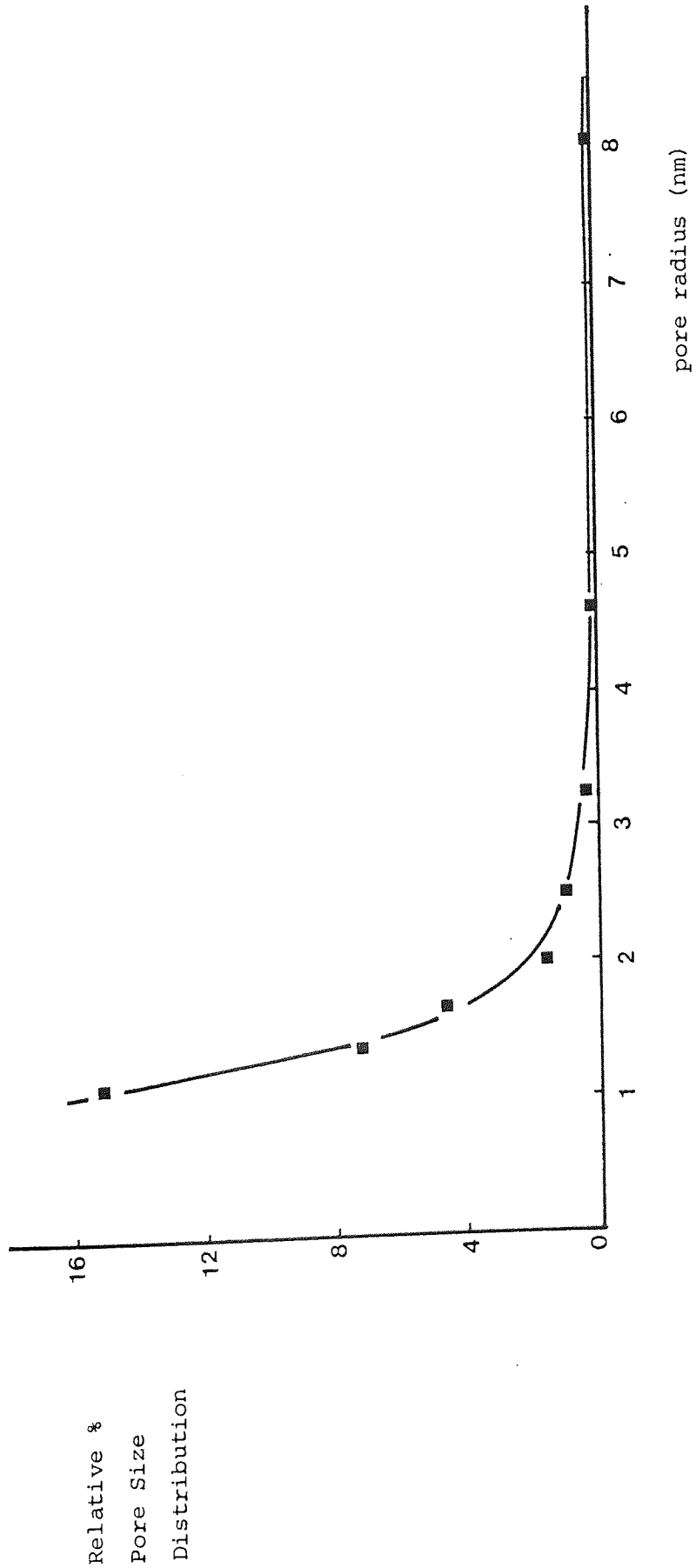


Figure 21 Pore Size Distribution of Diloxanide Furoate Batch 2616
by Nitrogen Adsorption

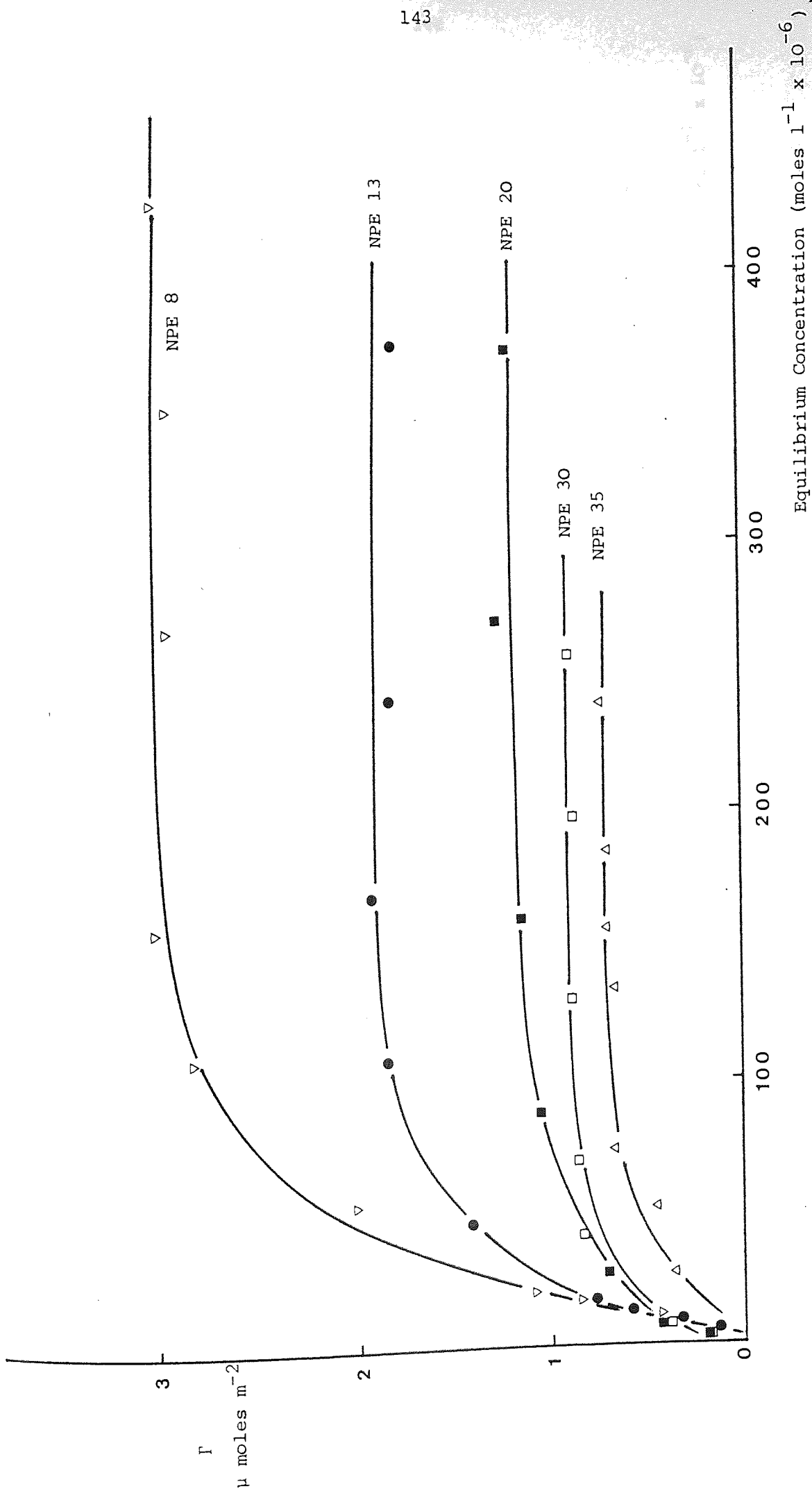


Figure 22 Adsorption Isotherms (25°C) of Nonylphenylethoxylates on Polystyrene Latex

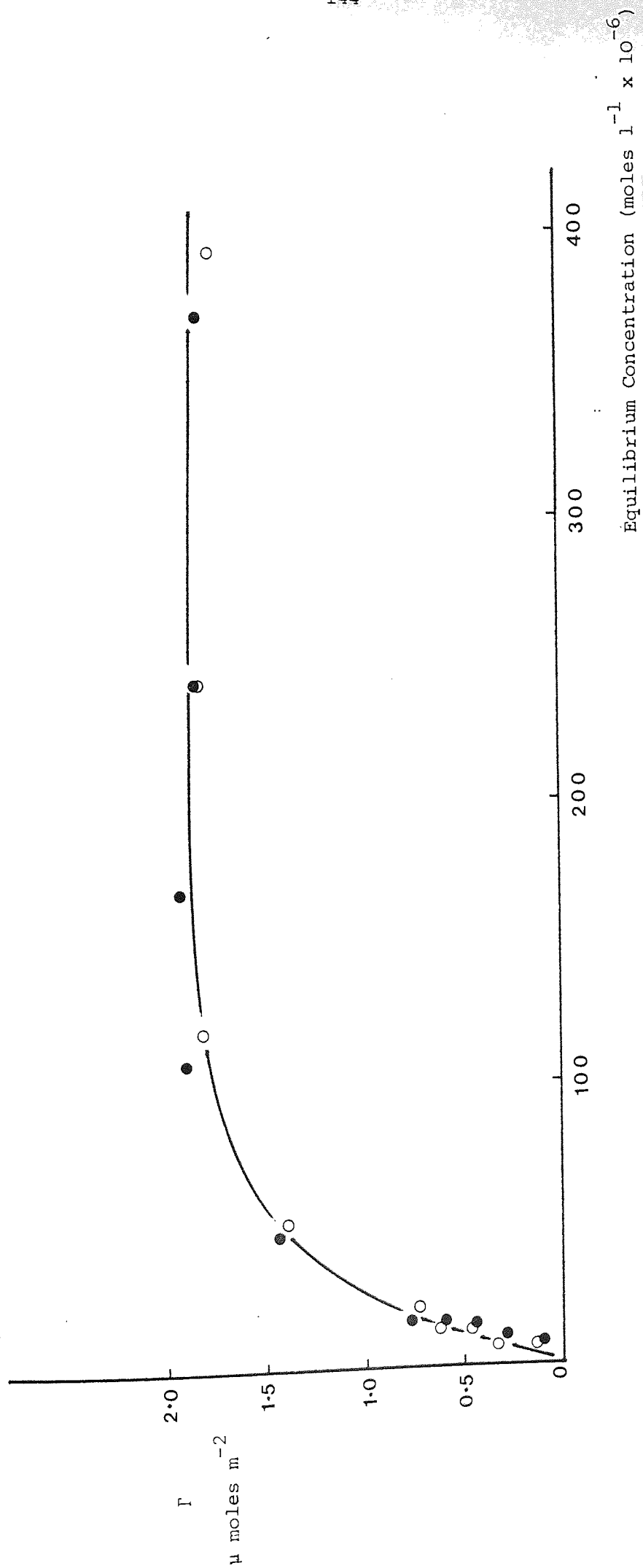


Figure 23 Adsorption Isotherms (25°C) of NPE 13 in Distilled Water (O) and at pH 2.3 (●) On Latex.

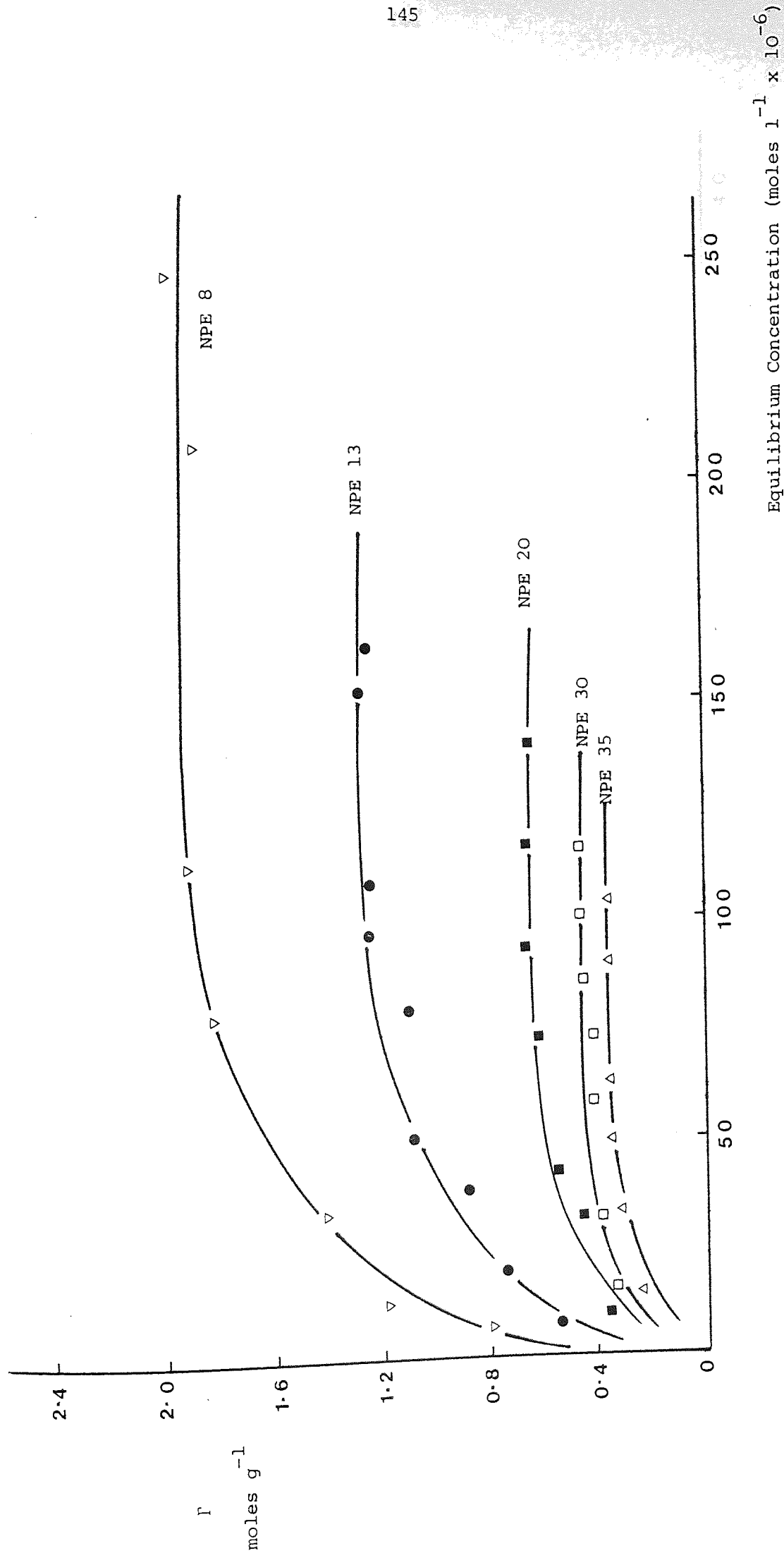


Figure 24 Adsorption Isotherms (25°C) of Nonylphenylethoxylates on Diloxanide Furoate B.P.

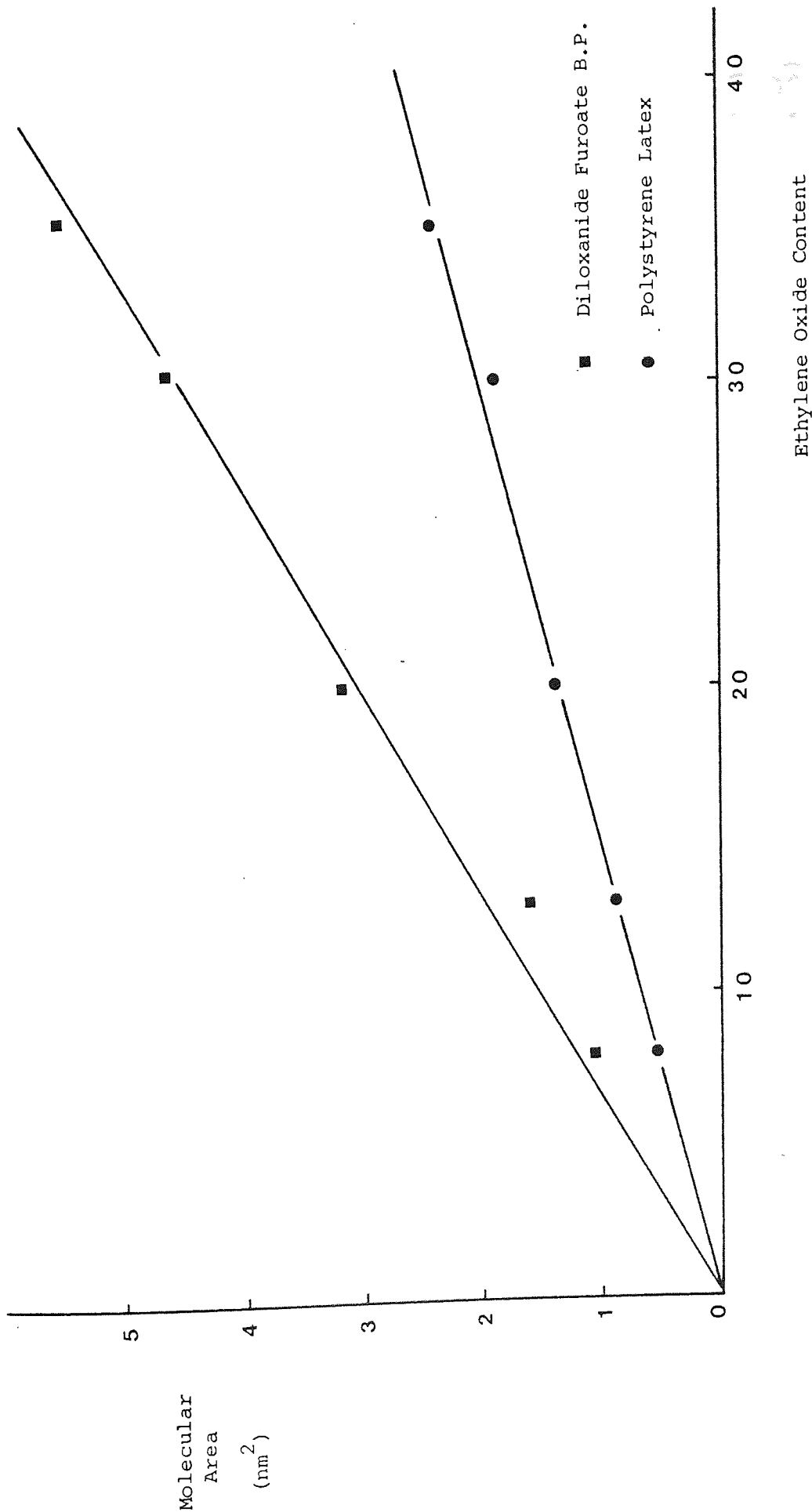


Figure 25 The Dependence of Molecular Area of Nonylphenylethoxylates on the Number of Ethylene Oxide Units per Molecule.

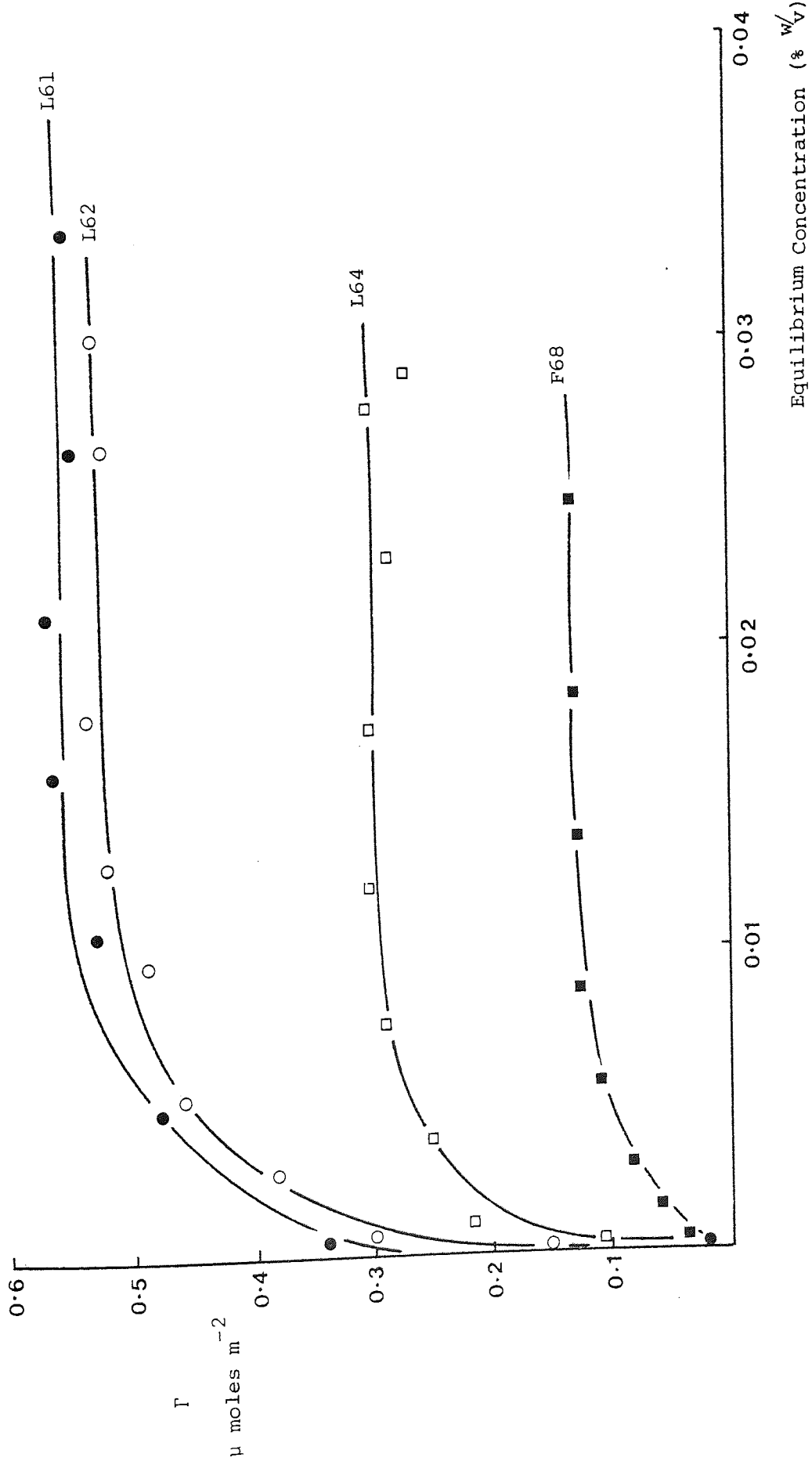


Figure 26 Adsorption Isotherms (25°C) of Pluronics on Polystyrene Latex

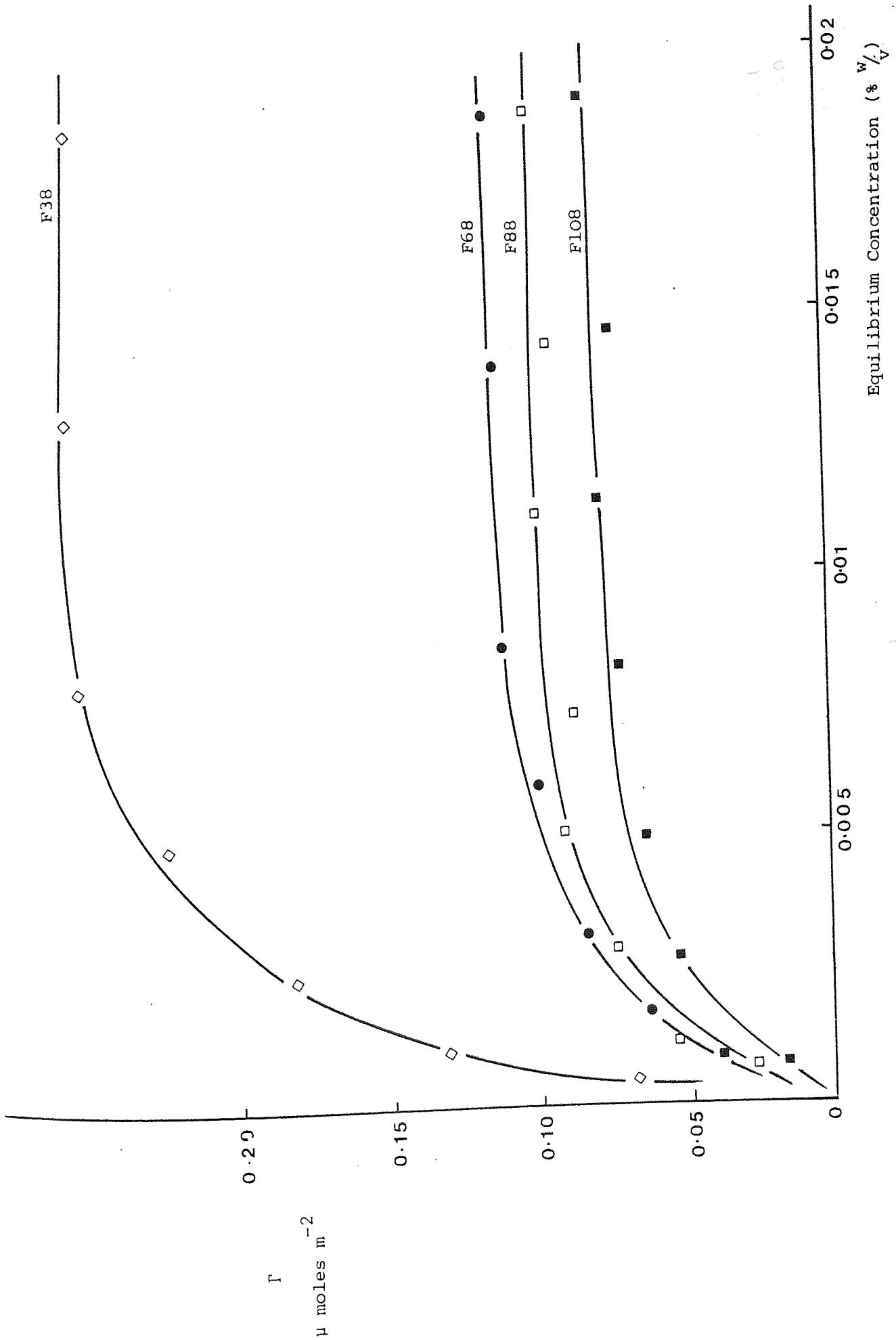


Figure 27 Adsorption Isotherms (25°C) of Plurionics on Polystyrene Latex

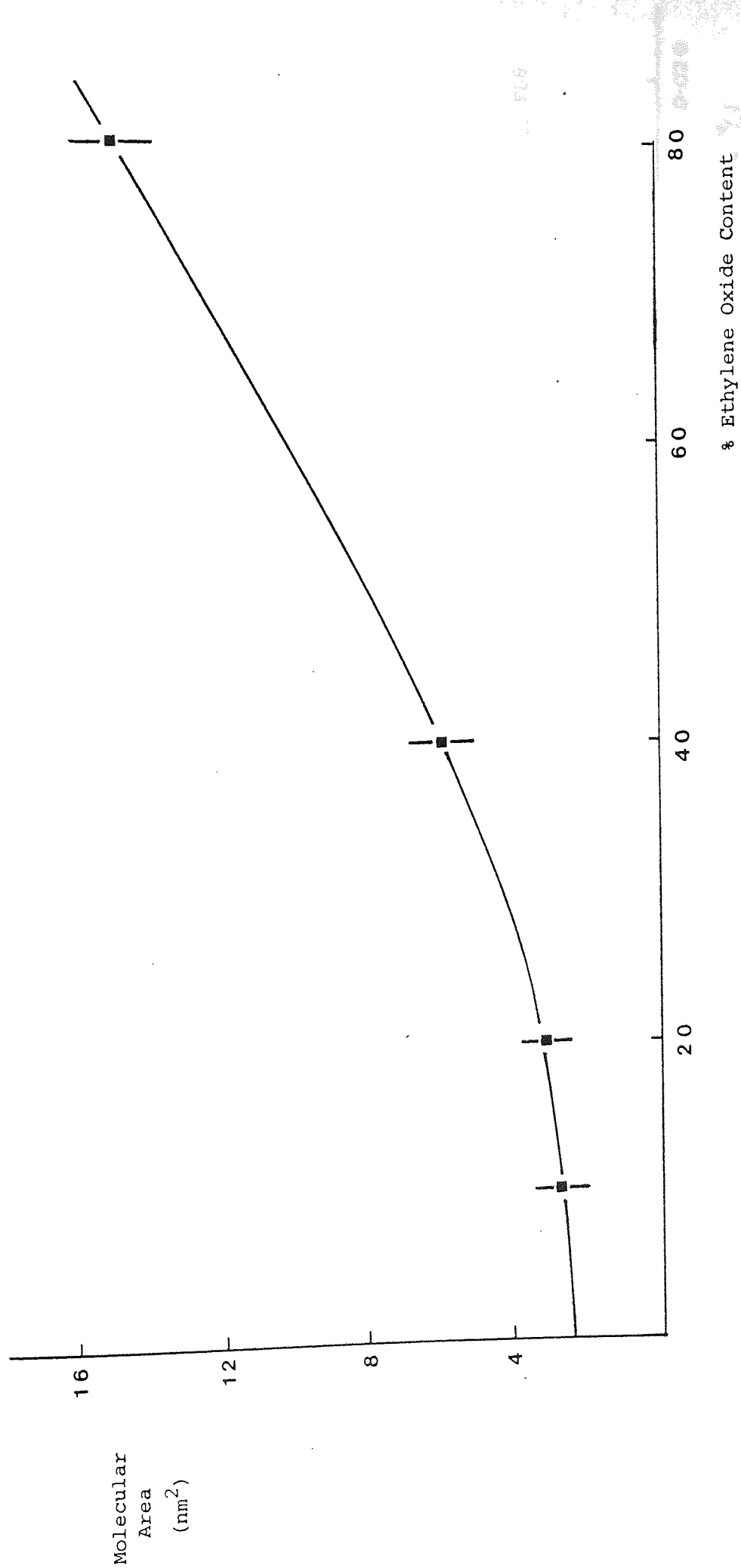


Figure 28 The Dependence of Molecular Area of Pluronics on Ethylene Oxide Content

- Polystyrene Latex

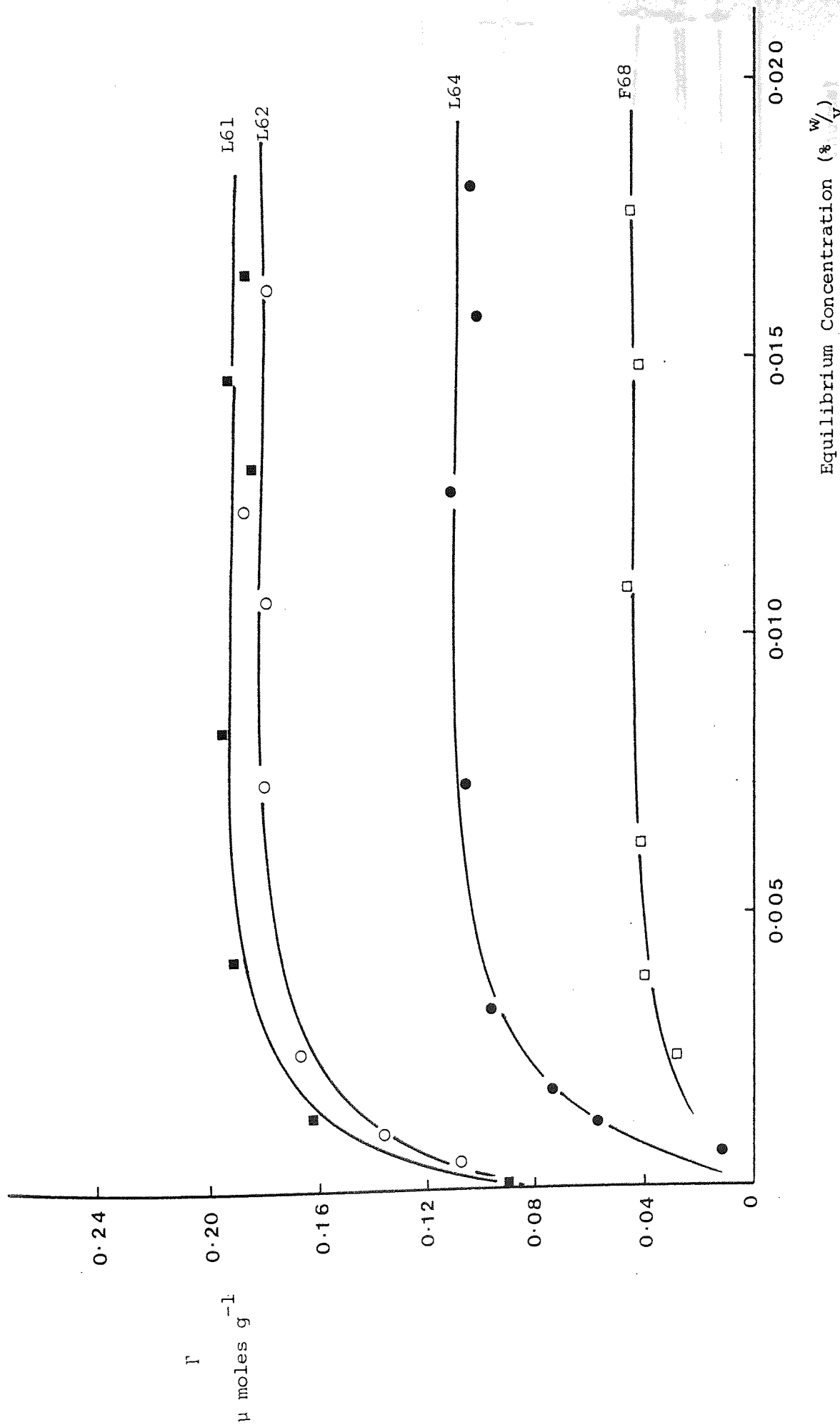


Figure 29 Adsorption Isotherms (25°C) of Pluronics on Diloxanide Furoate B.P.

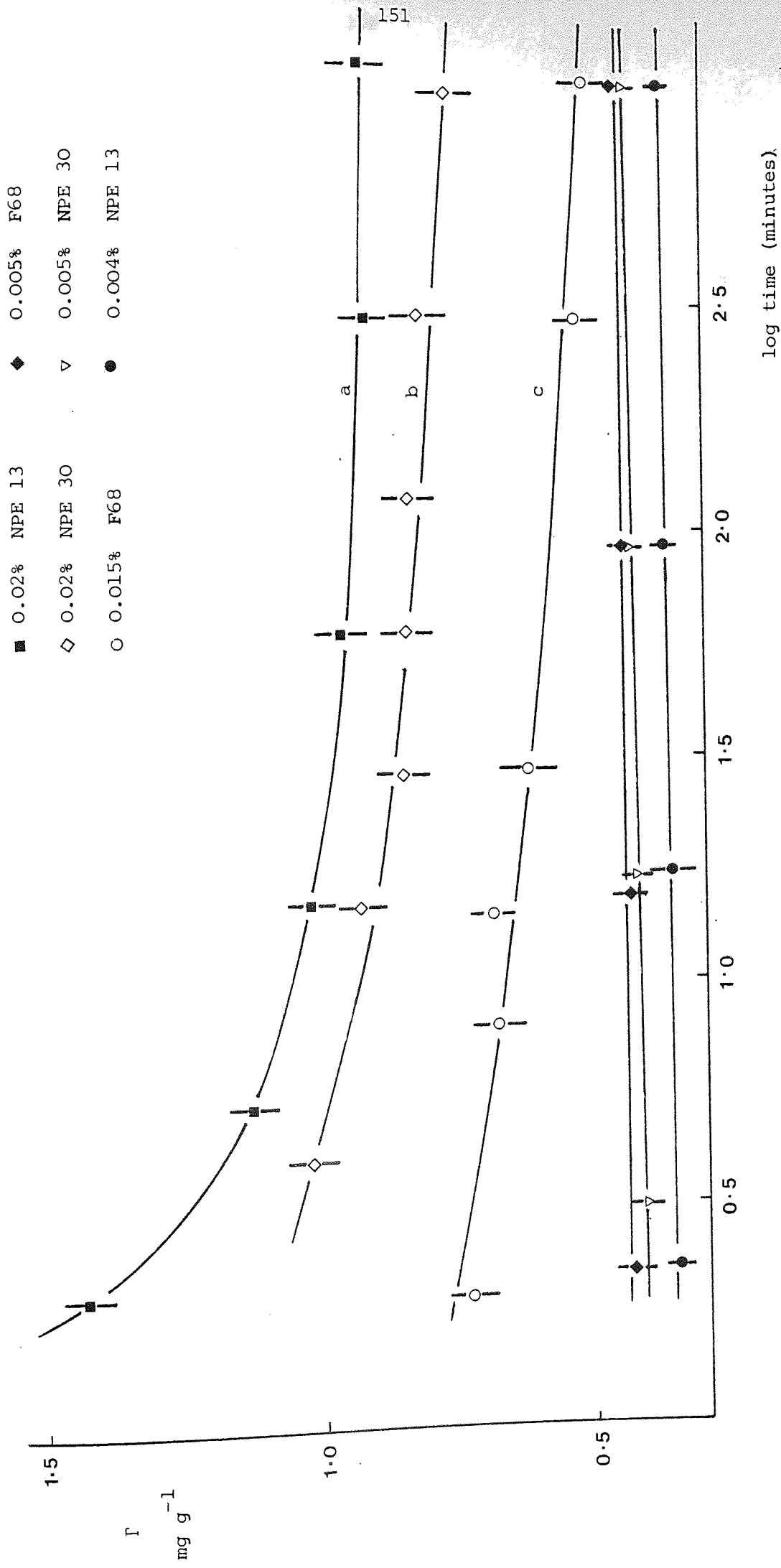


Figure 30 Effect of time on Surfactant Adsorption.

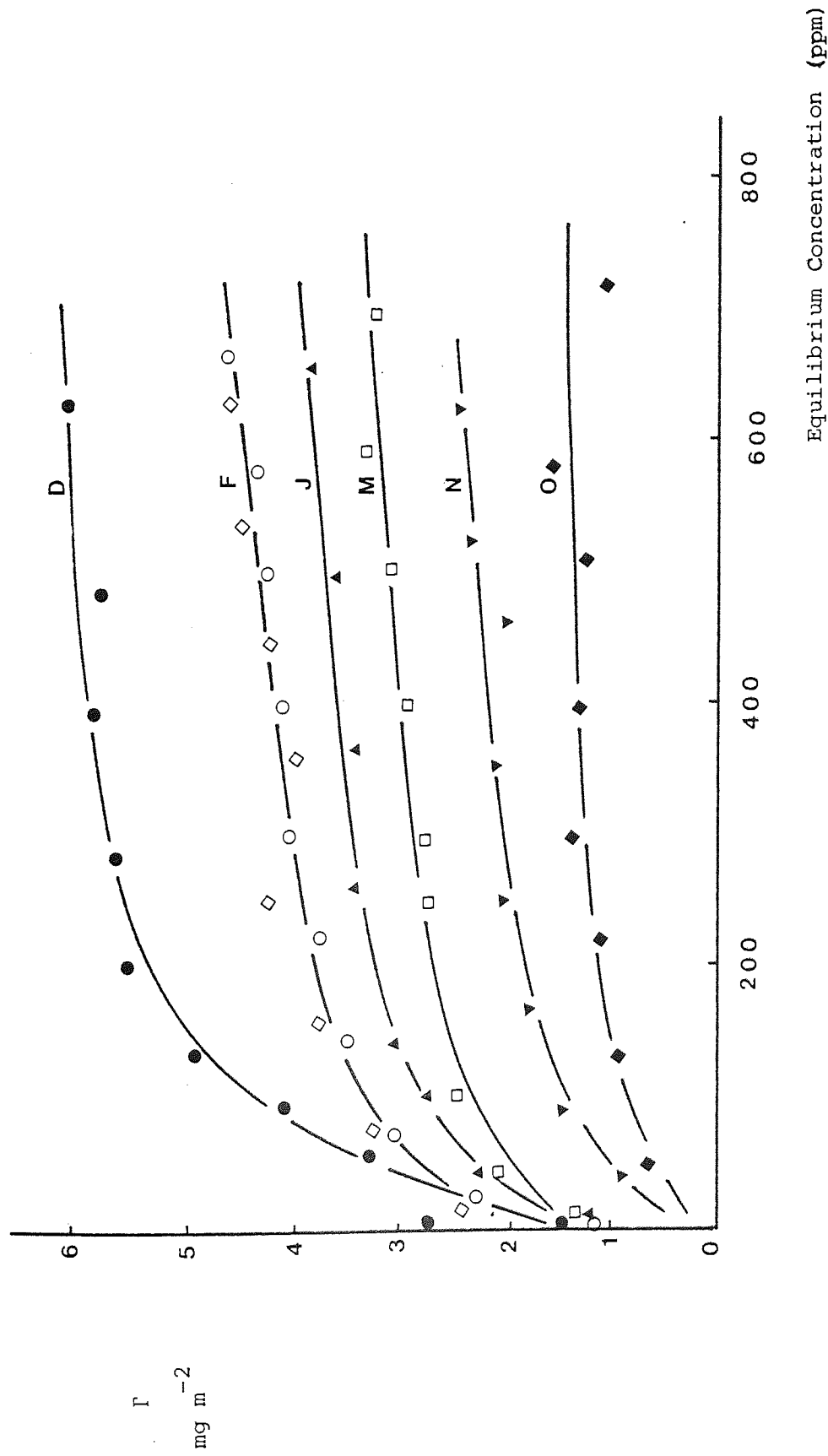


Figure 31 Adsorption Isotherms (25°C) of PVA on Polystyrene Latex in Distilled Water

(◇ measurements at pH 2,5)

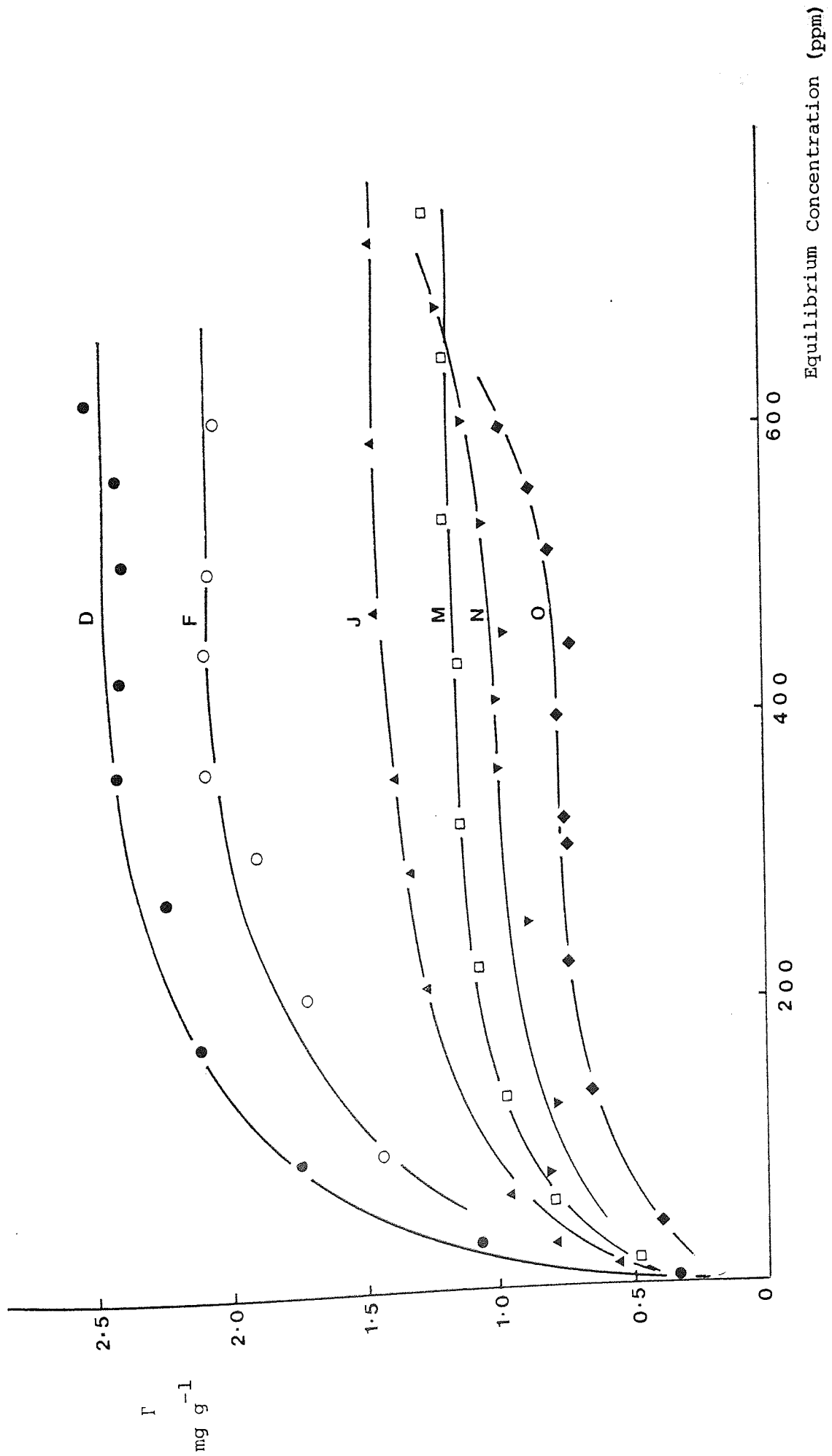


Figure 32 Adsorption Isotherms (25°C) PVA on Diloxanide Furoate

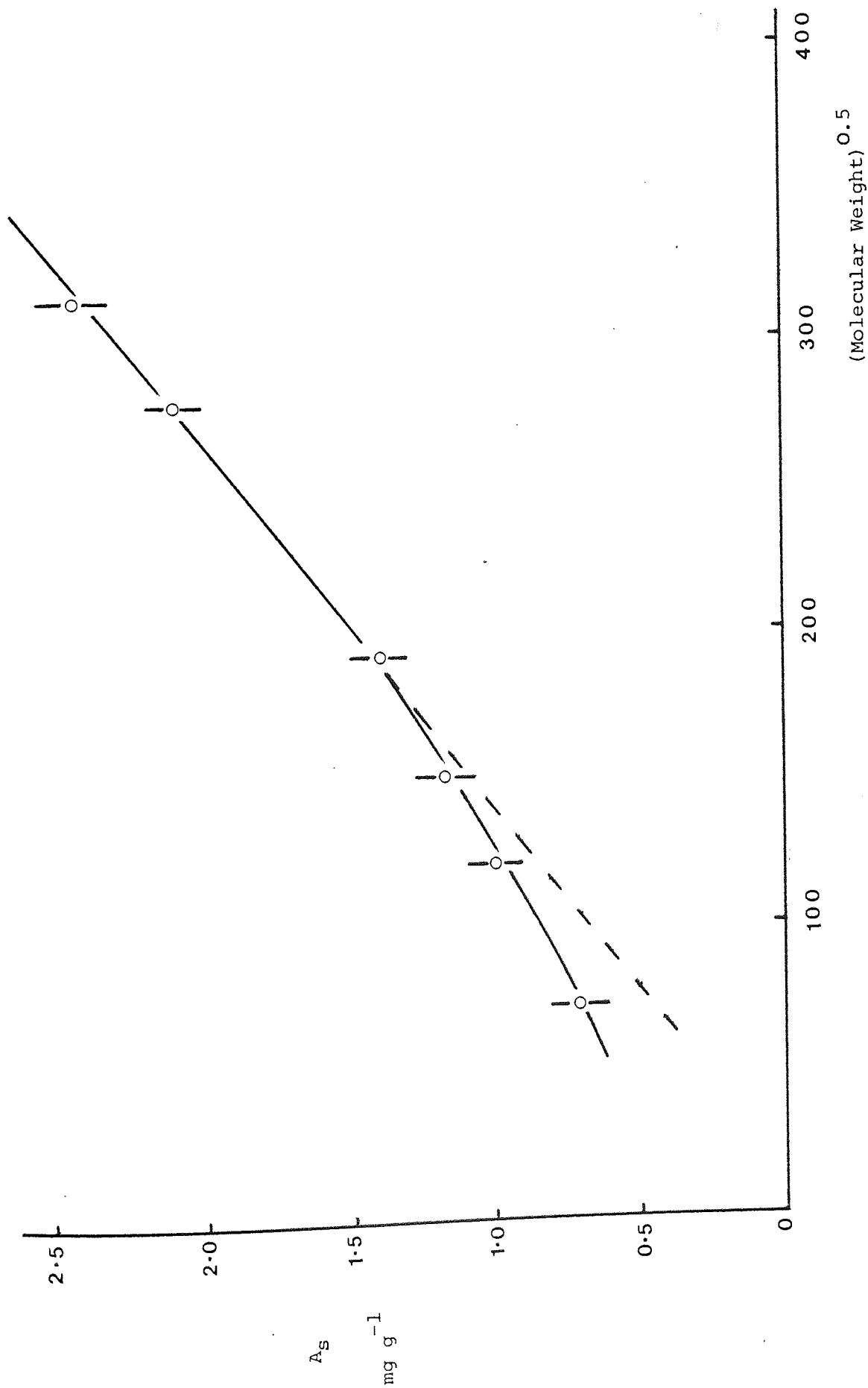


Figure 33 The Dependence of Saturation PVA adsorption on Diloxanide Furoate on the Square Root of Molecular Weight

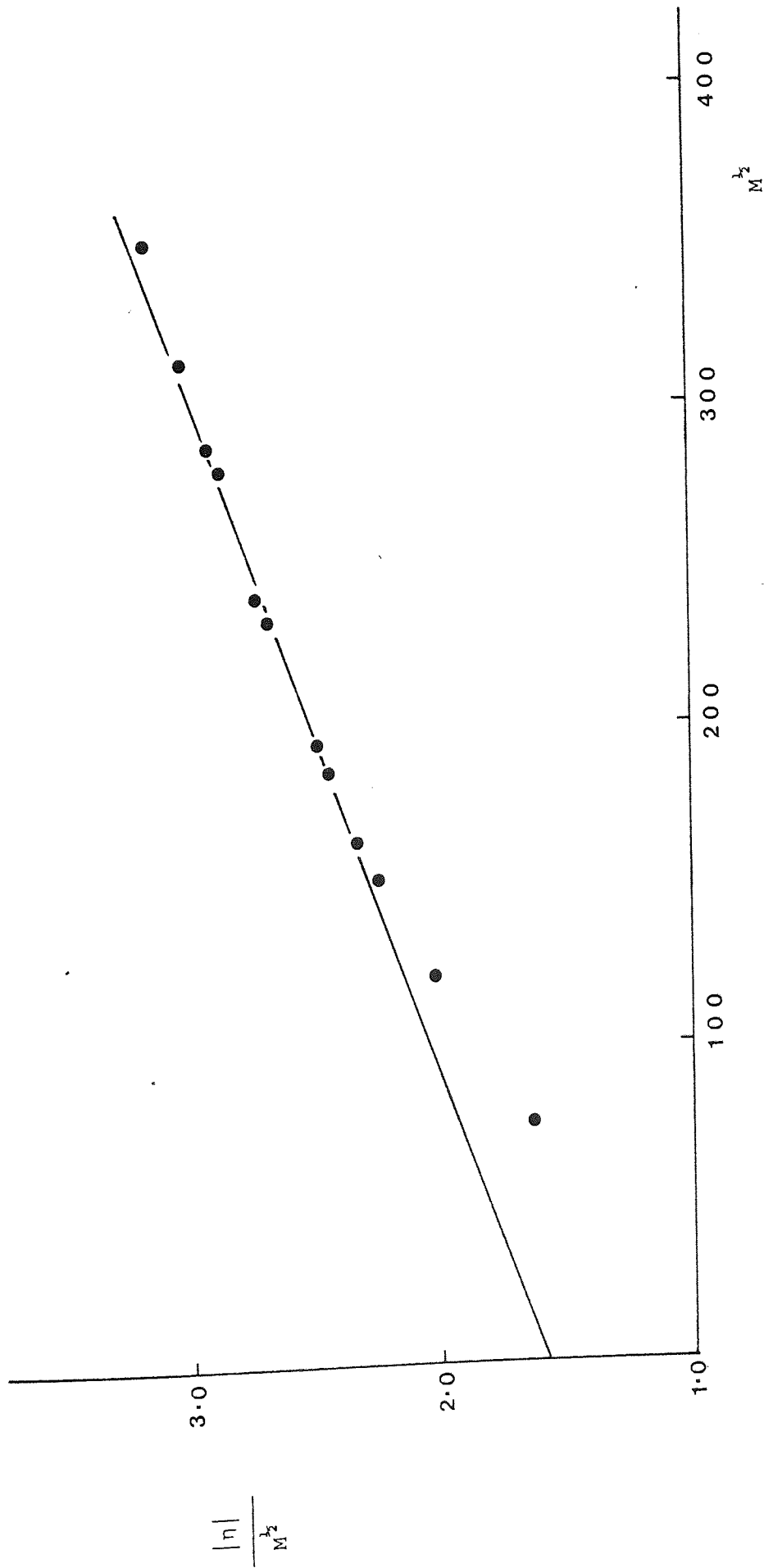


Figure 34 Stockmayer - Fixman plot for the Polyvinylalcohol Fractions

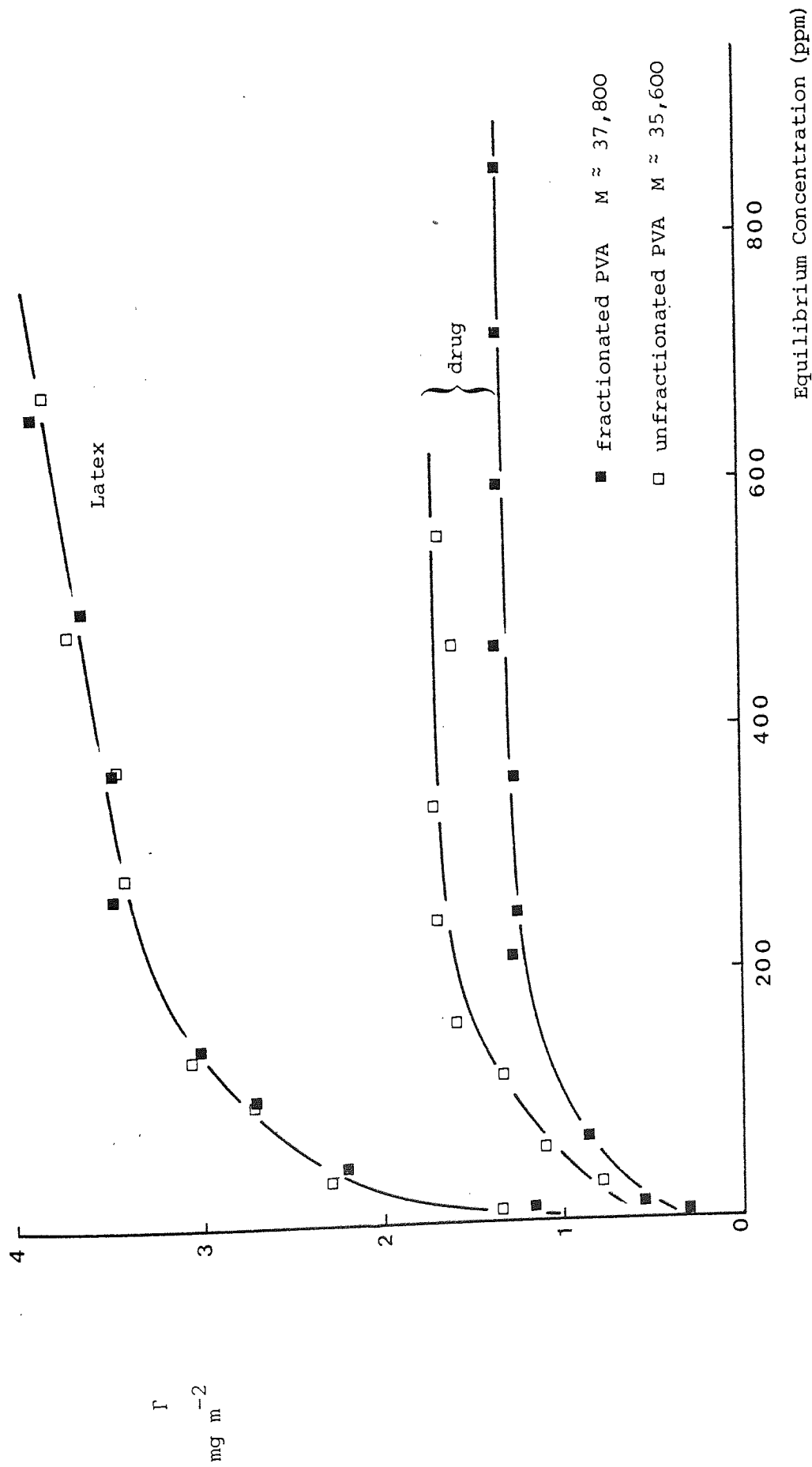


Figure 35 Adsorption of Fractionated and Unfractionated PVA on Polystyrene Latex and Diloxanide Furoate

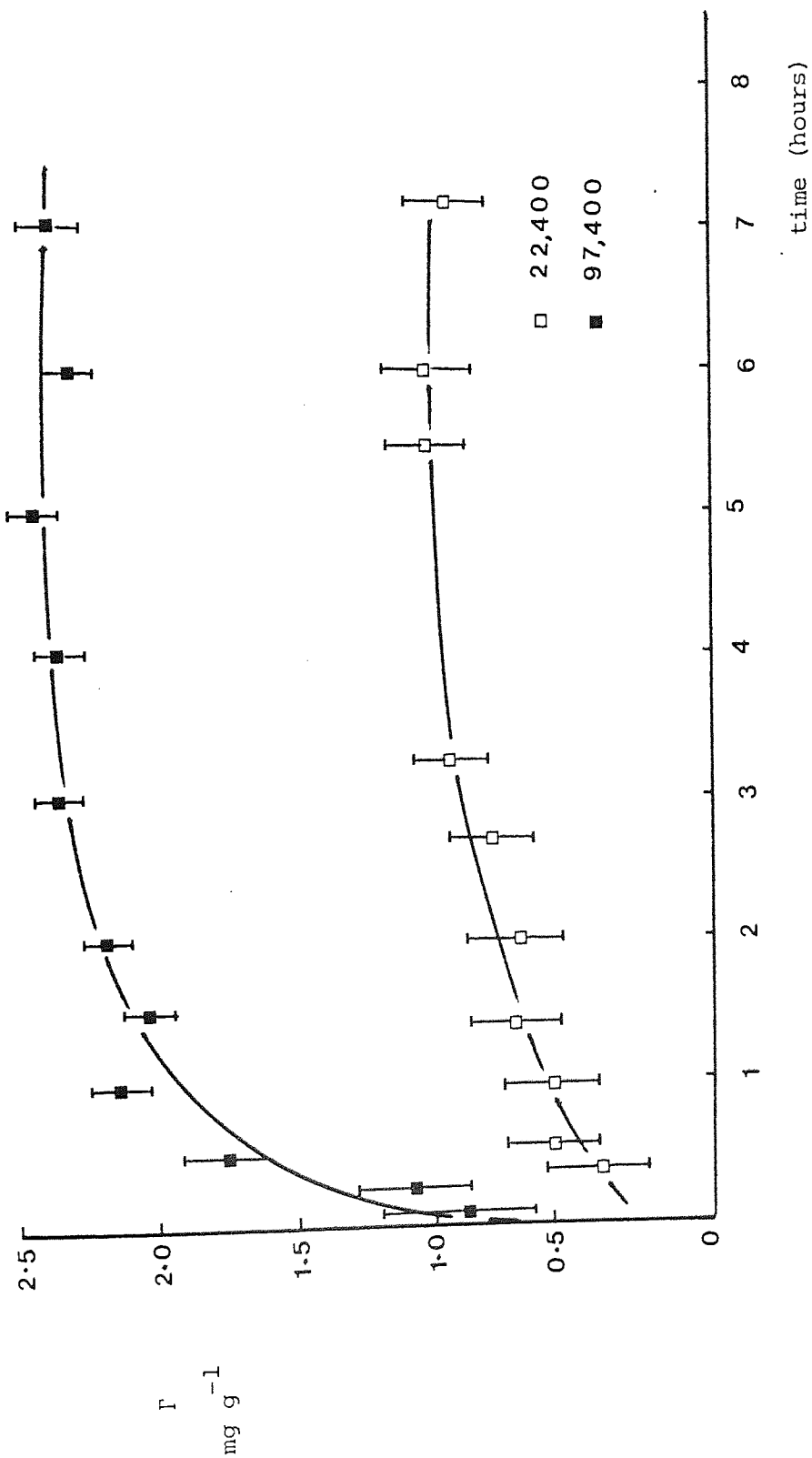


Figure 36 Adsorption Rate of Polyvinyl Alcohol onto Diloxonide Furoate B.P.

SECTION 5

adsorbed layer thickness

Section 5 Adsorbed Layer Thickness5:1:1 Microelectrophoresis

If a dispersion of negatively charged particles is placed between two electrodes and subjected to an electric field, movement of the particles and the attached ions of the Stern layer will take place towards the anode. Such movement is termed electrophoresis and is one of four related electrokinetic processes, the others being electro-osmosis, streaming potential and sedimentation potential. The experimentally determined electrophoretic mobility may be converted to a zeta potential measurement which is the potential at the plane of shear between the phases in relative motion. The exact location of the shear plane in the absence of adsorbed material is unknown, but it is usually assumed that it occurs at a marginally larger distance normal to the surface than the Stern plane. The zeta potential, ζ , is therefore assumed to be only slightly smaller than the Stern potential ψ_s and in general identity is usually assumed between these two parameters. The difference between ζ and ψ_s will be most pronounced at high potentials and high electrolyte concentrations.

The apparatus used to determine the electrophoretic mobilities of charged particles was the Rank Mark II Particle Microelectrophoresis Apparatus (Rank Bros., Bottisham, Cambridge). Essentially, this consists of a glass capillary tube into which the test dispersion is placed and across which a voltage is applied through electrodes placed at either end of the tube. Movement of the particles under the influence of the applied electric field is monitored by means of a suitable microscope system, mounted inside the constant temperature water bath surrounding the cell. Two types of cell were used for measurements in this work depending on the dispersion being tested. With the polystyrene latices

no appreciable sedimentation of the particles takes place and a thin walled capillary tube of circular cross section was used. For diloxanide furoate, the combination of large particle size and relatively high density ($1.52 \times 10^3 \text{ kg m}^{-3}$) produces rapid sedimentation of particles and causing them to fall out of the field of focus of the microscope. An additional problem with such systems in capillary tubes is that the sediment formed on the walls of the tubes disturbs the flow of fluid through the cell which may produce an invalid assessment of the electrophoretic mobility. For these reasons a flat cell was used where the dimensions of the cell are relatively large and sedimentation of particles does not interfere with fluid flow. The optical arrangement differs with the cell used. With the cylindrical cell illumination of the particles is from a lamp situation vertically above the tube and observation of the scattered light is at right angles to the incident beam. Focussing of the beam produces a short depth of field and only particles in the light path are illuminated. With the flat cell, direct viewing of the particles is used and consequently many particles are observed in the field of view. It is necessary to choose only those particles that are sharply in focus on which to perform measurements.

The apparatus was modified by use of a Pye Super Lynx LDM 0001 Television Camera mounted on the viewing head coupled with a Philips television monitor. The image observed is identical to that seen through the microscope eyepiece although the magnification is altered. A Churchill circulating water pump was used to provide a constant temperature water bath surrounding the cell ($25 \pm 0.5^\circ\text{C}$) in place of the thermostat provided with the apparatus.

Both microscope and television attachment were fitted with lmm

square grid graticules and calibration of these was by means of a stage micrometer divided in 0.1 and 0.01 millimeter divisions. Each side of the graticule square corresponded to 70μ and 35μ when viewed through the television monitor with x20 and x40 objectives respectively. Timings of the particles were measured using an electric stop watch accurate to 0.02 secs.

5:1:1:1 Electrodes

The electrodes used to apply the potential across the cell were platinum black as these are adequate for most salt concentrations commonly in use (208). Above concentrations of $10^{-2} \text{ mol dm}^{-3}$, 'gassing' at the electrodes occurs at high potentials resulting in a back-e.m.f. High salt concentrations also produce Joule heating at high applied potentials, however in this work all observations were made in solutions of $10^{-2} \text{ mol dm}^{-3}$ electrolyte or less and the above effects were not evident during the course of measurement. To determine the electrophoretic mobility, the exact distance between the two electrodes must be obtained. This was achieved by measuring the conductivity of standard solutions of potassium chloride at 25°C . These were measured using the Wayne-Kerr conductivity meter as described in Section 3:4:3. The interelectrode distance, l , is given by

$$K = \frac{l}{AR} \quad (5.1)$$

where A is the cross-sectioned area of the cell, R the measured resistance and K the specific conductivity of potassium chloride solutions, which is well documented. The cross-sectional area of the cell was determined from its diameter measured by focussing the objective on the inner walls of the cell by means of a vernier micrometer. For the flat cell the height was measured by means of a cathetometer. By these means the interelectrode distance was found to be 8.01 cm for the cylindrical cell and 8.22 cm for the flat cell.

5:1:1:2 Stationary Levels

The glass walls of the electrophoresis cell become charged in the presence of water and this causes electro-osmotic streaming in the vicinity of the walls when a potential difference is applied. Within the enclosed confines of the cell this necessitates a return flow of liquid with maximum velocity at the centre of the tube. The electrophoretic velocity of particles is superimposed on the liquid movement and true electrophoretic movement can only be observed where electro-osmotic flow and the return flow cancel. These clearly defined regions within the cell are termed 'stationary levels'. For a capillary of circular cross-section this stationary level occurs at $0.707R$ from the tube axis where R is the internal radius of the capillary (208). For a flat cell the position of the stationary level depends upon the width: depth ratio as given by Komagata (209):

$$\frac{s}{d} = 0.5 - \left[0.0833 + \frac{32}{\pi^5} \frac{d}{h} \right]^{1/2} \quad (5.2)$$

where d represents the depth, h the height and s is the position of the stationary level from the cell wall.

5:1:1:3 Optical Correction for Cylindrical Cells

The observation through the wall of a cylindrical cell may introduce the complication of an optical correction due to the lens effect of the curved glass. If the cell and surrounding water jacket are filled with water of refractive index N_w and that of the glass is N_g , then the correction term that must be subtracted from the apparent diameter, d_a , to give the correct diameter is $\frac{2t^2}{d_a}$ where $t = g \cdot \left[1 - \frac{N_w}{N_g} \right]$ and g is the glass thickness.

Substituting in appropriate values for N_g shows that this correction term is negligible even if g is as great as 100μ .

5:1:1:4 Operation

Prior to assembly the cell was cleaned with chromic acid and copious quantities of distilled water. When not in use it was kept full of distilled water and stoppered. All dispersions (except where stated) were prepared in 10^{-3} M sodium chloride solution and where necessary the pH was adjusted using sodium hydroxide or hydrochloric acid solutions using a PHM 64 Research pH Meter (Radiometer, Copenhagen) to monitor the pH. To obtain reproducible results it was found necessary to adopt the following procedure. The cell was washed with tap and distilled water and then rinsed with acetone and dried under reduced pressure. The dispersion was then used to rinse the cell before filling completely. Care was taken to avoid trapping air bubbles either in the tube or around the electrodes when they were placed in the supporting arms of the cell and all timings were made within 5 minutes of filling the cell. Particle velocities were measured by timing only those in sharp focus over a fixed distance on the calibrated graticule scale. The applied voltage was adjusted so that the time needed for a particle to cover the distance was ca 5 - 10 secs. This has been shown to be optimal with respect to errors produced by operator timing and displacements caused by Brownian motion. Alternate particles were timed in opposite directions by reversing the electrode polarity. This reduced the possibility of electrode polarization. The mean velocity V , was calculated from the timing of ten particles in each direction and from this the electrophoretic mobility, u was obtained by dividing the velocity by the field strength:

$$u = V/E \quad (5.3)$$

5:1:1:5 Conversion of Mobility to Zeta Potential

The zeta potential may be obtained from the experimentally determined electrophoretic mobility if the dimensions of the particle radius a , and the 'double layer thickness' ($1/\kappa$) are known. The magnitude of the

dimensionless quantity ka determines which form of the conversion expression to use.

The Huckel equation (210) may be used where ka is small (i.e. less than unity) and the particles may be treated as point charges. In this case

$$u = \frac{\epsilon\zeta}{1.5\eta} \quad (5.4)$$

where ϵ is the dielectric constant and η the viscosity of the solution surrounding the particles. Equation 5.4 has little applicability in aqueous solution as exceedingly low electrolyte concentration must be used to reduce ka to less than 1.0.

For large particles the double layer may be considered flat and for dispersions where $ka > 300$ the Smoluchowski equation (211) may be used.

$$u = \frac{\epsilon\zeta}{\eta} \quad (5.5)$$

$$\zeta = 12.85u \quad \text{at } 25^{\circ}\text{C in aqueous media}$$

where ζ is in mV and u in $10^{-8} \text{ m}^2 \text{ s}^{-1} \text{ V}^{-1}$.

Henry (212) has derived a general relationship between zeta potential and electrophoretic mobility for conducting and non-conducting spheres. For non-conducting spheres

$$u = \frac{\epsilon\zeta}{1.5\eta} f(ka) \quad (5.6)$$

$f(ka)$ depends upon the size of the particles and varies between 1.0 for small particles (Huckel) equation and 1.5 for large particles (Smoluchowski equation).

An important assumption made in deriving equation (5.6) is that the applied electric field does not in any way distort the electric double layer surrounding the particles. This effect is insignificant for $l > \kappa a > 300$ but for intermediate values of κa the relaxation effect becomes significant. This is due to the finite time required for the original symmetry of the ions in the diffuse region of the double layer to be restored after distortion by the applied electric field. A net movement of counter-ions in the directions opposite to that of the particle also occurs during electrophoresis producing a local movement of liquid opposing particle movement. This the retardation effect, is allowed for in the Henry equation.

Due to the distribution of ions in the double layer, the electrical conductivity in this region is greater than that in the bulk medium. This phenomenon affects the electric field distribution near the particle surface and through this alters the electrophoretic behaviour. Overbeek and Booth (213,214) derived expressions for spherical particles allowing for the effects of retardation, relaxation and surface conductance although the complexity of the equations obtained, limited their usefulness to zeta-potentials below 25mV. A more extensive treatment of the problem by Wiersema et al (215) has superceded the work of Overbeek and Booth and these results are tabulated in a readily useable form by Ottewill and Shaw (216) in terms of the zeta potential and κa . These tables were used in this work to convert the electrophoretic mobilities of polystyrene latex to zeta potentials.

All the above treatments assume that the effect of field strength on the permittivity ϵ and viscosity η near the shear plane are negligible. The possibility arises that dipole orientations of solvent molecules near the surface may be altered by the field strength resulting in a decreased

permittivity and/or an increased viscosity causing a retarding affect on the mobility. Lyklema and Overbeek (217) have concluded that the effect on ϵ is insignificant but that η does change significantly at high potentials and high electrolyte concentrations. However, Hunter (218) has suggested that the effect of field strength on both ϵ and η is negligible.

The applicability of equations such as those given above to convert mobilities to zeta potentials for non-spherical particles has been considered by Overbeek (219) who has demonstrated that the Smoluchowski equation is valid irrespective of the particle form provided ka is large at all points on the particle surface.

5:1:2 The Viscosimetric Thickness of the Adsorbed Layer

The Einstein equation describes the dependence of viscosity on the volume fraction of rigid uncharged particles (220)

$$\eta_r = 1 + K_E \phi_V \quad (5.7)$$

where η_r is the relative viscosity of the dispersion and ϕ_V is its solids volume fraction. K_E is the well known Einstein coefficient which for uncharged spheres takes a value of 2.5. K_E increases as the particle shape diverges from sphericity. Equation 5.7 is valid for a dilute dispersion of uncharged solids. For concentrated dispersions it may be necessary to add a further term in ϕ^2 to the above equation such that

$$\eta_r = 1 + K_E \phi_V + K_A \phi_V^2 \quad (5.8)$$

where K_A is a constant capable of giving an empirical fit to the data. Many values for K_A have been given (221) and Manley and Mason (222) consider that a value of K_A equal 9.2 describes much of the literature data. Mooney has also derived an equation to relate dispersion viscosity to

volume fraction (223):

$$\frac{1}{\ln \eta_r} = \frac{1}{2.5 \phi_V} - k_m \quad (5.9)$$

where k_m is a constant.

With charged spheres the above equations become inapplicable and the viscosity becomes a function of the ionic strength of the solution. This electroviscous effect is caused by the deformation of the electrical double layer surrounding the particle under shear and also by the overlap of two adjacent double layers. Under these circumstances, K_E increases with a decrease in ionic strength.

Where particles are covered with an adsorbed polymeric layer the volume fraction of the dispersed phase increases by a factor, f , where

$$f = \frac{\text{volume of polymer covered particle}}{\text{volume of uncovered particle}} = \frac{(a+\delta)^3}{a^3} \quad (5.10)$$

where a is the particle radius and δ is the adsorbed layer thickness.

Equations 5.7, 5.8 and 5.9 then become

$$\eta_r = 1 + 2.5f\phi_V \quad (5.11)$$

$$\eta_r = 1 + 2.5f\phi_V + K_A f^2 \phi_V^2 \quad (5.12)$$

$$\frac{1}{\ln \eta_r} = \frac{1}{2.5f\phi_V} = \frac{k_m}{f} \quad (5.13)$$

Suitable plots for the above three equations i.e. 1) η_r vs ϕ_V , 2) $(\eta_r - 1)/\phi_V$ vs ϕ_V , 3) $1/\ln \eta_r$ vs $1/\phi_V$ should give three linear lines and four independent values of f and hence δ .

The experimental measurements were carried out using latex A.

Volume fractions of latex used were 0.02 and lower. Measurements of viscosity were performed in a Grade A U-tube viscometer (British Standard: 188) at 25°C as described for the characterization of the PVA fractions in Section 3. Dispersions of known latex volume fraction were prepared by adding the requisite amount of latex to a PVA solution of such strength as to give maximum coverage of the latex surface. The electrolyte concentration was then adjusted to give a final ionic strength of 10^{-2} M potassium chloride which will suppress the electroviscous effect but which is not high enough to alter the configuration of the macromolecules in solution (147). Adsorption was then allowed to occur for 24 hours before measurements were made. To reduce the possibility of flocculation between particles the dispersions were filtered through a N^o2 sintered glass filter before viscosity measurements were made. The volume fraction of solids was then re-evaluated, after measurements, by evaporating to dryness and weighing the latex. The weight of PVA adsorbed contributing to this dried latex weight was determined from the adsorption isotherms in Section 4. The relative viscosity was obtained by centrifuging the dispersion at 16,000 rpm for 20 mins (M.S.E. HS18 centrifuge) and measuring the flow times of the supernatant. Adsorption onto the bore of the capillary viscometer was corrected for by allowing a 0.05% PVA solution to equilibrate with the glassware for 24 hours. The solution was then drained and the viscometer rinsed with small quantities of the dispersion under test prior to filling.

5:1:3 Intensity Fluctuation Spectroscopy (224)

This method depends on the measurement of the diffusion coefficient of the particles as they undergo Brownian motion. Particles in a dispersion medium will scatter light if their refractive index is different to that of the surrounding medium. Using a coherent optical source, the light is scattered and due to the random movement of the

particles a speckle pattern will be observed in the far field. As Brownian motion proceeds the intensity of scattered light at any one point will be seen to fluctuate and the time taken for one intensity minimum to replace a maximum at the photodetector corresponds approximately to the wavelength of light used. The photomultiplier converts the signal into a series of current pulses and a digital correlator measures directly the correlation function of the scattered light. The photocount correlation function $G^{(2)}(\tau_1)$ is given by

$$G^{(2)}(\tau_1) = B(1+\gamma_1^2 |g^{(1)}(\tau_1)|^2) \quad (5.14)$$

where (τ_1) is the correlation delay time, B is the known background value to which $G^{(2)}(\tau_1)$ decays after a long delay time and $|g^{(1)}(\tau_1)|$ is the normalised correlation function of the scattered electric field. γ_1 is a constant approximately equal to one. For monodisperse, non-interacting particles

$$|g^{(1)}(\tau_1)| = \exp(-\Gamma_1 \tau_1) \quad (5.15)$$

where the reciprocal coherence time Γ_1 is given by

$$\Gamma_1 = DK^2 \quad (5.16)$$

where D is the translational coefficient and K_1 is the scattering vector equal to

$$K = \frac{4\pi}{\lambda_0} n \sin\beta/2 \quad (5.17)$$

where λ_0 is the wavelength of light in vacuo, n is the refractive index of the dispersion and β is the scattering angle. A plot of Γ_1 against the (scattering vector)² will yield a straight of slope D which may then be related to the radius of the particle through the Stokes - Einstein relationship

$$a = \frac{kT}{6\pi\eta D} \quad (5.18)$$

Subtraction of the radius of the bare particles from the value of a , determined with the polymer coated particle gives the adsorbed layer thickness δ .

To prepare dispersions suitable for I.F.S. measurements, adsorption of the surfactants was permitted to proceed to equilibrium for 24 hours on 10^{-2} % w/v dispersions of Latex B. Filtration through 0.45μ membrane filters and dilution tenfold gave dispersions of suitable concentrations for analysis. The distilled water used in dilution was centrifuged at 20,000 rpm for 3 hours to remove dust. The final concentration of surfactant corresponds to a point on the plateau region of the adsorption isotherm in all cases. Viscosity effects due to the presence of the surfactants could be neglected. For example the viscosity of a 0.01% Fl08 solution relative to water was 1.0021 which gives rise to an error of 0.16nm in the radius of a 80nm radius particle. Light scattering measurements were made using a Malvern System 4300 photon correlation spectrometer (Precision Devices and Systems Ltd, Malvern) at the Physics Department, University of Manchester. This consisted of a scattering photometer with variable scattering angle facility through which a fine beam of coherent light was directed. The light source was a helium-neon laser (Spectra Physics Model 125) of wavelength 632.8nm. Scattered light was detected by an ITT FW-130 photomultiplier linked to a Malvern K7023 48 channel digital correlator. Experimental observations were determined over angular distributions of $60^\circ - 100^\circ$.

5:2 Results and Discussion

5:2:1 Microelectrophoresis

In addition to yielding useful information concerning the adsorption of material onto particle surfaces, the technique of microelectrophoresis may be used to give an estimate of the layer thickness provided certain assumptions are made. In this section the electrophoretic curves of

both latex and drug in the presence of an adsorbed polymer layer are discussed in the light of results obtained from adsorption isotherms and the thickness of such adsorbed layers is deduced from the electrophoretic results.

a) Polystyrene Latex. All measurements on Latex C where adsorbed surface active agent was present were performed in the plateau region of the mobility-pH plot for the base latex particles.

The effect that adsorption of nonionic polymers have on the zeta potential of a particle depends on the affect that the adsorbed species produce on the structure of the double layer surrounding the charged interface. In its simplest form this may be represented schematically by Figure 37 where low surface coverage is considered (61).

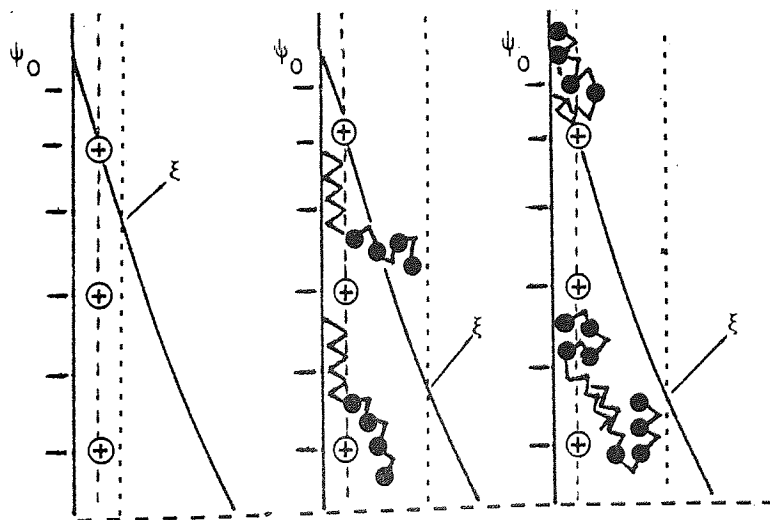


Figure 37 Schematic Representation of Adsorbed Polymer at a Charged Interface.

Two possible modes of attachment of the nonionic surfactant to the surface are considered where in Figure 37(b) adsorption occurs through the hydrophobic region of the molecule only and in Figure 37(c) both hydrophilic and hydrophobic regions take part in the adsorption process

but in addition multilayer adsorption occurs. If the adsorption energy of the adsorbed segments is greater than that of ions in the Stern plane desorption of some ions will occur resulting in a drop of the Stern potential. However in the case where this is not apparent the exponential drop in potential across the diffuse region of the double layer will be the same both in the presence or absence of adsorbed nonionic polymer. Whichever of the two adsorption mechanisms above occurs, for fairly high molecular weight molecules part of the molecule will project outwards into the surrounding bulk medium some way beyond the original shear plane (Figure 37a). Mechanical displacement of the shear plane away from the surface occurs resulting in a drop in the zeta potential. The lowering of ζ in the presence of adsorbed polymer will therefore reflect the thickness of this layer.

The mobility - concentration plot for polystyrene latex in the presence of the nonylphenylethoxylates is given in Figure 38. All curves show the same trend with mobility decreasing with an increase in surfactant concentration, until a plateau region is attained in the neighbourhood of the critical micelle concentration. This constant mobility value continues until at high concentrations a further decrease is observed.

Such observations has been reported previously by Elworthy and Florence (225) who investigated the variation in mobility of anisole, chlorobenzene and decane droplets in the presence of cetomacrogol and by Kayes (153) who studied the effect of a series of polyoxyethylene glycol monoethers of n-alkanols on latex mobility.

As the zeta potential reflects the adsorbed layer thickness it is apparent that below the critical micelle concentration the molecules must be in a more extended configuration on the surface and increasing

the bulk concentration which increases the amount adsorbed causes closer packing of the molecules which pushes the outer segments of the surfactant further out into the aqueous phase. At or near the cmc where saturation adsorption is attained no further adsorption takes place and the mobility remains constant.

The effect of increasing the ethylene oxide chain length is to cause a reduction in the electrophoretic mobility - a fact which may be explained by the displacement of the shear plane away from the interface on increasing the adsorbed molecules dimensions. The greater the number of ethylene oxide units the greater will be the displacement and consequently the mobility will be lower. Such an effect has been observed by Kayes (153) and by Daluja and Srivastava (226). From the results of nonionic surfactant adsorption on silver iodide sols Mathai and Ottewill concluded that below the cmc adsorption increased as ethylene oxide content decreased (164). Above the cmc comparison was difficult as multilayer adsorption was considered to have occurred in some cases. From Figure 38 it may be seen that an increase in adsorption with the smaller ethylene oxide chain lengths occurs both above and below the critical micelle concentration for the adsorption of the nonylphenyl-ethoxylates on latex. This confirms the results in Section 4 where the actual amount of surfactant adsorbed was investigated.

The electrophoretic mobility - concentration plots for the adsorption of the Pluronic block copolymers onto latex A is given in Figure 39. For a constant hydrophobic unit the mobility again decreases with an increase in ethylene oxide chain length. At high concentrations of surfactant the curves show a further decrease in mobility. The explanation for this further decrease beyond the plateau may be a result of further adsorption taking place or may simply be due to an increase in the viscosity at high surfactant concentrations. The latter

explanation was found to be correct. The viscosities of several concentrated Pluronic solutions (up to 5% $\frac{W}{V}$) were determined in a U-tube viscometer. Electrophoretic mobility is inversely proportional to the solution viscosity and allowance for the measured viscosities at high concentrations produces a continuation of the plateau region of the mobility curve. For example, the measured viscosity of a 5% solution of Pluronic F68 was 1.45 cp. At this concentration the measured mobility is $0.95 \times 10^{-8} \text{ m}^2 \text{ s}^{-1} \text{ v}^{-1}$. The corrected value allowing for dispersion viscosity is $1.54 \times 10^{-8} \text{ m}^2 \text{ s}^{-1} \text{ v}^{-1}$ which is in good agreement with the plateau value of ca $1.65 \times 10^{-8} \text{ m}^2 \text{ s}^{-1} \text{ v}^{-1}$. This substantiates the result obtained in Section 4 where it was shown that no further increase in adsorption occurs above 0.1%. Due to problems of solubility the microelectrophoretic technique could not be applied to highly concentrated L62 and L64 dispersions, thus it remains unclear as to whether multilayer adsorption occurs above the high cmc values quoted by some authors (see Table 1)

It may be seen that at very low surface coverages well below the equilibrium concentrations where saturation of the surface occurs, there is a marked reduction in mobility from that of the base latex. For Pluronics F38, F68, F88 and F108 the reduction in mobility is almost complete at surfactant concentrations of $0.5 \times 10^{-6} \text{ moles l}^{-1}$. This corresponds to a point on the adsorption isotherm where very little polymer (less than 10% of the maximum) has been adsorbed. It is therefore evident that with the Pluronics the thickness of the adsorbed layer is dependent on the first few molecules adsorbed and that subsequent adsorption of molecules does not produce a close packed formation with the outer segments being pushed away from the interface as the surface coverage increases. This contrasts with the results obtained for nonylphenylethoxylate adsorption where the thickness of the adsorbed layer

increases with concentration up to saturation of the surface. The reason for the behaviour of the Pluronics in this way may reside in the size of the surfactant molecules. The number of ethylene oxide units in each side chain for Pluronics F38, F68, F88 and F108 are approximately 43, 80, 102 and 148 respectively. Adsorption of these surfactants was shown to occur via both hydrophilic and hydrophobic units with the ethylene oxide chains forming loops around the surface. With such large numbers of hydrophilic units adsorption may occur through several of such segments. In order to pack the molecules closer together on adsorption of more molecules, desorption of these segments must occur simultaneously and this becomes statistically less probable the larger the number of segment-surface interactions occur. For the nonylphenylethoxylates there are relatively few segments per chain and consequently the number of attachments to the surface will be less if these chains are adsorbed as loops. These hydrophilic chains are therefore more easily desorbed from the surface and adsorption of further surfactant molecules will cause a bunching together of the chains, which is shown experimentally as a pushing out of the plane of shear from the surface resulting in decreased mobility.

Kayes (153) has demonstrated a linear relationship between the electrophoretic mobility and the number of ethylene oxide units per molecule of nonionic surface active agent. Figure 40 shows the decrease in mobility at the plateau region of the electrophoretic curve as a function of the ethylene oxide content. With the nonylphenylethoxylates an apparent linear decrease is observed in accord with the above work. For the Pluronics, where the mobility is plotted as a function of half the total ethylene oxide units per molecule, the graph shows a non-linear relationship between the two functions. It is probable that the linear relationship observed with the nonylphenylethoxylates is due to the limited

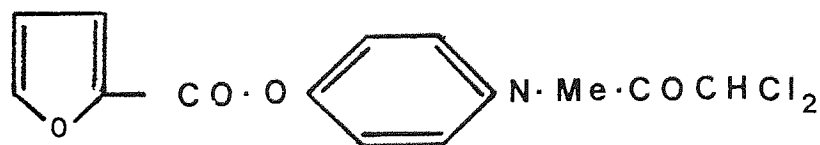
range of hydrophilic chain lengths that are covered with this series.

The results obtained with the Pluronic copolymers show that all the data points lie on the same curved line within experimental error demonstrating the independence of the layer thickness on the number of the hydrophobic POP units of the molecule. The results of the nonylphenylethoxylates may be superimposed on the graph obtained for the Pluronics to within $\pm 0.2 \times 10^{-8} \text{ m}^2 \text{ s}^{-1} \text{ v}^{-1}$. This agreement between nonionic surface active agents of different groups suggests that the electrophoretic mobility is dependent solely on the ethylene oxide content of the molecule. It is also apparent that the extent to which the hydrophobic region modifies the Stern potential, through adsorption or shielding of ions in this region, is either negligible or the same irrespective of the nature of the hydrophobic units. Due to the vast difference in size of the hydrophobic regions between the two groups and the much greater area that the Pluronics occupy at the interface, the latter argument is likely to be unsatisfactory.

The graph in Figure 41 shows the effect of increasing polyvinyl-alcohol concentration on the electrophoretic mobility of latex A. In Section 4 multilayer adsorption was considered likely to have occurred due to the large quantity of polymer adsorbed. However in Figure 41 no evidence of a two-stage adsorption process is seen which is in agreement with the adsorption isotherms. The mobility shows a very gradual lowering with increasing polymer concentration until a rapid decrease is observed at a point corresponding approximately to the rapid increase in adsorption in Figure 31. This type of mobility-concentration plot has been observed previously by Mathai and Ottewill (164) who found multilayer adsorption of nonionic surface active agents on silver iodide and by Tadros (227) who studied the adsorption of PVA onto a totally hydrophobic material, ethirimol. This work (227) showed that development

of a stepwise adsorption isotherm with the amount adsorbed at the first plateau corresponding to $6 - 8 \text{ mg m}^{-2}$ adsorbed. Multilayer adsorption cannot be discounted in this case, however micro-electrophoresis of the dispersion failed to detect any multilayer adsorption up to this plateau region and also at the concentration where a further step in adsorption occurred. This work is therefore in agreement with the above authors although the reason for the insensitivity of the technique to detect multilayer adsorption is unclear.

b) Diloxanide Furoate B.P. Figure 42 gives the mobility-pH plot for diloxanide furoate in 10^{-3} M and 10^{-2} M sodium chloride solution. Non-wetting of the particles and rapid sedimentation permitted measurement of only a few timings in both directions (ie. greater than ten but less than twenty) and the results are therefore subject to greater inaccuracy than results obtained with latex. At low pH a small positive charge exists which decreases to zero at ca pH 3.2. An increasing negative charge is acquired as the pH increases further with the attainment of constant mobility above pH 7 - 8. The structure of the drug is



and the positive charge at low pH can be attributed to protonation of the substituted amide function. Above pH 3.2 the increase in negative potential is probably due to the adsorption of hydroxyl ions onto the surface or the approach of anions closer to the surface than hydrated cations. The adsorption of hydroxyl ions was considered to be the charging mechanism in previous work on the electrophoretic properties of drug substances (228). In subsequent work where surface active agents and polymers were adsorbed measurements were performed in 10^{-3} M NaCl at pH 8 ± 0.5 corresponding to the plateau region of Figure 41.

Results of nonylphenylethoxylate and Pluronic adsorption are given in Figure 43 and 44 respectively for selected members of the surfactant series. In general the curves show the similar adsorption profiles found on polystyrene latex and thus demonstrate the use of latex systems as models for the drugs when considering the electrophoretic mobility. The results of PVA adsorption given in Figure 45 show a gradual decrease in mobility on increasing the polymer concentration. In this instance the results are not plotted logarithmically (as was the case for the latex systems) in order that a detailed analysis over relatively high concentrations ranges may be made when studying suspension stability (Section 6). If converted to the logarithmic form, these results show a more gradual decrease in mobility than found with the latex in the same concentration regions.

5:2:1:1 Estimation of Adsorbed Layer Thickness from Microelectrophoretic Measurements.

To estimate the adsorbed layer thickness a modification of equation 2.30 was used. This equation describes the decay of potential with distance over the diffuse region of the double layer and therefore applies to the potential decay from the Stern layer and not from the surface itself. ψ_s is substituted for ψ_0 and the zeta potential is used in place of ψ . In addition, as the equation applies only from the Stern layer a value for the thickness of this layer must be added as adsorption takes place onto the surface. Tadros (227) has given a value of 0.4nm for this distance and this is used here. The final equation then becomes

$$\kappa(\delta-0.4) = \ln \frac{(\exp(ze\zeta/2kT) + 1) (\exp(ze\psi_s/2kT) - 1)}{(\exp(ze\zeta/2kT) - 1) (\exp(ze\psi_s/2kT) + 1)} \quad (5.19)$$

where δ is the adsorbed layer thickness.

In order to apply equation 5.19 a value for ψ_s must be obtained. In general it is assumed that ψ_s and the zeta potential in the absence of adsorbed polymer ζ_0 are identical and significant deviations occur between these two parameters only at high potentials and high electrolyte concentrations. In a recent review of the anomalous behaviour of water at interfaces, Lyklema (229) has concluded that there are no thick stagnant layers of water surrounding the particles at close distances and consequently the practice of equating ψ_s and ζ_0 is viable.

Use of equation 5.19 to determine adsorbed layer thickness implies the use of several assumptions. These are that the adsorbed polymer does not affect

- 1) the surface charge density
- 2) the adsorption of specifically adsorbed ions
- 3) the distribution of ions within the diffuse mobile region of the electric double layer.

Conversion of electrophoretic mobilities to zeta potentials were performed using the tables of Ottewill and Shaw. At an electrolyte concentration of 10^{-3} M the value of $\frac{1}{\kappa}$ is 9.62nm and for latex C the dimensionless quantity κa becomes 16.12. It is therefore necessary to allow for the effects of retardation and relaxation using the above tables. In converting mobilities to zeta potentials, no account was taken of the increase in κa caused by the adsorption of the polymers. However, for particles the size of latex A, this effect is negligible, thus κa changes from 16.2 to 16.7 on adsorbing a polymer of layer thickness 10nm. Any changes in zeta potential due to this increase are insignificant.

Application of the above equation to the zeta potentials of polymer covered latex particles in the plateau region of the electrophoretic mobility-concentration curves gives the values of δ listed in Table 12.

Table 12

Adsorbed Layer Thickness of Surfactants by Microelectrophoretic Measurement
on Latex

Surfactant	Mobility ($10^{-8} \text{m}^2 \cdot \text{s}^{-1} \cdot \text{v}^{-1}$)	Zeta Potential (mV)	Adsorbed layer Thickness (nm)
Pluronic L62	-3.4 ± 0.10	-54.5 ± 2.0	0.9 ± 0.3
Pluronic L64	-3.13 ± 0.14	-49.3 ± 1.8	1.7 ± 0.3
Pluronic F68	-1.55 ± 0.20	-22.8 ± 2.4	8.7 ± 1.0
Pluronic F38	-2.32 ± 0.13	-34.8 ± 1.8	4.8 ± 0.5
Pluronic F88	-1.18 ± 0.18	-17.3 ± 2.0	11.3 ± 1.0
Pluronic F108	-0.95 ± 0.20	-14.0 ± 3.0	13.5 ± 2.0
NPE 8	-3.50 ± 0.10	-56.8 ± 1.5	0.40 ± 0.35
NPE 13	-3.25 ± 0.05	-54.0 ± 1.5	0.95 ± 0.22
NPE 20	-3.05 ± 0.10	-48 ± 2.0	2.8 ± 0.4
NPE 30	-2.68 ± 0.23	-41.25 ± 3.8	3.28 ± 0.8
NPE 35	-2.55 ± 0.20	-39.5 ± 2.1	3.50 ± 0.4

This method of determining adsorbed layer thickness has been used previously by Garvey, Tadros and Vincent (230) and by Tadros (227) who investigated the layer thickness of PVA coated particles, and by Kayes (228) who showed the thickness of the adsorbed layer on polystyrene latex of alkyl polyoxyethylene monoethers containing 30 and 60 ethylene oxide units to be 3.18 and 9.18 nm respectively. It may be observed that there is close agreement between these results and values of δ for NPE 30 and for F68 which contains ca 80 hydrophilic units in each side chain.

Staudinger has postulated two models for the configuration of the ethylene oxide chain which are dependent upon the number of repeating units per chain (231). Below 9 units the chain exhibits a zig-zag structure with the length of the repeating unit equal to 0.35nm. At greater degrees of polymerization chain contraction occurs leading to a meander configuration of unit length 0.2nm. The length of the polyoxyethylene chains in free solution may be determined from the number and length of

units per molecule and for the nonylphenylethoxylates the total chain length may be found by the addition of the hydrophobic region which has a value of 1.4nm for a branched nonylphenyl chain (138). In all cases given in Table 12 the results of δ are far less than lengths obtained from molecular models and therefore evidence of a looped monolayer is supported.

Consideration of the concentration of polymer at the interface derived from the adsorption isotherms and the adsorbed layer thickness given in Table 12 shows that for NPE 8 greater than 100% polymer is present while for NPE 13 a value of 89% polymer is obtained. This apparent error in the calculation is most probably due to an underestimation of the adsorbed layer thickness rather than due to the measured amount of polymer adsorbed. The reason for the failure of microelectrophoresis to provide a reasonable estimate for the layer thickness in the case of the two short chain nonionic polymers probably resides in one or more of the assumptions that are necessary to use equation 5.19. The effect of adsorbed polymers on the surface charge has been studied by several authors but no single conclusion may be drawn from the results except that different surfaces respond in different ways to the presence of polymer. For example Kavanagh, Posner and Quirk (195) found that the adsorption of PVA onto gibbsite has little effect on the properties of the Stern layer while Koopal and Lyklema (232) found that the same polymer adsorbed onto silver iodide sol significantly reduces the surface charge either by ion desorption or by a change in the average dielectric constant near the interface on replacing solvent molecules by polymer segments. However, if these mechanisms were accountable for a change in the surface charge, a decrease in surface charge and therefore zeta-potential would be expected. This is demonstrated experimentally by the work of Koopal and Lyklema who showed that at constant pAg the surface charge is reduced as more of the surface is covered by polymer. In

the results obtained in Figure 38 the values of ζ are too high for NPE 8 and NPE 13 to produce realistic values of the adsorbed layer thickness and therefore the modification of surface charge through polymer adsorption would appear unlikely. An alternative explanation may be that of expansion of the double layer caused by the adsorption of polymers as was found by Brooks (233) who studied the effects of dextran adsorption on the zeta potential of human erythrocytes. The adsorbed polymer alters the distribution of ions within the diffuse double layer region and at constant surface charge causes the zeta potential to increase. It is reasonable to expect that a change in the ionic distribution will occur on adsorption particularly with the lower ethylene oxide chain length surfactants as the polymer concentration within the adsorbed layer is relatively high.

To obtain a reasonable estimate of the adsorbed layer thickness, two approaches may be used. Either the extended length of the molecule or the radius of the surfactant micelle may be used. Elworthy and Florence (234) have used the micellar dimensions in order to construct potential energy diagrams for some emulsion systems with adsorbed layers of hexadecyl polyoxyethylene glycol surfactants whose micelles are spherical. Information regarding the micellar dimensions of the nonylphenylethoxylates is scant although Becher (235) has determined the micellar volume from light scattering studies. He has concluded that short chain surfactants form spherical micelles while higher ethylene oxide chain length surfactants most probably aggregate in the form of rods. For short chain surfactants the dimension of the monomers were in fair agreement with the extended length of the molecule and therefore in this work values of 4.2 and 4.0nm have been used for the thickness of NPE 8 and NPE 13 surfactant layers respectively. These values of δ produce adsorbed layer concentrations more in accord with adsorption at other interfaces (82, 234).

An estimation of the adsorbed layer thickness of the surfactants on diloxanide furoate from electrophoretic measurements in the plateau regions of Figures 43 and 44 were obtained using equation 5.19. The value of κa is very large with these systems in 10^{-3} M NaCl and therefore the Smoluchowski equation was used to convert mobilities to zeta potentials. The results are given in Table 13.

Table 13
Adsorbed Layer Thickness of Surfactants by Microelectrophoretic Measurement on Diloxanide Furoate B.P.

Surfactant	Mobility $10^{-8} m^2 s^{-1} V^{-1}$	Zeta Potential (mV)	Adsorbed Layer Thickness (nm)	Extended Length
Pluronic L62	-2.60 ± 0.15	-33.4 ± 1.9	3.00 ± 0.52	1.74
Pluronic L64	-1.83 ± 0.18	-23.5 ± 2.3	6.30 ± 0.90	2.65
NPE 20	-1.5 ± 0.20	-19.27 ± 2.6	8.15 ± 1.25	5.4
NPE 30	-0.90 ± 0.20	-11.55 ± 2.6	13.15 ± 2.15	7.4

The values of the experimentally determined adsorbed layer thickness are given alongside the length of the extended configuration of the molecule derived from molecular models (i.e. 0.2nm/EO unit for $EO > 9$, 0.35nm/EO unit for $EO < 9$ and 1.4nm for the length of the alkylphenyl residue). The extended length of the Pluronic molecules was taken to be that of the ethylene oxide side chain as the hydrophobic unit has been shown previously to adsorb flat onto the surface. It can be seen that there is a great discrepancy between these two values. The reason for this discrepancy probably lies in the displacement of ions in the double layer region during adsorption of the polymer. The mechanism of surface charge acquirement is thought to be due to the adsorption of hydroxyl ions onto the surface or the approach of these ions nearer to the surface than the cations. On polymer adsorption, some of these ions may be desorbed or displaced producing a lower than expected electrophoretic mobility. With the polystyrene latex the potential determining ions are

the carboxylic acid groups which are an integral part of the surface and cannot be desorbed during polymer adsorption. It would therefore appear that adsorbed layer thickness measurements may only be determined in circumstances when the potential determining ions are not displaced, unless surface charge measurements are performed in the presence of polymer as shown by Koopal and Lyklema (232).

5:2:2 Adsorbed Layer Thickness from Intensity Fluctuation Spectroscopy Measurements

The absolute accuracy of this technique in determining the particle radius can be seen by comparing the value of the particle radius found from electron microscopy (86nm) with that obtained using I.F.S. of 84nm. The measurement of the diffusion coefficient of the bare latex was performed in distilled water only and the particles are subject to a small electroviscous effect. Measurement in sufficient electrolyte to reduce this effect was not performed due to the probability of coagulation occurring. Duckworth, Lips and Staples (236) have used the same technique to measure particle radius to within $\pm 0.3\%$ of the mean particle diameter given by electron microscopy. From these results the electroviscous effect would appear negligible. Determination of particle diffusion coefficients were made only in the presence of adsorbed Pluronics F38, F68, F88 and F108 and results of diffusion coefficients and adsorbed layer thickness are given in Table 14

Table 14

Surfactant	Diffusion Coefficient $10^{-8} \text{ cm}^2 \text{ s}^{-1}$	Adsorbed Layer Thickness (nm)
Pluronic F38	2.745 ± 0.148	5.4 ± 4.8
Pluronic F68	2.654 ± 0.118	7.4 ± 5.1
Pluronic F88	2.556 ± 0.101	11.9 ± 3.8
Pluronic F108	2.579 ± 0.117	13.4 ± 4.5

Although the errors using I.F.S. are high due to the small thickness of the adsorbed polymer layer, the mean values agree with the microelectrophoretic results and both results are much lower than the extended length of the polyoxyethylene chains which is to be expected if the chains adsorb as loops on the surface. The results of Garvey et al (230) showed that using PVA as the adsorbing species the adsorbed layer thickness could not be accurately determined using an electrophoretic technique. Considering the mode of adsorption the present results measured by electrophoresis are within the expected range and the agreement with the I.F.S. measurements would indicate that the justification of using the double layer equations above is dependent on the type of polymer-substrate system studied.

5:2:3 Adsorbed Layer Thickness by Viscosimetric means

In interpreting the viscosity data it has been assumed that the increases in the apparent disperse phase volume on adsorbing polymer onto the latex surface are due solely to the presence of these solvated layers. Alternative explanations of particle asymmetry and particle flocculation were discounted for the following reasons. Electron microscopy of the colloids show the existence of smooth uniform sized spheres both before and after adsorption of the polymer although in the electron micrographs of polymer covered latex the edges of the spheres were indistinct and 'fuzzy'. Dilutions of the dispersions in a polyvinyl-alcohol solution of concentration approximately equivalent to that of the undiluted system showed no evidence of aggregation when viewed under a high resolution optical microscope.

The results are plotted in Figures 46 and 47 in terms of the Einstein and Mooney equations. Application of equation 5.12 to the data with a value of K_A of 9.2 (222) does not produce suitable plots from which to derive the adsorbed layer thickness. For the Einstein and

Mooney plots reasonable linear graphs are obtained and the values of δ obtained are given in Table 15. It may also be seen that results obtained where equilibrium of PVA solution with the viscometer were performed gave essentially the same data points where this correction was not applied. The reduction in the viscometer capillary bore due to polymer adsorption may therefore be neglected.

Table 15

Adsorbed Layer Thickness of PVA by Viscometry

<i>PVA fraction</i>	δ (nm) <i>Einstein Equation</i>	δ (nm) <i>Mooney Equation</i>
97,400	76.8 (0.99)	76.9 (0.99)
77,600	57.8 (0.99)	59.9 (0.98)
37,800	27.5 (0.98)	40.5 (0.98)
23,200	22.4 (0.98)	16.3 (0.97)
14,500	10.0 (0.97)	15.6 (0.97)

Figures in brackets denote correlation coefficient

These values of adsorbed layer thickness may be compared with the results obtained by Garvey for the adsorption of PVA on a latex system (145) and show values far in excess of his experimental data where monolayer adsorption was proposed. They are also in excess of values given by van den Boomgaard (133) who assumed that multilayer adsorption occurred. Both the above authors used intensity fluctuation spectroscopy to determine δ , but as it is known (237) that different techniques may produce significantly different values of δ for the same polymer-adsorbent system it would be injudicious to compare viscosimetric results with measurements by I.F.S. The thickness of the adsorbed layers reported in Table 15 greatly exceed the hydrodynamic diameters of the polymer molecules in free solution (Table 10) and also it may be seen that the apparent molecular area at the interface is far less than the projected

area of the free polymer molecule in solution. These results would therefore appear to substantiate the adsorption measurements that multilayer adsorption occurs with this system.

5:2:4 PVA Adsorbed Layer Thickness on Diloxanide Furoate B.P.

Due to the absence of a suitable model system for the drug, because of the occurrence of multilayer adsorption on the latex, a different approach must be adopted to provide an estimate of the extension of the adsorbed polymer into the solution. Hoffman and Forsman (55) have shown that at surface saturation the thickness of the adsorbed layer approaches the dimensions of the polymer in solution. Garvey et al (145) have postulated that in a good solvent environment the volume of a molecule at the interface is equal to the hydrodynamic volume in free solution. This method therefore provides an estimation of δ from the intrinsic viscosity of the polymer fractions and this approach is used here to obtain δ . The values obtained are shown in Table 16. At best these values may be used in a relative sense as certain arguments mitigate against the use of this approximation (145). The main argument is that the adsorbed layer thickness has been shown to be dependent on particle size (230). This is due to geometrical considerations of placing a polymer coil on a surface and shows that as particle size increases, the layer thickness also increases.

Table 16

PVA fraction	Hydrodynamic Volume (nm ³)	δ (nm)
97,400	3591.0	52.0
77,600	2438.0	38.5
37,800	648.0	13.8
23,200	301.6	9.2
14,500	141.1	4.6
5,400	25.7	1.6

The values of δ for the two lower fractions were determined using the extrapolated value of the molecular area to take into account adsorption into pores.

Using this procedure it may be seen that the adsorbed layer thickness is approximately proportional to the molecular weight. This is contrary to the predictions of the F.S.E. theory where dependence on $M^{\frac{1}{2}}$ is anticipated. However this prediction is for sparsely populated surfaces with no lateral interaction among the neighbouring molecules. The dependence of δ on M may be derived by use of equations 4.13, 3.5 and 2, assuming the volume of the polymer coil in solution is not altered upon adsorption (230) and a theory to account for this direct proportionality has been proposed (238).

These values of the adsorbed layer thickness are used in the following section to account for the stability of the coarse dispersions.

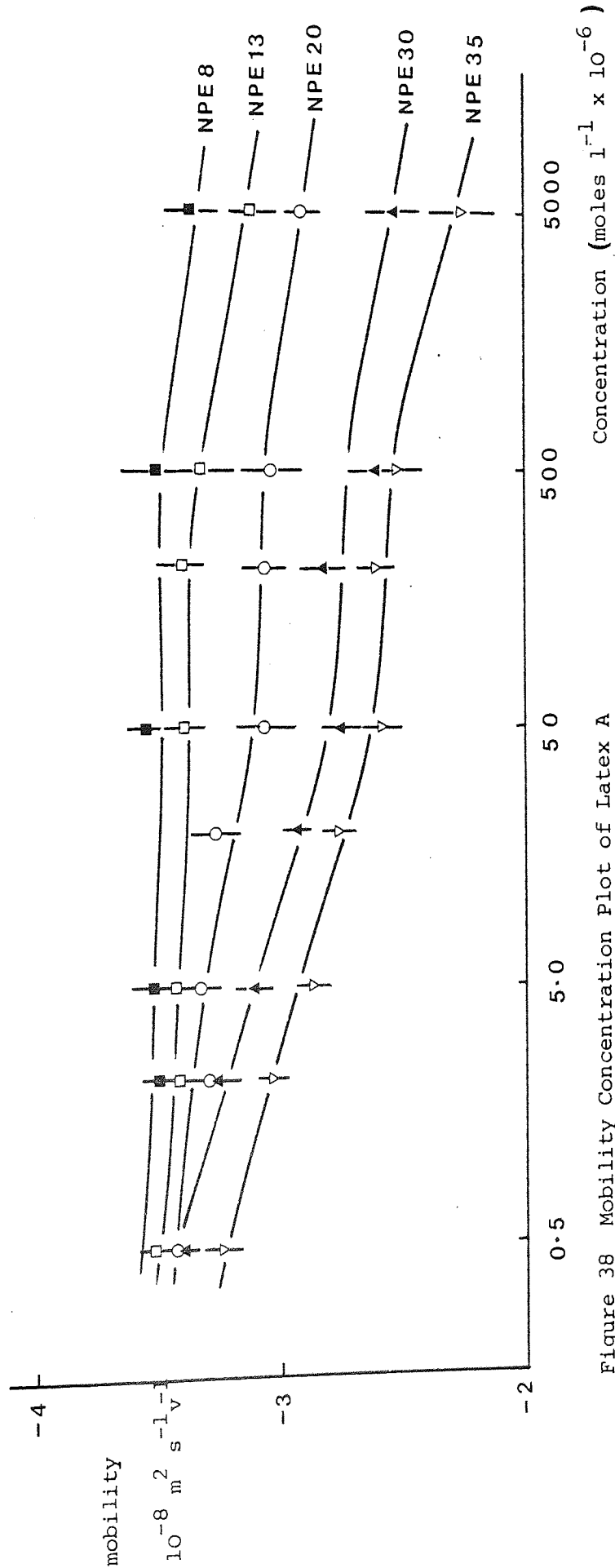


Figure 38 Mobility Concentration Plot of Latex A
in the presence of Nonylphenylethoxylates

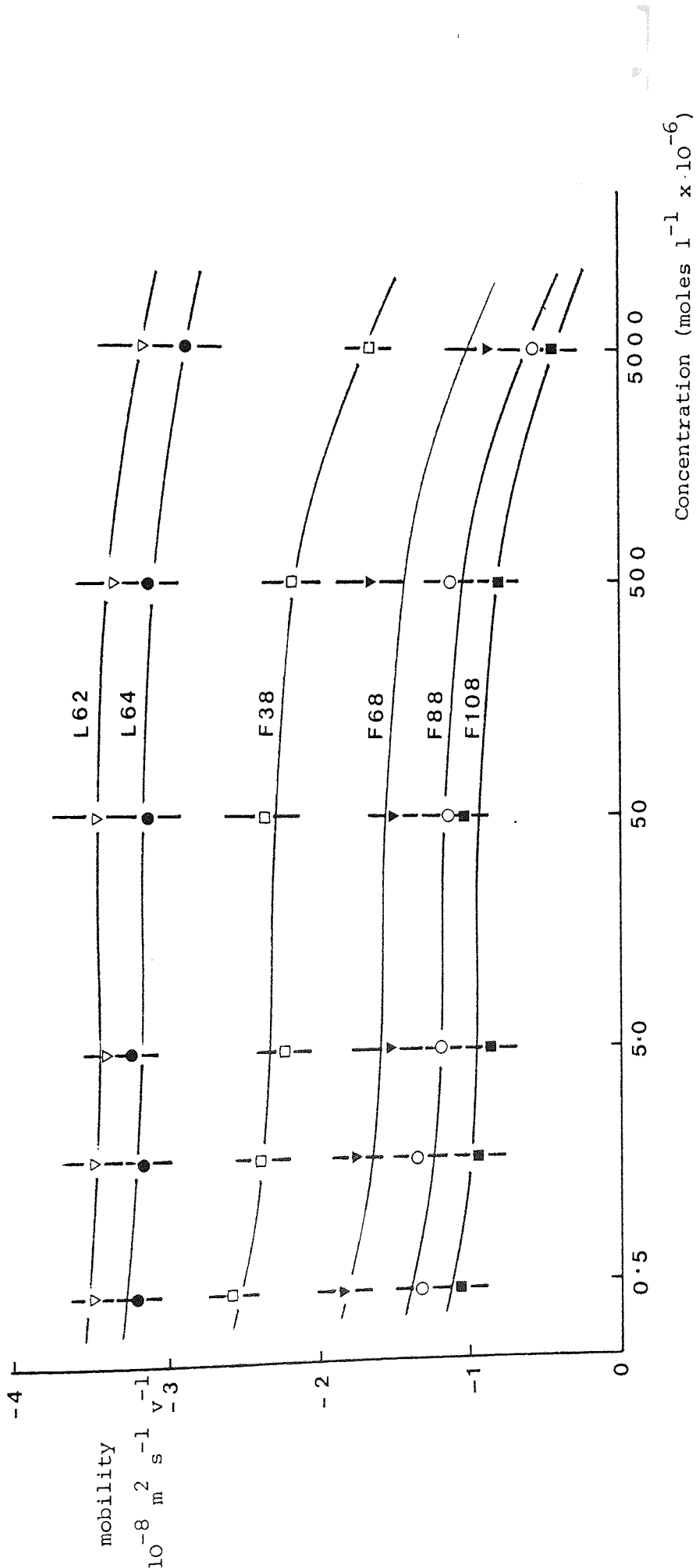


Figure 39 Mobility - concentration plot for Latex A in the presence of Pluronics

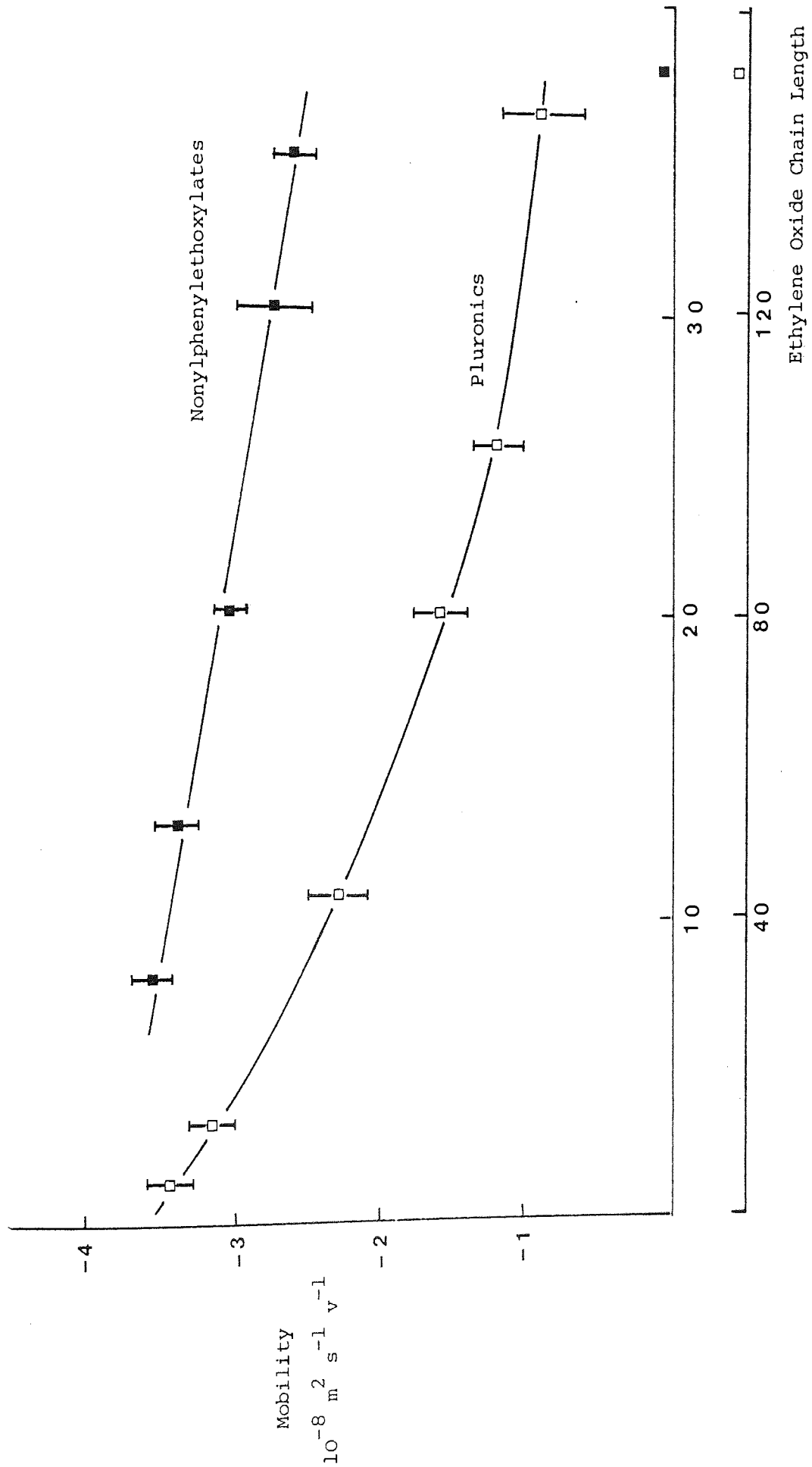


Figure 40 The Effect of Hydrophilic Chain Length on the Mobility of Latex A

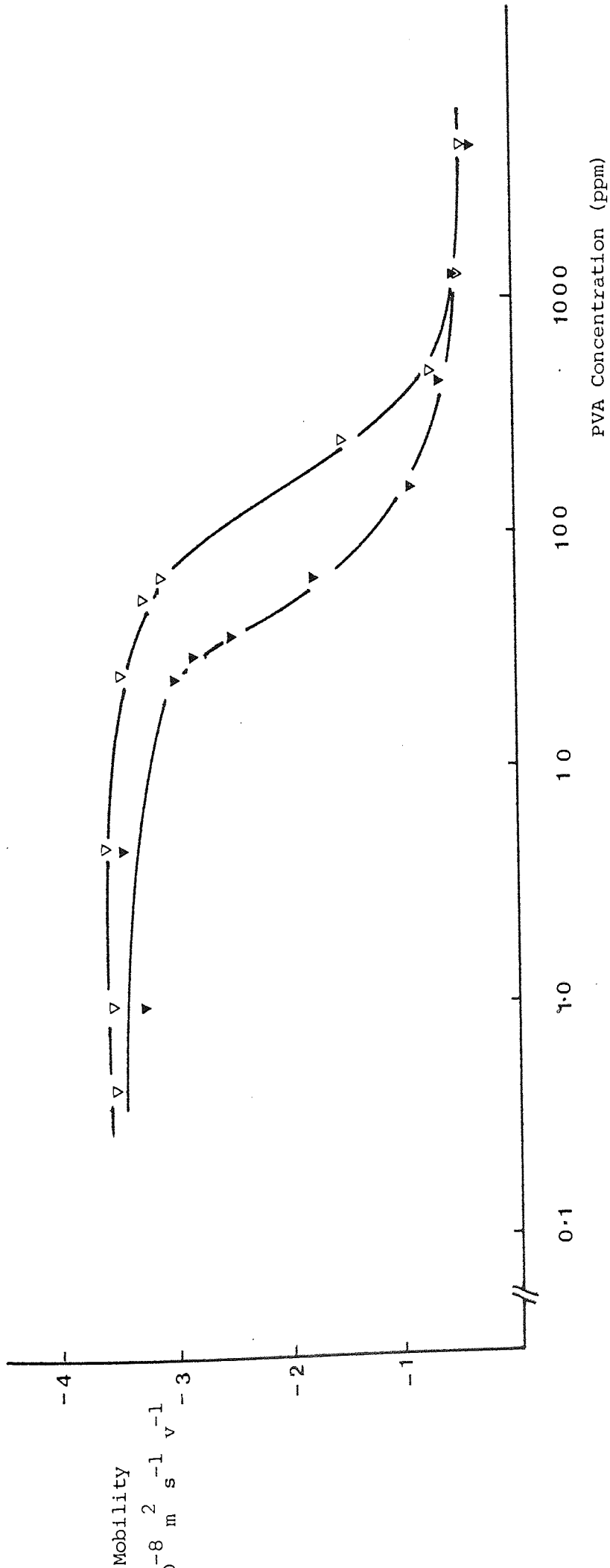


Figure 41 Mobility - concentration plot for Latex A in the presence of PVA

▽ 37,800 ▼ 97,400

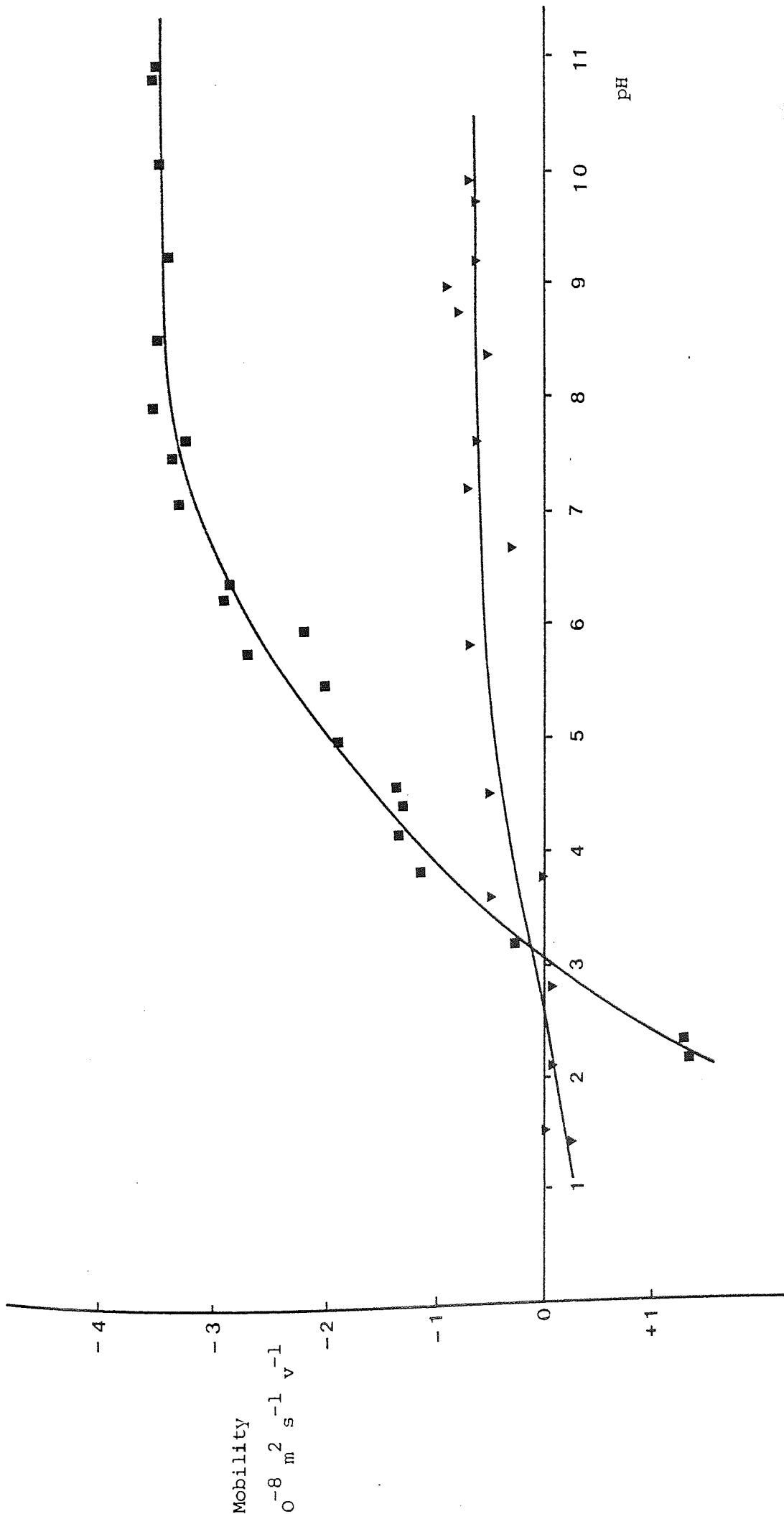


Figure 42 pH - mobility plot of Diloxanide Furoate B.P. (Batch 224231)
 in \blacksquare 10^{-3} molar and \blacktriangledown 10^{-2} molar NaCl solution

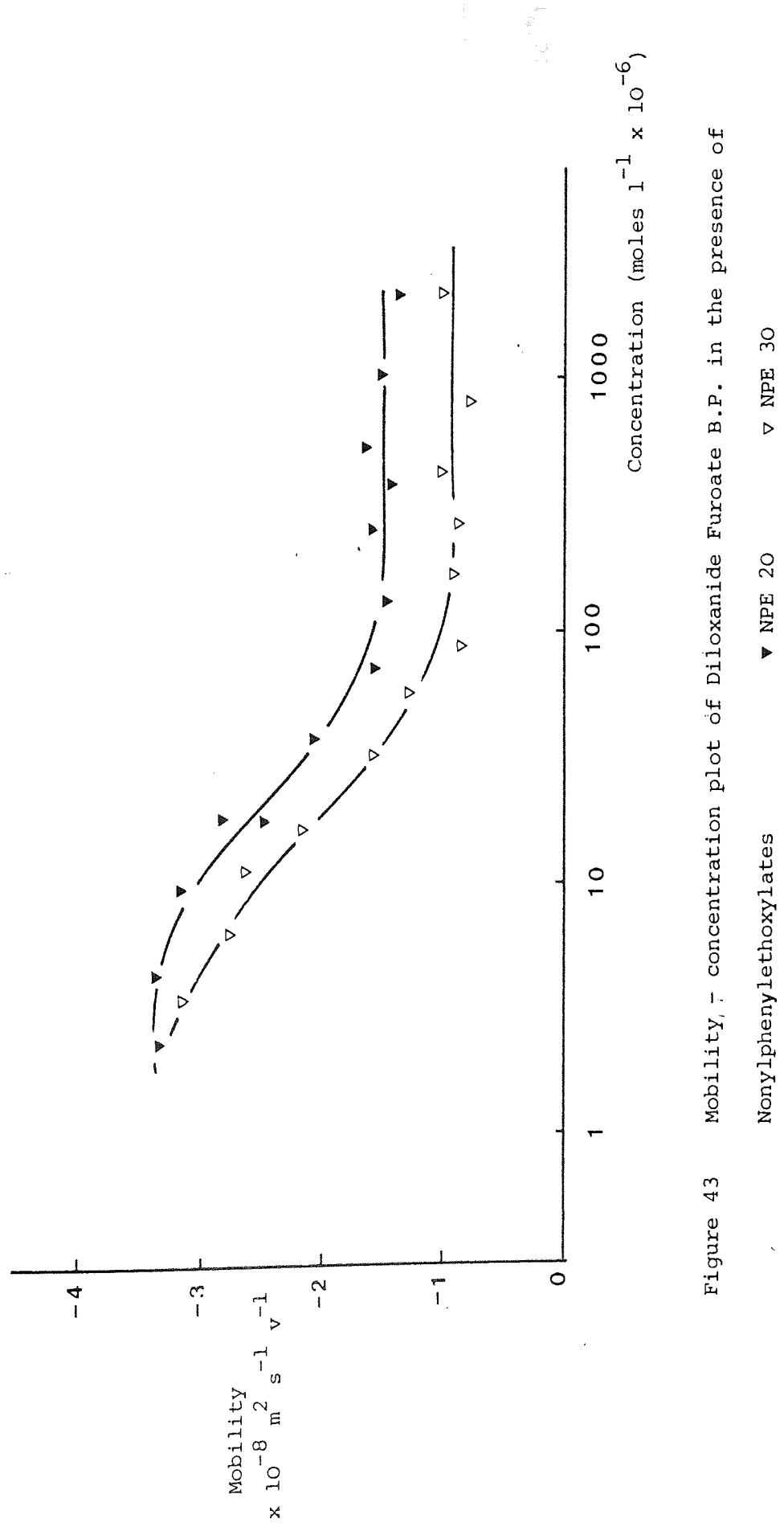


Figure 43 Mobility, τ concentration plot of Diloxanide Furoate B.P. in the presence of

Nonylphenylethoxylates

▼ NPE 20 ▽ NPE 30

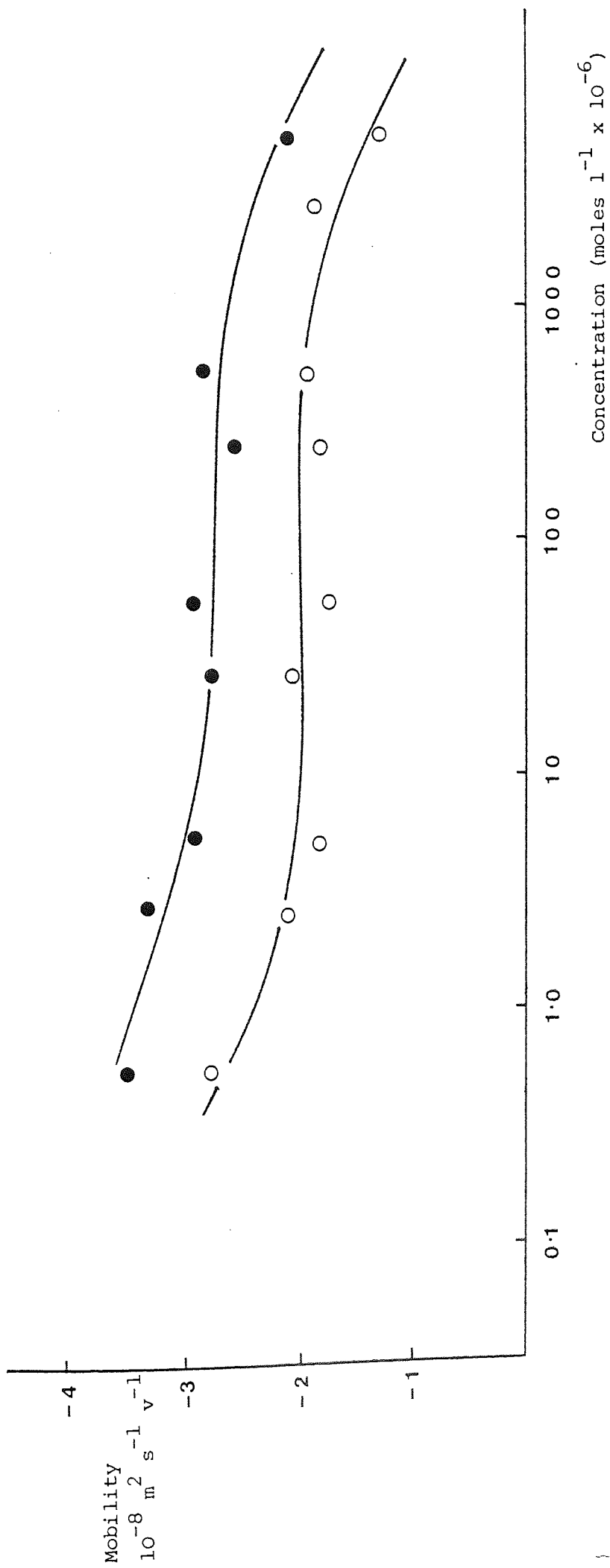


Figure 44 Mobility - concentration plot of Diloxanide Furoate B.P. in the presence of Pluronics

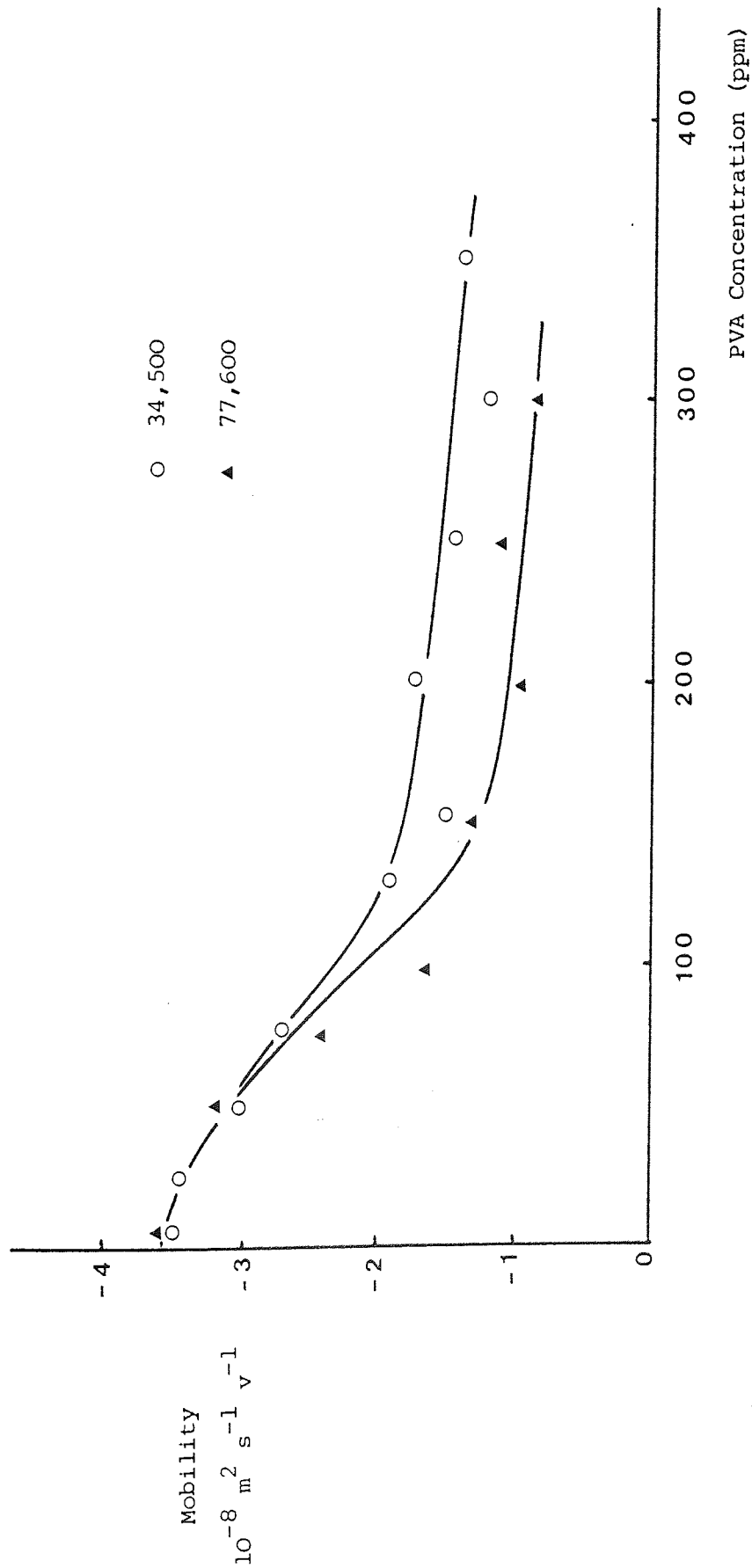


Figure 45 Mobility - concentration plot for Diloxanide Furoate B.P. in the presence of Polyvinylalcohol

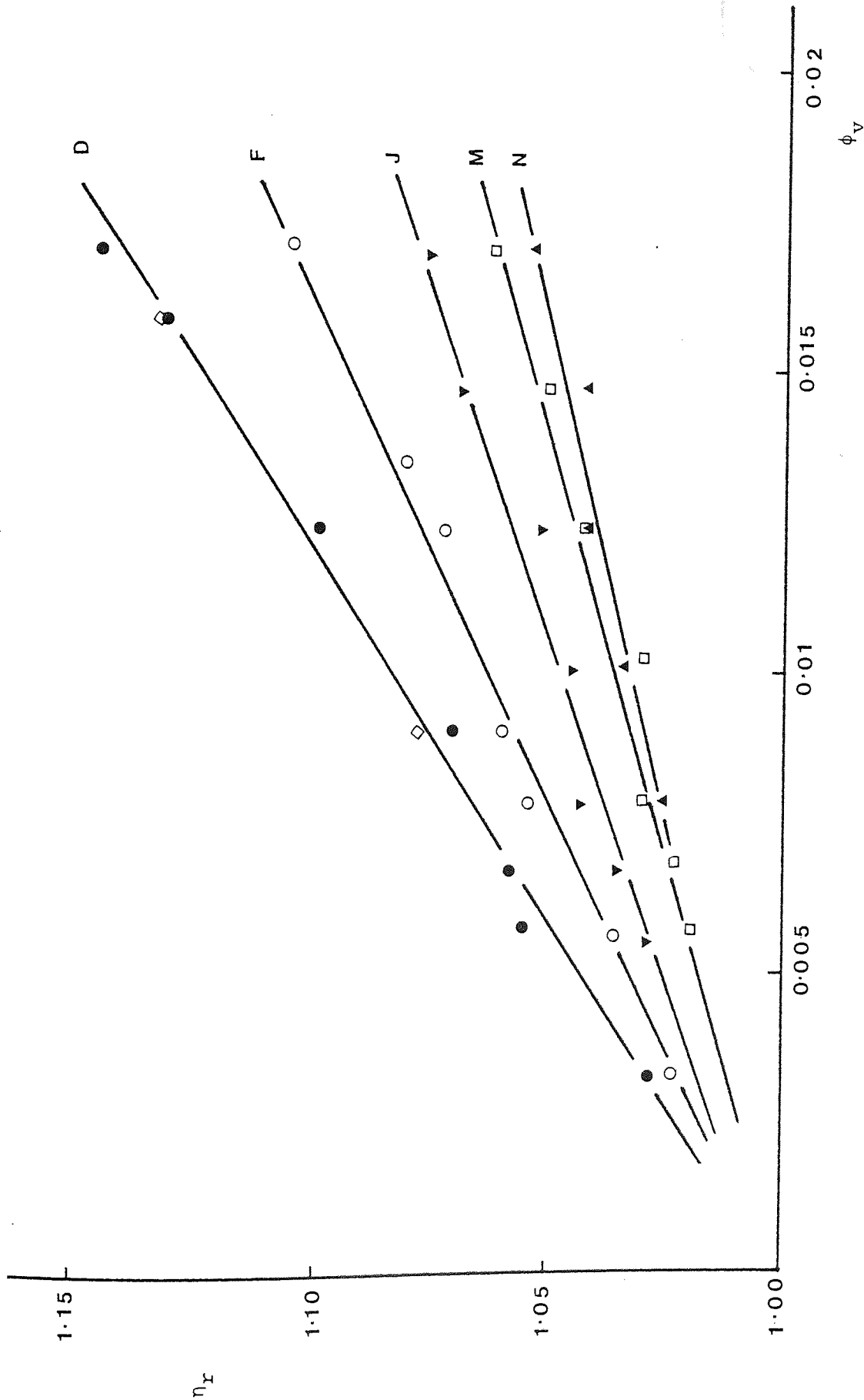


Figure 46 Graph of Relative Viscosity against Particle Volume Fraction for PVA on latex
 (◇ denotes equilibrium adsorption on glass viscometer)



Figure 47 Graph of Reciprocal logarithm(relative viscosity) against the Reciprocal of Particle Volume Fraction. *f* or PVA on latex

SECTION 6

dispersion stability

SECTION 6 - Dispersion Stability6:1 Methods6:1:1 Coarse Suspension Stability

Four criteria were used to assess the physical stability of the drug suspensions namely the appearance of the supernatant liquid, the appearance of the sediment, the sedimentation volume and the ease of redispersibility of the drug from the container base. The supernatant appearance gives a good indication of the attractive or repulsive forces operating between the particles. Thus, in a system where excess attractive forces predominate, complete aggregation of the particles occurs with the result that all particles form aggregates or 'flocs' which rapidly fall under gravity leaving a clear solution above the sediment. Where large repulsive forces are present the particles will remain as discrete entities as long as the long range van der Waals forces are of insufficient magnitude to overcome the repulsion. Sedimentation of these particles will occur and in accordance with Stokes' law the smaller sized particles of a polydispersed powder sample will take far longer to reach the container base than larger particles. This may take days or sometimes weeks to occur to completion depending on the particle size and density. The appearance of a cloudy supernatant or a slight haziness above the sediment is therefore an indication that the suspension is completely or partially deflocculated. The appearance of the sediment is an important consideration not only in discussing the type of interactions operating between particles but also in determining patient acceptability of the final product. An open-textured sediment indicates that aggregation of the particles has occurred while a dense, compact sediment shows deflocculated behaviour of the particles. The degree of aggregation determines the appearance of the final product. Hiestand considers that the aim of the formulator is to produce the 'single-floc' condition and that this one aggregate should extend throughout the entire suspension (239). In the case of a low solid volume fraction suspension such

a large aggregate would produce an extremely open-structured, inelegant sediment which may not have the desired appearance.

The sedimentation volume of a suspension is by itself meaningless due to the lack of a reference. Ward and Kammermayer (240) overcame this difficulty by expressing this characteristic in terms of the ratio of the settled height H_u , to the original height H_o . Thus the sedimentation volume (S.V.) is equal to

$$S.V. = H_u/H_o \quad (6.1)$$

Dintenfass (241) used the same ratio in terms of the sediment volume to describe the relative floc structures

$$S.V. = V_u/V_o \quad (6.2)$$

This ratio is used in the present work to describe the degree of suspension aggregation.

The resuspendibility of the suspensions were evaluated by rotating the tubes containing the dispersions in a vertical plane about the mid-point of the tube. A variable speed motor was used for this purpose (Palmer Ltd., E.P. Recording Drum) to which a shortened apparatus clamp was attached. Lateral movement of the tube centre from the axis of rotation amounted to 1cm on revolving the tube. The number of revolutions necessary to resuspend the drug was noted and this was termed the Redispersibility Value (R.V.). The end-point of the experiment was in some cases difficult to detect as compacted material forming a thin ring around the base circumference was difficult to resuspend even after prolonged rotation. For this reason the redispersibility value was taken to be the number of revolutions required to expose three quarters of the container base. The error involved in using this procedure was low, as the suspensions in which compaction occurred produced very high redispersibility values. In general the number of revolutions required to procede from

half to full container base exposure was no greater than 5% of the redispersibility value. For the sake of simplicity, those suspensions producing low redispersibility values (i.e. 1 - 5 revolutions) were all assigned a R.V. of 4.

Suspensions of diloxanide furoate (Batch 224231) were prepared in 30ml glass vials having polyethylene stoppers. Preparation of the dispersions was the same as for those used in determining the adsorption isotherms (Section 4:1) except that the total volume of liquid added was 25ml. All suspensions used in these studies were made in a final concentration of 10^{-2} M sodium chloride solution. At this strength the maximum electrophoretic mobility is $-0.5 \times 10^{-8} \text{ m}^2 \text{ s}^{-1} \text{ v}^{-1}$ (Figure 41) which corresponds to a zeta potential of -7mV. This potential is insufficient to produce a repulsion capable of stabilizing the drug particles of this size and therefore any changes in suspension characteristics will be due solely to the presence of the adsorbed polymer layer. The diameter of the tubes was ca. 25mm which is large enough for 'wall effects' to be considered absent (18). Subsequent to shaking on a water bath for 24 hours, the tubes were placed vertically in the water bath for 3 days before the suspension characteristics were noted. This has previously been shown to be adequate time for suspensions to adopt their equilibrium sedimentation volume (20). All suspensions were kept after testing and left at room temperature ($22 \pm 3^\circ\text{C}$) for one year before retesting.

6:1:2 Polystyrene Latex Stability

Preliminary studies on the stability of polymer coated latices by determining the optical density of the dispersions after coagulation had occurred gave irreproducible results. This is probably because small 'flocs' were observed to attach themselves to the glass container walls in preference to sedimenting under gravity. For this reason the method

used by Long et al (242) was adopted. For spherical non-absorbing particles, the relationship between the turbidity or optical density (τ') of the dispersion and the wavelength at which this was measured (λ) is given by

$$(\tau'/c)_{c \rightarrow 0} = k\lambda^{-n'} \quad (6.3)$$

where c is the particle concentration and k is a numerical constant. The value of the exponent n' decreases on increasing particle size. For very small particles ($\lambda/10$), $n' = 4$ which corresponds to Rayleigh scattering. n' may therefore be used to assess the degree of aggregation because as coagulation occurs the average particle size increases and hence n' will decrease. The above equation may be rewritten :

$$n' = - \left(\frac{d \log \tau'}{d \log \lambda} \right)_c + \left(\frac{d \log k}{d \log \lambda} \right) \quad (6.4)$$

For polystyrene latices k is virtually constant over the wavelength region considered here and hence n' is given by the slope of the log turbidity - log wavelength plot.

A latex of 0.716 μ diameter was used in these experiments. This dispersion was prepared by an aqueous phase polymerization technique (153) using potassium persulphate as the initiator and therefore has similar surface characteristics to the latices prepared as in Section 3. The rationale for its use was that under identical conditions of an adsorbed polymer layer a large particle latex would more readily aggregate than smaller particles due to larger van der Waals forces. To assess the effectiveness of a surface active agent in preventing coagulation a series of latex dispersions were made in 10ml glass vials with screw-on bakelite tops. To the dispersion various quantities of a stock solution of surfactant solution were added in order that a range of surface coverages of the latex by the adsorbed surfactant could be obtained. The volume

fraction of particles in the final dispersion was low enough for changes in the surfactant concentration after adsorption to be considered negligible. After equilibration for 24 hours, aggregation was induced by the addition of a volume of barium nitrate solution sufficient to give a final electrolyte concentration of 30mM. This concentration may be shown to be of sufficient strength to coagulate the bare, unprotected latex but in addition it is too low to cause salting out of the ethylene oxide surfactant chains (243). To prevent sedimentation of any aggregates the dispersions were subjected to a gentle rocking action at a frequency of 2 min^{-1} . The dispersions were then poured into 1,2,5 or 10mm absorbance cells and the optical densities were determined as a function of wavelength over the range 400-600nm using a Pye Unicam SP600 Series 2 spectrophotometer. The slope and correlation coefficient of the log (optical density) - log wavelength plots were analysed to give values of n' .

6:1:3 Determination of Hamaker Constants

To determine the Hamaker constants of all the pure materials used in this work the extrapolative dispersion technique of Gregory (244) was used. The Hamaker constant, A , of a material is given by

$$A = \pi^2 q^2 \mu \quad (6.5)$$

where q is the number of atoms or molecules per unit volume and μ is given by

$$\mu = \frac{3}{4} h v_0 \alpha_0^2 \quad (6.6)$$

h is Planck's constant, v_0 is the characteristic oscillatory frequency of the molecules and α_0 is the static polarizability which is related to v_0 by

$$\alpha_0 = \frac{e^2}{4\pi^2 M_e} \cdot \frac{s}{v_0^2} \quad (6.7)$$

where e and M_e are the charge and mass of the electron respectively and s is the effective number of dispersion electrons which is related to the molar refraction R by

$$R = \frac{n^2 - 1}{n^2 + 2} \cdot \frac{M}{\rho} = \frac{e^2 N_o}{3\pi M_e} \cdot \frac{s}{v_o^2 - v^2} \quad (6.8)$$

Substitution of equation 6.7 into equation 6.8 yields

$$\frac{n^2 + 2}{n^2 - 1} = \frac{3Vm}{4\pi N_o \alpha_o} \cdot \frac{v_o^2 - v^2}{v_o^2} \quad (6.9)$$

A plot of $(n^2 + 2)/(n^2 - 1)$ against frequency v^2 gives a straight line from which v_o is obtained from the gradient and α_o from the intercept. Substitution of these values into equations 6.6 and 6.5 gives the required quantity A .

The refractive index n , of the materials at various frequencies was measured using an Abbé 60 refractometer (Bellingham and Stanley Ltd., Tunbridge Wells). To improve the contrast between observed colour bands the compensating Amici prism was removed. The accuracy of the instrument was determined firstly by measuring the refractive index of water at the sodium D line and then comparing values of n at other frequencies with literature values and secondly by measuring n at different frequencies for benzene after standardizing the instrument with water. In all cases the error was ± 0.0001 . Five wavelengths were used namely 589nm (sodium) 546 and 436nm (mercury) and 644 and 480nm (cadmium). Where surfactants were solid at room temperature, the refractometer prisms were heated to 60°C by circulated water. All surfactants were a clear liquid at this temperature. Corrections for the variations of n with temperature and wavelength were allowed for by use of tables supplied with the instrument. This technique could not be applied to polyvinylalcohol or to the drug powder. In the case of PVA a film of dry polymer was prepared by

evaporating a thin film of concentrated aqueous solution onto a glass slide and repeating the process until a film of suitable thickness was obtained. This film was then clamped between the two refractometer prisms and the refractive index measured using monobromonaphthalene as the contact liquid. To obtain the Hamaker constants for diloxanide furoate the powder was first recrystallized from chloroform to produce large crystals and the refractive index of these crystals determined using the Becke-line method (245). The procedure involves immersing the crystals in a liquid of known refractive index and observing the direction of movement of the 'halo of light' which surrounds the particle (the Becke line) through a microscope when the objective is raised or lowered. Raising the microscope tube causes the Becke line to move towards the medium having the higher refractive index. The composition of the immersion fluid is changed until the Becke line disappears at which point the refractive index of the crystals equals that of the immersion fluid. The fluids used were saturated solutions of diloxanide furoate in cinnamon oil and propan-1-ol mixtures allowing a refractive index of up to 1.601 to be measured. Only four wavelengths could be used due to difficulties in isolating the individual wavelengths. The error involved in determining n for the crystals was ± 0.0015 .

6:1:4 Potential Energy Diagrams

Due to the time consuming nature of the calculations, Fortran programs were written to evaluate the potential energy of interactions between two particles. All programs were run on the ICL 1904S computer at the University of Aston in Birmingham. Three main files were created suitable for calculating:

- a) The potential energy of attraction between two semi-infinite flat plates coated with an adsorbed polymer layer, taking the effect of retardation into account (Equations 2.50, 2.51).
- b) The total interaction of attraction between semi-infinite plates with

no adsorbed layer present, taking retardation into account, plus the steric stabilization contribution calculated from HVO theory (Equation 2.50, 2.51, 2.22).

c) The potential energy of attraction between two spherical particles coated with an adsorbed polymer layer taking retardation into account (90).

To calculate the attractive potential between two semi-infinite plates the value of the Hamaker constant of the adsorbed layer composed of polymer and solvent was determined from the expression (90):

$$A_{p+s} = \left| F_p (A_p^0)^{1/2} + (1-F_p) (A_s^0)^{1/2} \right|^2 \quad (6.10)$$

where F_p is the volume fraction of component p and A_p^0 and A_s^0 are the Hamaker constants of the pure polymer and solvent respectively.

6:2 Results and Discussion

6:2:1a Suspension Characteristics

The suspension characteristics after standing undisturbed for three days are given in Tables 17 - 19. It should be noted that the polymer concentrations referred to are the initial concentrations and do not take into account the adsorption of material onto the drug surface.

For all those suspensions which are deflocculated at high polymer concentrations it is observed that at lower concentrations a more open-textured sediment is formed with a correspondingly high sedimentation volume. This may be the result of either primary minimum coagulation or may be due to bridging flocculation. It is doubtful whether the latter explanation could be applied to the surfactants used here as this mechanism involves the linking of two particles by polymer bridges. Such a situation is feasible for high molecular weight polymers where a terminally anchored chain extends a long way from the particle surface

and can adsorb onto a second neighbouring surface. The surfactants used here are of relatively low molecular weight (e.g. 572 for NPE 8) and in these cases it is more probable that aggregation occurs due to attraction between the large bare patches of particle surface exposed.

A low sedimentation volume indicates that a strong repulsive force is present and that this force is sufficient to overcome the attractive forces between particles. This is found with all the nonylphenylethoxylates and the higher molecular members of the polyvinylalcohol series. The Pluronic polymers do not provide sufficient steric stabilization even at high concentrations where complete saturation of the surface will have occurred, and therefore aggregation of the particles will take place resulting in a high sedimentation volume product. The types of suspension formed are discussed in Section 6:2:4 where potential energy diagrams are used to describe the interactive forces based on theoretical grounds.

The redispersibility values are plotted as a function of the initial concentration for the nonylphenylethoxylates in Figure 48 and for the polyvinylalcohols in Figure 49. Two different types of plot are obtained for the two polymer groups. On increasing the surfactant concentration (Figure 48) the redispersibility of the suspensions increases rapidly over a small concentration range to a maximum value after which a plateau is attained at high concentrations. For PVA (Figure 49), this maximum was not observed and the redispersibility increases to a more or less constant value. For the higher molecular weight polyvinylalcohols relatively high redispersibility values (R.V.) were found at very low concentrations.

Ohno et al (246) have demonstrated that a maximum in the viscosity of Veegum suspensions occurs on adding increasing amounts of a polyoxyethylene hydrogenated castor oil to the system. Adsorption of this

nonionic surface active agent onto the particle surface was shown to be multilayer in form and the maximum in the measured viscosity coincided with the inflection point of the adsorption isotherm. Maximum flocculation was also observed at this concentration. The authors interpret their results in terms of the hydrophobicity of the exposed surface. Adsorption of the surfactant was assumed to have occurred via the hydrophilic chain only so that the hydrophobic hydrocarbon chain projected into the aqueous phase. Up to the inflection point in the adsorption isotherm, two similarly coated particles could approach each other and aggregation was thought to have occurred through hydrophobic bonding of the hydrocarbon chain projecting from the surfaces. Above the inflection point further adsorption of surfactant molecules occurred, with these additional molecules oriented with their hydrophilic head group towards the aqueous phase. This produced a steric repulsion between particles and little aggregation of particles occurred after this point causing a maximum in the 'flocculation' and apparent viscosity of the dispersion at this concentration. This mechanism cannot be used to explain the results in this work where a maximum in the redispersibility curve is observed for two reasons. Firstly, multilayer adsorption of the NPE s onto diloxanide furoate does not occur (see Section 4) and secondly those suspensions where R.V. is a maximum are deflocculated in nature and not highly flocculated as found by the above authors.

A more detailed investigation of the redispersibility behaviour of the suspensions was carried out using NPE 20 and PVA ($M = 34,500$ - fraction K) as the adsorbing species. Results of these investigations are shown in Figures 50 and 51 respectively. The suspensions were prepared in 10ml glass vials as described in Section 6:1:2 and the final dispersion consisted of 1g of drug powder plus 10ml of solution of the required polymer strength at an ionic strength of 10^{-2} M sodium chloride. The results of sedimentation volumes and redispersibility values are presented here

Table 17

Characteristics of Suspensions with Adsorbed Nonylphenylethoxylate
layers after 3 days at 25°C

Initial Conc ⁿ % w/w	S.V.	R.V.	Sediment Appearance	Supernatant Appearance
<u>NPE 8</u>				
0.005	0.16	4	Aggregated	Clear
0.010	0.06	23	↑	Clear
0.015	0.06	57	↑	↑
0.020	0.05	90	caked	Cloudy
0.025	0.05	77	↓	↓
0.030	0.06	72	↓	↓
0.035	0.06	65	↓	↓
<u>NPE 13</u>				
0.005	0.12	4	Aggregated	Clear
0.010	0.05	134	↑	↑
0.015	0.05	112	↑	↑
0.020	0.06	95	caked	Cloudy
0.025	0.06	95	↓	↓
0.030	0.06	86	↓	↓
0.035	0.06	85	↓	↓
<u>NPE 20</u>				
0.003	0.14	4	Aggregated	Clear
0.008	0.06	46	↑	Clear
0.010	0.06	1140	↑	Clear
0.015	0.06	190	caked	↑
0.020	0.06	180	↓	Cloudy
0.025	0.06	107	↓	↓
0.030	0.06	90	↓	↓

Cont'd.

Table 17 (Continued)

<u>NPE 30</u>			<i>with Adsorbed Phosphate</i>	
0.003	0.23	4	Aggregated	Clear
0.004	0.25	4	Aggregated	Clear
0.006	0.12	4	Aggregated	Clear
0.007	0.15	105	↑	↑
0.008	0.06	1129		
0.010	0.06	1906		
0.015	0.06	600		
0.020	0.06	660	↓	↓
0.025	0.06	480		
0.030	0.06	520		
<u>NPE 35</u>				
0.003	0.25	4	Aggregated	Clear
0.008	0.06	1543	↑	↑
0.009	0.06	2119		
0.010	0.06	1372		
0.015	0.06	900		
0.020	0.06	970	↓	↓
0.025	0.09	910		
0.030	0.10	940		

Table 18

Characteristics of Suspensions with Adsorbed Pluronic Layers

after 3 days at 25°C.

Initial Conc ⁿ % w/v	S.V.	R.V.	Sediment Appearance	Supernatant Appearance
<u>L61</u>				
0.003	↑	↑	↑	↑
0.008				
0.010	0.28	4	Aggregated	Clear
0.015	↓	↓	↓	↓
0.020				
0.025				
0.030	↓	↓	↓	↓
<u>L62</u>				
0.003	↑	↑	↑	↑
0.008				
0.010				
0.015	0.28	4	Aggregated	Clear
0.020	↓	↓	↓	↓
0.025				
0.030	↓	↓	↓	↓
<u>L64</u>				
0.003	↑	↑	↑	↑
0.008				
0.010	0.24	4	Aggregated	Clear
0.015	↓	↓	↓	↓
0.020				
0.025				
0.030	↓	↓	↓	↓

Cont'd.....

Table 18 (Continued)

<u>F68</u>				
0.003	0.18	4	Aggregated	Clear
0.008	0.10	16		
0.010	↑	92	↑	↑
0.015		142	caked	Clear
0.020	0.06	109		
0.025	↓	115	↓	↓
0.030		97		

Table 19

Characteristics of Suspensions with Adsorbed Polyvinylalcohol layers
after 3 days at 25°C.

Initial Conc ⁿ p.p.m.	S.V.	R.V.	Sediment Appearance	Supernatant Appearance
<u>M = 5,400</u>				
100	0.28			
200	0.28			
300	0.25			
400	0.25	4	Aggregated	Clear
500	0.28			
600	0.28			
700	0.25			
800	0.28			
<u>M = 14,500</u>				
100	0.25			
200	0.25			
300	0.28			
400	0.25	4	Aggregated	Clear
500	0.18			
600	0.25			
700	0.25			
800	0.28			
<u>M = 23,200</u>				
100	0.18	4	Aggregated	Clear
200	0.12	14		Clear
300	0.06	19		Clear
400	0.06	26		
500	0.06	28	caked	Slight haze
600	0.06	32		
700	0.06	26		

Cont'd....

Table 19 (Continued)

800	0.06	32		
<u>M = 37,800</u>				
100	0.12	8	Aggregated	Clear
200	↑	42	↑	↑
300		29		
400		36		
500	0.06	27	caked	Slight haze
600	↓	43	↓	↓
700		32		
800		32		
<u>M = 77,600</u>				
100	0.06	39		Clear
200	0.06	46	↑	↑
300	0.06	51		
400	0.04	45	caked	Slight haze
500	0.06	40	↓	↓
600	0.06	40		
700	0.06	40		
800	-	45		
<u>M = 97,400</u>				
100	↑	48	↑	↑
200		46		
300		55		
400	0.06	51	caked	Slight haze
500	↓	52	↓	↓
600		47		
700		58		
800		45		

in conjunction with the adsorption isotherms of the polymers onto the drug. For NPE 20 it is apparent that the sedimentation volume rapidly decreases over a small increase in the equilibrium concentration and that the lowest sedimentation volume attained occurs just before the onset of the plateau region of the adsorption isotherm. In contrast, the maximum in the redispersibility value occurs at approximately two-thirds of maximum surface coverage. Results with the other nonylphenylethoxylates show that in general this maximum occurs between $\frac{1}{3}$ and $\frac{2}{3}$ of maximum surface coverage.

A recent paper by Rupprecht and Hofer (247) showed similar results with nonylphenylethoxylates adsorbed onto silica particle surfaces. In this case a maximum in the viscosity of the dispersion was obtained at exactly half saturation coverage and this was co-incident with a maximum in the electrophoretic mobility of the particles. They suggest that at this adsorption level, complete surface saturation occurs by the particles aggregating, thereby reducing the available surface area on which the polymers may adsorb. This aggregation produces the high dispersion viscosity observed at half saturation coverage. Two mechanisms were suggested for the increase in electrophoretic mobility at this point. The surface charge density on the silica particles was assumed constant throughout the NPE adsorption and the dielectric constant of the adsorbed film decreased from a value of ca. 80 in an aqueous environment to ca. 10 when the polymer was adsorbed. Under these conditions the surface potential is inversely proportional to the square root of the dielectric constant (247). Hence reducing the value of the dielectric constant through polymer adsorption increases the surface potential and therefore the electrophoretic mobility. Alternatively the aggregation of the particles disturbs the electrical double layer and counter-ions are displaced out of the interaction zone. This results in a higher electric charge on the floc surface yielding a large zeta-potential. These

results were shown to be particle size dependent, thus particles of mean diameter less than 30 microns exhibited high viscosities at half saturation adsorption while particles in the micron range showed no tendency to aggregate.

These mechanisms proposed to explain the high viscosities observed at partial surface coverage do not however apply to the drug system considered in this work. As in the work of Ohno et al (246), Rupprecht's results show that flocculation of the particles occurs before sedimentation is complete and the high viscosities measured in his work reflect the degree of this particle aggregation. With the diloxanide furoate suspensions coated with an adsorbed nonylphenylethoxylate layer, the particles remain as individual species except at very low surfactant concentrations where primary minimum coagulation occurs. Therefore the observed maximum in the redispersibility curve cannot be due to the above explanation of particle 'flocculation'.

To interpret the redispersibility behaviour observed in Figures 50 and 51 a model is devised which relates the suspension behaviour to the stabilization of the particles produced by adsorbed polymer layers. This is shown diagrammatically in Figure 52. The adsorption isotherm is divided into three sections corresponding to the redispersibility behaviour:

- Region A - zone of low R.V.
- Region B - zone of maximum R.V.
- Region C - zone of plateau R.V.

In Region A very low surface coverage of the drug particles occurs and in this state the surfactant molecules may be envisaged as being in an extended form on the surface. There is therefore no effective repulsion provided by these adsorbed molecules and large bare patches of

drug surface will be exposed to the aqueous medium. Approach of a second similarly coated particle will produce strongly attractive forces between the bare patches of surface and as a result of this, aggregation (or primary minimum coagulation) will occur. This aggregation is rapid and a highly open-textured, randomly packed 'floc' will result. Sedimentation of these flocs to the container base produces a very large sedimentation volume. Such sediments are easily redispersed as the open network of particles permits the passage of the aqueous medium throughout the sediment and this fluid movement assists in breaking up the floc structure. Although the interparticulate bond strength will be high, the co-ordination number of the particles will be small and therefore the amount of shear required to separate the particles will be low giving very low redispersibility values.

In Region C saturation coverage of the particle surface occurs and in this state the nonylphenylethoxylate molecules lie in the form of loops upon the surface. The high concentration of ethylene oxide chains projecting into the surrounding medium provides a very strong steric repulsion between particles and this will outweigh the force of attraction due to the long range van der Waals forces. The particles will therefore sediment slowly and individually. The repulsion between particles permits them to roll over each other on reaching the container base and smaller particles will fill in the voids created between large particles. A small, dense sediment will be formed in this case. Upon rotation of the container, fluid movement within this compact is restricted and the major force separating the particles will be the 'crashing' motion of the supernatant onto the sediment surface. The interparticulate bonds in this case will be relatively weak but due to the small sediment volume the co-ordination number of all the particles will be very high. Because of the high particle concentration in this region the effective viscosity of the sediment compact will be high and

consequently a high energy input must be given to the system to separate and redisperse the particle.

At Region B a situation intermediate to Regions A and C occurs. There is sufficient surfactant adsorbed for the molecules to project some way into the aqueous phase but in addition there may well be patches of drug surface exposed between these molecules. Due to adequate steric stabilization the particles settle individually and a small sedimentation volume is formed in the manner described for Region C. Due to the intimate contact of particles within the sediment, van der Waals attraction or crystal bridging may occur between the bare surface patches, and this effect coupled with the high viscosity of the sediment gives rise to a very high redispersibility value. This effect of 'partial steric stabilization' can therefore be used to explain the maximum in the redispersibility curves for the nonylphenylethoxylates

Results obtained with a large diameter (3 - 4 micron) polystyrene latex covered with an adsorbed layer of the nonionic surfactants - the polyoxyethylene n hexadecanols - support this concept of 'partial steric stabilization' (248) although in this case the observed maximum in the R.V.-concentration plot is not as marked as with the drug used above. This is probably due to the effect of density. The density of the drug ($1.52 \times 10^3 \text{ kg m}^{-3}$) is far greater than that of latex ($1.055 \times 10^3 \text{ kg m}^{-3}$). With the drug suspensions the attraction between sub-maximally covered particles will be enhanced by the weight of the upper sediment layers pressing down on the lower layers and forcing these particles closer together. The results with the latex also indicate that it is the attraction between bare patches rather than crystal bridging which is responsible for the maximum in the redispersibility curve. Stability studies of polystyrene latex at sub-maximal surface coverage substantiate the occurrence of partial steric stabilization (Section 6:2:2).

From Figure 51 it can be seen that the adsorption of polyvinyl-alcohols onto the drug surface does not produce a maximum in the redispersibility curve. The explanation for this probably lies in the dimensions of the molecules at the interface. At very low surface coverage the bridging mechanism described by Healy and La Mer (11) will apply and the suspensions produced will be flocculated. This is achieved by the long chain polymers adsorbing onto two particle surfaces simultaneously. Increasing the surface coverage causes the polymers to adsorb in the form of distorted random coils and extension of these coils upon the surface takes place. This flattened configuration of the macromolecules will completely cover the drug surface and further adsorption of polymer only serves to crowd the molecules together, thereby increasing the adsorbed layer thickness. The presence of an effective steric stabilizing action at low surface coverages can be observed from Figure 49 where for the higher molecular weight fractions a low sedimentation volume-high redispersibility suspension is produced at initial polymer concentrations of 100 p.p.m. Figure 45 shows the mobility - concentration plot for diloxanide furoate in the presence of increasing amounts of PVA. In this graph the initial concentrations will be approximately equal to that of the equilibrium concentration as the amount of drug present in these experiments is very low and hence little change in solution concentration will occur on adsorption. These graphs may therefore be related directly to the adsorption isotherms in Figure 51. At a concentration of 100 p.p.m. more than half of the surface saturation by the polymer has taken place and the redispersibility value is increasing at this point. This is in contrast to the nonylphenylethoxylate adsorption where at half saturation, the redispersibility value approaches the maximum. Considerable extension of the polymer from the surface is apparent from the electrophoretic mobility measurements at this concentration and this provides the stabilizing force between the particles. At this concentration therefore a combination of total

surface coverage of the drug by the polymer and extension of the molecules into the aqueous medium produces the redispersibility curves observed in Figure 49. There is no direct evidence in this work to show that at low polymer adsorption the molecules do extend over the surface and effectively 'hide' the surface against attraction from other particles. The work of Fleer, Koopal and Lyklema (85) showed that maximum adsorption of PVA onto a silver iodide sol. was 1.5 mg m^{-2} . At half of maximum surface coverage the degree of occupancy of segments in the first adsorbed layer approached 100% (232) as deduced from potentiometric titration and therefore it would appear reasonable that a similar situation occurs on the diloxanide furoate surface.

The work of Otsuka et al (35) showed that the sedimentation volume of deflocculated suspensions increased as the ethylene oxide chain length of the stabilizing adsorbed surfactants increased. This was not apparent in the present work as shown in Tables 17 - 19 and would not be expected to occur as the thickness of the adsorbed layer is at maximum ($M = 97,400$) less than 1% the particle radius.

6:2:1b Long Term Storage of Suspensions

Matthews and Rhodes (20) have prepared suspensions of griseofulvin and assessed their degree of redispersibility after nine months storage. The systems used were all coagulated and it was found that no significant change in sedimentation volume occurred over this period and that redispersibility of the sediments required little effort. The same is true of all the aggregated systems studied in this work irrespective of the mechanism of aggregation i.e. bridging flocculation with low concentrations of PVA, primary minimum coagulation with low concentrations of NPE's and restricted coagulation with the Pluronics and low molecular weight PVA's. All these systems redispersed within 1-5 revolutions of the suspensions.

The redispersibility values of the suspensions stored for one year are shown in Figure 53 for the nonylphenylethoxylates and Figure 54 for the polyvinylalcohols. The curves are essentially similar to those obtained after only three days of storage although in each case the redispersibility value is higher after prolonged storage. A possible explanation for this may be the crystal growth of particles in intimate contact during storage. Carless and Foster (249) have investigated the effect of temperature cycling on the crystal growth of suspended particles and demonstrated that the mean particle size increases with the number of temperature cycles. In this work the fluctuation in temperature on prolonged storage was 6°C which is far less than that used by the above authors of 20°C . However the time of storage of one year would allow numerous changes in small temperature cycling to take place and this may permit changes in particle size to occur. Carless and Foster also noted that crystal growth is retarded in the presence of increasing concentrations of nonionic surfactant despite the increase in drug solubility caused by solubilization. They ascribe this retardation to an interfacial interaction between the surfactant and drug. This is in contrast to the work of Tadros (250) who studied the solubilization and crystal growth of a pesticide dispersion stabilized with polyvinylalcohol and one of the Pluronic series. Dispersions in the Pluronic showed higher growth rates than those in the PVA and this was attributed to the solubilization of the pesticide causing an increase in the flux of solute diffusing to the crystal surfaces.

The particle size distributions of these suspensions were measured using the Coulter Counter as described in Section 3:4:4 and results of the surface volume mean diameter (d_{sv}) are given in Table 20. In an attempt to measure the particle size of the aggregated suspensions, 1ml of a 2.5% w/v of PVA Mowiol 8-88 was added to the suspensions which were

then sonified for 1 minute and shaken in a water bath for 12 hours. In every case deflocculated suspensions were produced using this technique.

Table 20

Surface-volume Mean Diameters of Suspensions After 1 Years Storage

Initial Conc $\frac{n}{\% w/v}$	$d_{(sv)}$ microns	Initial Conc $\frac{n}{\% w/v}$	$d_{(sv)}$ microns
<u>L67</u>		<u>L64</u>	
0.003	19.4	0.003	18.9
0.008	20.5	0.008	18.1
0.010	26.3	0.010	20.4
0.015	26.3	0.015	23.5
0.020	25.7	0.020	21.6
0.025	24.4	0.025	24.6
0.030	23.4	0.030	23.9
<u>NP20</u>		<u>NP30</u>	
0.003	20.5	0.003	22.0
0.008	16.6	0.004	31.0
0.010	12.4	0.006	26.0
0.015	12.5	0.007	26.0
0.020	12.7	0.008	14.6
0.025	11.4	0.010	14.7
0.030	11.5	0.015	11.4
		0.020	12.9
		0.025	12.7
		0.030	-
<u>PVA</u> 23,200		<u>PVA</u> 97,400	
0.01	13.4	0.01	11.4
0.02	13.4	0.02	12.5

Table 20 (Continued)

0.03	13.4	0.03	11.4
0.04	13.4	0.04	11.8
0.05	11.1	0.05	14.0
0.06	11.1	0.06	12.1
0.07	12.9	0.07	14.4
0.08	13.0	0.08	14.1

The mean diameter of those suspensions previously aggregated (e.g. Pluronics L61 and L64) are far greater than the original diameter of the particles (13 μ). Microscopic examination of these suspensions reveals that weak aggregation of the particles occurs despite the appearance of being completely deflocculated.

No conclusive results were obtained with the deflocculated suspensions due to the wide scatter of the results but their diameters are close to that of the original material. Therefore it would appear that only slight changes in particle size occur but this small change may be sufficient to increase the problem of redispersion on storage due to crystal bridging.

It is generally recognized that aggregated systems, whether flocculated or coagulated, redisperse more easily than deflocculated ones and this is borne out by the results in Tables 17-19. However, it was of interest to relate the redispersibility values to ease of dispersion by hand. Those suspensions corresponding to the final plateau region of the R.V. curve were studied by shaking the tubes by hand and noting the ease of redispersion. For the higher chain length nonylphenylethoxylates redispersion was very difficult and these

suspensions would not be suitable as pharmaceutical products. However it was found that those suspensions stabilized by NPE 8 or NPE 13 could readily be dispersed despite being deflocculated with low sedimentation volumes. In some cases it would therefore appear that deflocculated suspensions may be used pharmaceutically. Such suspensions are quite elegant although the long periods necessary for complete sedimentation may detract from their use.

6:2:2 Polystyrene Latex Stability

To demonstrate that an adequate steric stabilization exists at low surface coverages for repulsion between particles to be experienced, the aggregation of a model polystyrene latex was observed. Figure 55 shows the results obtained on plotting $\log \tau$ against $\log \lambda$ for the 0.716 micron diameter latex. Linear relationships are found illustrating the applicability of the approximate form of equation 6.4. Long et al found that for large diameter latices the $\log \tau - \log \lambda$ plots were slightly curved (242), but there is no indication of this in the present work, the lines in Figure 55 having correlation coefficients of better than 0.97. This graph also shows the results for two different particle concentrations from which it can be seen that the slope n' , is the same in both cases. For a stable, deflocculated latex the value of n' is therefore independent of the solids content of the dispersion.

Figure 56 shows the effect of time on the aggregation of latices covered with an adsorbed layer of Pluronics. In all cases, concentrations were chosen so that complete surface saturation took place and aggregation appears complete after 4 hours. The final degree of aggregation can be seen to increase with a decrease in the ethylene oxide chain length. A dispersion covered with Pluronic L61 shows no stability against aggregation since the n' -time curve is superimposed on that for the bare latex particles. No theoretical analysis exists

to derive the rate of particle aggregation from these curves, however the initial decay of n' with time is faster for the short chain length Pluronics than for those higher in the series and this would indicate qualitatively that the restricted primary minimum is deeper for the short chain length surfactants.

The effects of increasing concentration of surfactant on the stability of the latex is shown in Figure 57 where the degree of stability n' is given as a function of the initial surfactant concentration. In common with the microelectrophoretic curves differences in initial and equilibrium surfactant concentrations will be insignificant as the surface area of latex available for adsorption is very low. Direct comparisons may be made with the adsorption isotherms. Three stability curves are shown for NPE 20, L64 and F68. In every case maximum stability is demonstrated at a concentration corresponding to the onset of the plateau regions of the adsorption isotherms as indicated by the arrows. In addition the same degree of stability is found at concentrations well below this point e.g. NPE 20 and Pluronic F68 show maximum stability at approximately one order of magnitude below the surface saturation concentration. These demonstrate that the concept of partial steric stabilization introduced in Section 6:2:1 does occur and that such a mechanism can be used to explain the anomalous redispersibility behaviour observed with drug suspensions coated with the nonylphenylethoxylates. The results of Kalley, Krznarić and Cegelj (251) demonstrate that the rate of silver iodide sol aggregation decreases as the surfactant concentration increases. A large reduction in the rate was found at the critical micelle concentration although no attempt was made to relate this to the amount of polymer adsorbed. Similar conclusions were reached by Mathai and Ottewill (164) and Ottewill and Walker (162) for work on the stabilization by nonionic surface active agents on a silver iodide sol and polystyrene latex respectively, however the degree of stability was

not monitored continuously as a function of surface coverage.

Reference to the adsorption isotherms of Pluronic L64 and NPE 20 shows that at equal fractional surface coverage of latex by the surfactants, L64 is less effective in stabilizing the particles against aggregation. This may be expected on the grounds that NPE 20 will provide a larger adsorbed layer thickness capable of giving a stronger steric stabilization. L64 exhibits partial steric stabilization and maximum stabilization is provided at fractional surface coverages of approximately one half.

Long, Osmond and Vincent (242) have questioned whether a unique value for the depth of the minimum in the potential energy curves exist below which aggregation occurs and above which a system is colloiddally stable. They have demonstrated the close similarity between particle aggregation and molecular condensation from vapour to the liquid phase and show that equilibrium is established between particles in the flocs and singlets remaining in the dispersion. It is also shown that the depth of the potential energy minimum at which aggregation occurs is a function of particle size and also that a critical volume fraction of latex exists above which aggregation will only take place. Lambe et al (252) postulated that such an effect would be observed on maintaining the particle size constant but altering the dimensions of the adsorbed polymer layer. However with their system, location of the critical volume fraction could not be achieved. This was due to two possible reasons (i) the high molecular weights of polymer used reduced the depth of the minimum to such an extent that no coagulation was possible within the latex concentration range available for study (ii) the aggregation was complicated by the presence of unadsorbed polymer remaining in solution.

The effect of particle concentration on dispersion stability is seen

in Figure 58 where the degree of stability n' , is plotted against the volume fraction of latex in the dispersion. The concentration of surfactant was chosen to give complete surface saturation of the latex. The effect of unadsorbed polymer on the dispersion stability can be seen from the results with adsorbed L64. The open circles represent a surfactant concentration twice as great as that of the closed symbols and in this case it appears that extraneous polymer has little effect on stability. The critical coagulation volume fraction decreases with ethylene oxide chain length indicating the relative ease with which the latex coagulates when dispersed with the lower members of the Pluronic series. No aggregation could be found with Pluronic F68 or with any of the nonylphenylethoxylates. The results therefore show that stability of dispersions is not solely dependent on the hydrophilic chain length, as for example L64 (chain length 13 ethylene oxide units) will aggregate whereas NPE13 (chain length 13 ethylene oxide units) will not aggregate within the range studied here.

The possibility that drug suspensions coated with adsorbed nonylphenylethoxylates will not aggregate because they are below the critical volume fraction may be discounted. The critical volume fraction decreases with an increase in particle size and Long et al have shown that for a 490nm radius particle the c.f. ϕ is less than 1×10^{-5} (242). The drug particles used in the present work are of approximate radius 6 microns and are used at a volume fraction of ca. 2.5×10^{-2} . In addition, aggregation has been shown to occur with diloxanide furoate particles coated with other polymeric substances used in this work.

6:2:3 Hamaker Constants

The results of the Hamaker constants of all the materials used in this work are given in Table 21 together with the characteristic frequencies and polarizabilities. Figures 59 - 62 show the graphs from

which this data was derived and the applicability of the dispersion equations to these materials.

The values of the Hamaker constant obtained for the nonionic surfactants are in good agreement with those reported by Elworthy and Florence (234) for surfactants of the cetyl polyoxyethylene glycol ether group. An increase in A was found on increasing the ethylene

Table 21
Optical Dispersion Data of Materials

Material	Temp °C	ν_0 $\times 10^{15}$ sec^{-1}	α_0 $\times 10^{-17}$ $\text{m}^3 \text{mol}^{-1}$	A $\times 10^{-20}$ J
Water	25	3.27	14.50	3.78 [*]
Polystyrene latex	20	-	-	7.80 [†]
Diloxanide furoate	25	2.48	2.49	5.88
L61	25	3.64	20.15	7.11
L62	25	3.60	22.35	7.11
L64	25	3.60	29.35	7.15
NPE 8	25	3.11	6.06	6.88
PVA (Mowiol 8-88)	25	3.72	378.90	8.72
L61	60	3.59	19.88	6.69
L62	60	3.58	22.05	6.74
L64	60	3.57	29.08	6.81
F68	60	3.54	86.79	6.97
NPE 8	60	3.29	5.99	7.00
NPE 13	60	3.31	8.18	6.91
NPE 20	60	3.31	11.19	6.85
NPE 30	60	3.32	15.39	6.79
NPE 35	60	3.33	17.76	6.78

oxide chain length (234) but in the present work both increases and decreases are found depending on the surfactant group under study. Little change in the Hamaker constant is apparent on raising the temperature from 25 to 60°C and therefore the higher temperature values were used for the surfactants in calculating the potential energy diagrams. The value of the Hamaker constant for polyvinylalcohol is in excellent agreement with that given by Visser (253) in his review article on the subject. Tadros has shown that using the dispersion technique, two values of A can be found for ethirimol crystals corresponding to the different orientation of the crystals (227). No evidence of anisotropy could be found for the drug crystals within the limited range of immersion fluids available. The values of 5.88×10^{-20} J can be compared with the values of $6.52 - 7.76 \times 10^{-20}$ J for ethirimol and may give some idea of the range of values for organic crystals.

It is well known that the value of the Hamaker constant depends upon the method of determination. Thus coagulation (254), interfacial tension (255) and dispersion data all give different values for the Hamaker constant and it is necessary to use only one type of result in order that direct comparisons may be made. Only data obtained from optical dispersion measurements are used in the present work.

6:2:4 Potential Energy Diagrams

The rationale for using specific equations in estimating the potential energies of attraction and repulsion is explained as follows.

For all cases where the attraction between particles of the drug is considered, equations for semi-infinite flat plates have been used. Due to the non-sphericity of the drug particles (being approximately twice as long as they are wide) and due to the large irregularities on

the surface, equations for spherical particles were considered inappropriate. Use of spherical particle equations would also lead to very large values of the restricted primary minimum depth which could not be reconciled with the experimental evidence that in some cases stabilization of the dispersions does occur. Flat plate equations were therefore used although the values of the energy minima determined may be used only in a qualitative manner to predict whether aggregation will take place. When spherical particles are considered, it has been suggested that a critical minimum energy depth exists above which aggregation will not take place as the thermal motion of the particles will overcome the tendency for aggregation to occur. This depth has been given values of 1 - 20kT units by several authors (see 242). When considering flat-plate interactions no such critical minimum depth has been put forward. Thus the problem of predicting whether aggregation will take place is avoided.

In studying the mechanisms of particle aggregation, Evans and Napper (92) concluded that aggregation is probably induced as a result of the attraction between the stabilizing adsorbed layer sheaths rather than the attraction between the core particles. They claim this would apply in the case where the core and sheath attractions are of the same magnitude, but that such a situation would not apply as, for example with metal sols where the core attraction may dominate. This mechanism has been used in the present work and calculations of V_A based upon the equations of Vincent (90) have been performed which take into account the effect of the presence of adsorbed layers and retardation on V_A (Equations 2.50, 2.51).

The presence of the adsorbed layer presents certain difficulties in calculating the depth of the restricted primary minimum as these equations for V_A predict that upon contact of the adsorbed layers V_A tends to

- ∞ . To overcome this difficulty a few layers of solvent molecules are envisaged bound to the ethylene oxide chains and this provides a cut-off point at which V_s increases rapidly. In the present work, V_A is calculated from Vincent's equations and the cut-off point is taken to be 0.6nm, corresponding to 4 molecules of bound water sandwiched between the interacting polymer layers (109).

This method of obtaining V_p obviates the need to calculate V_s exactly and incorporate it into the potential energy diagram. This is advantageous as the determination of the polymer-solvent interaction parameter χ is difficult to assess and the value of V_s is heavily dependent upon its value. For example, V_s is proportional to $(0.5 - \chi)$, (see equation 2.13) and for polyvinylalcohols the limiting value of χ is around 0.475 (133). Small experimental errors in the evaluation of χ may therefore lead to large errors in the calculation of V_s . This is further complicated as χ is polymer concentration dependent and therefore an accurate value for the adsorbed layer concentration is required to calculate V_s .

Ottewill and Walker (162) have demonstrated that when $\chi < 0.4$, V_s is positive and rises very steeply with decreasing distance between the particles. Therefore in the case of the ethylene oxide nonionic surfactants it is justifiable to represent V_s by a straight line rising nearly vertically from the V_A curve at $H = 0.6\text{nm}$, as Florence and Rogers have given values of χ for various chain length ethylene glycols of 0.16 - 0.35 (256).

Calculations of V_A at a surface separation of 0.6nm are shown in Figures 63 and 64 for data corresponding to:

- a) Hamaker constant of core variable while that of the adsorbed layer is constant at 4.5×10^{-20} J.

- b) Hamaker constant of the adsorbed layer variable while that of the core is constant at 5.88×10^{-20} J.

The depth of the minimum in the potential energy curve ($H = 0.6\text{nm}$) is more strongly effected by the Hamaker constant of the adsorbed layer than by that of the core particle. For example when the adsorbed layer thickness is 1nm , a change in the Hamaker constant of the adsorbed layer from 4×10^{-20} to 7×10^{-20} J causes a twenty-fivefold increase in the value of V_A . Changing the Hamaker constant of the core particle over the same range only doubles depth of the minimum. These calculations substantiate the view of Evans and Napper (92) that it is the attraction between adsorbed layer sheaths which is primarily responsible for the promotion of particle aggregation.

The effect of adsorbed layer thickness on the depth of V_A is also demonstrated in Figures 63 and 64. The effect on V_A of altering the Hamaker constant of the core particle decreases with increasing δ (Figure 64) and at $\delta = 10\text{nm}$ no significant change in V_A occurs over the whole range of Hamaker constants studied here.

Potential energy diagrams of drug particles covered with adsorbed layers of nonylphenylethoxylates, Pluronics and polyvinylalcohols are shown in Figures 65, 66 and 67. The depths of the minima in these diagrams are tabulated in Table 22 together with the type of suspension that is formed on adsorbing the polymers onto the drug surface at maximum surface coverage.

Table 22

Restricted Primary Minimum Depth and Suspension

Types

Polymer	$V_A (H = 0.6\text{nm})$ $kT.\text{nm}^{-2} \times 10^{-3}$	Suspension Aggregation
<u>PVA</u>		
5,400	- 17.60	✓
14,500	- 3.27	✓
23,200	- 1.60	-
37,800	- 1.04	-
77,600	- 0.31	-
97,400	- 0.22	-
<u>Pluronics</u>		
L61	- 12.48	✓
L62	- 13.15	✓
L64	- 5.94	✓
F68	- 0.27	-
<u>NPE's</u>		
8	- 4.80	-
13	- 4.23	-
20	- 3.51	-
30	- 2.65	-
35	- 2.07	-

The agreement between the depth of the energy minimum and the suspension type is reasonable if a value of ca. $5 \times 10^{-3} kT.\text{nm}^{-2}$ is taken as the critical depth above which aggregation will not occur. However this applies only to those polymers of the ethylene oxide surfactant type as PVA 14,500 demonstrates an exception to this rule. The probable explanation of why the polyvinylalcohols do not conform to

the critical depth-suspension type relationship is due to the fact that in all these calculations a mean-segment concentration of polymer within the adsorbed layer is assumed. This is reasonable for the short chain ethylene oxide condensates where the chains only extend a few nanometres from the surface. For the polyvinylalcohols and other long chain polymers the segment concentration decreases exponentially away from the surface and the above model is therefore unrealistic. A further explanation may be due to the measurement of the adsorbed layer thickness. This value is critical, particularly for the short chain polymers, as it controls the polymer concentration of the adsorbed phase and through this the Hamaker constant of this layer and V_A . The measurement of this thickness for the PVA's was not performed directly but was obtained from a knowledge of the amount adsorbed and from the polymer dimensions in solution. Whilst it has been shown that the volume of polymer molecules does not change upon adsorption onto polystyrene latex (145) the same cannot be conclusively said of adsorption onto diloxanide furoate and the determination of the adsorbed layer thickness is only obtained on applying this assumption. In order to obtain a value of $5 \times 10^{-3} \text{ kT.nm}^{-2}$ for this polyvinylalcohol, calculations show that for the same amount of polymer adsorbed, the layer thickness would have to be ca. 3.5nm instead of 4.6nm. This calculation takes into account changes in Hamaker constant on reducing δ . This reduction represents a 25% change in the volume of the adsorbed molecule which in the light of previous work (54,145) seems unlikely to occur.

Figure 68 shows the variation in restricted primary minimum depth as a function of molecular weight for the polyvinylalcohols. Increasing the molecular weight decreases the attraction between particles. The depth of the minimum of the uncoated drug particles is $-4.22 \times 10^{-2} \text{ kT.nm}^{-2}$ and it can be seen for PVA 5,400 that adsorbing polymer onto the particles increases the attraction. The same is found for several of the Pluronics

and nonylphenylethoxylates and confirms the results of Elworthy and Florence who found increased attraction on emulsion droplets coated with nonionic surfactants (234).

The attraction between particles is therefore dependent upon the concentration of polymer in the adsorbed phase and these values are given in Table 23.

Table 23
Concentration of Polymer in the Adsorbed Phase

Polymer	NPE 8	NPE 13	NPE 20	NPE 30	NPE 35	
Conc $\frac{n}{\%}$ w/v	22	21	18	16	16	
Ethylene Oxide						
Conc $\frac{n}{\%}$ w/v	13	15	14	13	14	
Polymer	<u>L61</u>	<u>L62</u>	<u>L64</u>	<u>F68</u>		
Conc $\frac{n}{\%}$ w/v	34	36	15	4		
Ethylene Oxide	3	7	6	3		
Conc $\frac{n}{\%}$ w/v						
PVA	<u>5,400</u>	<u>14,500</u>	<u>23,200</u>	<u>37,800</u>	<u>77,600</u>	<u>97,400</u>
Conc $\frac{n}{\%}$ w/v	35	17	12.2	9.6	5.2	4.4

The concentrations of the Pluronics which promote particle aggregation have significantly higher values than the nonylphenylethoxylates. In addition, the concentrations of the stabilizing moieties, the ethylene oxide groups, are far less in the Pluronic series and therefore the repulsive force due to steric interactions will not be as great as those of the nonylphenylethoxylates. Aggregation of particles coated with an adsorbed layer of Pluronics L61, L62 and L64 may therefore be due to a combination of two mechanisms:

- a) high interparticulate attraction due to high interfacial polymer concentration
- b) insufficient steric stabilization to prevent aggregation.

With the polyvinylalcohols the aggregation may again be explained by the high concentration of polymer at the interface increasing the attractive potential between particles. Complications arise due to the concentration dependence of the polymer-solvent interaction parameter χ . Peppas and Merrill (257) have shown that at 20°C χ increases from 0.475 to 0.495 on increasing the volume fraction of polymer from 0.05 to 0.10. From Table 23, the volume fractions of the two lowest molecular fractions are in excess of 0.10 and it is conceivable that in these cases χ is greater than 0.5 which would result in an attraction between particles due to the steric term alone as V_s would be negative. This effect may also explain why aggregated systems are found with these two polymers.

A major difficulty in constructing potential energy diagrams is determining the effective adsorbed layer thickness at which steric repulsion first occurs. Garvey, Mitchell and Smith (258) have used a two dimensional compression technique to study these forces and have ascertained that repulsion originates at an interparticulate distance of 150nm whereas the hydrodynamic adsorbed layer thickness was 44nm. They state that serious difficulties may arise in calculating V_s if the free draining portion of the adsorbed layer is not accounted for. The polymer used was polyvinylpyrrolidone (PVP) and Najib, Kellaway and Marriott have shown that for low molecular weight species of this polymer long tails extend from the surface (259). It is likely that these tails produce the long range steric repulsion between particles. For PVA such tails have not been shown to occur and with the polymer adsorbing as random coils a loop distribution of the chains is likely although the

possibility of adsorbed tails may not be discounted

Table 23 shows that high concentrations of polymer exist at the drug-solution interface. Cloud point studies of relatively dilute solutions of some of the surfactants are shown in Figure 69 where low cloud point temperatures are found for Pluronic L62 and NPE 8. The value for NPE 8 ($25 - 26^{\circ}\text{C}$) is close to that at which the measurements in this work were performed (25°C) and hence instability of suspensions and latex dispersions coated with an adsorbed layer of this surfactant might be expected due to dehydration of the polymer chains. This is not found experimentally as the results of Table 17 show and therefore the molecules at the interface cannot adopt the same configuration as those molecules in the bulk solution.

Potential energy diagrams for spherical particles were also constructed for the 0.716 micron diameter latex used in the stability experiments using Vincent's equations allowing for retardation (90). The curves obtained in Figures 70 and 71 reflect the relative stabilities of the latex when coated with nonylphenylethoxylates and Pluronics respectively. Experimental instability was found for Pluronics L61, L62 and L64 while all the remaining nonionic surfactant displayed no evidence of aggregation. This is accounted for by the potential energy diagrams where a value of approximately 16 to $20kT$ may be taken as the critical depth below which aggregation occurs. In these calculations the presence of the adsorbed layer reduces the attraction below that found for the uncoated latex.

Long et al (242) have attempted to relate the critical coagulation volume fraction (c.f. ϕ) of latex (Fig, 58) to the depth of the minimum in the potential energy curve using an equation analogous to vapour liquid condensation equations, viz:

$$L_D = L_F \exp(-BV_m/kT) \quad (6.11)$$

where L_D and L_F are the volume concentrations of latex in the dispersed and floc phases respectively, B is the co-ordination number of particles within the floc and V_m is the depth of the potential energy minimum. Use of equation 6.11 with values of L_D and B giving the closest agreement of V_m with that obtained from potential energy diagrams shows marked differences between the two values. Values of V_m obtained from equation 6.11 were always greater than those obtained through use of energy diagrams. This observation was also found by Long et al for larger particle size latices although they claimed good agreement when the particle diameter was less than 500nm.

The equations of Hesselink, Vrij and Overbeek (88) have been used in combination with those of Vincent (90) to permit the construction of potential energy diagrams for polyvinylalcohol adsorbed onto flat plates of diloxanide furoate allowing for the exponential segment density distribution of polymer normal to the surface. Figure 72 shows the three components of the total interaction curve namely the osmotic, volume restriction and attraction terms. The attraction term V_A was calculated by neglecting the effect of the adsorbed layer and choosing a composite value for the Hamaker constant of the particle of 4.5×10^{-20} J. These results are based on data for $M = 37,800$ obtained in previous sections. The osmotic term operates well before the volume restriction term and in further calculations this minor term has been neglected. However for smaller molecular weight polymers the volume restriction term may dominate, but the equations for this effect when M is small become less accurate (88).

Total potential energy diagrams for the PVA's using the HVO theory for an equal loop size distribution are given in Figure 73 for all the

fractions used in this work. Increasing energy minima are found on decreasing the molecular weight which is in agreement with calculations based on a mean segment density distribution (Figure 67). For the smaller molecular weight fractions the distance at which repulsion starts to occur is however much greater than twice the thickness of the adsorbed layer determined in Section 5 while for higher fractions the reverse applies. This arises because of the exponential decrease in segment density which according to theory only becomes zero when the distance from the surface tends to infinity. The use of such equations is at the present time therefore limited and the energy minima calculated in this way should be viewed with caution.

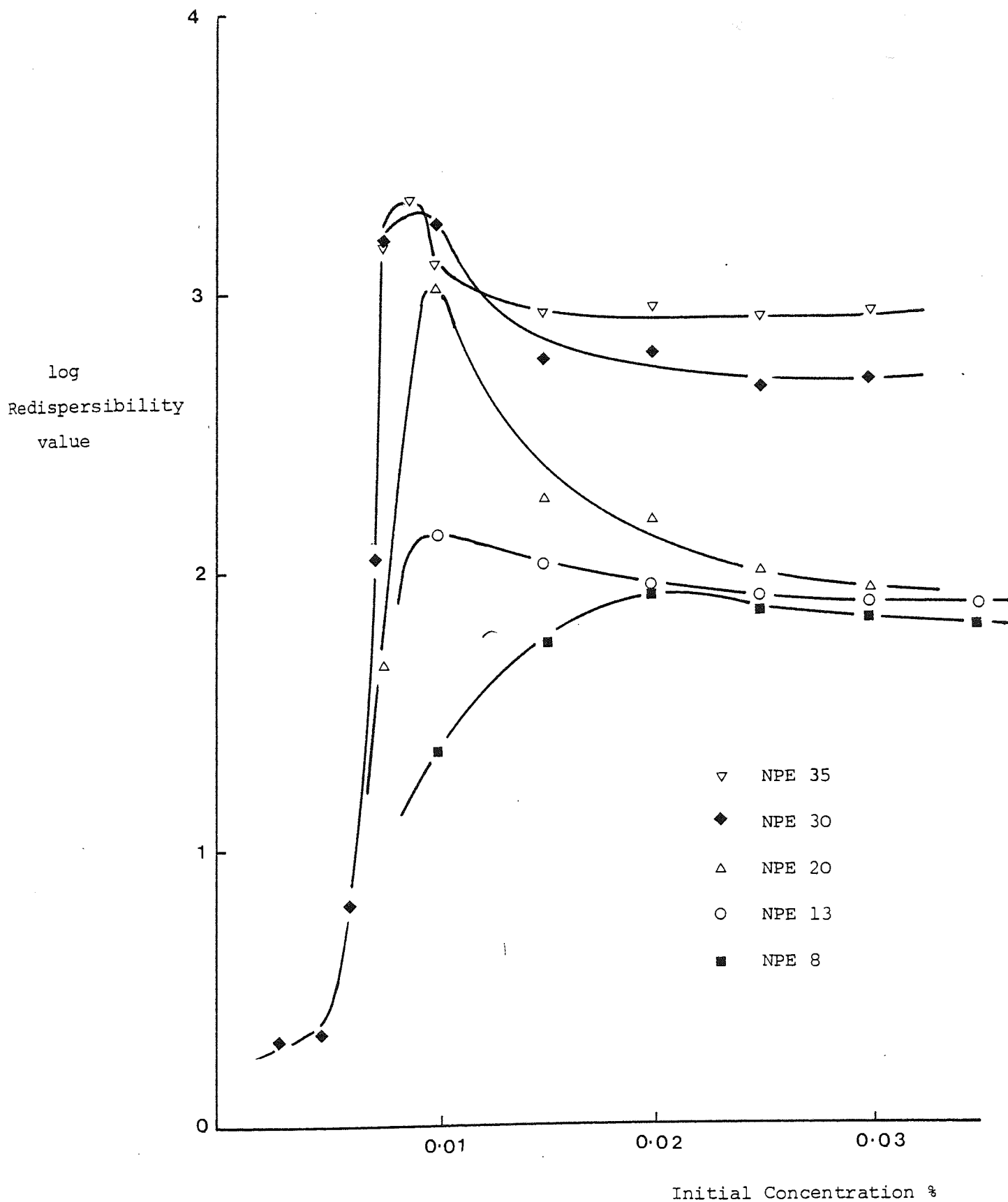


Figure 48 Redispersibility Data for Drug Suspension in the Presence of Nonylphenylethoxylates after 3 days Storage.

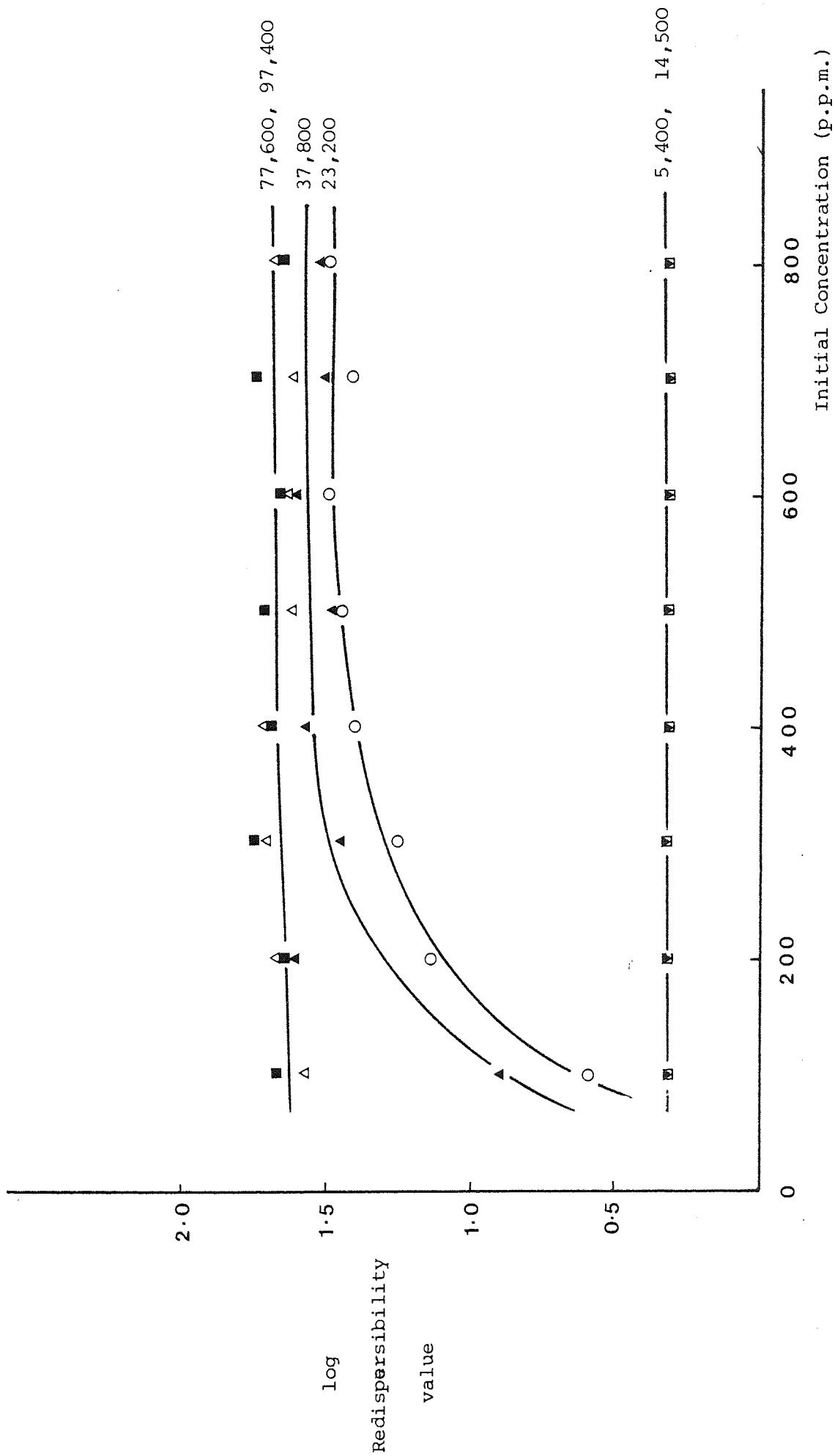


Figure 49 Redispersibility Data for Drug Suspension in the Presence of Polyvinylalcohols

After 3 Days Storage.

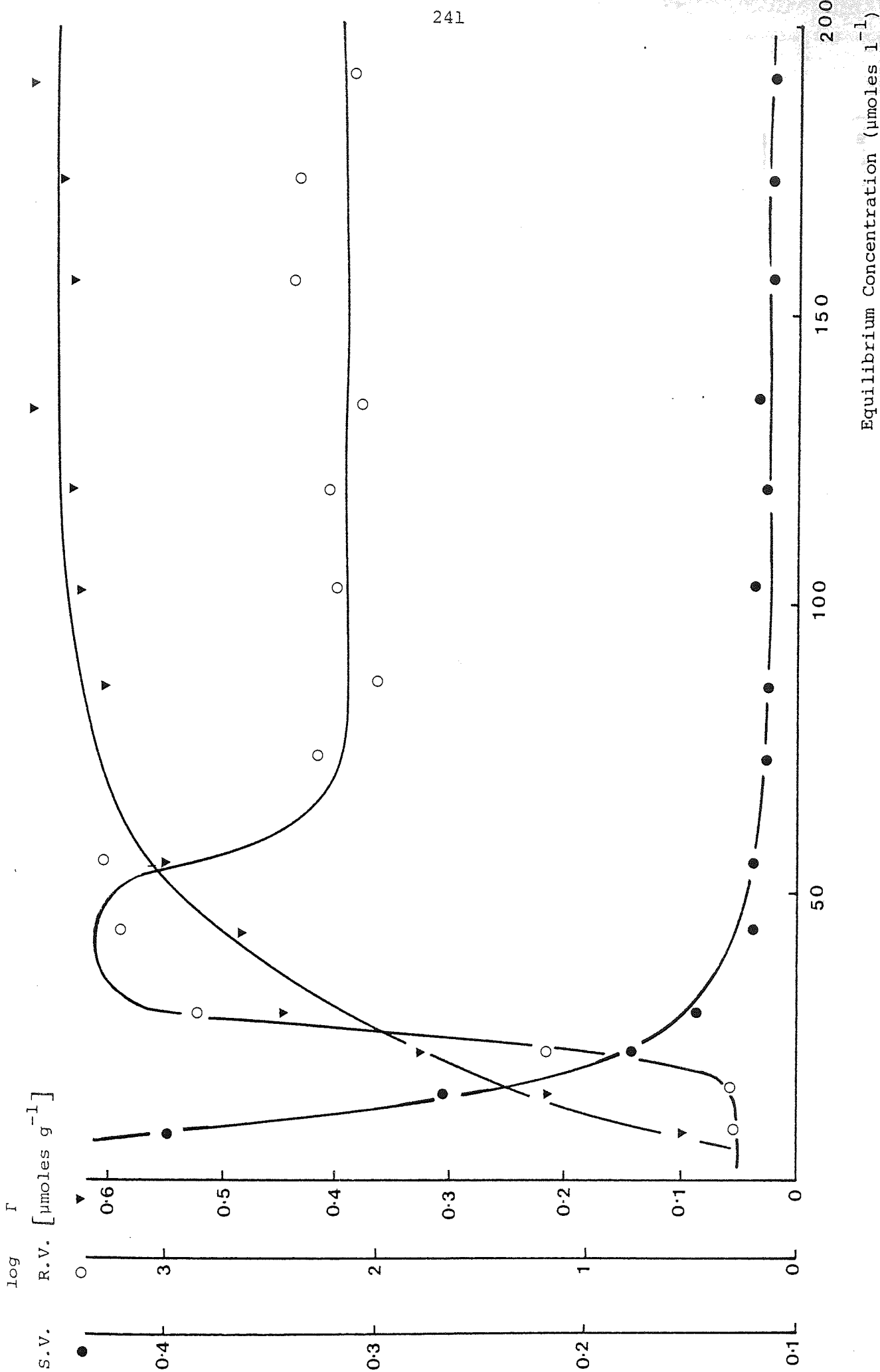


Figure 50 Suspension Characteristics in the Presence of NPE 20

After 3 days Storage.

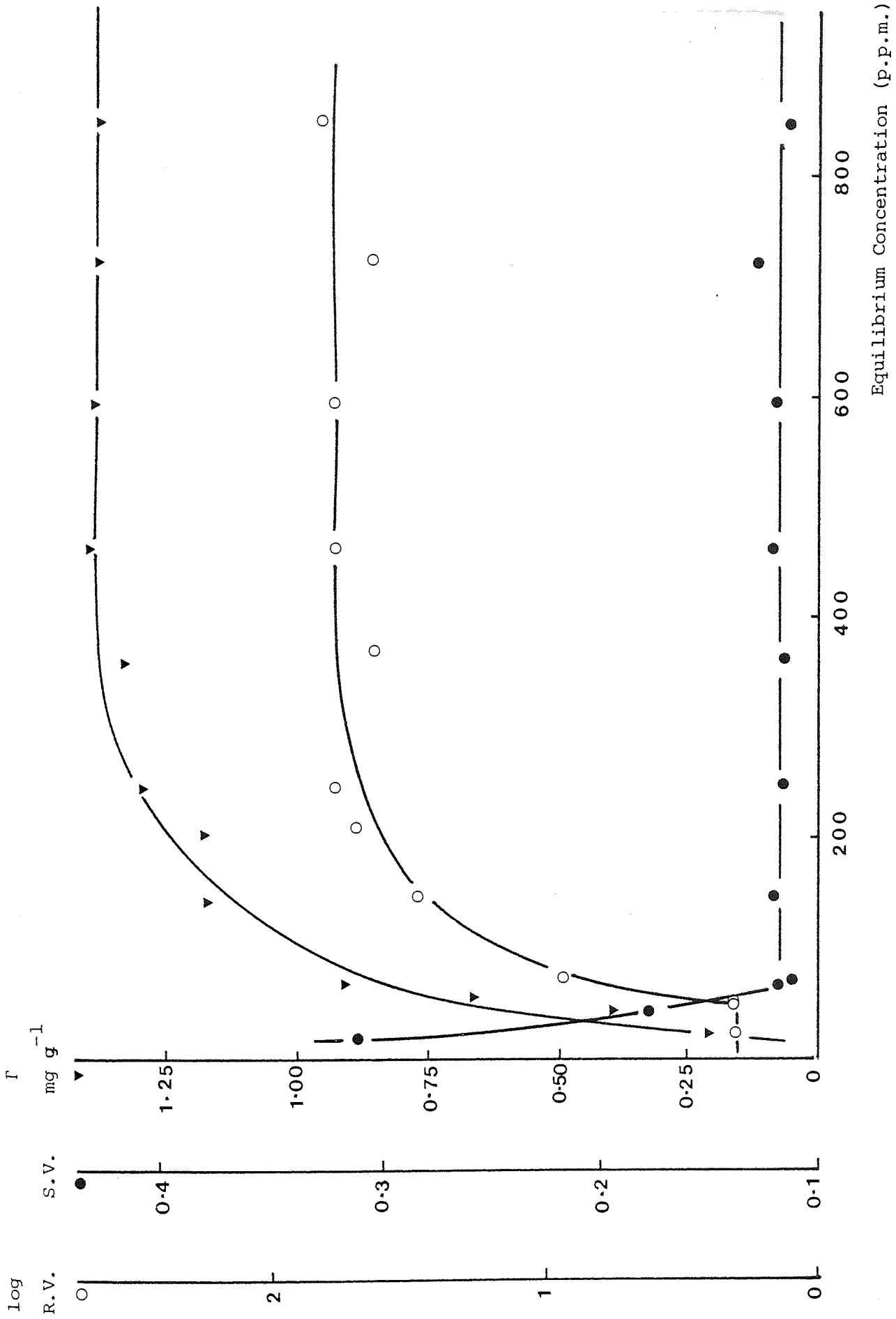


Figure 51 Suspension Characteristics in the Presence of PVA 34,500 After 3 days.

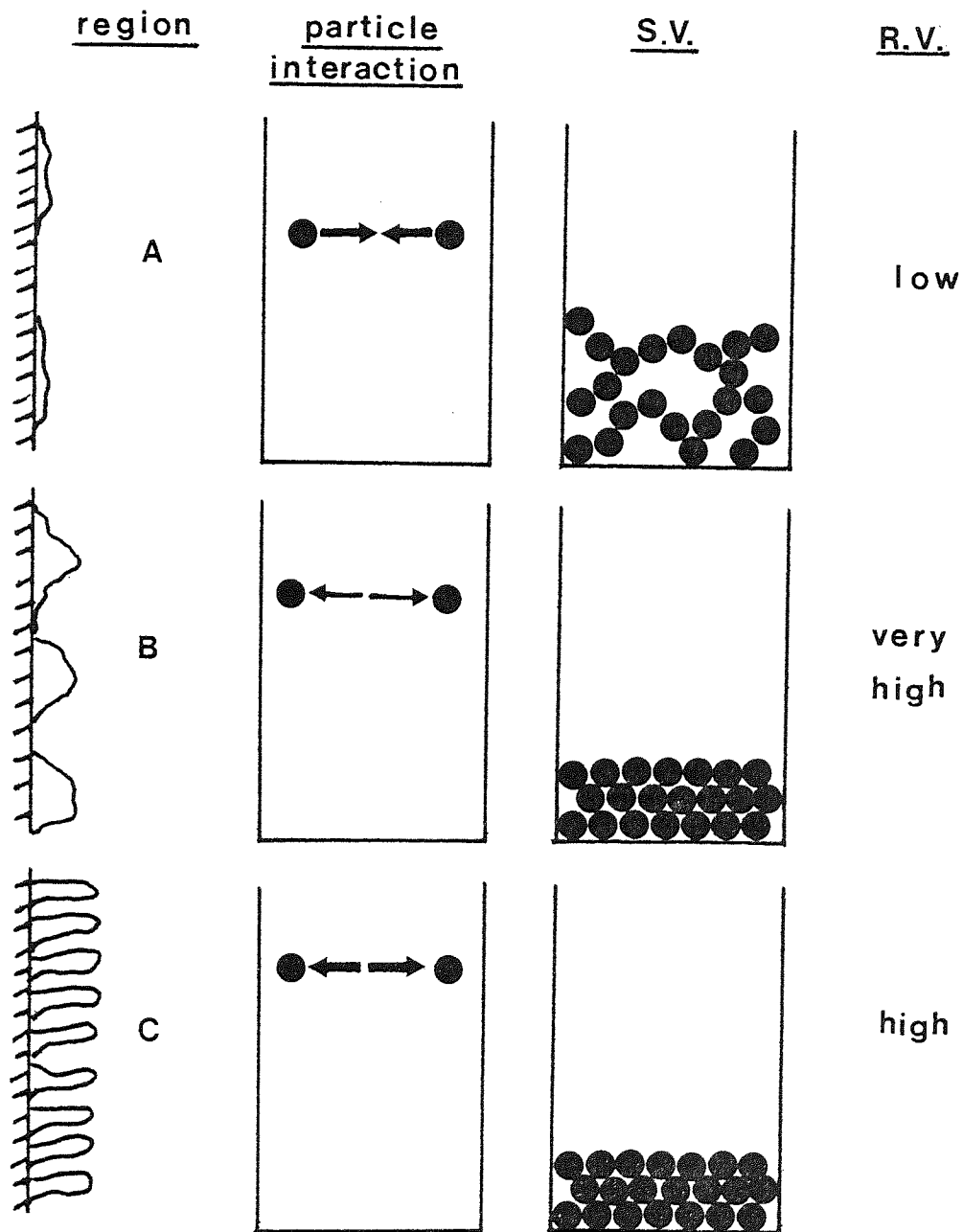
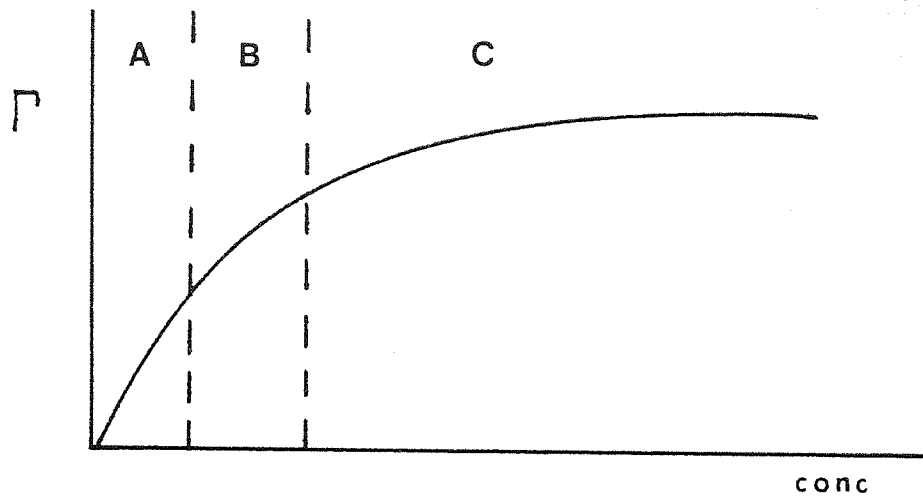


Figure 52 Schematic Representation of Partial Steric Stabilization

(see text for explanation)

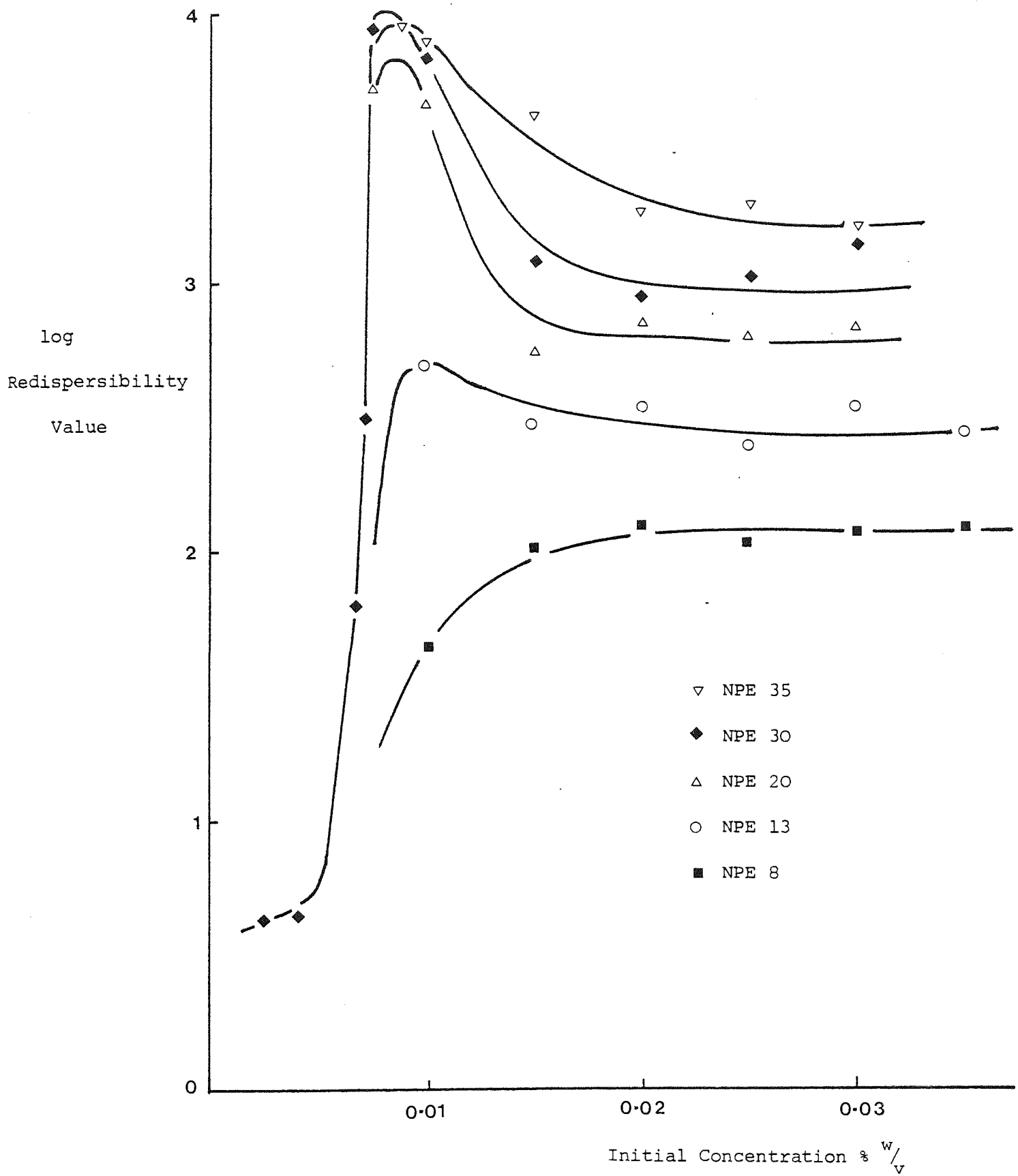


Figure 53 Redispersibility Data for Drug Suspensions in the Presence of Nonylphenylethoxylates after 1 year Storage.

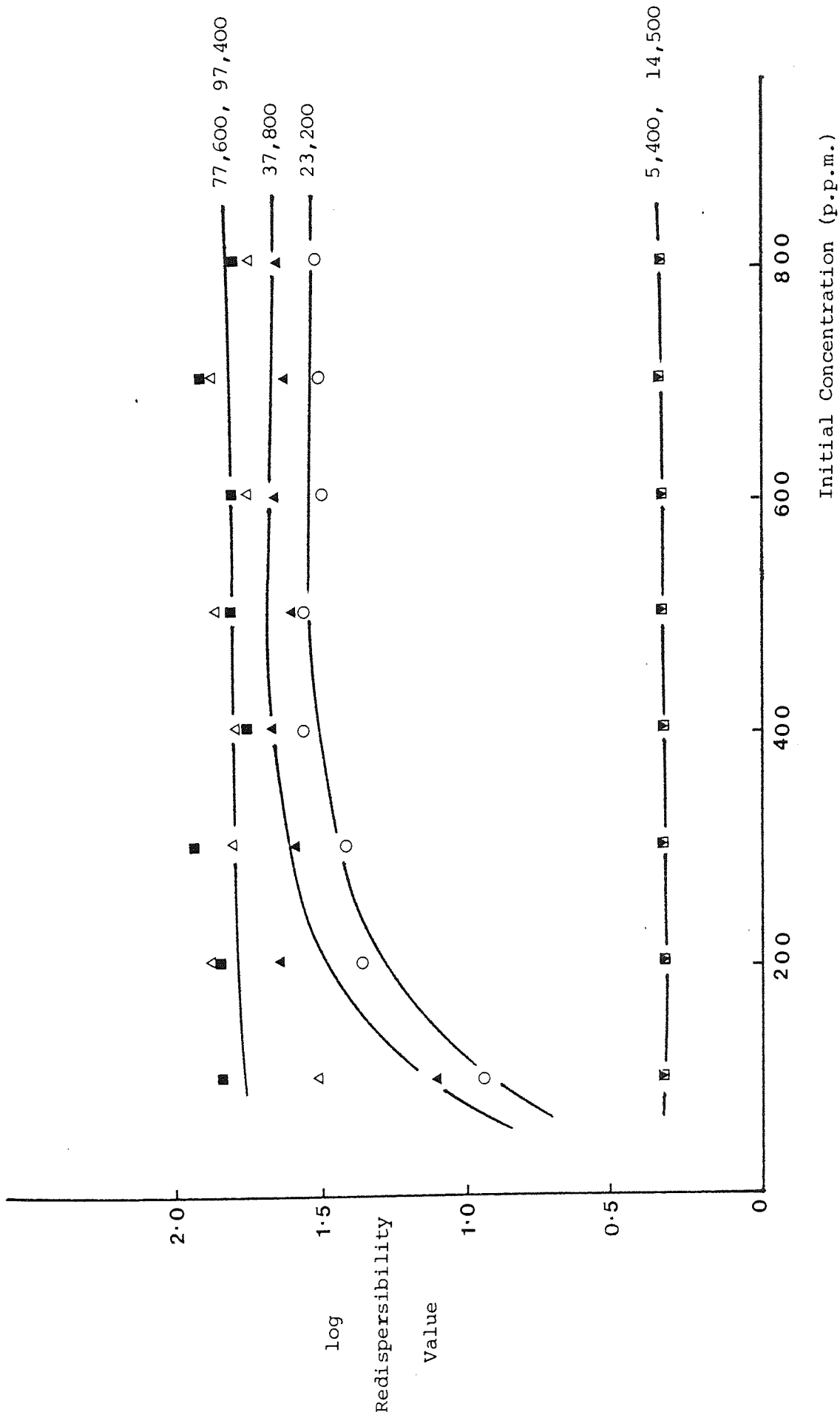


Figure 54 Redispersibility Data for Drug Suspensions in the Presence of Polyvinylalcohol After 1 year Storage.

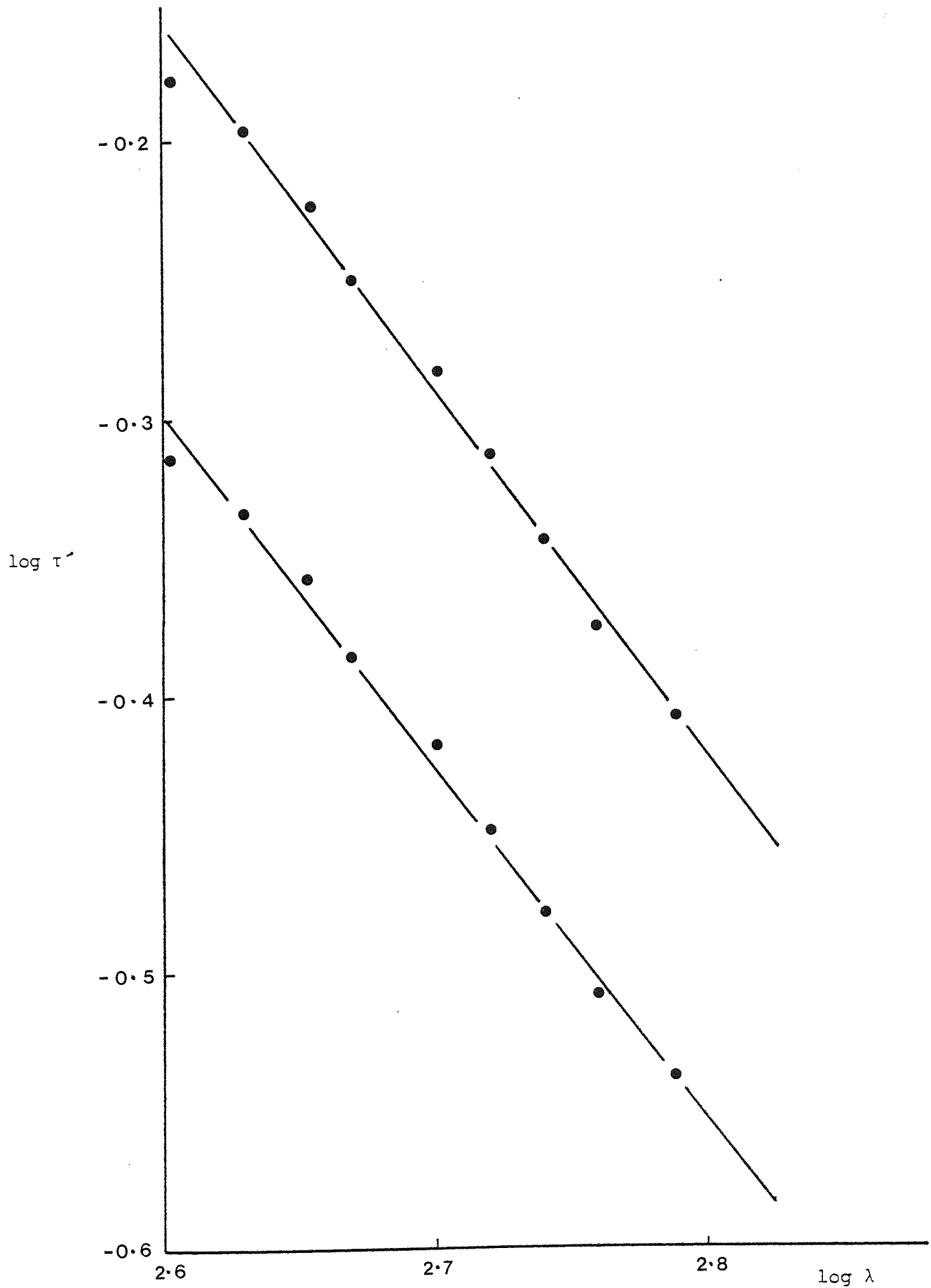


Figure 55 $\log \tau'$ vs $\log \lambda$ plots for 0.716 micron diameter latex

for two particle concentrations.

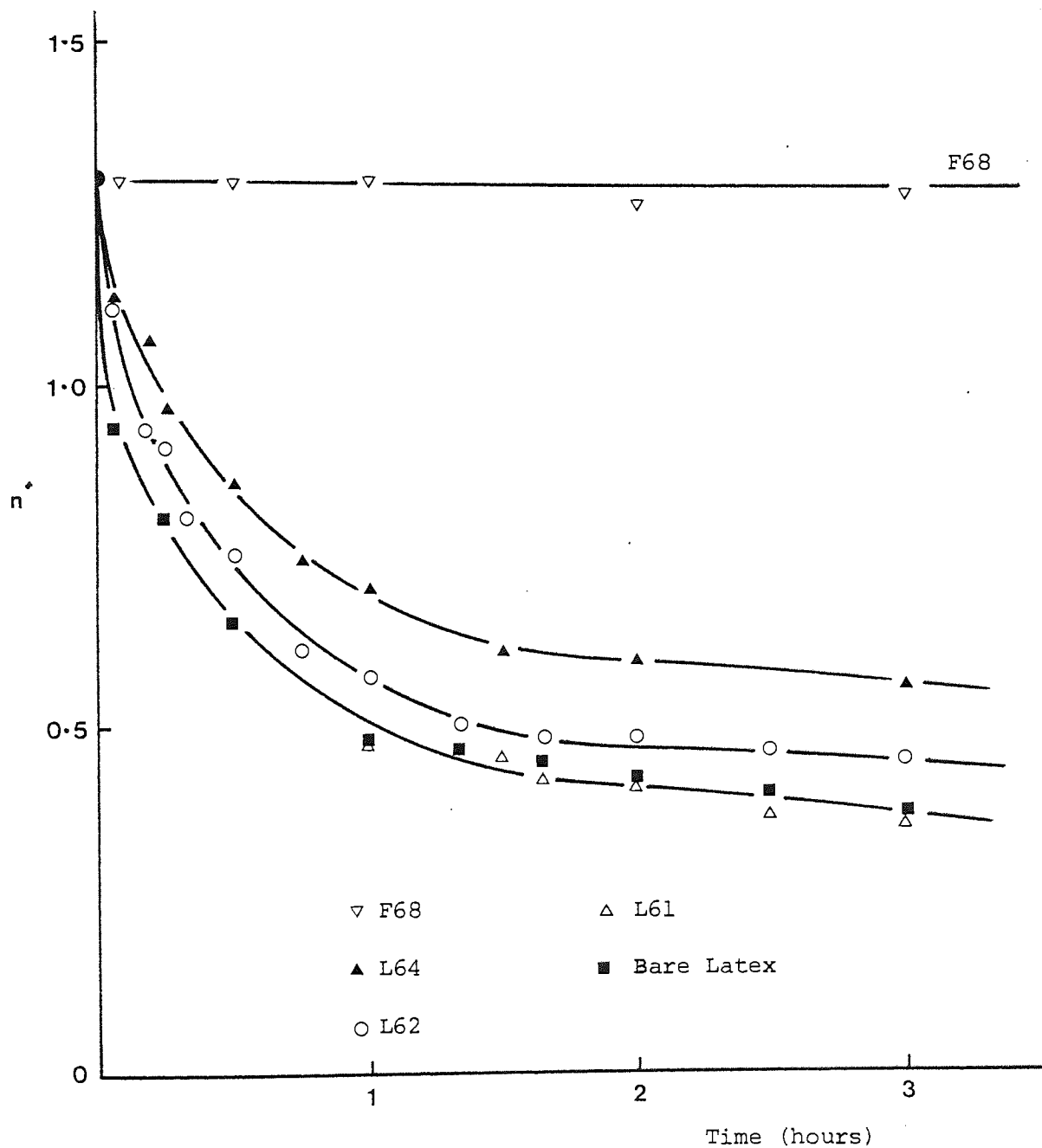


Figure 56 n' vs time plots for latex in the presence of adsorbed Pluronics.

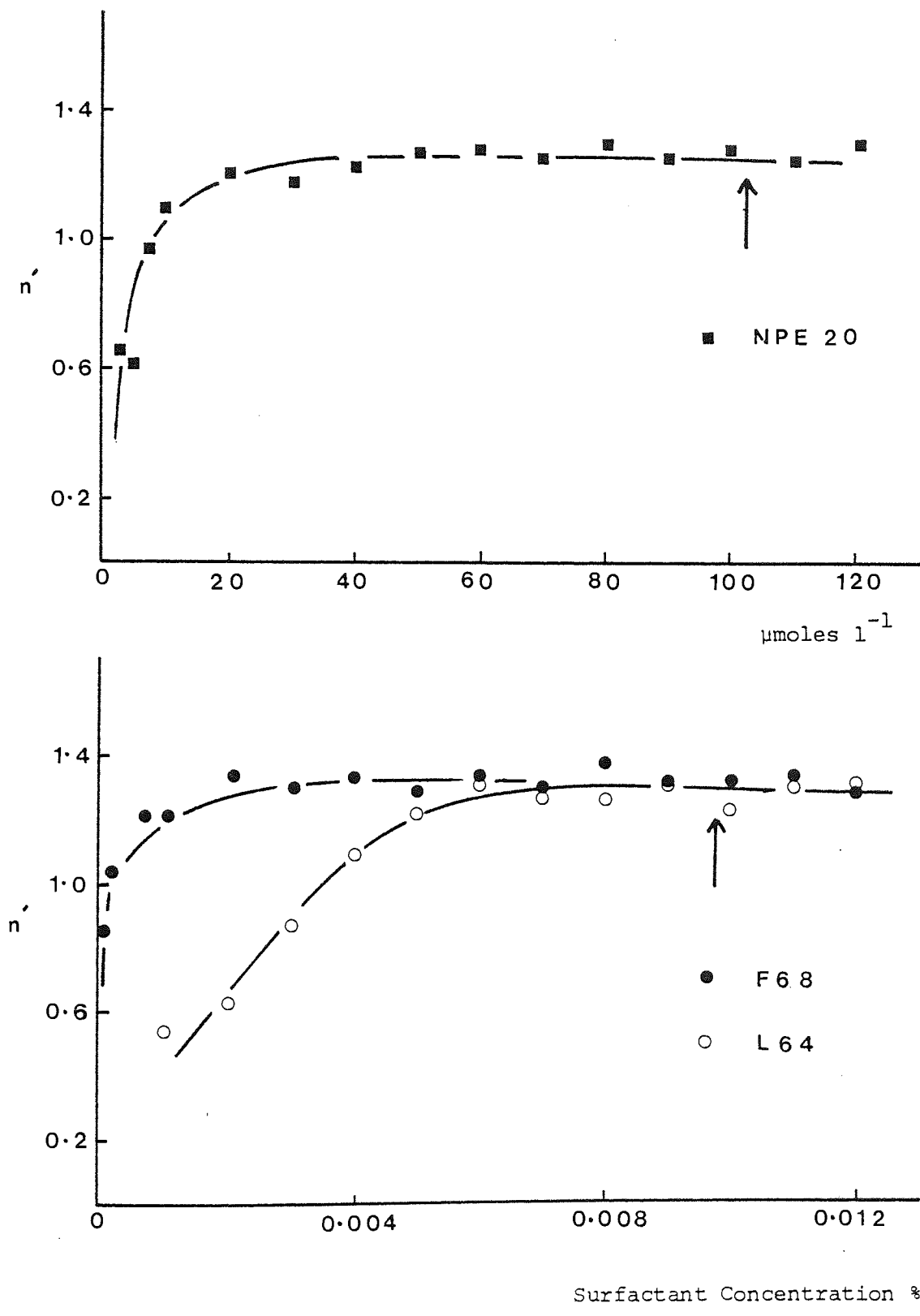


Figure 57 The Effect of Surfactant Concentration on Latex Stability

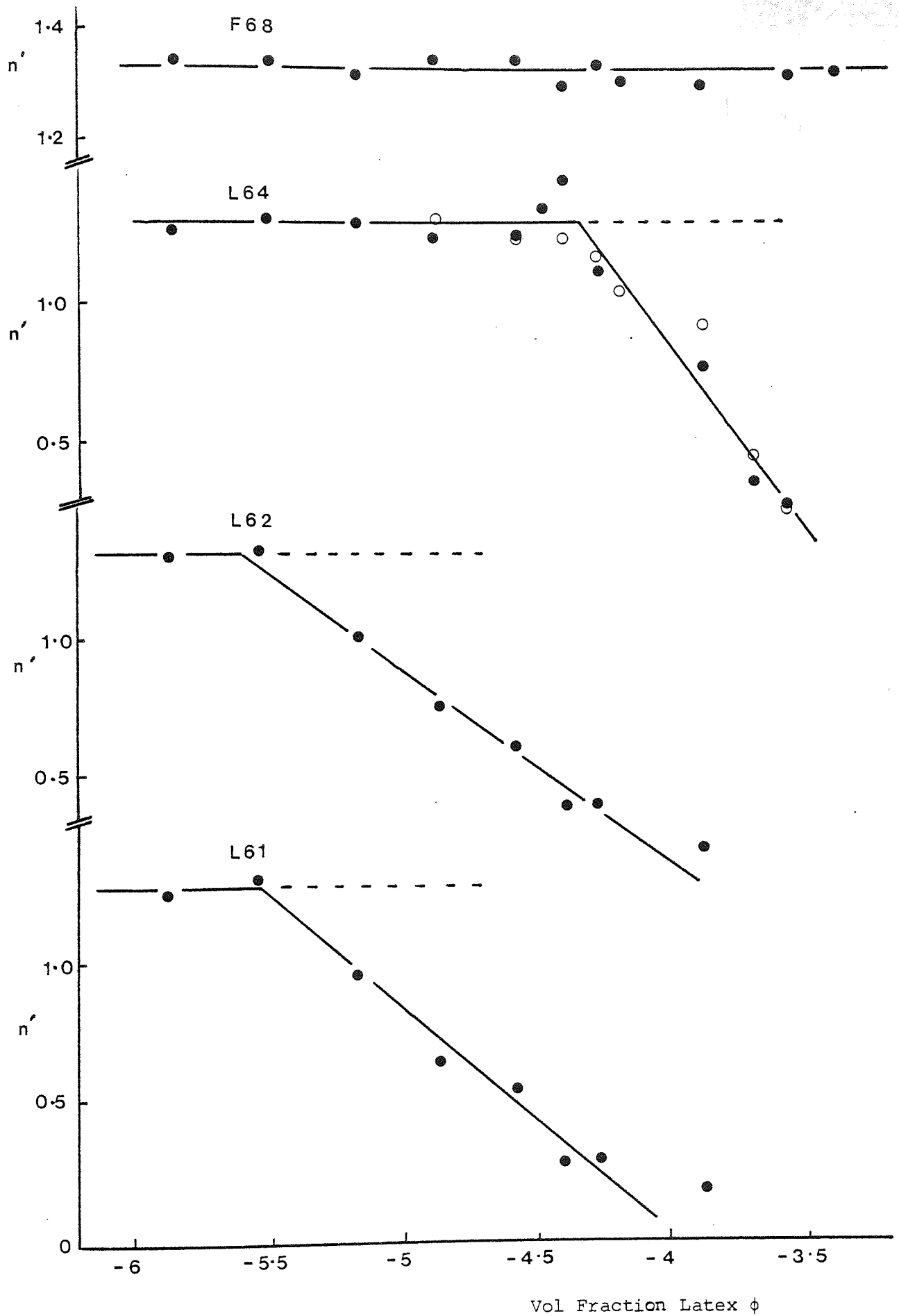


Figure 58 The Effect of Latex Concentration on Stability

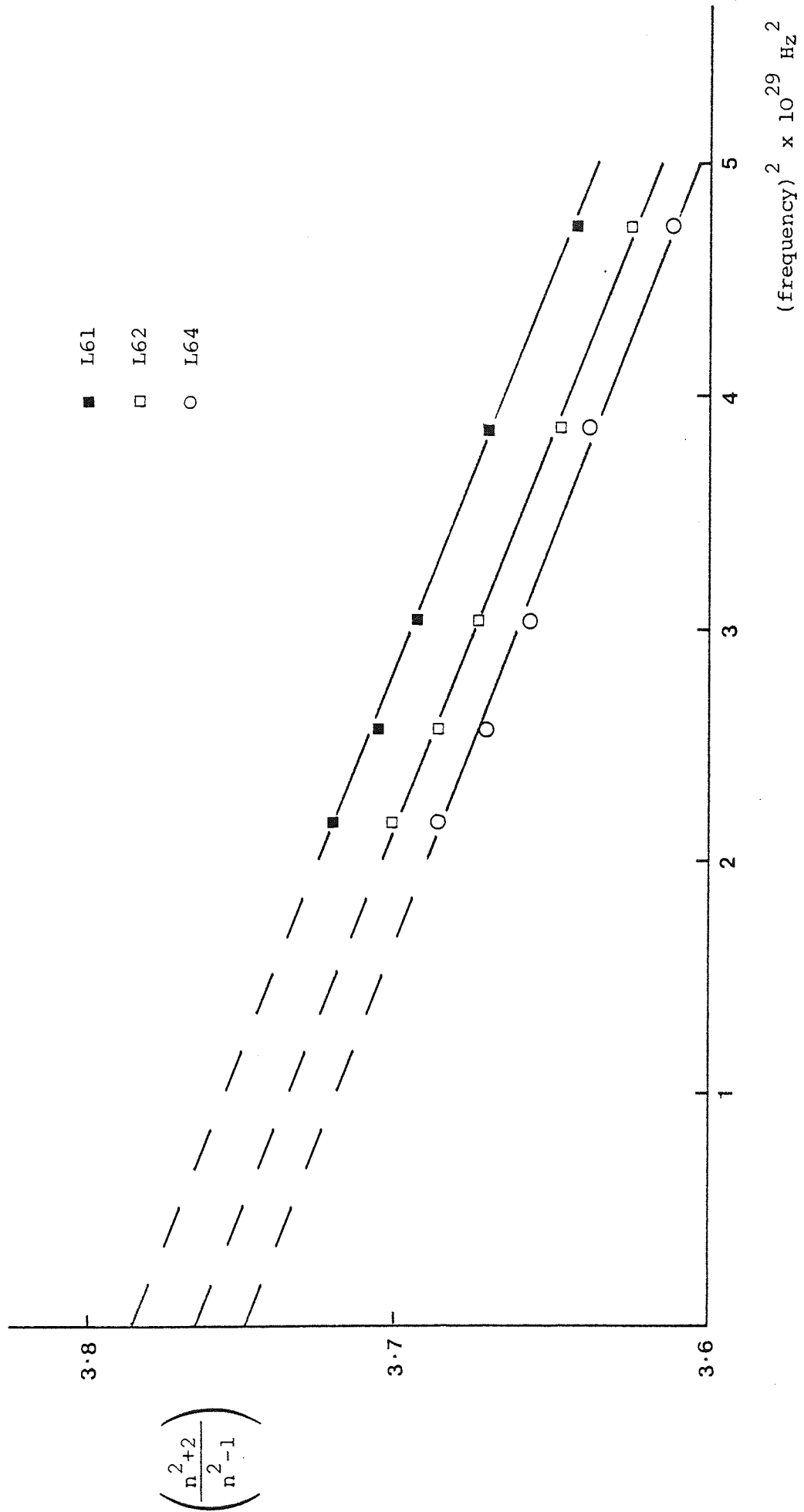


Figure 59 Optical Dispersion Plots for Pluronics at 25°C.

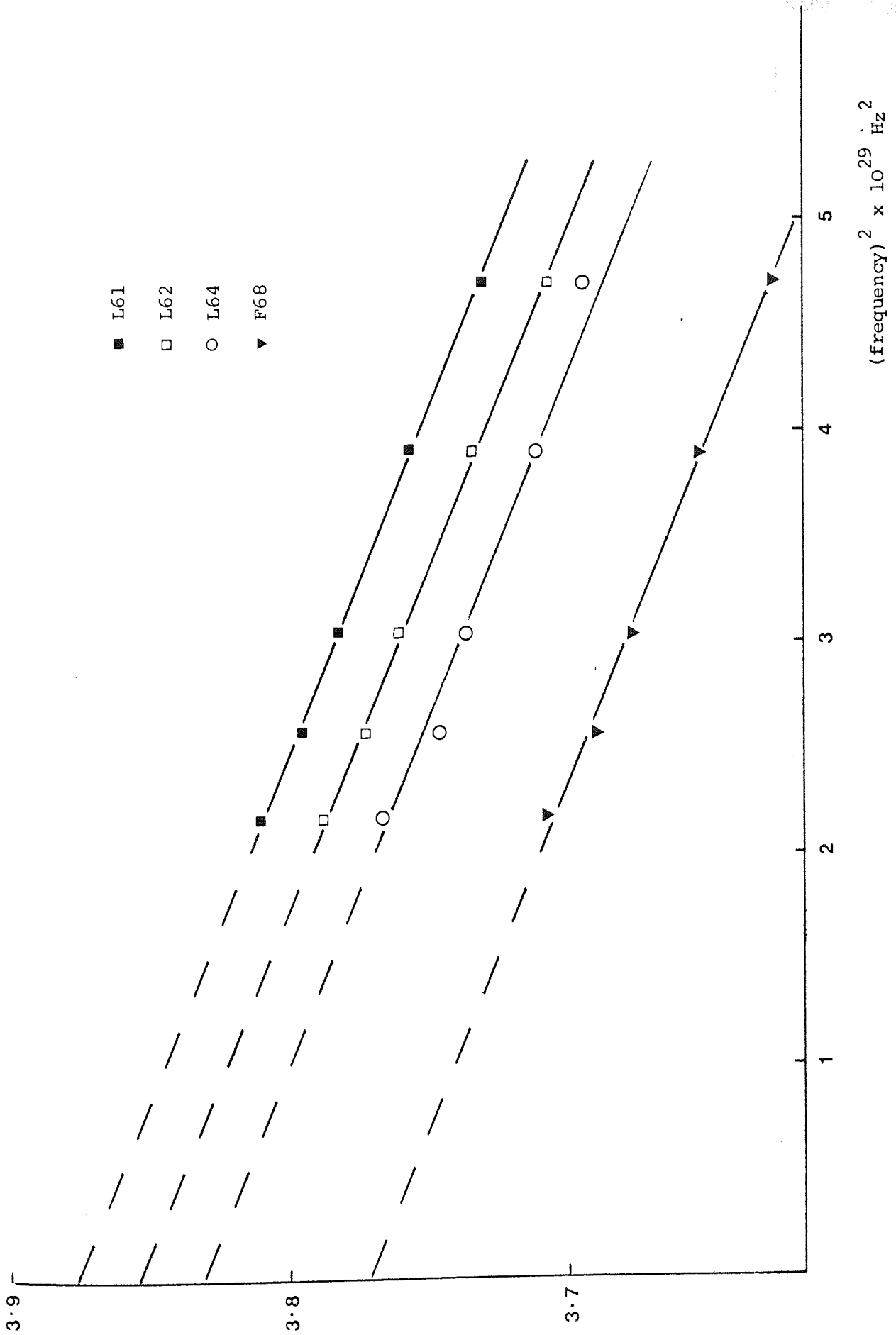


Figure 60 Optical Dispersion Plots for Pluronics at 60°C

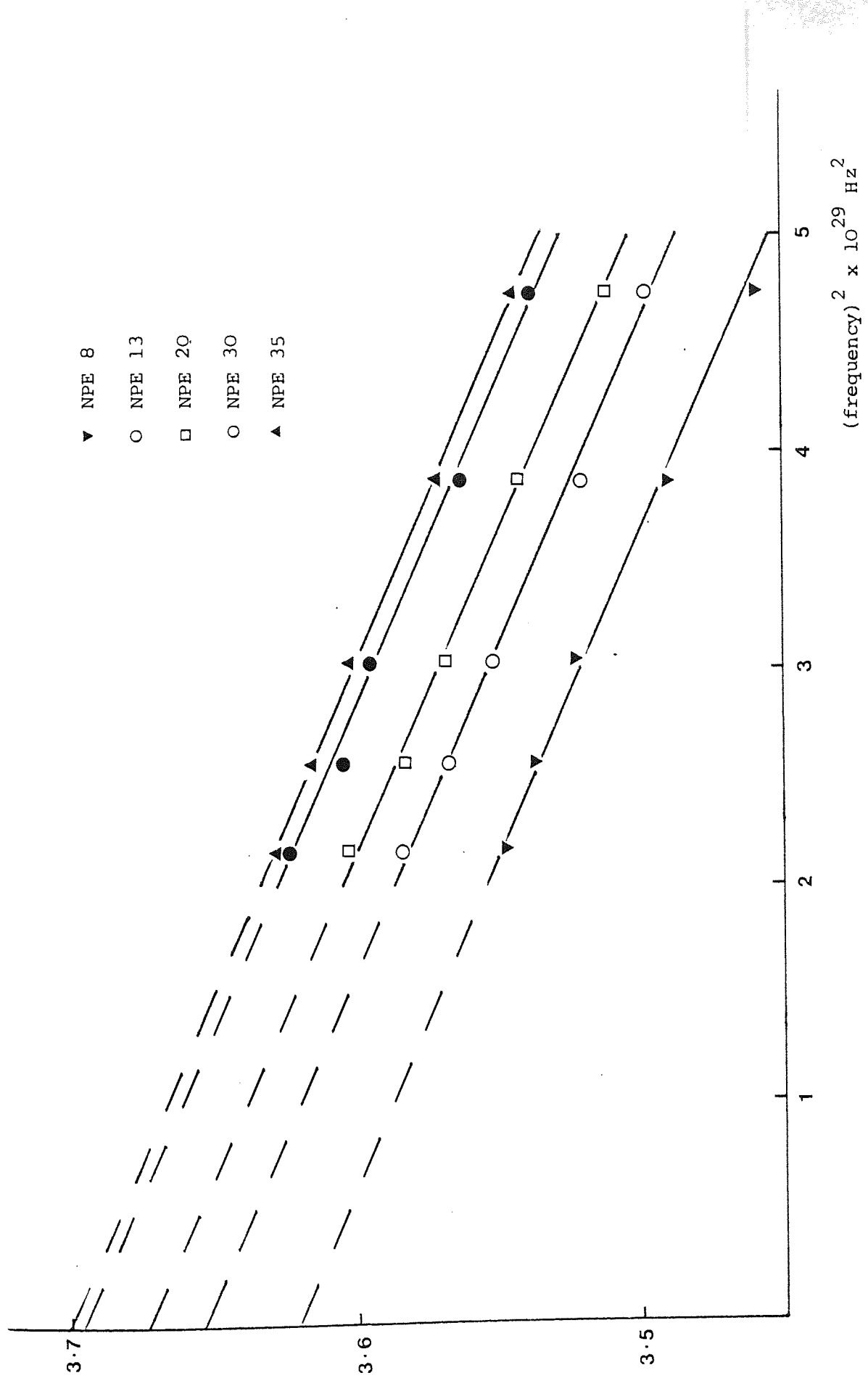


Figure 61 Optical Dispersion Data for Nonylphenylethoxylates at 60°C

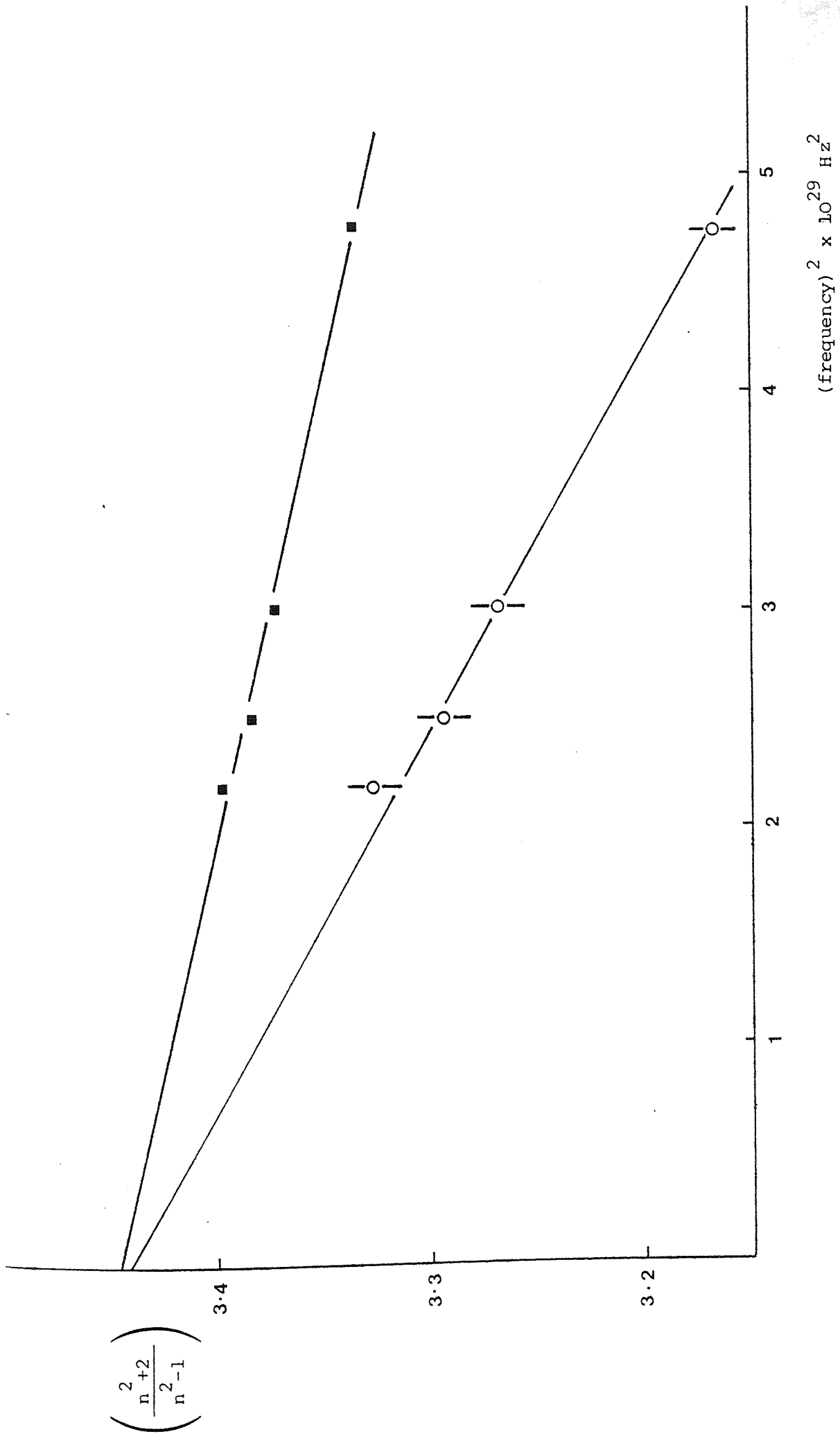


Figure 62 Optical Dispersion Plots for Diloxanide Furoate B.P. (o) and Polyvinylalcohol (■)

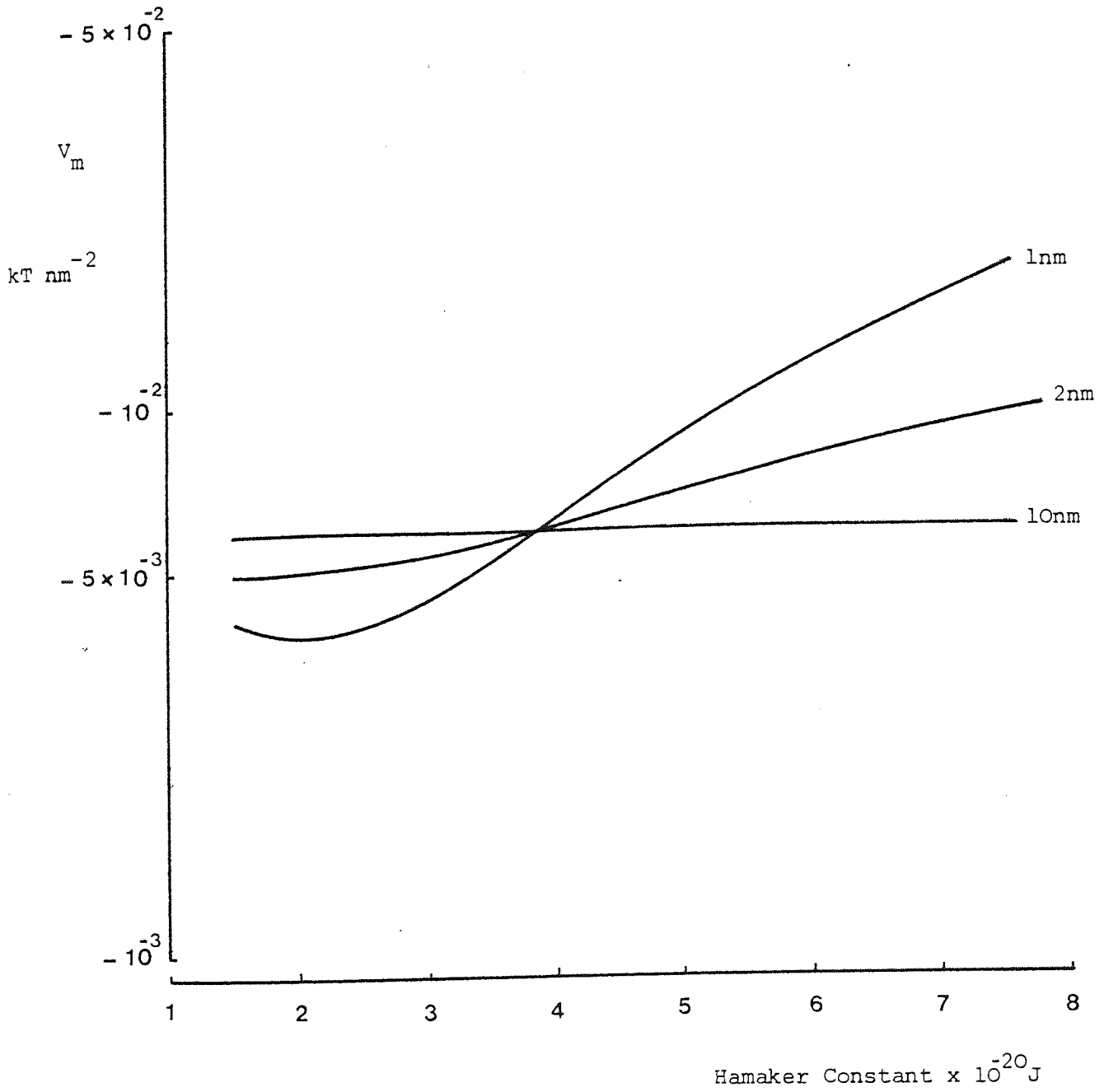


Figure 63 The Effect of Particle Core Hamaker Constant on the Primary Minimum ($H = 0.6 \text{ nm}$)

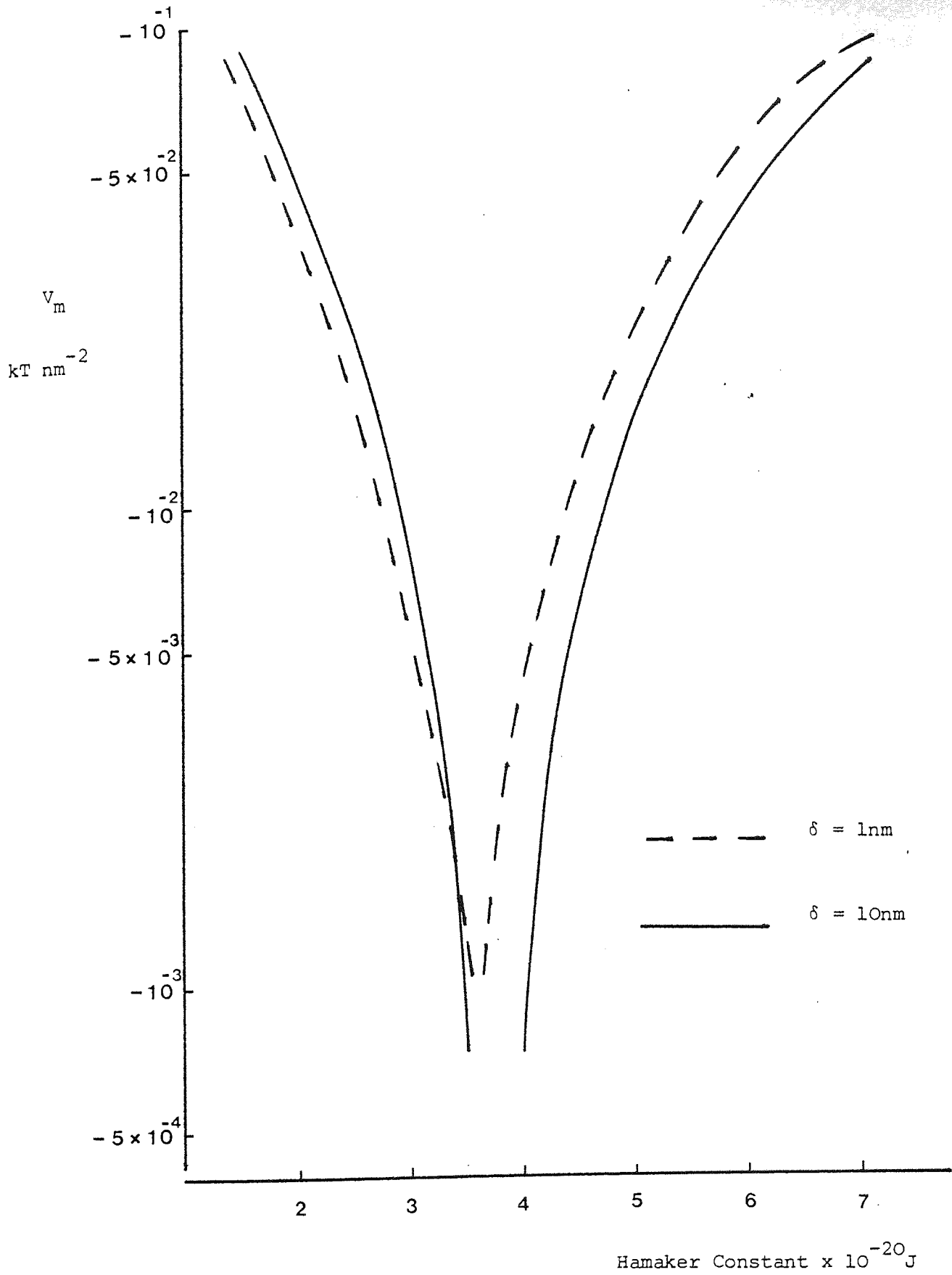


Figure 64 The Effect of Adsorbed Layer Hamaker Constant on the Primary Minimum ($H = 0.6 \text{ nm}$)

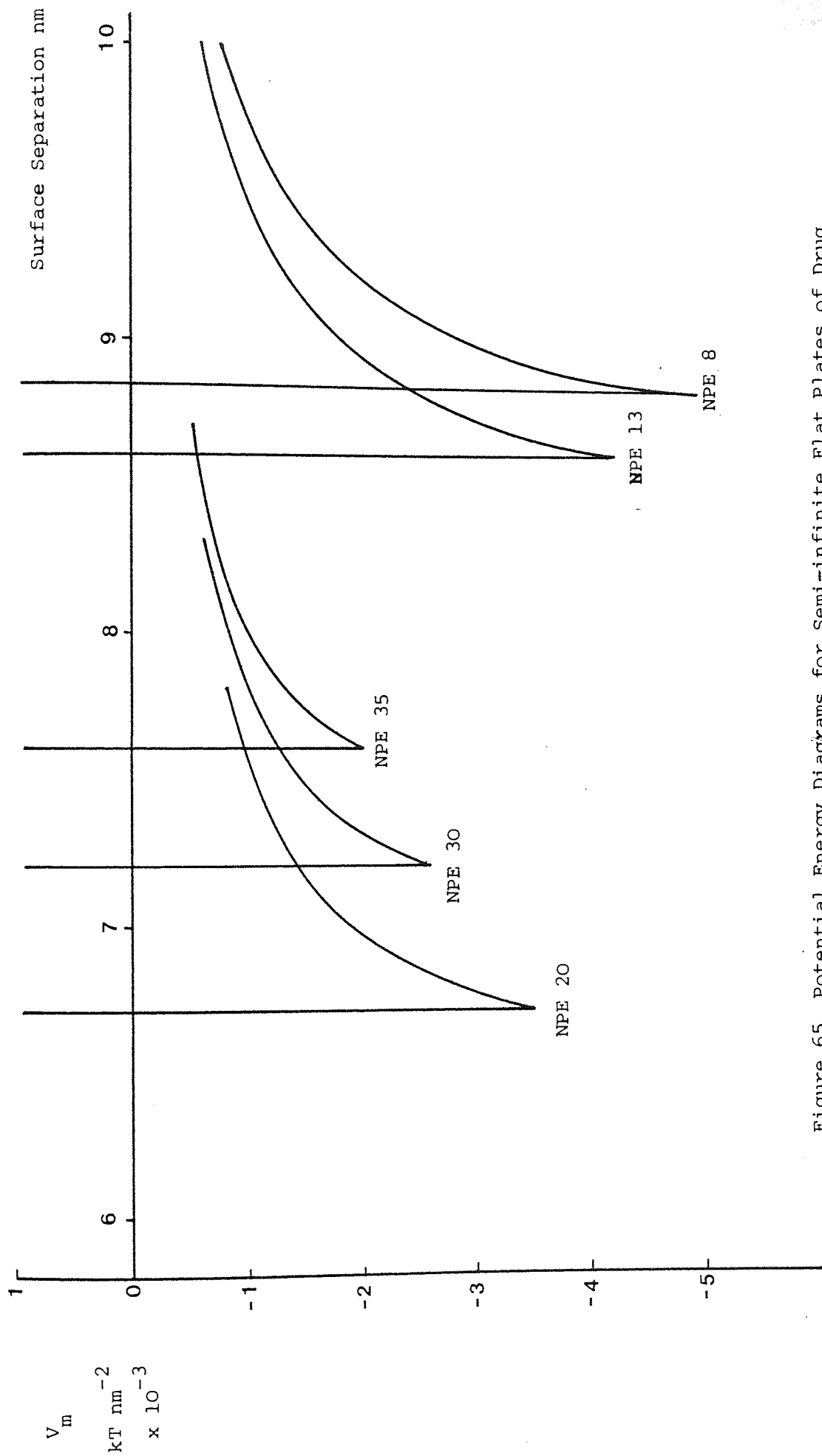


Figure 65 Potential Energy Diagrams for Semi-infinite Flat Plates of Drug

Coated with Adsorbed Nonylphenylethoxylates.

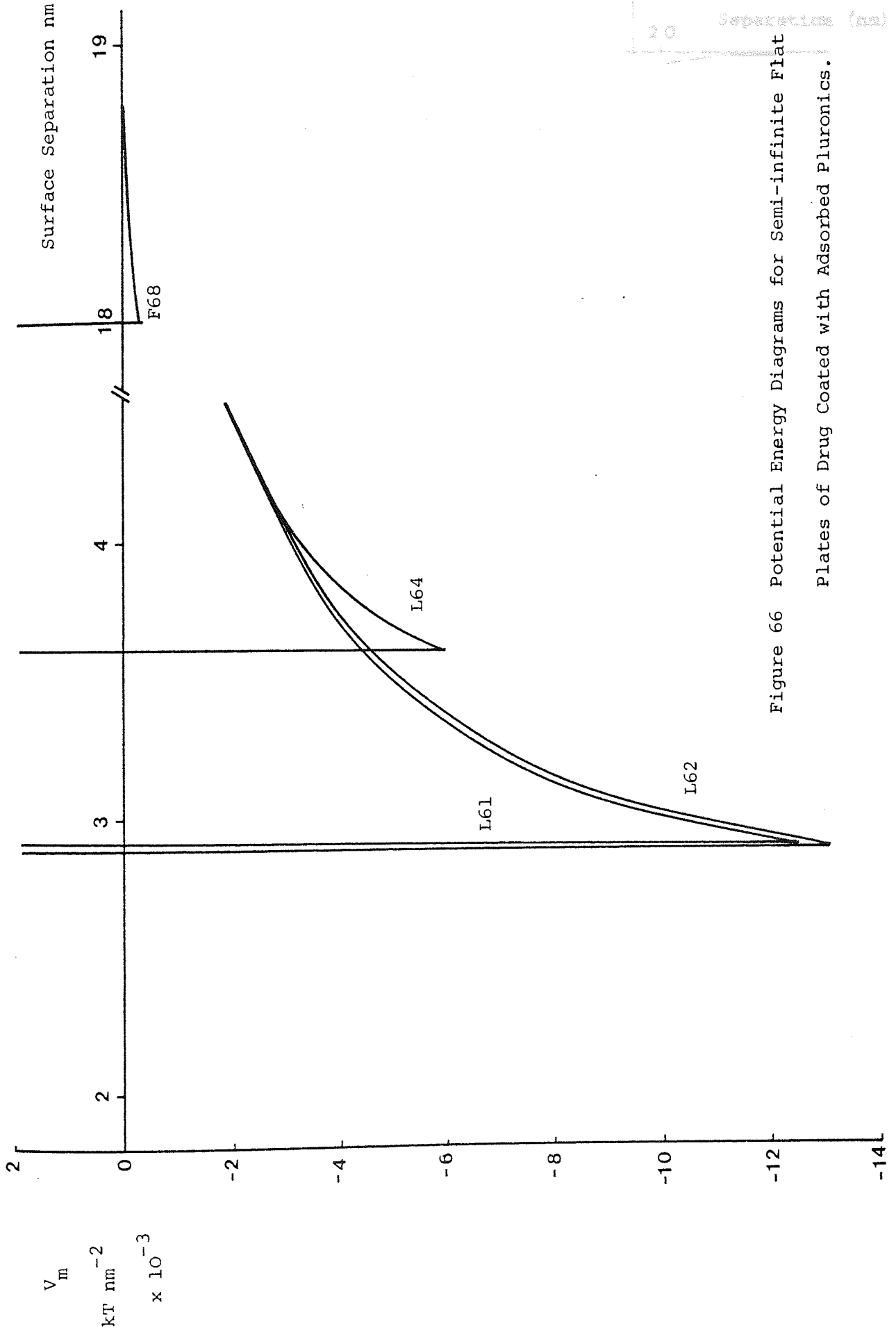


Figure 66 Potential Energy Diagrams for Semi-infinite Flat Plates of Drug Coated with Adsorbed Pluronic.

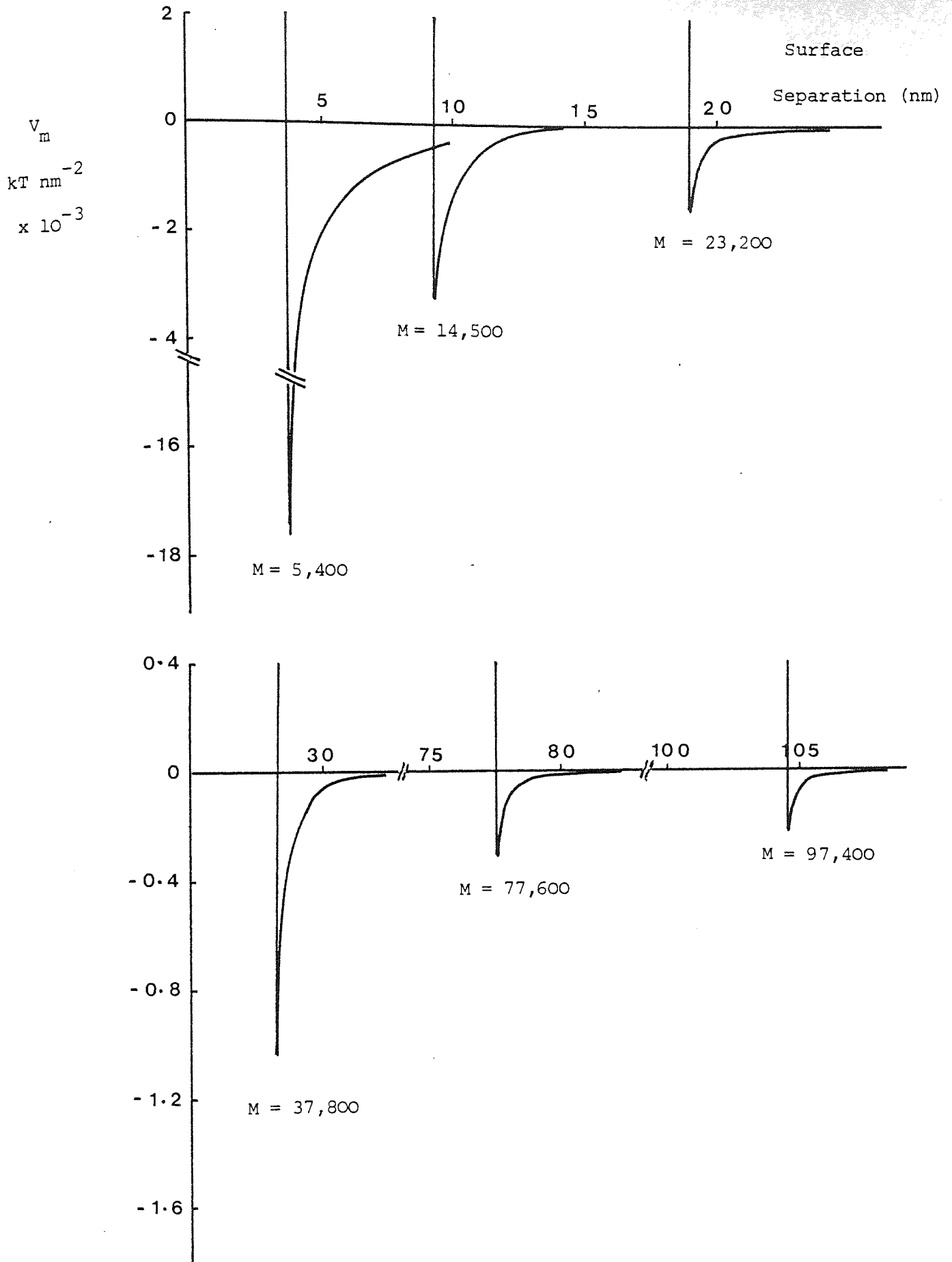


Figure 67 Potential Energy Diagrams for Semi-infinite Drug Plates of Drug Coated with Adsorbed Polyvinylalcohols

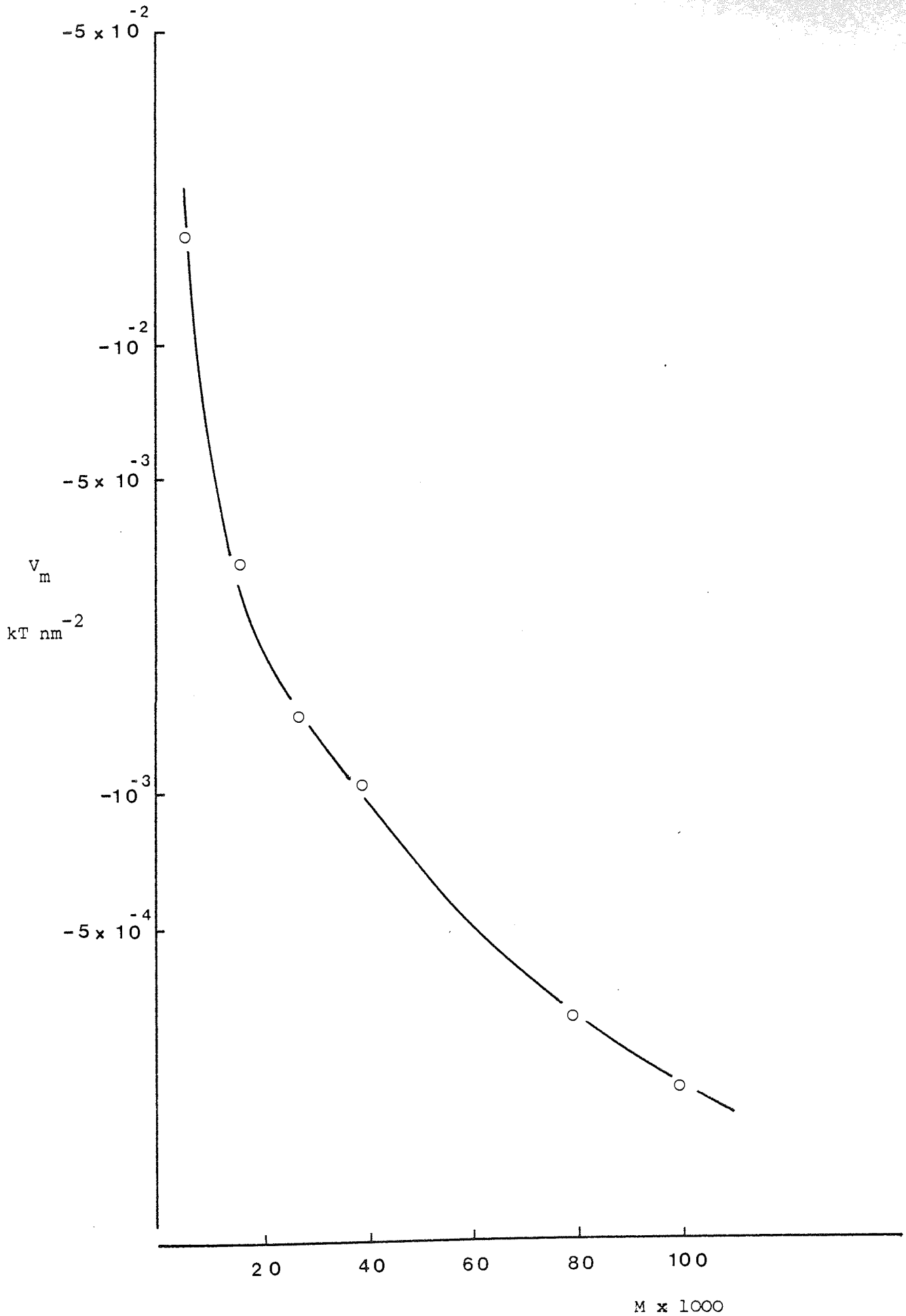


Figure 68 Variation of Restricted Primary Minimum Depth as a Function of Polyvinylalcohol Molecular Weight.

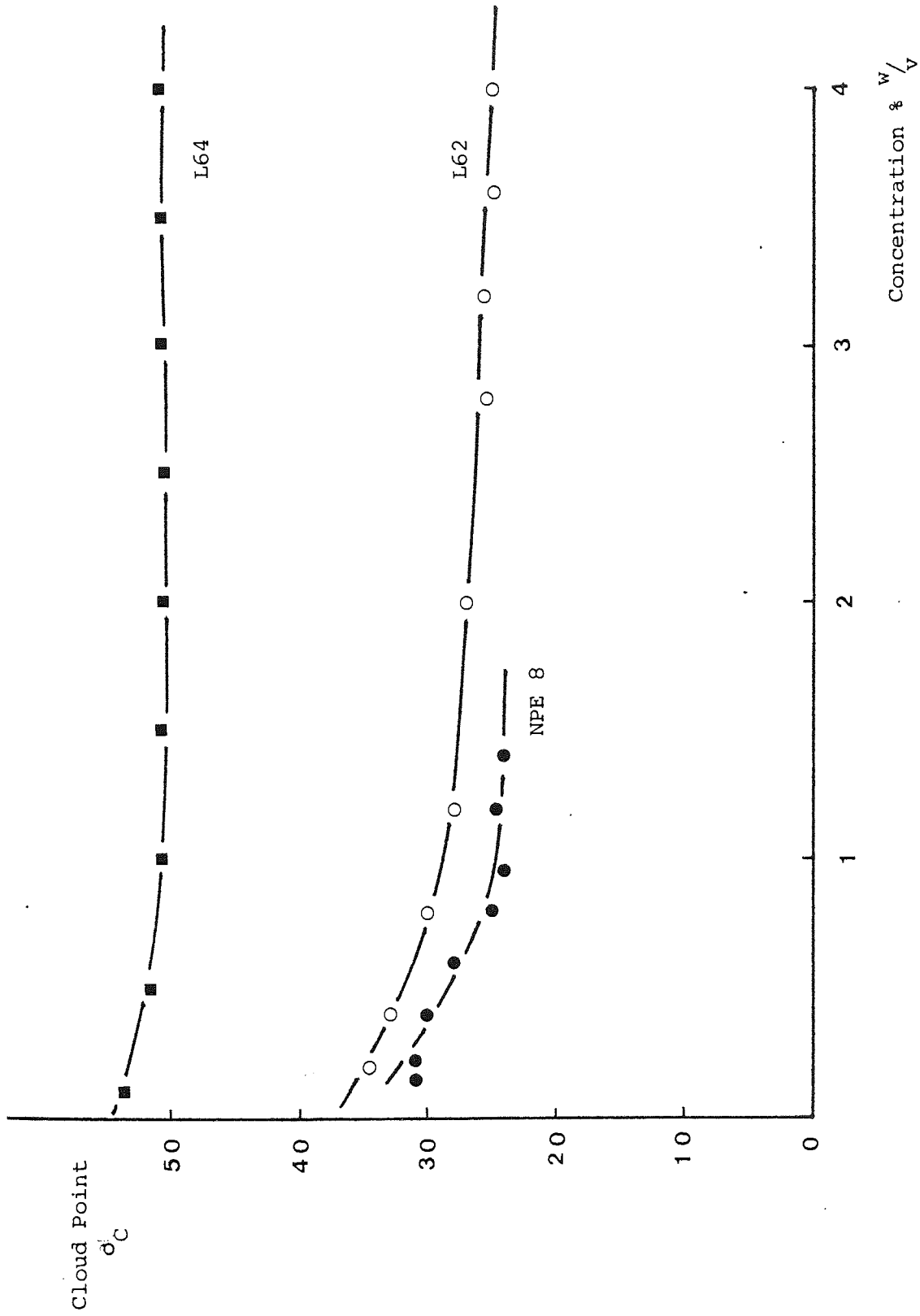


Figure 69 Cloud Point Diagrams for some Surfactants

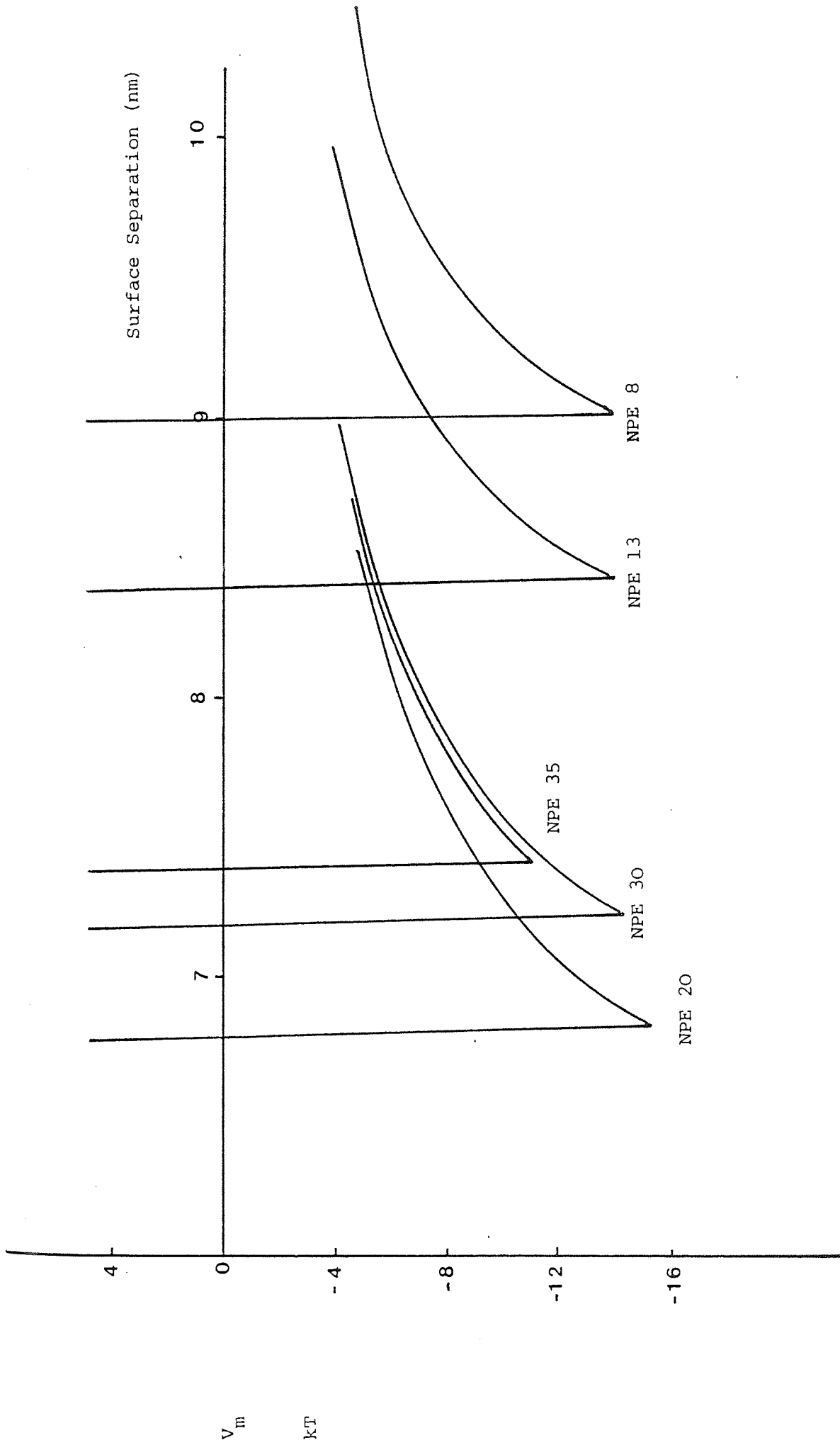


Figure 70 Potential Energy Diagrams for 0.716 μ latex coated with Adsorbed Nonylphenylethoxylates.

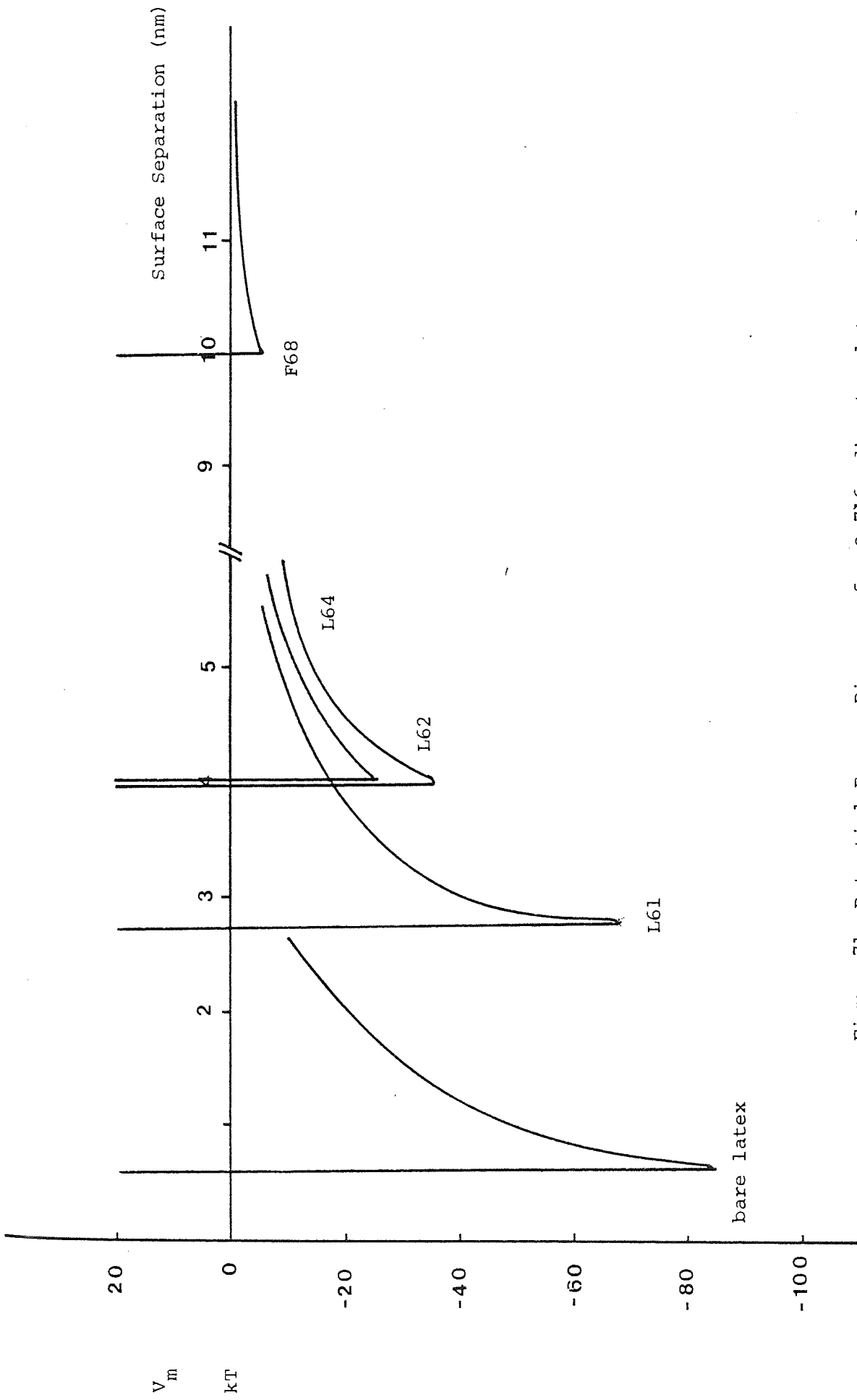


Figure 71 Potential Energy Diagrams for 0.716 μm diameter latex coated with Adsorbed Pluronics

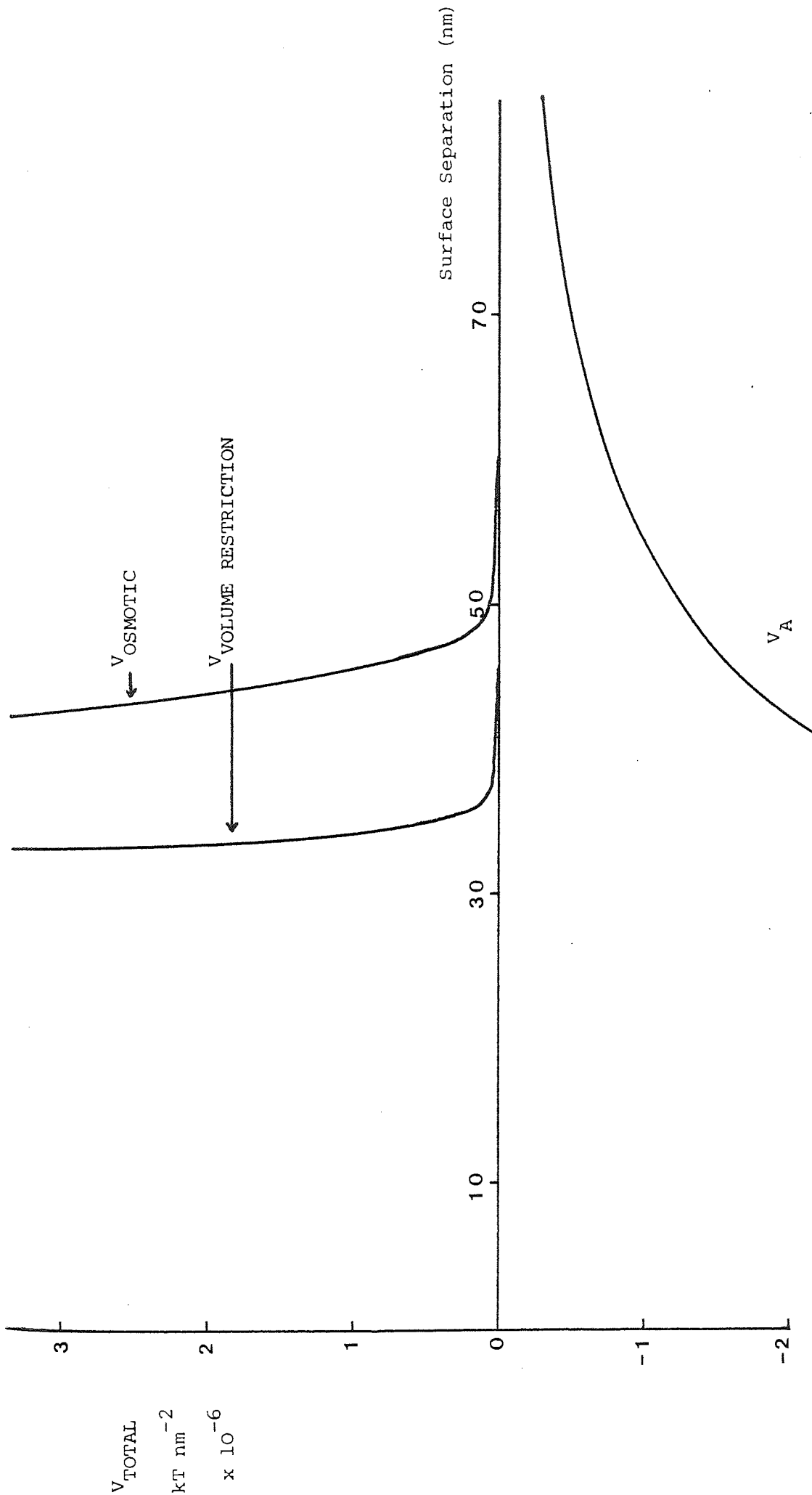


Figure 72 Potential Energy Curves for V_A , V_{RS} , $V_{OSMOTIC}$ calculated for an exponential Segment Density Distribution for PVA 37,800.

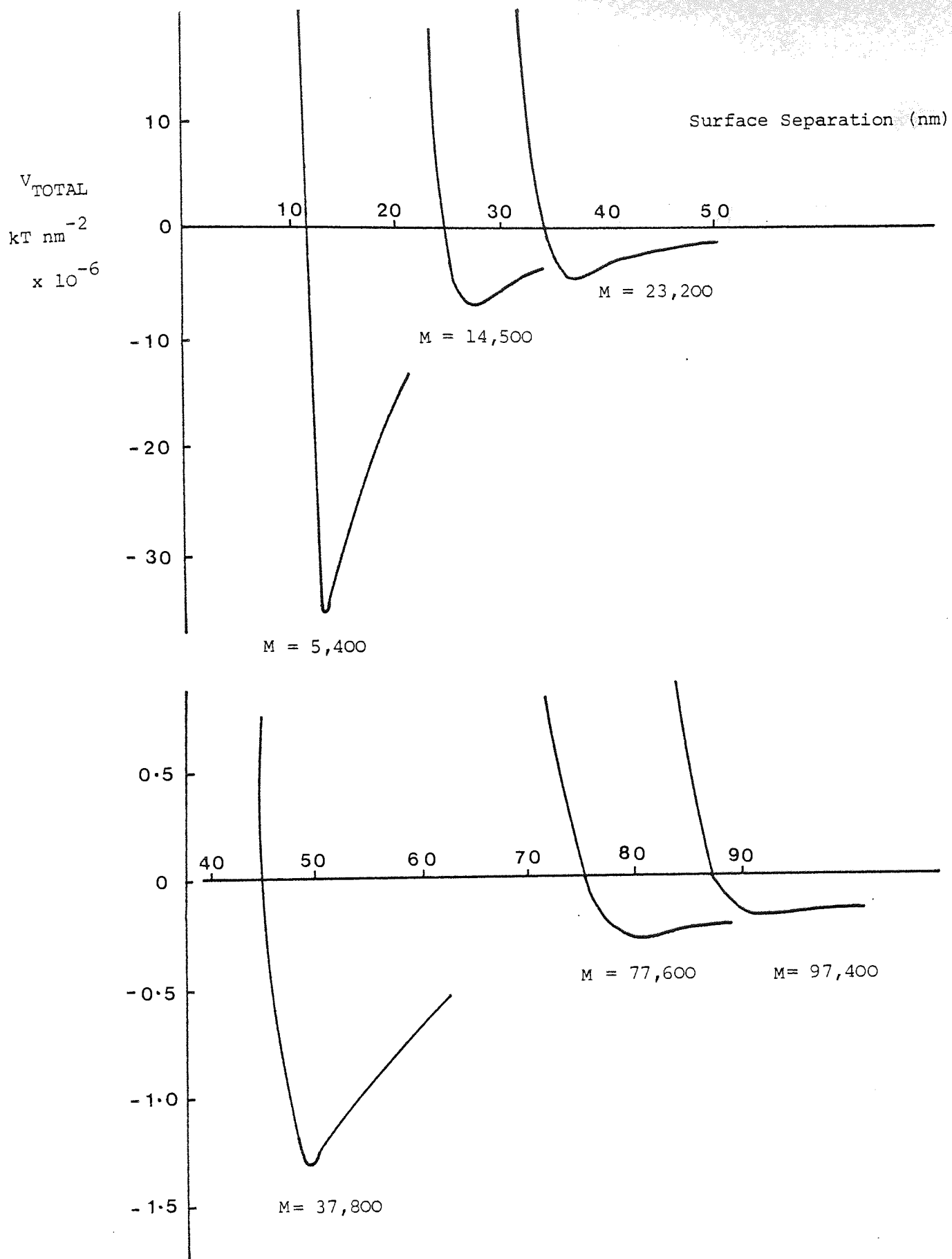


Figure 73 Potential Energy Diagrams for Semi-infinite Flat Plates

of Drug Coated with Adsorbed Polyvinylalcohols using HVO Theory.

SECTION 7

dissolution studies

SECTION 7 Dissolution Studies All Inta points

In order to elicit the desired pharmacological response, a drug molecule in an orally administered delivery system must undergo both dissolution from that system and adsorption through the gut wall. The concentration of drug in the bloodstream is dependent upon several kinetic processes such as dissolution, absorption, excretion, metabolism and distribution. The rate of drug absorption is limited by the first two of these processes - the slowest of the two being the rate determining step. A major factor in the development of biopharmaceutics has been the realization that formulation variables may have a significant effect on the bioavailability of a drug from a dosage form. A review of this topic has been given by Garrett (260).

Berlin et al (261) have determined the bioavailability of diazepam formulations from plasma concentration data. Tablets and suspensions were compared and it was found that suspensions produced lower plasma levels than tablets of the same dose indicating incomplete absorption from this dosage form. Bates et al (262) have attempted to correlate in vitro dissolution data of tablet and suspension formulations of salicylamide. In this case suspensions gave much greater dissolution rates and the same order was found for the biological activity.

Howard et al (263) have investigated the effect that hydroxypropylmethylcellulose has on the dissolution profile of prednisolone acetate crystals. A decrease in the release rate was observed on addition of the polymer such that after 1000 seconds the weight fraction of powder undissolved when polymer was present was 0.75 compared with a value of 0.5 in the absence of polymer. Florence et al (264) have studied the effects of several polymers on the dissolution rate of potassium and sodium chlorides and related the dissolution rate constant

k, to the effective polymer solution viscosity. All data points fitted one curve indicating the independence of the nature of the polymer chains on dissolution. Similar effects were observed by Barzegar-Jelali and Richards (265). A rank order correlation was shown to exist between the various dissolution parameters obtained from dialysis measurements and the viscosity of several suspending agents solutions used. Using a similar technique Shah and Sheth (266) studied the dissolution - dialysis of nitrofurantoin suspensions using various grade methylcellulose as suspending agents. They conclude that the reduced rate of dialysis observed is a result of complexation between drug molecules and polymer and also due to the formation of microscopic regions of high viscosity surrounding the particles which leads to a reduction in the diffusion of drug away from the surface. This work may give an explanation to the results of Seager (41) who found decreased absorption of the drug in vivo when using the same drug-polymer system. Najib, Kellaway and Marriott have demonstrated that adsorbed layers of polyvinylpyrrolidone decreased the amount of drug released from drug suspensions (267). A linear relationship was found between the amount dissolved at a particular time and the adsorbed layer thickness.

A number of papers have dealt with the dissolution of solids into surfactant solutions (eg. 268, 269). The present work also utilizes surfactants but only bulk concentrations less than the critical micelle concentration. In this way the effect that adsorbed layers of surfactant may have on dissolution rates may be observed. The effect of adsorbed polyvinylalcohols is similarly investigated.

7:1 Methods

7:1:1 Saturated Solubility of Drug in Water

Two techniques were used to ascertain the maximum aqueous solubility. In the first, a known weight of drug was solubilized in 500ml of a 0.6% $\frac{w}{v}$ hexadecyl polyoxyethylene glycol monoether containing 60 ethylene oxide units per molecule (Texafor A60). Dilutions of this solution were prepared from which a calibration graph was constructed using the absorbance of these solutions at a wavelength of 261nm. The absence of interference due to background absorption of the Texafor A60 was checked by comparing the spectra of these solutions with that of a sub-saturated solution of the drug where no additive was present. The maximum solubility was then measured by shaking an excess of drug with distilled water for 6 days at 25°C and determining the solubility of the filtrate by comparison of these absorption peaks with the calibration curve. The effect of pH was monitored by adding quantities of 0.1M NaOH or HCl to the dispersions before shaking.

The second technique involved dissolving the drug in methanol and making suitable dilutions from this before adding an equal volume of water. Calibration curves of the drug in the 50 : 50 methanol-water mixtures were constructed from the absorbance readings at 259nm. An equal volume of methanol was then added to the saturated drug solution prepared as above and the absorbances of these solutions were compared with the calibration curve.

7:1:2 Polymer Desorption

Dispersions of diloxanide furoate B.P. were prepared in 10ml of polymer solution sufficient to give saturation coverage of the surface according to the adsorption isotherms in Section 4. After equilibration for 24 hours, 6ml of the supernatant were removed and replaced by the

same volume of distilled water. A further equilibration period was then allowed before the supernatant was filtered and assayed for polymer content. The percentage of polymer desorbed was then evaluated from the mean of three replicate experiments.

7:1:3 Solubility in Polymer Solutions

Calibration curves for these systems were prepared by making different concentrations of drug in 0.5% $\frac{w}{v}$ polymer solutions in 50:50 methanol-water systems. To obtain the maximum solubilities, an excess of drug was equilibrated with the polymer solutions for a period of 10 days in a shaking water bath at 25°C. After equilibration, the polymer solutions were diluted with suitable volumes of methanol and water to give solutions of the same composition as the calibration solutions

7:1:4 Dissolution Studies

The apparatus used for the dissolution studies consisted of a 1-litre round bottomed flask with three sampling ports, clamped rigidly in a viscometer bath operating at 25°C. The volume of dissolution medium used was 1100ml. Stirring was effected by a Citenco variable speed motor positioned vertically above the central sampling port, coupled with a Quickfit PTFE T-paddle stirrer. The base of the stirrer blade was positioned 1cm above the flask base during experimental runs. The geometry of the glass vessel in combination with the optimum depth of stirrer blade, produced a movement of fluid which prevented sedimentation of drug particles at stirrer speeds of greater than 260 r.p.m. Calibration of the motor speed was found from stroboscopic measurements. A known weight of drug was dispersed in 4ml of polymer solution sufficient to give maximal surface coverage and allowed to equilibrate for 24 hours at 25°C. After this period the contents were poured into the dissolution chamber and the suspension container washed out with a further 5ml of dissolution medium, the

washings being added to the round bottomed flask. At predetermined time intervals approximately 4ml of dissolution fluid was removed and filtered through pre-soaked 0.45 micron membrane filters. The first portion of the filtrate was discarded to reduce the effects of adsorption onto the filter assembly. The concentration of the drug in solution was determined from the solution absorbance at 261nm measured on a Pye Unicam SP500 spectrophotometer.

7:1:5 Preparation of Drug Crystals

Preliminary studies of the dissolution rate of diloxanide furoate B.P. Batch 2616 using the above method gave solution rates too fast to be measured accurately. To reduce the rate of release, larger crystals were prepared, thereby decreasing the surface area from which dissolution occurs. A supersaturated solution of drug in methanol was prepared at 45°C and undissolved drug was removed by decanting. Using a slow stirring rate a volume of water equal to half that of the methanol was added. After five minutes the same quantity of water was again added. The crystals were obtained after a further 30 minutes of stirring by filtration and washed with copious quantities of water to prevent the occurrence of crystal bridging. Drying was achieved at 45°C in a vacuum oven. Those crystals retained on a 125 micron sieve were used in further dissolution studies.

7:2 Theory

The solubility of diloxanide in aqueous solution is so small that changes in surface area of the crystals during the initial dissolution period may be neglected. The dissolution process can be regarded as consisting of two simultaneously occurring processes.

- a) The zero order reaction involving transfer of drug molecules from the solid surface to the solution with rate constant k_1
- b) The first order reaction for the migration and deposition of solute

molecules from the solution onto the surface with rate constant k_2 . The rate of change of the bulk solution concentration then becomes

$$\frac{dc}{dt} = k_1 - k_2 c \quad (7.1)$$

Integrating this equation with the condition that at $t = 0$, $c = 0$ the equation becomes

$$c = \frac{k_1}{k_2} (1 - e^{-k_2 t}) \quad (7.2)$$

Expansion of this equation yields

$$\frac{c}{t} = k_1 - \frac{k_1 k_2 t}{2} + \frac{k_1 k_2^2 t^2}{6} - \frac{k_1 k_2^3 t^3}{24} \quad (7.3)$$

Terms in t^2 and higher powers can be neglected at times early in the dissolution process giving

$$\frac{c}{t} = k_1 - \frac{k_1 k_2 t}{2} \quad (7.4)$$

The rate constants k_1 and k_2 may then be evaluated from the intercept and slope of the plot of c/t against t .

When equilibrium is reached

$$\frac{dc}{dt} = 0 = k_1 - k_2 c_s \quad (7.5)$$

where c_s is the saturation solubility. Thus

$$k_2 = k_1 / c_s \quad (7.6)$$

Either k_1 or k_2 may be found from equation 7.6 provided the other constant is known.

7:3 Results and Discussion

7:3:1 Solubility of Drug in Water and Polymer Solutions.

Measurements of the aqueous solubility of diloxanide furoate B.P. by both methods have similar results with values of $2.37 \pm 0.06 \text{ mg } 100\text{ml}^{-1}$

by the solubilization technique and $2.30 \pm 0.04 \text{mg } 100\text{ml}^{-1}$ by the mixed solvent-system assay method. Further shaking of the dispersion for one week did not affect the values obtained. These values therefore represent the equilibrium solubility.

Solubility was constant over the range pH 2.5 to 5.6 and showed no indication of increasing at low pH where protonation of the tertiary amide group of the molecule occurs as demonstrated by microelectrophoretic measurements. Above an equilibrium value of pH 6.0 the solution became discoloured and the absorption in the ultraviolet region of the spectrum showed very different peaks to that of the original material. Hydrolysis of the ester linkage may be responsible for the decomposition. The transition from a stable colourless solution to a decomposed solution occurs over a very small pH range, thus no evidence of decomposition was apparent at pH 5.6 while at pH 6.0 a deep brown solution was produced. This decomposition appears to have no effect on the microelectrophoretic mobility-pH curve of the drug as only a small increase in mobility is observed above pH 5.6 and the curve obtained is consistent with the adsorption of hydroxyl ions only. Hydrolysis of surface drug molecules therefore does not take place.

Previous cloud point experiments have shown that the surfactant adsorbed at the interface does not have the same configuration as a molecule in bulk solution. These molecules will not be able to solubilize drug to the same extent as those in the micelle and therefore measurement of the solubility of drug in the adsorbed film were not performed with the nonylphenylethoxylates or Pluronics. A range of polyethylene glycols were used in place of the surfactants as these represent the hydrophilic part of the surfactant chain which projects into the surrounding medium from the particle surface.

The results of the solubility measurements in a range of polyethylene glycols of molecular weights 200, 400, 600, 1500 and 6000 are shown in Figure 74 as a function of polymer concentration. All curves show an increase in solubility with an increase in polymer concentration but differences are found between the molecular weight polymer functions. This is in contrast to the results of Elworthy and Lipscomb (270) who measured the solubility of griseofulvin in a series of polyethylene glycols and found all curves to be superimposable. The pattern that emerges from Figure 74 is that at any given polymer concentration the solubility first increases to a maximum with PEG 400 and then decreases to a constant value as the polymer chain length increases. It is of interest to observe that the maximum occurs at a chain length corresponding to approximately 9 ethylene oxide units - i.e. the chain length where transformation from the zig-zag to meander configurations of the ethylene oxide polymers is thought to occur (231).

The solubility of diloxanide furoate in polyvinylalcohol solutions increases with an increase in polymer concentration (Figure 75) but there is no significant difference in the amount of drug in solution on increasing the PVA molecular weight from 35,600 to 81,700. Eagland, Wardlaw and Thorn (206) have shown that spherical polymer units similar to micellar species of surfactants are found with polyvinylalcohol solutions at approximately 1% $\frac{w}{v}$ concentration. No evidence was found in this work for solubilization of drug at this concentration as smooth solubility-concentration plots were obtained over the concentration range studied. The likely reason for this is due to the composition of the polyvinylalcohol molecules. For surfactants the molecules consist of two different regions - one hydrophilic and one hydrophobic and on micellization the hydrocarbon chain form a hydrophobic core in which organic compounds become solubilized. On aggregation of polyvinylalcohol molecules the production of an essentially hydrophobic core cannot take

place due to the long chain homogenous nature of the molecules. The presence of randomly distributed acetate groups along the chain could conceivably form a more hydrophobic centre, however this would involve considerable distortion of the polymer chains upon aggregation.

Najib (271) has determined the solubility of nystatin in aqueous solutions of polyvinylpyrrolidone and has found an increase in solubility on increasing the polymer concentration. However at any one concentration, the solubility decreased with an increase in PVP molecular weight. This effect was attributed to larger excluded volume effects on increasing the chain length. No such effect was found in the present work with polyvinylalcohol polymers.

7:3:2 Desorption of Polymers from the Drug Surface

In this method of dissolution testing the drug is first equilibrated with polymer solution to permit maximum adsorption to occur but it is subsequently poured into a large volume of dissolution medium containing no added polymer. The potential for polymer desorption exists under these conditions due to the non equilibrium of free and adsorbed polymer species. Desorption studies were performed on all the polymers used. The results are given in Table 24 in terms of the percentage of the previously adsorbed polymer desorbed from the surface.

Table 24

Journal of Tadros (272)

The Desorption of Polymers from the Drug Surface

Time (hours)	Percentage Desorbed	
	0.5	12
<i>Polymer</i>		
<u><i>Nonylphenylethoxylates</i></u>		
<i>NPE 8</i>	60 ± 8	65 ± 5
<i>NPE 20</i>	42 ± 3	53 ± 7
<i>NPE 30</i>	55 ± 11	59 ± 5
<u><i>Pluronics</i></u>		
<i>L61</i>	5 ± 2	6 ± 3
<i>L64</i>	2 ± 1	3 ± 2
<i>F68</i>	2 ± 2	-
<u><i>PVA</i></u>		
<i>Mowiol 8-88</i>	6 ± 3	4 ± 2
<i>Polyviol W25/L40</i>	2 ± 2	4 ± 2

All figures refer to desorption from a previously saturated drug surface.

With the nonylphenylethoxylates, 40 - 60% of the total polymer adsorbed at the interface was desorbed within 30 minutes and little change in desorption occurred after a further 11½ hours. The desorption values reflect the binding strength of polymers at the interface and the rapid loss of the NPE's show the relative ease with which these surfactants lose contact with the surface. The Pluronics show little tendency to desorb even after 12 hours and these results reflect the affinity of the surface for the hydrophobic central region of the

molecules. The results confirm the observations of Tadros (272) that Pluronic adsorption is essentially non-reversible. The unfractionated samples of polyvinylalcohol also show little tendency to desorb from the surface which is due to the numerous segmental-surface contacts. Thus, although the proportion of the total chain segments adsorbed is small, the total number of segments adsorbed at any one time, will be high. For desorption to occur, all segment-surface contacts must be broken simultaneously but this is statistically unlikely. The data of Stromberg, Grant and Passaglia (273) on the desorption of polystyrene from chrome surfaces shows similar effects with desorption rates depending on the surface coverage, and time of adsorption prior to desorption. Where sub-maximum surface coverages were studied no detectable desorption occurred over a period of three weeks. This occurs because there are a higher number of segment-surface contacts per molecule at sub-maximum surface coverage than at complete surface coverage.

7:3:3 The Effect of Stirring Rate on Suspension Dissolution Rates.

To investigate this effect, 60mg of drug were used with a small quantity of NPE 13 as wetting agent. The amount of NPE 13 added was insufficient to cause complete saturation of the drug surface. Typical graphs of absorption vs time curves and the corresponding c/t vs t curve are shown in Figure 76. Allowance was made for previously dissolved diloxanide furoate by subtracting the absorbance reading when $t = 0$ from all subsequent readings. Due to the low absorbance values, small errors in these readings may cause a wide scatter of points in the c/t vs t plot, particularly at low values of t . The linear plot of this graph was therefore determined from points at larger values of t . For the nonylphenylethoxylates the final concentration of surfactant in the dissolution medium was so low that the UV absorption of these molecules at 261nm could be neglected.

The effect of stirring speed on the dissolution rate was determined over the range 125 - 600 r.p.m. and the results of these observations are shown in Figure 77. NPE 13 was again used as the wetting agent. Above 200 r.p.m. a linear relationship applies between the logarithm of the rate constant k_1 , and the logarithm of the stirrer speed. Below this speed, k_1 decreases rapidly. Visual observation of the dissolution chamber showed that at low speeds there was insufficient agitation to maintain the drug particles in a dispersed state throughout the vessel and a layer of particles accumulated around the wall of the vessel at the same height as the stirrer paddle. The effect of this is to reduce the available surface area from which dissolution can take place and to reduce the flow of liquid over the particle surface. As a consequence of this the dissolution rate constant will decrease. In further experiments the stirrer speeds used were between 200 and 600 r.p.m.

Bircumshaw and Riddiford (274) have suggested that for a diffusion controlled process the velocity constant of a first order rate constant (k_2) can be written as

$$k_2 = D'A/Vh \quad (7.7)$$

where D' is the diffusion coefficient of the solute, A the area of surface exposed to the dissolution medium of volume V and h is the diffusion layer thickness. Elworthy and Lipscomb (268) further suggest that the zero order rate constant k_1 is proportional to $D'A/h$. In both cases a reduction in A due to the settling of particles at low stirrer speeds will cause a reduction in the rate constants as observed in Figure 77.

The relationship between dissolution rate k_1 , and the stirring speed S is found to be of the form (274) $k_1 = a S^b$

while for transport processes that are purely diffusion controlled to Elworthy and Lipscomb (268) have given

$$k_1 = a S^{0.5} \quad (7.8)$$

The value of the slope of the $\log k_1$ against $\log S$ plot above 200 r.p.m. is 0.34. This relatively low value does not preclude the possibilities that the dissolution process is diffusion controlled. Factors which are known to account for unusual dissolution rate - agitation rate relationships are:

- 1) Surface film formation due to the deposition of solvent insoluble substance which is chemically different to that of the dissolving material (275)
- 2) Interfacial reaction controlled dissolution (276)
- 3) Surface effervescence (277)
- 4) Surface pitting (278)

In the case of suspended particles further complications arise due to the motion of particles within the dissolution fluid. This has the effect of reducing the velocity of liquid over the crystal faces in comparison to a disc of the drug where the disc is stationary relative to the moving fluid. For example it has been found (279) that the dissolution rate - agitation rate relationship of griseofulvin has a slope of 0.54 when the drug is presented as a tablet but the same drug in powdered form gives a value of 0.21 for the constant b . It was not possible to perform dissolution studies on diloxanide furoate tablets due to the poor compaction properties of the pure drug. Thus confirmation of a diffusion controlled dissolution process could not be provided directly.

7:3:4 The Effect of Drug Quantity on Diloxanide Rate

According to equation 7.7 and the corresponding equation for a

zero order reaction the rate constants, k_1 and k_2 are proportional to the surface area of drug exposed to the dissolution medium. Figure 78 gives confirmation of the validity of these equations as linear relationships are found between k_1 and the weight of drug used in the experiments. It was found that this relationship held even for small weights of drug where it might be expected that the dissolution process would erode the particles to such an extent that the zero order forward reaction rate would not apply due to the continuing decrease in surface area with time. However with these low weights of drug there was no evidence for deviation from linearity in the plots of c/t against t . Calculations for spherical particles of 125 micron diameter show that at 10% of complete dissolution the reduction in surface area of a drug suspension initially containing 30mg of powder is approximately 6%. This is unlikely to cause serious problems in the dissolution process.

7:3:5 The Effect of Adsorbed Layers on Dissolution Rate

Figure 79 shows the effect of adsorbing nonylphenylethoxylates onto the drug prior to dissolution testing. In all cases the final concentration of surfactant in the dissolution medium was far below the critical micelle concentration (greater than a fivehundredfold dilution) therefore changes in the saturated solubility of drug in the bulk solution can be neglected.

The results indicated that increasing the ethylene oxide chain length of the surfactant molecule has no effect on the dissolution characteristics of the drug as all data points can be fitted to the same linear plot. In addition this graph is similar to the results of Figure 77, where sub-maximum surface coverage of the drug occurred. Thus adsorption of these surfactants onto diloxanide furoate produces no observable change in the rate of drug release. The poor wetting properties of the uncoated drug particles did not permit the rate

constants for the pure drug to be evaluated. of the dissolution

solutions per

The most likely explanation of why these surfactants do not cause any rate changes is due to the desorption of these molecules from the surface. Table 24 indicates that after 30 mins desorption time 40 - 60% of previously adsorbed material was desorbed in 10ml of solution. If the adsorption-desorption is a true equilibrium process, more polymer would be desorbed in the same time on increasing the volume of solution to 1100ml. The rate constants obtained in these cases will therefore approach the rate for the uncoated, bare drug particles.

The effect of adsorbed Pluronics on the drug dissolution is shown in Figure 80. For the short chain surfactants L61, L62 and L64 no measurable variation is found between these polymers whereas F68 containing 80 ethylene oxide units per side chain, a small but discernable decrease was found in the drug release rate. Desorption does not occur with these materials and hence the reduced dissolution rate must be due to the presence of the adsorbed polymer layer. This effect is greater when the dissolution from polyvinylalcohol covered particles is considered (Figure 81). In all cases the rate constant increases on increasing the stirrer speed indicating the importance of the thickness of diffusion layer surrounding the particles on drug dissolution. The results imply that the polymer layer contributes to only a part of the diffusion layer. If this were not so, and the adsorbed layer constituted the complete diffusion layer the rate constant would be independent of stirrer speed. The diffusion layer thickness h , has been determined by Collett et al (280) for solvent flowing linearly over the surface of salicylic acid tablets using the Nelson equation (281):

$$h = \left(\frac{\eta}{\rho_m S} \right)^{\frac{1}{2}} \quad (7.9)$$

where η and ρ_m are the viscosity and density of the dissolution medium respectively and S is the stirrer speed in revolutions per second. The values of h obtained varied between 600 micron and 6mm depending upon the conditions used. For the suspension systems the agitation will not be as effective in reducing the diffusion layer thickness due to the motion of particles within the fluid. Values of h calculated from equation 7.9 will therefore underestimate the true diffusion layer thickness. However, in view of the results of Fage and Townsend (283) it appears unlikely that diffusion layers of this magnitude can exist at the interface. These authors examined the laminar flow of water along the walls of a tube and observed fluid movement to within 0.6 microns of the surface. The maximum adsorbed layer thickness measured was 52nm for the highest molecular weight polyvinylalcohol. Therefore even with stationary diffusion layers of 0.1 micron thickness, a large proportion of the layer will consist of solvent rather than polymer chains.

The total dissolution process therefore consists of three sub-processes, i.e. initial solvation of drug molecules at the interface, diffusion through the polymer barrier and diffusion through the solvent diffusion layer of which - the second process being the rate determining step. The total process can be considered as diffusion through laminated structures for which the following expression has been derived (283)

$$dM/dt = \Delta C/R_T \quad (7.10)$$

where dM/dt is the rate of mass transport across laminated barriers and ΔC is the instantaneous concentration difference across the whole system. The total diffusional resistance R_T is given by

$$R_T = \frac{h_1}{D_1 K_1} + \frac{h_2}{D_2 K_2} + \dots + \frac{h_n}{D_n K_n} \quad (7.11)$$

where h_n represents the thickness of the individual layers, D_n and K_n represent the diffusion coefficient and partition coefficient of the n th layer respectively.

As diffusion through the polymer layer is the rate determining step, the thickness, partition coefficient and diffusion coefficient relating to this layer are of prime importance. Figure 83 shows the relative diffusion rates of molecules through polymer solutions determined by viscometric means as a function of concentration and molecular weight. As expected increases in both these parameters decrease the diffusion of drug through the polymer network. Using U-tube viscometers it was impractical to determine relative diffusion coefficients at those concentration of polymer found at the interface. A further difficulty in attempting to explain the dissolution through an adsorbed polymer layer is that according to theory, the segment concentration within the adsorbed layer is not uniform but decays exponentially (88). D and K will therefore vary with distance from the surface.

A similar decrease in the dissolution behaviour of drug in the presence of adsorbed PVP on increasing the molecular weight has been found by Najib et al (267). They attribute this effect to saturation of the adsorption sites and they therefore claim that the polymer segment density is independent of polymer fraction - the reduced dissolution being due to film thickness on increasing M . Results of polymer concentration at the interface however show that the average polymer segment concentration decreases as M increases (see Table 23 and Ref. 133). In addition, theoretical predictions of a segment density distribution predict that it is dependent on polymer molecular weight, (56, 57, 52). Accepting the premise that at surface saturation the number of adsorption sites occupied is independent of molecular weight, the exponential decrease in segment density normal to the surface will be slower for

higher molecular weight polymers. The decrease of dissolution rate with increase in M may therefore reflect the exponential nature of the polymer segment density distribution. This idealized view is complicated by the fact that the solubility of drug in the adsorbed layer is polymer concentration dependent (Figure 75) and the rate of transport of drug from the polymer layer to the solvent diffusion layer is dependent upon the concentration difference across this interfacial barrier. The dissolution of drug from the solid surface through an adsorbed polymer layer appears to be a complex process involving the solubility and diffusion of drug molecules within that layer.

In conclusion it may be said that adsorption of polymers at the drug-solution interface affects not only the physical stability of the resulting dispersion but in addition may alter the bioavailability of the product.

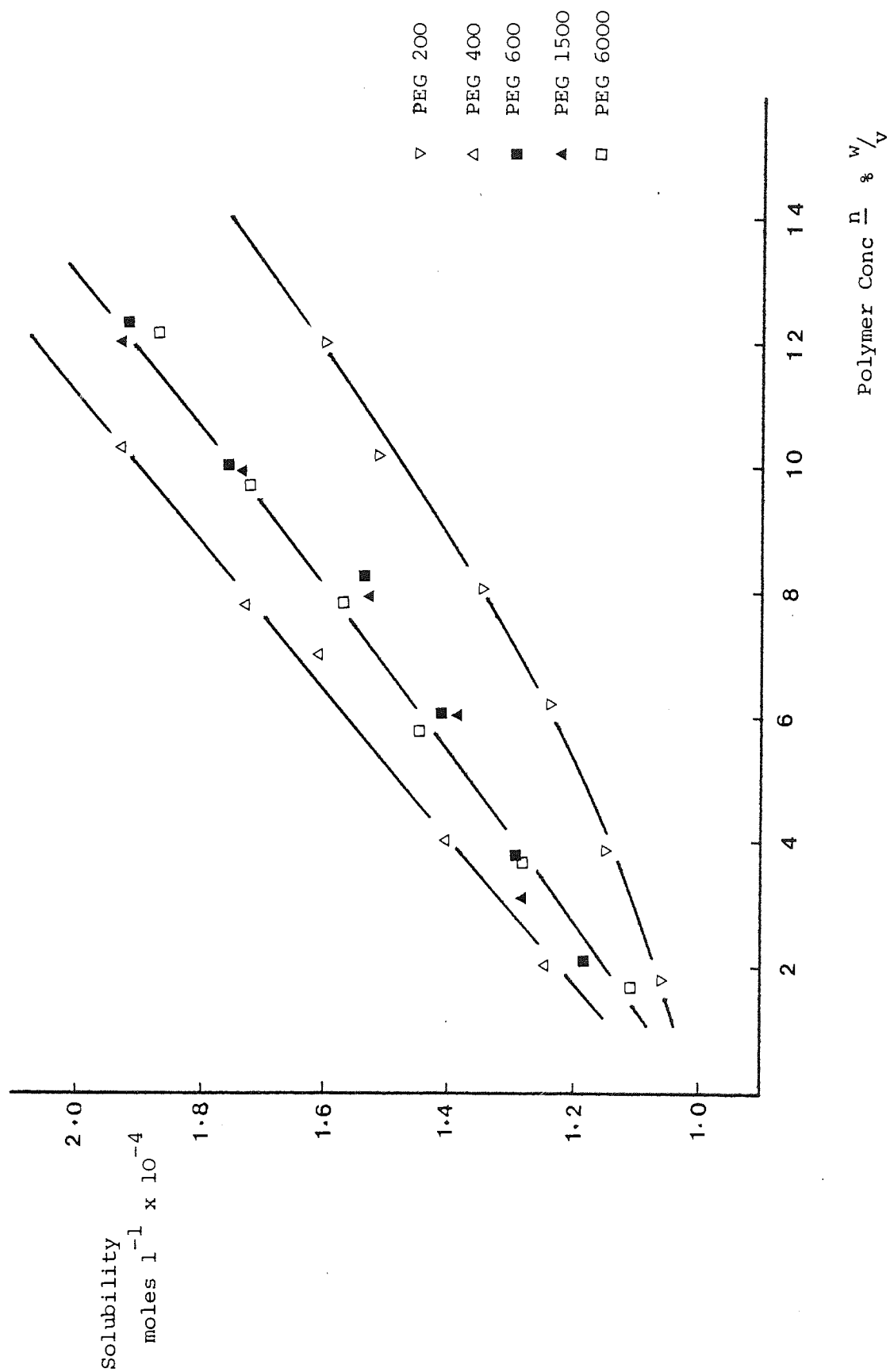


Figure 74 Solubility of Diloxanide Furoate B.P. in Polyethylene Glycol Solutions.

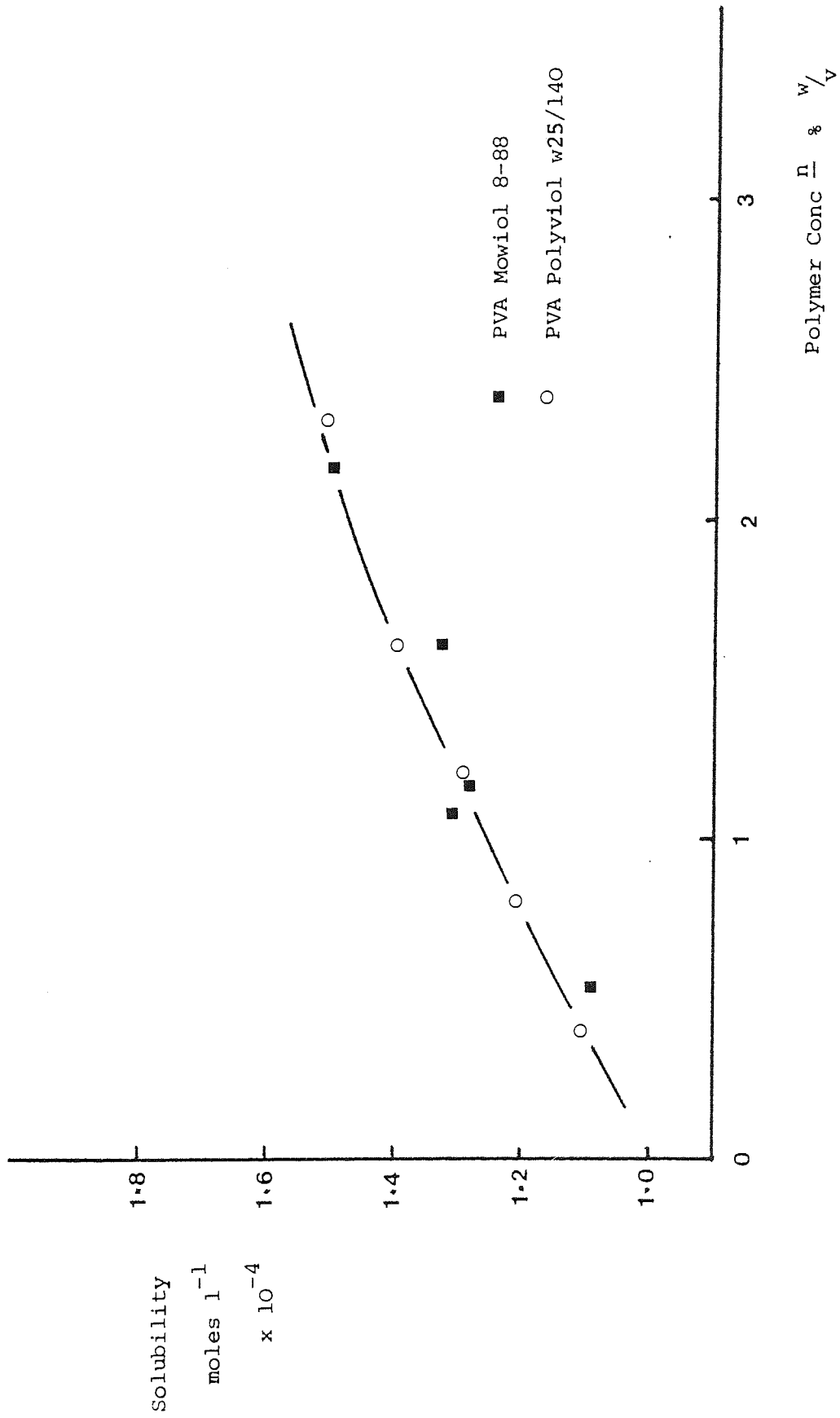


Figure .75 Solubility of Diloxanide Furoate B.P. in Polyvinylalcohol Solutions.

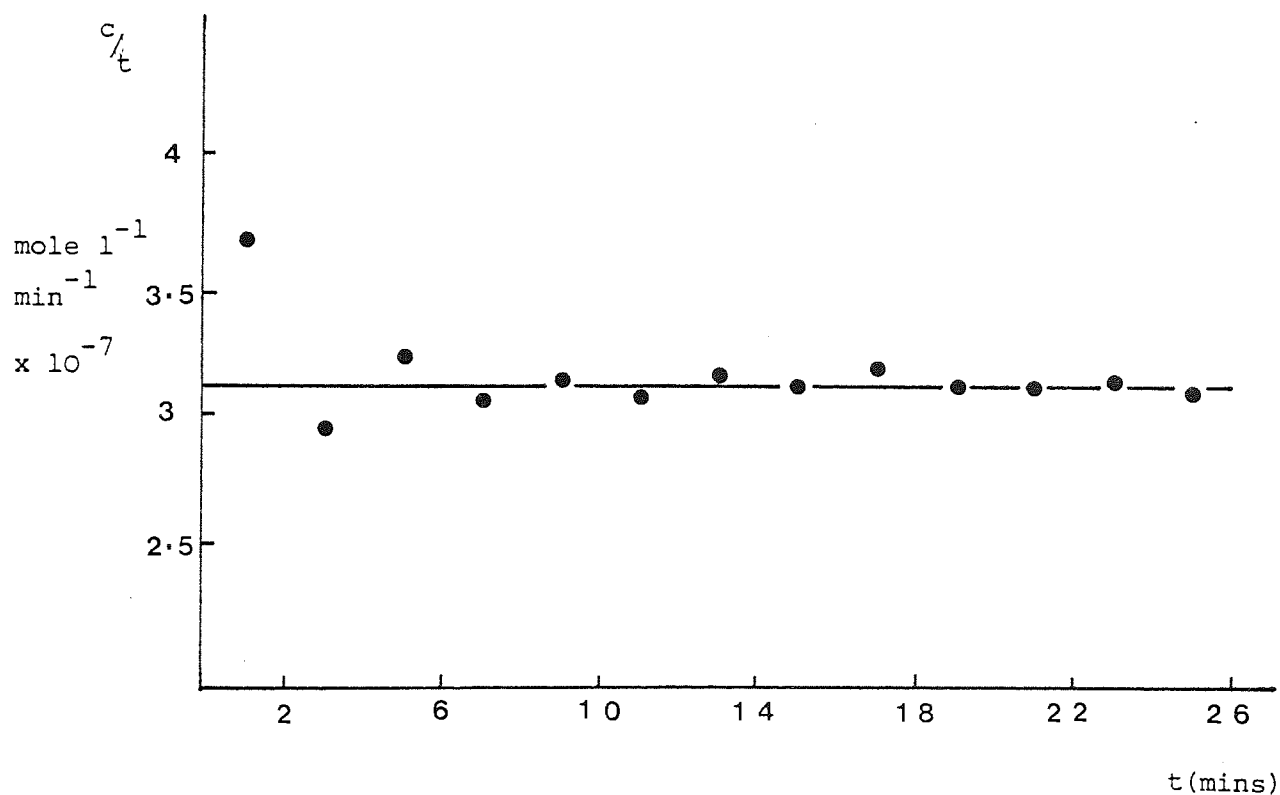
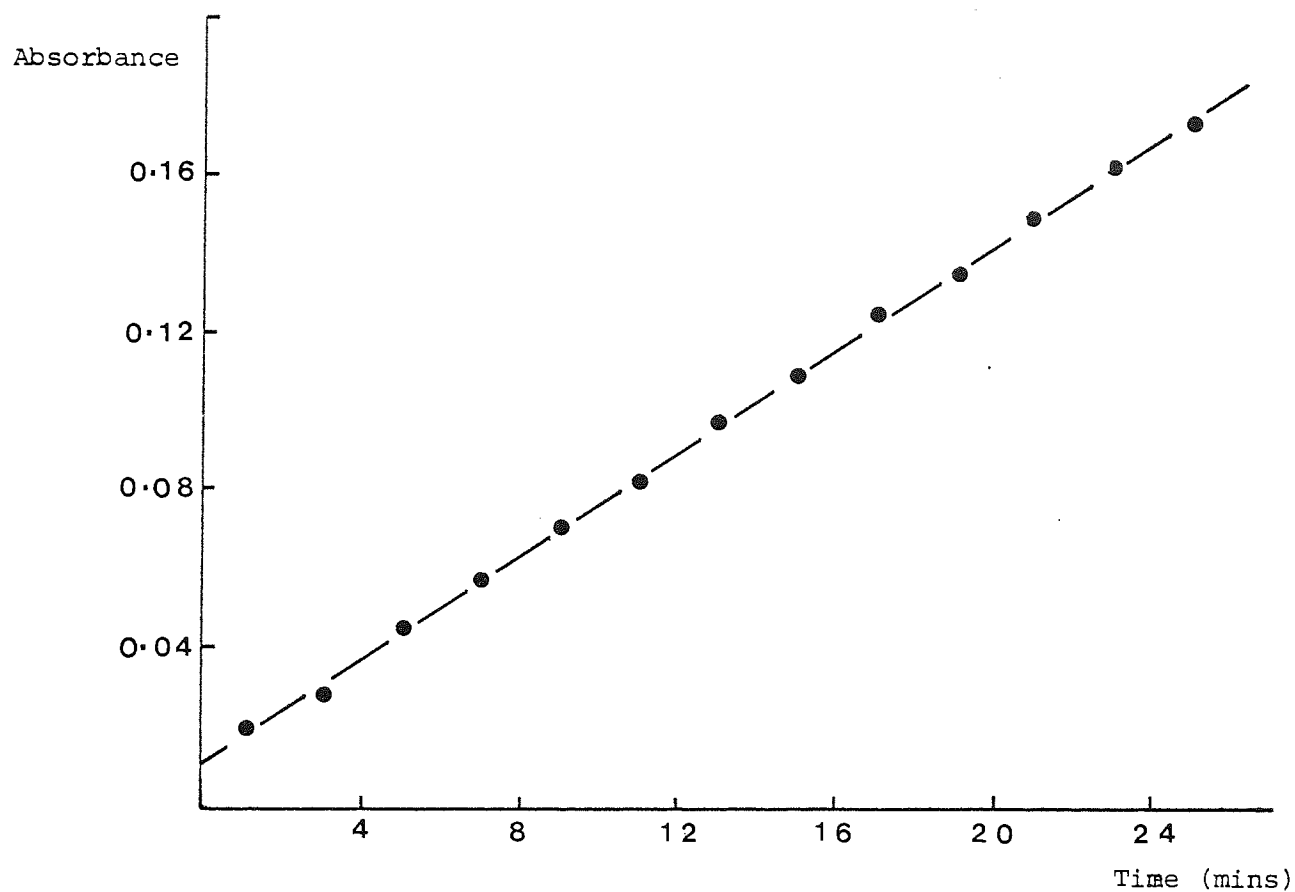


Figure 76 Dissolution Curves of Diloxanide Furoate B.P.

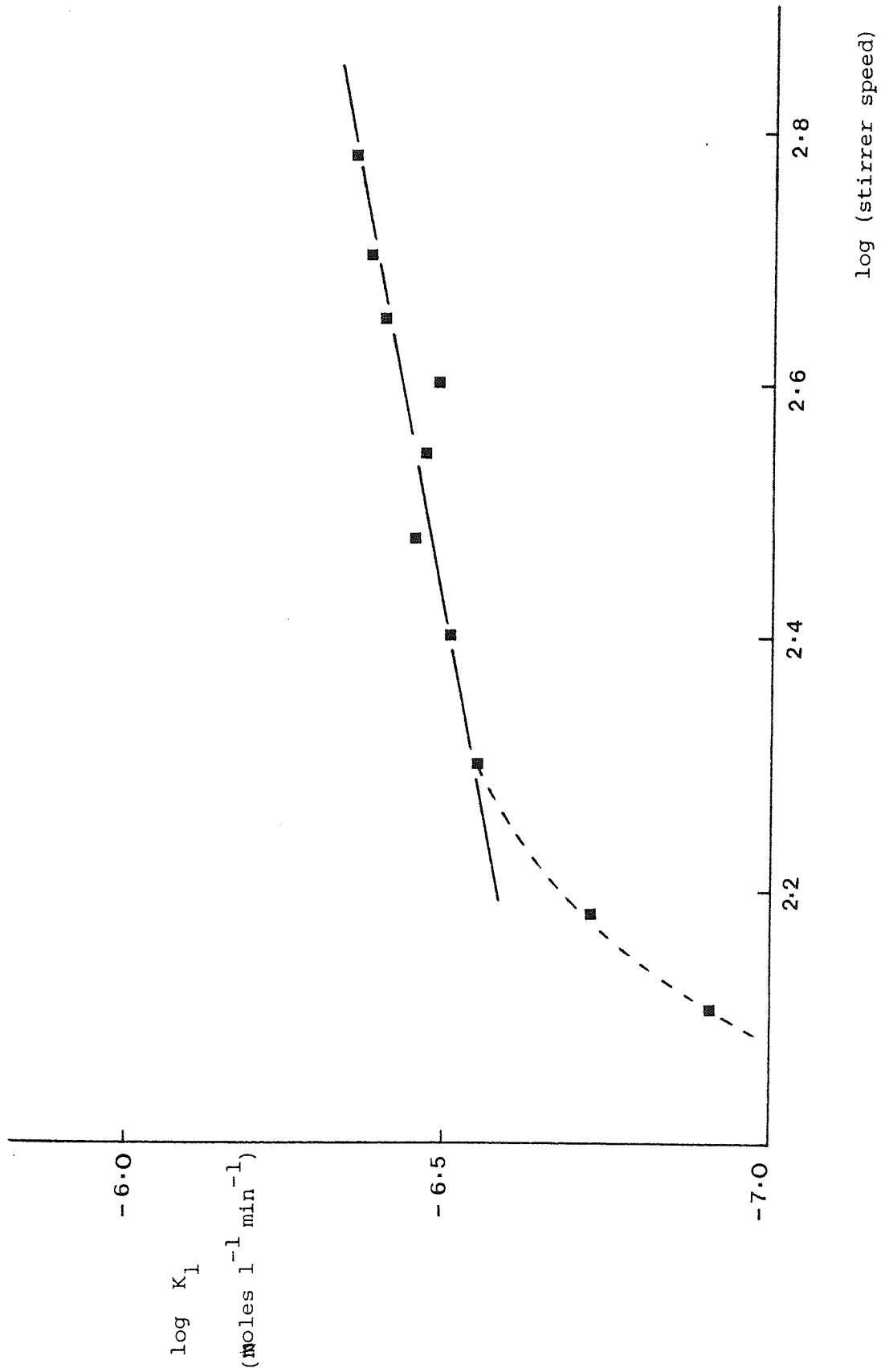


Figure 77 Effect of Agitation on Drug Dissolution

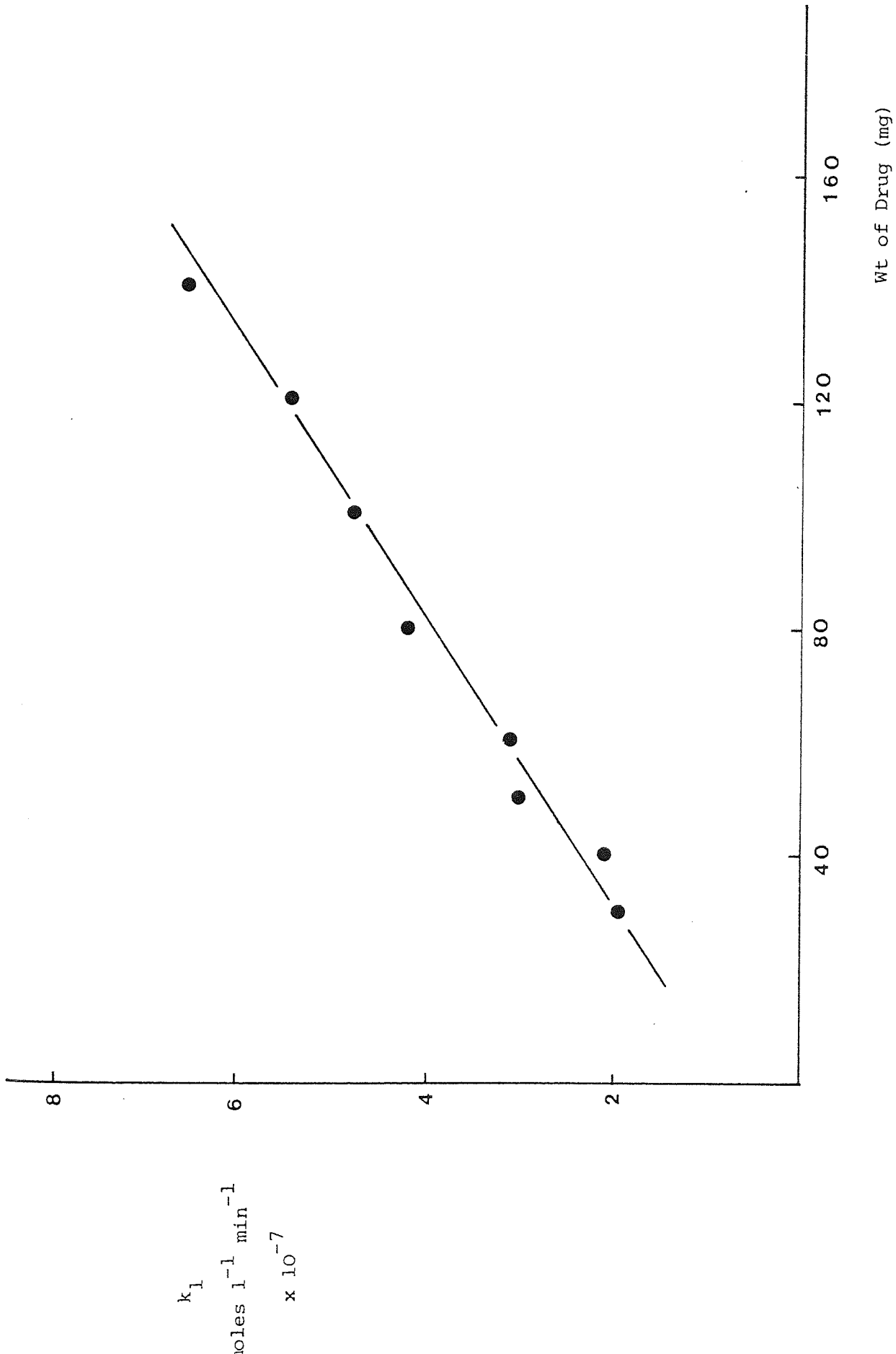


Figure 78 Effect of Quantity of Drug on Dissolution Rate

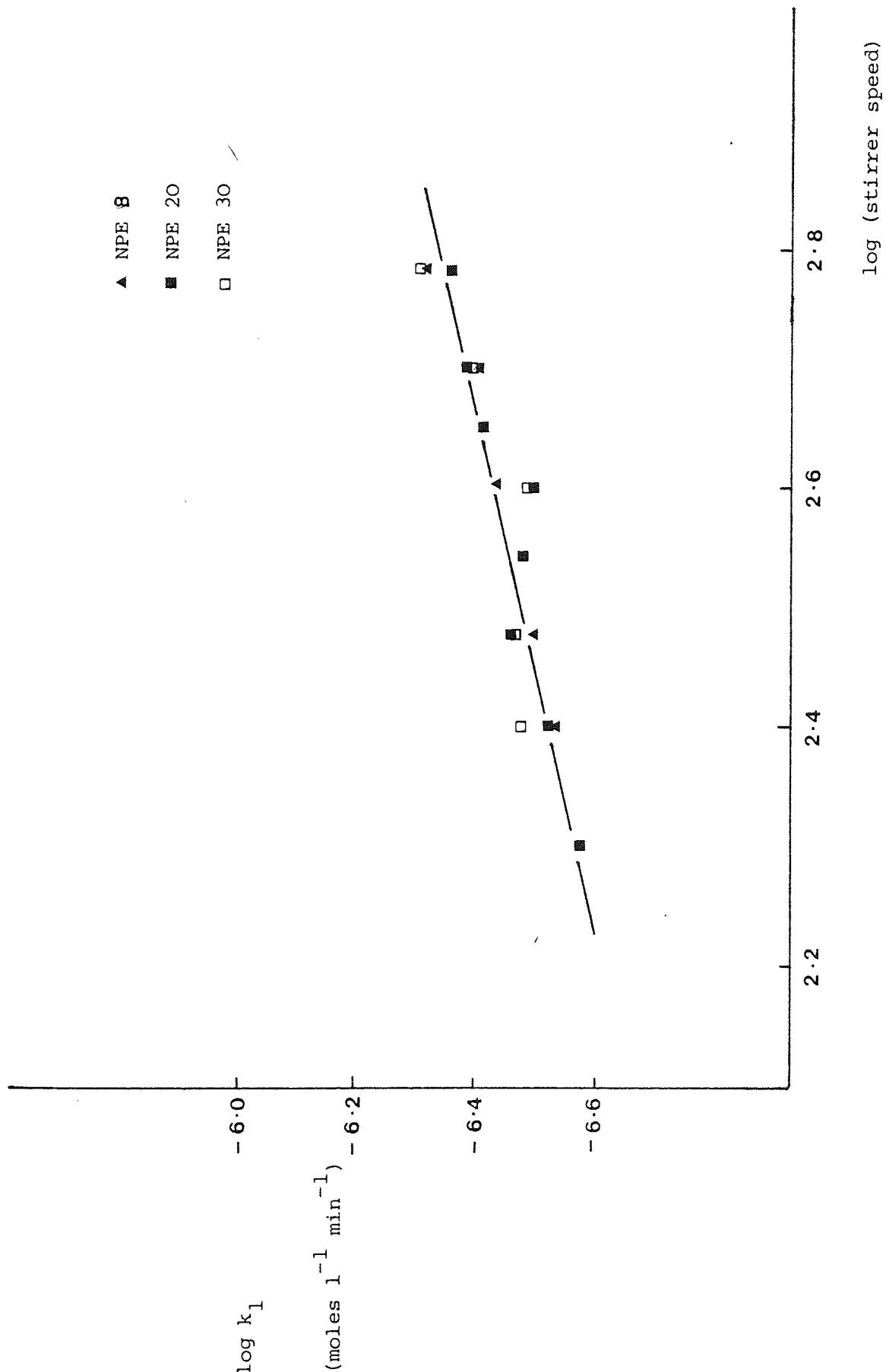


Figure 79 Effect of Adsorbed Nonylphenoxyethoxylates on Dissolution Rates

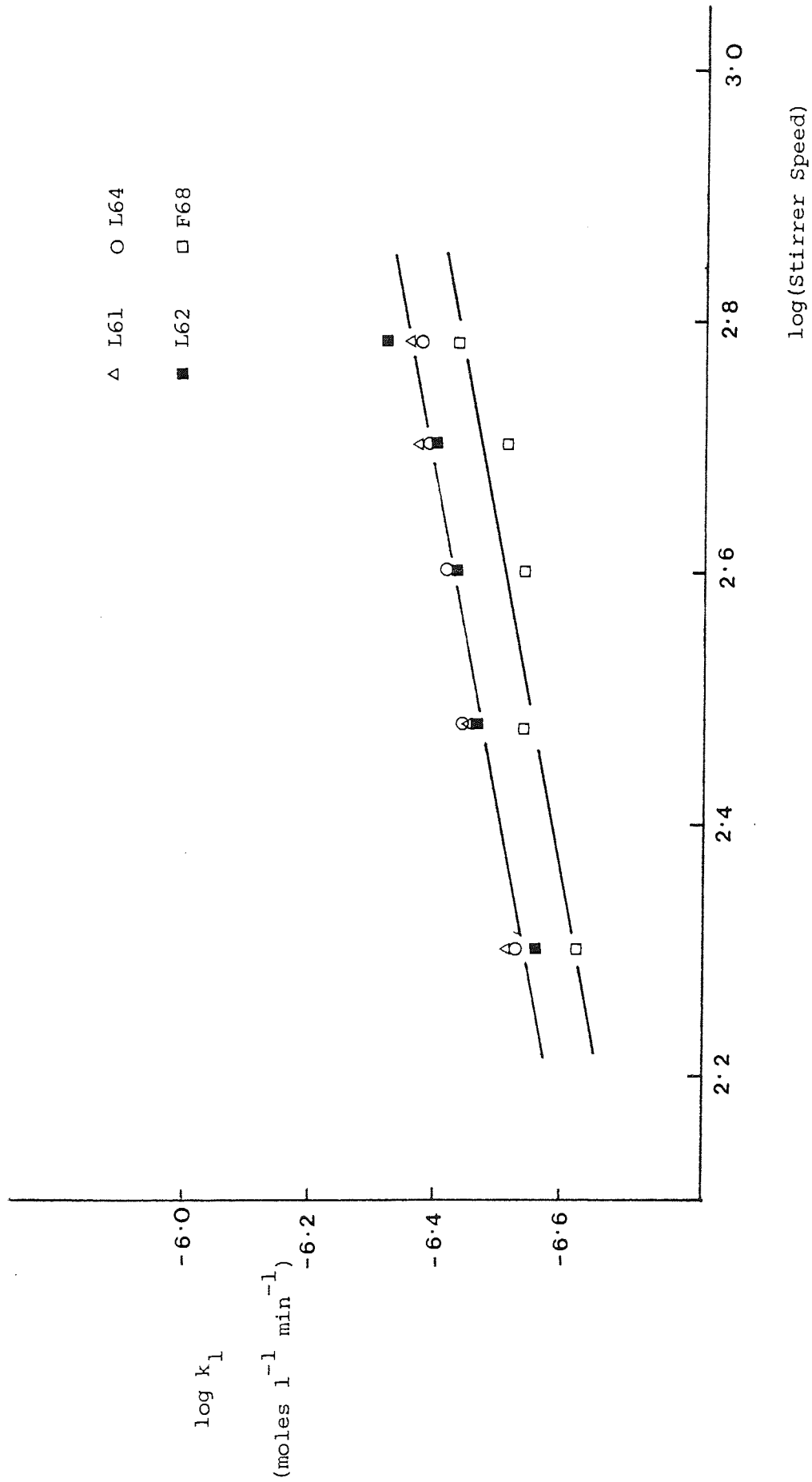


Figure 80 Effect of Adsorbed Pluronics on Dissolution Rate

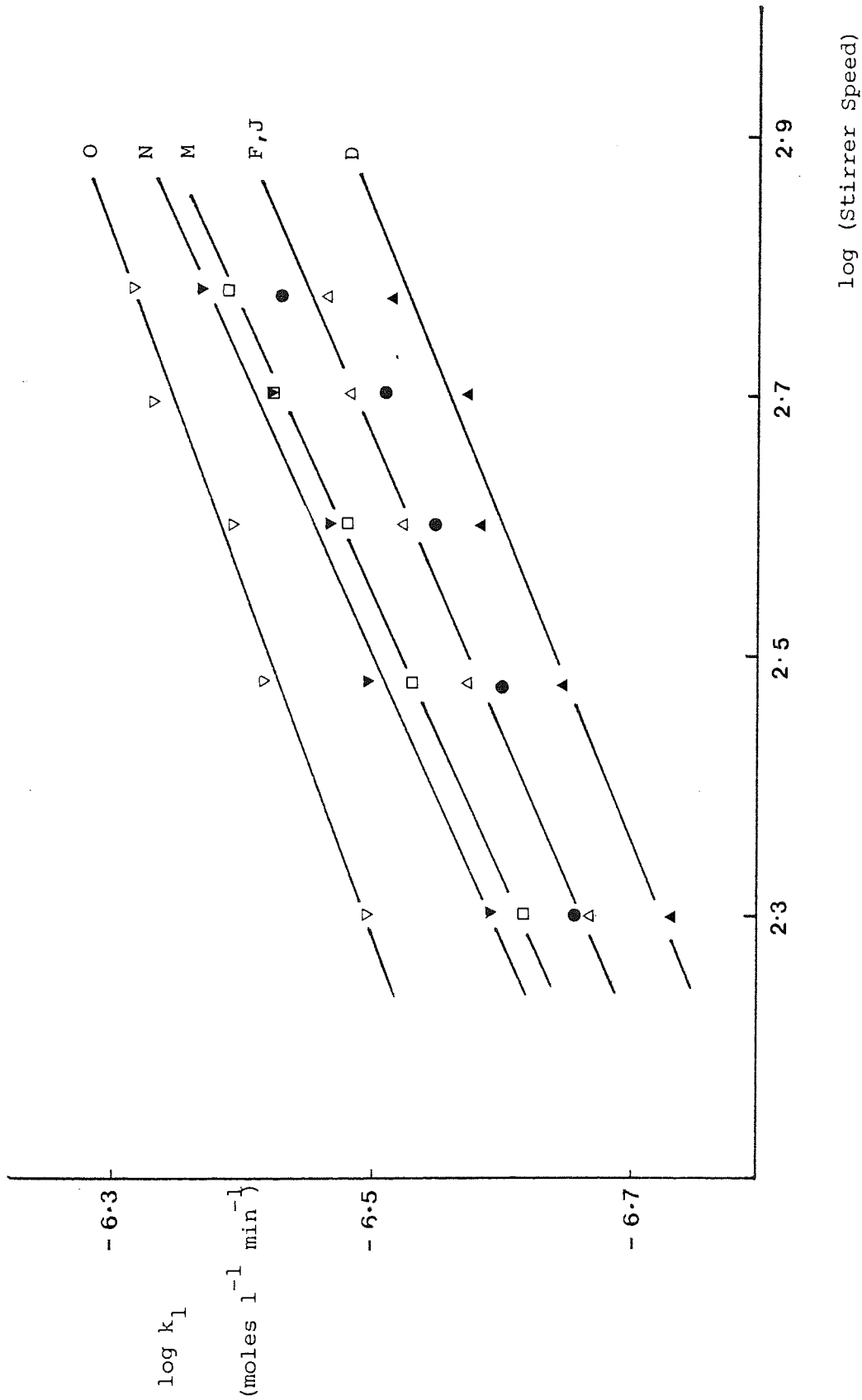


Figure 81 Effect of Adsorbed Polyvinylalcohols on Dissolution Rate

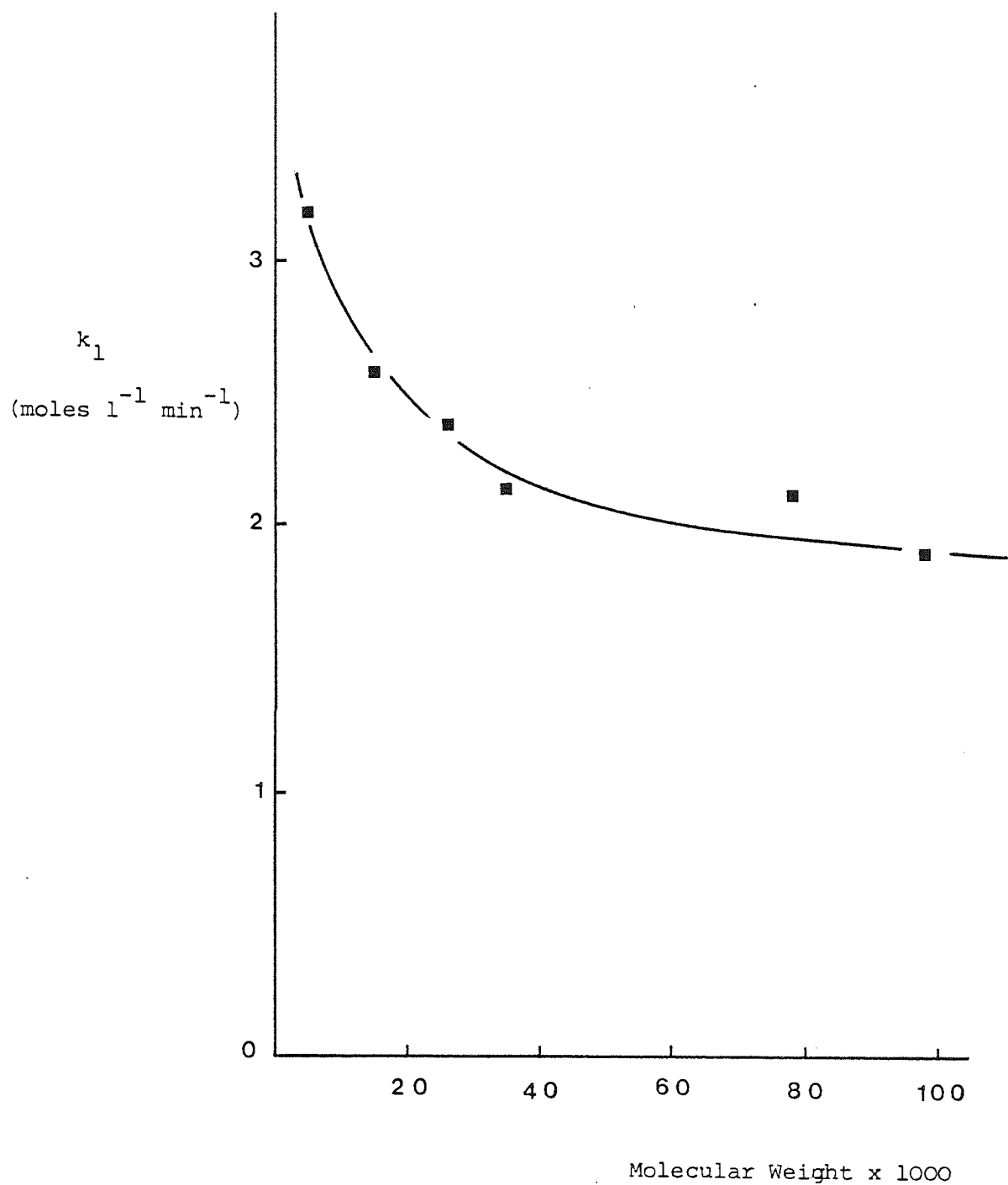


Figure 82 Effect of PVA Molecular Weight Dissolution Rate
at 200 r.p.m.

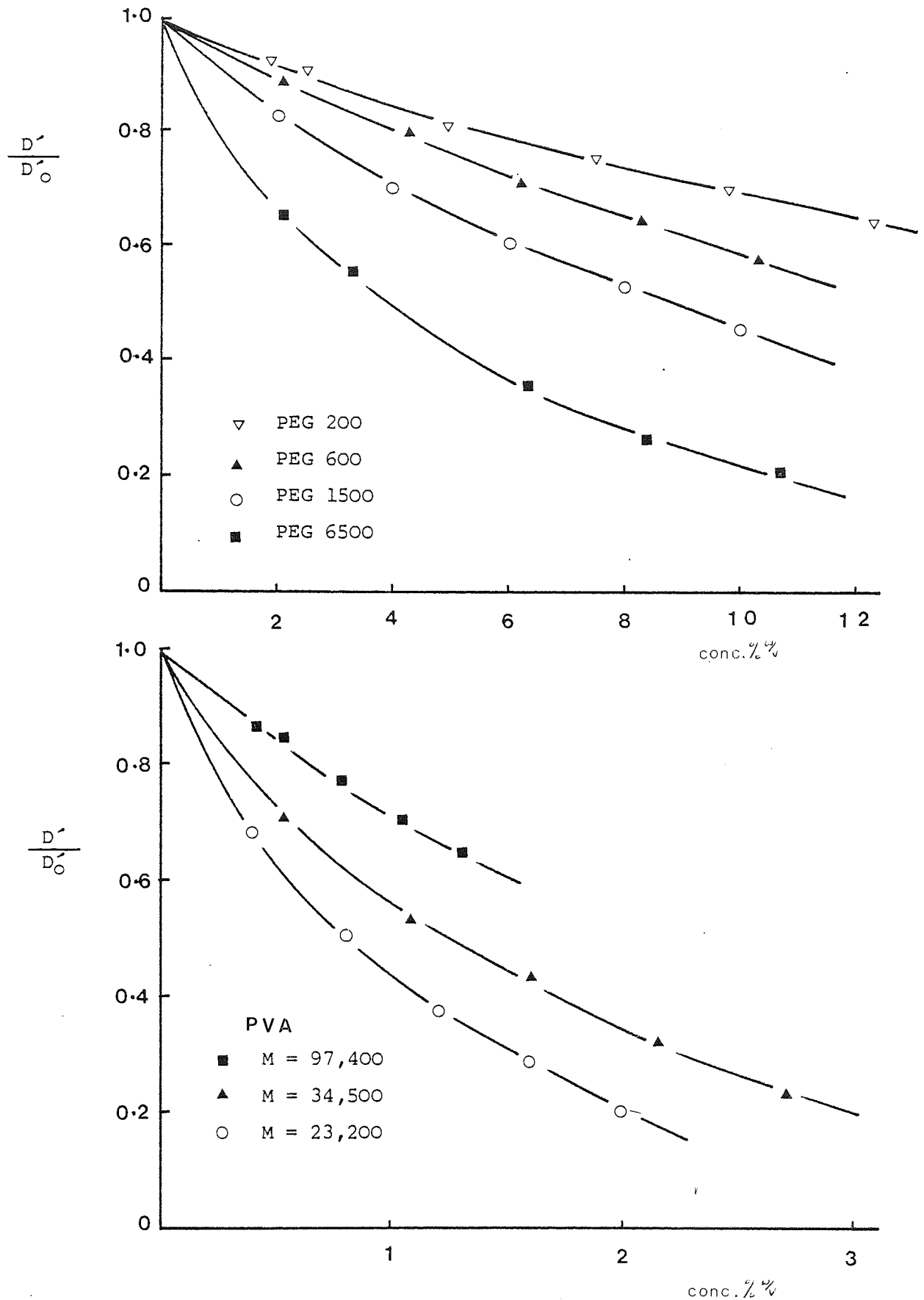


Figure 83 Relative Diffusion Rates of Molecules through Polymer Solutions. by Viscosity Measurement assuming Applicability of Stokes-Einstein Equation

SECTION 8

conclusions

SECTION 8 Conclusions

The adsorption of two groups of nonionic surfactants and a series of fractionated polyvinylalcohols onto a polystyrene latex and a drug substance diloxanide furoate B.P. have been investigated. The mass adsorption isotherms for the nonionic surfactants followed the Langmuir equation with a saturated monolayer of material being formed in the region of the measured critical micelle concentration. The area occupied at the interface increased on increasing the ethylene oxide content of the molecule indicating that adsorption occurred through the hydrophobic and hydrophilic regions of the molecule. For the Pluronic nonionic surface active agents there is some dispute as to the value of the critical micelle concentration or indeed whether micelles actually form at all. The present work has shown that a rapid rise in adsorption occurs at a concentration corresponding approximately to the measured apparent c.m.c. determined by an iodine solubilization technique. This concentration is in agreement with the low values obtained by other workers but extension of the adsorption isotherm to cover equilibrium concentrations in excess of the higher reported c.m.c. values for one of the Pluronics studied gave no evidence for the occurrence of further adsorption.

The adsorption of polyvinylalcohol at the drug-solution interface could similarly be fitted to the Langmuir isotherm and the maximum amount adsorbed A_s , increased with polymer molecular weight. For low molecular weight fractions, deviations in the $\log A_s - \log M$ plot occurred and this was explained by the adsorption of these smaller molecules into the drug pores. Confirmation of the existence of pores within the surface was provided by mercury porosimetry and nitrogen adsorption measurements. The measured diameter of the pores corresponded to the molecular dimensions of the polymer molecules in free solution for

the polymer fraction where deviation in the above plot took place. The adsorption of fractionated and unfractionated polymer samples also confirmed the presence of pores. The polymer dimensions in solution were obtained from the intrinsic viscosity using dilute polymer solution theory. Such values were used to construct potential energy diagrams.

Adsorption of polyvinylalcohol onto the polystyrene latex produced maximum adsorption values far in excess of those normally found for monolayer formation of this polymer at interfaces. Multilayer formation was considered to have occurred - a fact which is substantiated by previous work on the same polymer - substrate system (133). The difference in adsorption patterns onto the two solid surfaces was explained by the more hydrophobic nature of the latex producing a stronger affinity for the adsorption segments of the polymer chain. Static contact angle measurements were used to assess the hydrophobic nature of the surfaces and a significantly higher contact angle was found for the latex-water system.

The adsorbed layer thickness at the latex-solution interface was determined by three methods : microelectrophoresis, intensity fluctuation spectroscopy and viscosity measurements. For the Pluronics good agreement was found for the first two methods and microelectrophoresis was therefore applied to nonylphenylethoxylate adsorption. In all cases the value of δ obtained was considerably less than the extended length of the molecule, providing further confirmation that adsorption of these surfactants occurred in the form of a looped monolayer. Viscosimetric thickness of PVA adsorbed onto latex gave values too large to be explained by monolayer adsorption and these results in combination with the adsorption results indicate the presence of multilayer formation. Measurements of the adsorbed layer thickness of polymers on the diloxanide furoate surface using microelectrophoresis gave values

which were greater than the extended length of the molecules. This occurred due to desorption of the adsorbed hydroxyl potential determining ions on adsorption of surfactants. Such an effect gives lower than expected plateau mobility values from which large adsorbed layer thicknesses are obtained. The results with polystyrene latex indicate that microelectrophoresis may be used to determine the adsorbed layer thickness of surfactants at interfaces. However as a precaution the results obtained in this manner should be confirmed by independent means.

The stability of drug suspensions was monitored as a function of polymer concentration in the absence of any significant electrostatic repulsive forces. The main criteria used to assess stability were the sedimentation volume and the redispersibility of the product. When coated with adsorbed nonylphenylethoxylates the drug suspensions exhibited unusual redispersibility characteristics with this value going through a maximum at one to two thirds of maximum surface coverage. These dispersions were all deflocculated and the observed redispersibility effect was attributed to the 'partial steric stabilization' of the drug particles at sub-maximum surface coverages coupled with attraction between the bare batches of exposed surface in the final sediment. Polyvinylalcohol did not show the same redispersibility characteristics despite the production of deflocculated systems and the difference between these two groups of adsorbing species was interpreted in terms of the dimensions of the polymers at the interface.

The Hamaker constants of all the materials used were determined by an optical dispersion technique and these values were used to construct potential energy diagrams between interacting particles. The microscopic approach to particles attraction was used and effects of adsorbed layers and attractive retardation were taken into account through

use of appropriate equations. Good correlation was observed between the type of suspension formed and the depth of the restricted primary minimum based on the potential energy of attraction between particles for short chain ethylene oxide surfactants. The correlation for adsorbed polyvinylalcohols was not as good and this was attributed to the use of a mean segment density in the adsorbed layer in calculating V_A , whereas an exponential segment density distribution would be more appropriate for these long chain polymers.

The short chain ethylene oxide Pluronics produced aggregated suspensions when adsorbed at the interface due to two mechanisms, a) increased attraction due to high concentration of surfactant at the interface b) insufficient repulsion due to the low concentration of stabilizing ethylene oxide chains within the adsorbed layer.

Long term stability testing over a period of one year showed that those suspensions which were initially aggregated remained so after prolonged storage. Deflocculated suspensions showed an increase in redispersibility due to crystal bridging between particles.

The dissolution characteristics of the drug dispersions were investigated and the effect of adsorbed polymers studied. No significant effect was observed when an adsorbed layer of nonylphenylethoxylate was present on the surface but this was probably due to desorption of these molecules on dilution in the dissolution medium. Adsorbed polyvinylalcohol reduced the dissolution rate and this reduction became greater as the molecular weight of the polymer increased. The cause of this effect is due to the reduction of drug diffusion through the adsorbed polymer layer.

This work has shown the usefulness of adsorbed polymers and

surfactant in altering the characteristics of drug suspensions in the absence of any electrical factors. Both aggregated and non-aggregated systems may be obtained depending on the concentration and type of polymer used and a theoretical understanding of the interacting forces between particles has been applied to interpret the suspension characteristics observed. Adsorbed polymers may affect the bioavailability from pharmaceutical suspensions, thus in vitro testing of the final formulated product is advisable to monitor adverse dissolution problems.

REFERENCES

REFERENCES

1. British Pharmaceutical Codex (1954) The Pharmaceutical Press, London.
2. British Pharmaceutical Codex (1973) The Pharmaceutical Press, London.
3. Data Sheet Compendium 1978/9 A.B.P.I. London.
4. Rainsford, K.D. J. Pharm. Pharmacol (1978) 30 129.
5. 'Physical Pharmacy' Martin, A.N., Swarbrick, J. and Cammarata, A., Chap. 19 Lea and Febiger (1969) Philadelphia.
6. Deryaguin, B.V. and Landau, L. Acta Phys-Chim. URSS (1941) 14 633.
7. Verweey, E.J.W. and Overbeek, J.Th.G. 'Theory of the Stability of Lyophobic Colloids' Elsevier (1948).
8. Israelachvilli, J.N. Faraday. Disc. Chem. Soc. (1978) 65 20.
9. Heller, W. and Pugh, T.L. J. Chem. Phys. (1954) 22 1778.
10. Ottewill, R.H. in 'Colloid Science' Vol 1 Chemical Society, London 1973.
11. Healy, T.W. and La Mer, V.K. J. Colloid Sci. (1964) 19 343.
12. Slater, R.W. and Kitchener, J.A. Disc. Faraday Soc. (1966) 42 267.
13. Ecanow, B., Grundman, R. and Wilson, R. Am. J. Hosp. Pharm. (1966) 23 404.
14. Bondi, J.V., Schnaare, R.L., Niebergall, P.J. and Sugita, E.T. J. Pharm. Sci. (1973) 62 1731.
15. van Olphen, H. 'Introduction to Clay Colloid Science' (1963) Interscience, New York.
16. Worrall, W.E. and Green, C.V. Trans. Brit. Ceram. Soc. (1953) 52 528.
17. Norton, F.H. 'Fine Ceramics' p.60 (1970) McGraw-Hill, New York.
18. Hiestand, E.N. J. Pharm. Sci. (1964) 53 1.
19. Bagchi, P. in 'Colloidal Dispersions and Micellar Behaviour' Ed. Mittal, K.L. (1975) A.C.S. Symposium Series 9.
20. Mathews, B.A. and Rhodes, C.T. J. Pharm. Pharmacol. (1968) 20 2045.

21. See Reference 5 page 313. Japan (1976) 96 110.
22. Weissberger, A. 'Technique of Organic Chemistry' Vol 3 (1950) page 388. Interscience, New York.
23. Kolthoff, I.M., Proc. Koninkl. Nederland Akad. Wetenschap (1937) 40 82.
24. Haines, B.A. and Martin, A.N. a) J. Pharm. Sci. (1961) 50 228
b) J. Pharm. Sci. (1961) 50 753
c) J. Pharm. Sci. (1961) 50 756
25. Kayes, J.B. J. Pharm. Pharmacol (1976) 29 199.
26. Wilson, R.G. and Ecanow, B. J. Pharm. Sci. (1963) 52 757.
27. Ecanow, B., Gold, B. and Ecanow, C. Amer. Perfum. Cosmet. (1969) 84 27.
28. Schenkel, J.H. and Kitchener, J.A. Trans. Faraday Soc. (1960) 56 161.
29. Tabor, D. and Winterton R.H.S. a) Nature (London) (1968) 219 1120
b) Proc. Roy. Soc. (1969) A312 435
c) J. Colloid. Interface. Sci. (1969) 31 364.
30. Matthews, B.A. and Rhodes, C.T. J. Pharm. Sci. (1968) 57 569.
31. Jones, R.D.C., Mathews, B.A. and Rhodes, C.T. J. Pharm. Sci. (1970) 59 518.
32. Ecanow, B. and Takruri, H. J. Pharm. Sci. (1970) 59 1848.
33. Mathews, B.A. and Rhodes, C.T. J. Pharm. Sci. (1970) 59 521.
34. Short, M.P. and Rhodes, C.T. Can. J. Pharm. Sci. (1973) 8 46.
35. Otsuka, A., Surrada, H. and Yonezawa, Y. J. Pharm. Sci. (1973) 62 751.
36. Caramella, C. and Cocchi, G.A. Boll. Chim. Pharm. (1976) 115 658.
37. Felmeister, A., Kuchtyak, G.M., Koziol, S. and Felmeister, C.J. J. Pharm. Sci. 62 2026.
38. Najib, N., Kellaway, I.W. and Marriott, C. J. Pharm. Pharmacol. (1977) 29 43P.

39. Otsuka, A. and Kakuichi, C. J. Pharm. Sci. Japan (1976) 96 110.
40. Farley, C.A. and Lund, W. Pharmaceutical Journal (1976) June 26th.
41. Seager, H., J. Pharm. Pharmacol. (1968) 20 968.
42. Perkel, R. and Ullman, R. J. Polym. Sci. (1961) 54 127.
43. Jenckel, E. and Rumbach, B. Z. Elektrochem (1951) 55 612.
44. Frisch, H.L., Simha, R. and Eirich, F.R. J. Phys. Chem. (1953) 57, 584, J. Phys. Chem. (1954) 58 507, J. Phys. Chem. (1955) 59 633
J. Chem. Phys. (1953) 21 365, J. Chem. Phys. (1957) 27 702.
45. Higuchi, W.I. J. Phys. Chem. (1961) 65 487.
46. Lal, M. and Stepto, R.F.T. J. Polym. Sci. Polymer Symposium (1977) 61 401.
47. Forsman, W.C. and Hughes, R.E. J. Chem. Phys. (1963) 38 2130.
48. Silberberg, A. (a) J. Phys. Chem. (1962) 66 1872, (b) J. Phys. Chem. (1962) 66 1884.
49. Hoeve, C.A.J., DiMarzio, E.A. and Peyser, P. J. Chem. Phys. (1965) 42 2558.
50. Roe, R.J. Proc. Natl. Acad. Sci. U.S. (1965) 53 50
51. Silberberg, A. (a) J. Chem. Phys. (1967) 46 1105, (b) J. Chem. Phys. (1968) 48 2835.
52. Rubin, R.J. J. Chem. Phys. (1965) 43 2392.
53. Clark, A.T., Lal, M. and Turpin, M.A. Far. Disc. Chem. Soc. (1975) No 59 189.
54. Hoeve, C.A.J. J. Polym. Sci. Polymer Symposium (1977) 61 389.
55. Hoffman, R.F. and Forsman, W.C. J. Polym. Sci. (1970) A2 8 1847.
56. Hesselink, F.Th. J. Phys. Chem. (1969) 73 3488.
57. Hoeve, C.A.J. J. Chem. Phys. (1965) 43 3007.
58. Flory, P.J. 'Statistical Mechanics of Chain Molecules' (1969) Wiley-Interscience.
59. Flory, P.J. 'Principles of Polymer Chemistry' (1953) Ithaca-New York.
60. Napper, D.H. J. Colloid. Interface. Sci. (1970) 32 109.

61. Ottewill, R.H. in 'Nonionic Surface Active Agents' Ed. Schick, M.J. (1967) Dekker.
62. Napper, D.H. and Hunter, R.J. MTP Int. Review of Science - Series One Vol 7 p. 279.
63. Elworthy, P.H. J. Pharm. Pharmacol (1960) 12 260T
64. Elworthy, P.H. and MacFarlane, C.B. J. Chem. Soc. (1964) Pt 1 311.
65. El Eini, D.I.D., Barry, B.W. and Rhodes, C.T. J. Pharm. Pharmacol. (1973) 25 166P.
66. Schott, H. J. Colloid. Interface. Sci. (1967) 24 193.
67. Corkill, J.M., Goodman, J.F. and Tate, J.R. Trans. Faraday. Soc. (1966) 62 979.
68. Ottewill, R.H. Ann. Reports (1969) 66 183.
69. Evans, R., Davison, J.B. and Napper, D.H. J. Polym. Sci. (1972) BIO 449.
70. Evans, R. and Napper, D.H. J. Colloid Interface. Sci. (1975) 52 260.
71. Napper, D.H. Kolloid - Z u. Z Polymere (1969) 234 1149.
72. Napper, D.H. Ind. Eng. Chem. Prod. Res. (1970) 9 467.
73. Flory, P.J., Ellenson, J.L. and Eichinger, B.E. Macromolecule (1968) 1 279.
74. Flory, P.J. Disc. Far. Soc. (1970) 49 7.
75. Shaw, D.J. 'Introduction to Colloid and Surface Chemistry' 2nd Ed. (1970) Butterworths, London.
76. Mackor, E.L. J. Colloid. Sci. (1951) 6 492.
77. van der Waarden, M. J. Colloid. Sci. (1950) 5 317.
78. Clayfield, E.J. and Lumb, E.C. (a) J. Colloid. Interface. Sci. (1966) 22 269, (b) Disc. Far. Soc. (1966) 42 314, (c) J. Colloid. Sci. (1966) 22 285.
79. Cowell, C., Li-in-on, R. and Vincent, B. J. Chem. Soc. Faraday I. (1978) 74 337.
80. Evans, R. and Napper, D.H. Kolloid-Z.u.Z. Polymere (1978) 251 409.

81. Fischer, E.W. Kolloid-Z.u.Z. Polymere (1958) 160 120.
82. Ottewill, R.H. and Walker, T. Kolloid-Z.u.Z. Polymere (1968) 227
108.
83. Doroszkowski, A. and Lambourne, R. J. Polym. Sci. (1971) 34 253.
84. Bagchi, P. J. Colloid. Interface. Sci. (1974) 47 86,100.
85. Fleer, G.J., Koopal, L.K. and Lyklema, J. Kolloid-Z.u.Z. Polymere
(1972) 250 689.
86. Meier, D.J. J. Phys. Chem. (1967) 71 1861.
87. Flory, P.J. and Krigbaum, W.R. J. Chem. Phys. (1950) 18 1086.
88. Hesselink, F.Th., Vrij, A. and Overbeek, J.Th.G. J. Phys. Chem. (1971)
75 2094.
89. Hesselink, F.Th. J. Phys. Chem. (1971) 75 65.
90. Vincent, B. J. Colloid. Interface. Sci. (1973) 42 270.
91. Evans, R. and Napper, D.H. Kolloid-Z.u.Z. Polymere (1973) 251 329.
92. Osmond, D.W.J., Vincent, B. and Waite, F.A. Colloid and Polymer
Sci. (1975) 253 676.
93. Hesselink, F.Th. J. Polym. Sci. Polymer Symposium (1977) 61 439.
94. Doroszkowski, A. and Lambourne, R. J. Colloid. Interface. Sci. (1973)
43 97.
95. Smitham, J.B., Evans, R. and Napper, D.H. J. Chem. Soc. Faraday I
(1975) 71 285.
96. Dolan, A.K. and Edwards, S.F. Proc. Roy. Soc. (1974) A337 509.
97. Dobbie, J.W., Evans, R., Gibson, D.V., Smitham, J.B. and Napper, D.H.
J. Colloid. Interface. Sci. (1973) 45 557.
98. Jackel, K. Kolloid Z (1964) 197 143.
99. Evans, R., Smitham, J.B. and Napper, D.H. Colloid Polymer Sci. (1977)
255 161.
100. Haydon, D.A. Recent Prog in Surface Membrane Science (1964) 1 147.
101. Gouy, G. J. Phys. Rad. (1910) 9 457.
102. Chapman, D.L. Phil. Mag. (1913) 25 475.

103. Stern, O. Z. Elektrochem (1924) 30 508.
104. Grahame, D.C. Chem. Revs. (1947) 41 441.
105. Visser, J. in 'Surface and Colloid Science' Ed Matijevic, E.
Vol. 8 (1976) Wiley-Interscience.
106. Levine, S. and Bell, G.M. J. Colloid Sci. (1962) 17 838.
107. Lyklema, J. and Overbeek, J.Th.G. J. Colloid. Sci. (1961) 16 501.
108. Hogg, R., Healy, T.W. and Furstenau, D.W. Trans. Farad. Soc. (1966)
62 1638.
109. see reference 15.
110. Le Neveau, D.M., Rand, R.P. and Parsegian, V.A. Nature (London)
(1976) 259 601.
111. Hunter, R.J. and Leyendekkers, J.V. J. Chem. Soc. Faraday I
(1978) 74 450.
112. Marcejla, S. and Radic, N. Chem. Phys. Letts (1976) 42 129.
113. Barclay, L.M. and Ottewill, R.H. Spec. Disc. Faraday Soc. (1970)
1 169.
114. van der Waals, J.D. University of Leiden, Thesis (1873).
115. Keesom, H. Proc. Acad. Sci. Amsterdam (1920) 18 939.
116. Debye, P. Phys. Z (1920) 178.
117. London, F. Z.F. Physik (1930) 60 245.
118. Kallman, H. and Willstatter, M. Naturwiss (1932) 20 952.
119. Hamaker, H.C. Physica (1937) 4 1058.
120. Casimir, H.G.B. and Polder, D. Phys. Rev. (1948) 73 360.
121. Schenkel, J.H. and Kitchener, J.A. Trans. Faraday Soc. (1960)
56 161.
122. Clayfield, E.J., Lumb, E.C. and Miller, W.L. Proc. Int. Congress.
Surface Active Subst. (1969) 2 25.
123. Lifshitz, E.M. Zhur. eksp. teor. Fiz. (1955) 29 94.
124. Parsegian, V.A. and Ninham, B.W. J. Colloid. Interface. Sci. (1971)
37 332.
125. Haydon, D.A. and Taylor, J. Nature (London) (1968) 217 739.

126. Parsegian, V.A. and Ninham, B.W. Nature (London) (1969) 224 1197.
127. Smith, E.R., Mitchell, D.J. and Ninham, B.W. J. Colloid. Interface. Sci. (1973) 45 55.
128. Evans, R. and Napper, D.H. J. Colloid. Interface. Sci. (1973) 45 138.
129. Nir, S. and Adams, S. J. Colloid. Interface. Sci. (1974) 49 203.
130. Vold, M.J. J. Colloid. Interface. Sci. (1961) 16 1.
131. Osmond, D.W.J., Vincent, B. and Waite, F.A. J. Colloid. Interface. Sci. (1973) 42 262.
132. Pluronic Grid. The Wyandotte Chemical Corporation.
133. van den Boomgaard, Th., King, T.A., Tadros, Th.F., Tang, H. and Vincent, B. J. Colloid. Interface. Sci. (1978) 66 68.
134. Goodwin, J.W., Hearn, J., Ho, C.C. and Ottewill, R.H. Colloid and Polymer Science (1974) 252 464.
135. Ross, S. and Olivier, J.P. J. Phys. Chem. (1959) 63 1671.
136. Kuno, H. and Abe, R. Kolloid-Z.u.Z. Polymere (1961) 177 40.
137. Hsio, L., Dunning, H.N. and Lorentz, P.B. J. Phys. Chem. (1956) 60 1057.
138. Schick, M.J., Atlas, S.M. and Eirich, F.R. J. Phys. Chem. (1962) 66 1328.
139. Schmolka, I.R. and Raymond, A.J. J. Amer. Oil. Chem. Soc. (1965) 44 1088.
140. Becher, P. in Ref 171.
141. Saski, W. and Shah, S.G. J. Pharm. Sci. (1965) 54 71.
142. Huggins, M.L. J. Amer. Chem. Soc. (1942) 64 2716.
143. Tanford, C. 'Physical Chemistry of Macromolecules' (1963) Wiley New York.
144. Morawetz, H. 'Macromolecules in Solution' (1966) Wiley-Interscience New York.
145. Garvey, M.J., Tadros, Th.F. and Vincent, B. J. Colloid. Interface. Sci. (1974) 49 57.

146. Brandrupp, J. and Immergut, E.H. 'Polymer Handbook' (1975)
2nd Edition. Wiley-Interscience.
147. Fleer, G.J. Meded Landbouwhogeschool, Wageningen, (1971).
148. Goodwin, J.W., Hearn, J., Ho. C.C. and Ottewill, R.H. Br. Polym.
J. (1973) 5 347.
149. Ottewill, R.H. and Shaw, J.N. Kolloid Z.u.Z. Polymere (1967) 218 314.
150. Hearn, J., Ottewill, R.H. and Shaw, J.N. Br. Polym. J. (1970)
2 116.
151. Yates, D.E., Ottewill, R.H. and Goodwin, J.W. J. Colloid. Interface.
Sci. (1977) 62 356.
152. van den Hul, H.J. and vander Hoff, J.W. Br. Polym. J. (1970) 2 121.
153. Kayes, J.B. Kolloid Z.u.Z. Polymere (1972) 250 939.
154. Stone-Masui, J. and Watillon, A. J. Colloid. Interface. Sci.
(1975) 52 479.
155. Herden, G. 'Small Particle Statistics' 2nd Edn. (1960) Butterworths.
156. Baleaux, M.B. C.R. Acad. Sci. Paris (1972) 274 1617.
157. Rootare, H.M. and Prenzlou, C.F. J. Phys. Chem. (1967) 71 2733.
158. Allen, T.A. 'Particle Size Measurements' 2nd Edn. 1974
Chapman and Hall, London.
159. Kossen, N.W.F. and Heertjes, P.M. Chem. Eng. Sci. (1965) 20 543.
160. Lerk, C.F., Schoonen, A.J.M. and Fell, J.T. J. Pharm. Sci. (1976)
65 843.
161. Tanford, C. in 'The Hydrophobic Effect' 1973. Wiley-Interscience
New York.
162. Ottewill, R.H. and Walker, T. J. Chem. Soc. Faraday I (1974) 70
917.
163. Lambe, R., Tadros, Th.F. and Vincent, B. J. Colloid. Interface.
Sci. (1978) 66 77.
164. Mathai, K.G. and Ottewill, R.H. Trans. Faraday Soc. (1966) 62 750.
165. Akers, R.J. and Riley, P.W. J. Colloid. Interface. Sci. (1974) 48 162.

166. Abe, R. and Kuno, H. Kolloid-Z.u.Z. Polymere (1962) 181 70.
167. McCracken, J.R. and Datyner, A. J. Colloid. Interface. Sci. (1977) 60 201.
168. Stryker, H.K., Helin, A.F. and Mantell, G.J. J. App. Polym. Sci. (1966) 10 81.
169. Rupprecht, H. and Liebl, H. Kolloid-Z.u.Z. Polymere (1970) 239 685.
170. Elworthy, P.H. and Guthrie, W.G. J. Pharm. Pharmacol. (1970) 22 1145.
171. Heydegger, H.R., and Dunning, H.N. J. Phys. Chem. (1959) 63 1613.
172. Bell, W.E. J. Phys. Chem. (1959) 63 299.
173. Howard, G.J. and McConnel, P. J. Phys. Chem. (1967) 71 2981, 2991.
174. Anderson, R.A. Pharm. Acta. Helv. (1972) 47 304.
175. Mankowich, A.M. J. Phys. Chem. (1954) 58 1028.
176. Cowie, J.M.G. and Sirriani, A.F. J. Amer. Oil. Chem Soc. (1966) 43 572.
177. Dwiggin, C.W., Bolen, R.J., Dunning, H.N. J. Phys. Chem. (1960) 64 1175.
178. McDonald, C. and Wong, C.K. J. Pharm. Pharmacol. (1974) 26 557.
179. Wong, C.K. M.Sc. Thesis, Manchester University (1974).
180. Prasad, K.N., Luong, T.T., Florence, A.T., Paris, J., Vaution, C., Seiller, M., and Puisieux, F. J. Colloid. Interface. Sci. (1979) 69 225.
181. Sadron, C., Pure Appl. Chem. (1962) 4 347.
182. Hillsom, P.J. J. Photograph. Sci. (1963) 11 225.
183. Glazmann, Y. and Blaschuk, Z., J. Colloid. Interface. Sci. (1977) 62 158.
184. Lang, J., Auburn, J.J. and Eyring, E.M. J. Colloid. Interface. Sci. (1972) 41 484.
185. Enyeart, C.R. in 'Nonionic Surfactants' Ed. M.J. Schick 1967. Marcel Dekker N.Y.
186. Lipatov, Yu. S. and Sergeeva, L.M. 'Adsorption of Polymers' 1974.

187. Kolthoff, I.M. and Gutmacher, R.G. J. Phys. Chem. (1952) 56 740
Wiley and Sons.
188. Johnson, G.A. and Lewis, K.E. Br. Polym. J. (1969) 1 266.
189. Lankveld, J.M.G. and Lyklema, J. J. Colloid Interface Sci. (1972)
41 475.
190. Silberberg, A. J. Colloid. Interface. Sci. (1972) 38 217.
191. Tadros, Th.F. J. Colloid. Interface. Sci. (1978) 64 36.
192. Fleer, G.J. and Smith, L.E. 'Colloid and Interfacial Science'
Vol. 5 p. 501. Ed. M. Kerker - Academic Press (1976).
193. Davydov, V.Y., Kiselev, A.V. and Zhuravlev, L.T. Trans. Faraday.
Soc. (1964) 60 2254.
194. Kipling, J.J. 'Adsorption from Solutions of Non-Electrolytes'
Academic Press (1965) London.
195. Kavanagh, B.V., Posner, A.M. and Quirk, J.P. Far. Disc. Chem. Soc.
(1975) 59 242.
196. Garvey, M.J. Ph.D. Thesis, University of Bristol.
197. Stockmayer, W.H. and Fixman, M. J. Polym. Sci. Part C (1963) 1 137.
198. Ptitsyn, O.B. and Eisener, Yu.E. Soviet Tech. Phys. (1960) 4 1020.
199. Flory, P.J. and Fox, T.G. J. Amer. Chem. Soc. (1951) 73 1904.
200. Berry, G.C. J. Chem. Phys. (1967) 46 1338.
201. Banks, W., Greenwood, C.T. and Sloss, J. Makromol. Chemie (1970)
140 119.
202. Eltekov, Yu.A. and Kiselev, A.V. J. Polym. Sci. Symposium (1977)
61 431.
203. Ottewill, R.H. and Shaw, J.N. Kolloid-Z.u.Z. Polymere 215 165.
- 203a Stromberg, R.R., Kunststoffe (1965) 12 12.
204. Howard, G.J. and McConnel, P. J. Phys. Chem. (1967) 71 2995.
205. Peterson, C. and Kwei T. J. Phys. Chem. (1961) 65 1331.
206. Eagland, D., Wardlaw, G.C. and Thorn, I. Colloid Polymer Sci. (1978)
256 1073.
207. Ottewill, R.H. and Vincent, B. J. Chem. Soc. Faraday I (1972) 68 1533.

208. Shaw, D.J. in 'Electrophoresis' Academic Press London and New York 1969.
209. Komagata, S. J. Electrochem. Soc. Japan (1933) 1 97.
210. Huckel, E. Phys. Z. (1924) 25 204.
211. von Smoluchowski, M. Bull. Acad. Sci. Cracovie (1903) page 182.
212. Henry, D.C. Proc. Roy. Soc. (1931) A133 106.
213. Overbeek, J.Th.G. Adv. Colloid Sci. (1950) 3 97.
214. Booth, F. Nature (1948) 161 83.
215. Wiersema, P.H., Loeb, A.L. and Overbeek, J.Th.G. J. Colloid Interface Sci. (1966) 22 78.
216. Ottewill, R.H. and Shaw, J.N. J. Electroanal. Chem. (1972) 37 133.
217. Lyklema, J. and Overbeek, J.Th.G. J. Colloid Sci. (1961) 16 501.
218. Hunter, R.J. J. Colloid Interface Sci. (1966) 22 231.
219. Overbeek, J.Th.G. and Wiersema, P.H. in 'Electrophoresis' Vol II Ed. Bier, M. Academic Press 1967.
220. Einstein, A. Ann. Physik. (1906) 19 289.
221. Doroszkowski, A. and Lambourne, R. J. Colloid Interface Sci. (1968) 26 214.
222. Manley, R.St.J. and Mason, S.G. Can. J. Chem. (1954) 32 763.
223. Mooney, M. J. Colloid Sci. (1951) 6 162.
224. Pusey, P.N. in 'Industrial Polymers - Characterisations by Molecular Weight' Ed. Green, J.H.S. and Dietz, R. Transcripta Books 1973.
225. Elworthy, P.H. and Florence, A.T. J. Pharm. Pharmacol. (1967) 19 140S
226. Daluja, K.L. and Srivastava, S.N. Indian J. Chem. (1969) 7 790.
227. Tadros, Th.F. in 'Colloidal Dispersions and Micellar Behaviour' Ed. Mittal, K.L. A.C.S. Symposium Series 9 Washington (1975).
228. Kayes, J.B. Ph.D. Thesis University of Aston in Birmingham (1975).
229. Lyklema, J. J. Colloid Interface Sci. (1977) 58 242.
230. Garvey, M.J. Tadros, Th.F. and Vincent, B. J. Colloid Interface Sci. (1976) 55 440.

231. Staudinger, H. Die hochmolekularen organischen Verbindungen, Springer, Berlin (1960) new edn.
232. Koopal, L.K. and Lyklema, J. Faraday Disc. Chem. Soc. (1975) 59 230.
233. Brooks, D.E. J. Colloid Interface Sci. (1973) 43 700.
234. Elworthy, P.H. and Florence, A.T. J. Pharm. Pharmacol (1969) 21 79S.
235. Becher, P. J. Colloid. Sci. (1961) 16 14.
236. Duckworth, D.S., Lips, A. and Staples, E.J. Faraday Dis. Chem. Soc. (1978) 65 288.
237. Young, C. M.Sc. Thesis Bristol University (1976).
238. See Ref 133.
239. Hiestand, E.N. J. Pharm. Sci. (1972) 61 269.
240. Ward, H.T. and Kammemayer, K. Ind. Eng. Chem. (1940) 32 622.
241. Dinterfass, L. Kolloid-Z.u.Z. Polymere (1959) 163 48.
242. Long, J.A., Osmond, D.W.J. and Vincent, B. J. Colloid Interface Sci (1973) 42 545.
243. Boucher, E.A. and Hines, P.D. J. Polymer Sci. (Physics) (1976) 14 2241.
244. Gregory, J. Adv. Colloid Interface Sci. (1968/70) 2 400.
245. El-Hinnawi, E.E. "Methods in Chemical and Mineral Microscopy" (1966) Elsevier.
246. Ohno, Y., Sumimoto, Y. Ohshima, M. Yamada, M., Shimamoto, T. Chem. Pharm. Bull. (1974) 22 2788.
247. Rupprecht, H. and Hofer, J. Paper presented at Surface Active Agent Symposium Nottingham September 1979.
248. Law, S-L. University of Aston in Birmingham (1979) - Private Communication.
249. Carless, J.E. and Foster, A.A. J. Pharm. Pharmacol. (1966) 18
250. Tadros, Th.F. S.C.I. Monograph (1973) 38 221.
251. Kallay, N. Krznaric, I. and Cegelj, Z. Colloid and Polymer Science (1979) 257 75.
252. Lambe, R., Tadros, Th.F. and Vincent, B. J. Colloid Interface Sci. (1978) 66 77.

253. Visser, J. Adv. Colloid Interface Sci. (1972) 3 331.
254. Force, C.G. and Matijevic, E. Kolloid-Z.u.Z. (1968) 224 60.
255. Fawkes, F.M. Ind. Eng. Chem. (1964) 56 40.
256. Florence, A.T. and Rogers, J.A. J. Pharm. Pharmacol. (1971) 23 153.
257. Peppas, N.A. and Merrill, E.W. J. Polym. Sci. (Chemistry) (1976) 14 459.
258. Garvey, M.J., Mitchell, D. and Smith, A.L. Colloid and Polymer Science (1979) 257 70.
259. Najib, N., Kellaway, I.W. and Marriott, C. J. Pharm. Pharmacol. (1978) 30 3P.
260. Garrett, E.R. in 'Safer and More Effective Drugs' A.Ph.A. Washington (1967).
261. Berlin, A., Siwers, B., Augurell, S., Hiort, A., Sjoquist, F. and Strom, S. Clin. Pharmacol. Ther. (1972) 13 733.
262. Bates, T.R., Lambert, D.A. and Johns, W.H. J. Pharm. Sci. (1969) 58 1468.
263. Howard, S.A., Mauger, J.W. and Phusanti, L. J. Pharm. Sci. (1977) 66 557.
264. Florence, A.T., Elworthy, P.H. and Rahman, A. J. Pharm. Pharmacol. (1973) 25 779.
265. Barzegar-Jelali, M. and Richards, J.H. Int. J. Pharm. (1979) 2 195.
266. Shah, N.B. and Sheth, B.B. J. Pharm. Sci. (1976) 65 1618.
267. Najib, N., Kellaway, I.W. and Marriott, C. J. Pharm. Pharmacol. (1978) 30 1P.
268. Elworthy, P.H. and Lipscomb, F.J. J. Pharm. Pharmacol. (1968) 20 923.
269. Collett, J.H. and Rees, J.A. J. Pharm. Pharmacol. (1975) 27 647.
270. Elworthy, P.H. and Lipscomb, F.J. J. Pharm. Pharmacol. (1968) 20 817.
271. Najib, N. Ph.D. Thesis University of Nottingham (1979).
272. Tadros, Th.F. Private Communication (1978).

273. Stromberg, R.R., Grant, W.H. and Passaglia, E. J. Res. Natl. Bur. Std. (1964) A68 391.
274. Bircumshaw, L.L. and Riddiford, A.C. Q. Rev. (1952) 6 157.
275. Levy, G. and Procknal, J.A. J. Pharm. Sci. (1962) 51 294.
276. Hamlin, W.E. Nelson, E., Ballard, B.E. and Wagner, J.G. J. Pharm. Sci. (1962) 51 432.
277. Higuchi, W.I. J. Pharm. Sci. (1958) 47 376.
278. Levy, G. J. Pharm. Sci. (1963) 52 1039.
279. Elworthy, P.H. and Lipscomb, F.J. J. Pharm. Pharmacol (1969) 21 273.
280. Collett, J.H., Rees, J.A. and Dickinson, N.A. J. Pharm. Pharmacol (1972) 24 724.
281. Nelson, E. J. Pharm. Sci. (1957) 46 607
282. Fage, A. and Townend, H.C.H. Proc. Roy. Soc. (1932)A 135 656.
283. Flynn, G.L., Yalkowski, S.H. and Roseman, T.J. J. Pharm. Sci. (1974) 63 479.